

VOL. 13 NO. 4 APRIL 1967

PUBLISHED MONTHLY

completing volume 13

JOURNAL OF

# ELECTROANALYTICAL CHEMISTRY

## AND INTERFACIAL ELECTROCHEMISTRY

International Journal devoted to all Aspects  
of Electroanalytical Chemistry, Double Layer  
Studies, Electrokinetics, Colloid Stability, and  
Electrode Kinetics.

EDITORIAL BOARD:

J. O'M. BOCKRIS (Philadelphia, Pa.)  
B. BREYER (Sydney)  
G. CHARLOT (Paris)  
B. E. CONWAY (Ottawa)  
P. DELAHAY (New York)  
A. N. FRUMKIN (Moscow)  
L. GIERST (Brussels)  
M. ISHIBASHI (Kyoto)  
W. KEMULA (Warsaw)  
H. L. KIES (Delft)  
J. J. LINGANE (Cambridge, Mass.)  
G. W. C. MILNER (Harwell)  
R. H. OTTEWILL (Bristol)  
J. E. PAGE (London)  
R. PARSONS (Bristol)  
C. N. REILLEY (Chapel Hill, N.C.)  
G. SEMERANO (Padua)  
M. VON STACKELBERG (Bonn)  
I. TACHI (Kyoto)  
P. ZUMAN (Prague)

E L S E V I E R

## GENERAL INFORMATION

See also Suggestions and Instructions to Authors which will be sent free, on request to the Publishers.

### *Types of contributions*

- Original research work not previously published in other periodicals.
- Reviews on recent developments in various fields.
- Short communications.
- Bibliographical notes and book reviews.

### *Languages*

Papers will be published in English, French or German.

### *Submission of papers*

Papers should be sent to one of the following Editors:

Professor J. O'M. BUCKRIS, John Harrison Laboratory of Chemistry,  
University of Pennsylvania, Philadelphia 4, Pa. 19104, U.S.A.

Dr. R. H. OTTEWILL, Department of Chemistry, The University, Bristol 8, England.

Dr. R. PARSONS, Department of Chemistry, The University, Bristol 8, England.

Until June 1967: Gates and Crellin Laboratories of Chemistry, California Institute of  
Technology, Pasadena, Calif. 91109, U.S.A.

Professor C. N. REILLEY, Department of Chemistry,  
University of North Carolina, Chapel Hill, N.C. 27515, U.S.A.

Authors should preferably submit two copies in double-spaced typing on pages of uniform size. Legends for figures should be typed on a separate page. The figures should be in a form suitable for reproduction, drawn in Indian ink on drawing paper or tracing paper, with lettering etc. in thin pencil. The sheets of drawing or tracing paper should preferably be of the same dimensions as those on which the article is typed. Photographs should be submitted as clear black and white prints on glossy paper. Standard symbols should be used in line drawings, the following are available to the printers:

▼ ▽ ■ □ ● ⊙ ■ □ ⊕ ⊖ ⊗ ⊘ ⊙ ⊙ ⊕ ⊕ ⊗ ⊗ ⊘ ⊘ ⊙ ⊙ ⊕ ⊕ ⊗ ⊗ ⊘ ⊘ ⊙ ⊙ ⊕ ⊕ ⊗ ⊗ ⊘ ⊘

All references should be given at the end of the paper. They should be numbered and the numbers should appear in the text at the appropriate places.  
A summary of 50 to 200 words should be included.

### *Reprints*

Fifty reprints will be supplied free of charge. Additional reprints can be ordered at quoted prices. They must be ordered on order forms which are sent together with the proofs.

### *Publication*

The *Journal of Electroanalytical Chemistry and Interfacial Electrochemistry* appears monthly and has four issues per volume and three volumes per year.

Subscription price: £ 18.18.0 or \$ 52.50 or Dfl. 189.00 per year; £ 6.6.0 or \$ 17.50 or Dfl. 63.00 per volume; plus postage. Additional cost for copies by air mail available on request. For advertising rates apply to the publishers.

### *Subscriptions*

Subscriptions should be sent to:

ELSEVIER PUBLISHING COMPANY, P.O. Box 211, Amsterdam, The Netherlands.



## CONSTRUCTION AND OPERATION OF A ROTATING DISC ELECTRODE FOR ELEVATED TEMPERATURES

J. WOJTOWICZ\* AND B. E. CONWAY

*Department of Chemistry, University of Ottawa (Canada)*

(Received March 1st; in revised form, May 13th, 1966)

## INTRODUCTION

Rotating disc techniques, the principles of which have been adequately described elsewhere<sup>1,2</sup>, are required in the study of the kinetics of certain anodic oxidations<sup>3</sup>, *e.g.*, of hydrocarbons, formate ion and hydrazine<sup>4</sup>, where a region of anodic potentials exists over which the rates tend towards a limiting current and where in some cases, the direction of the current-potential curve becomes reversed (passivation effect<sup>3,5</sup>). In these cases, it is important to evaluate the extent to which the reaction becomes diffusion-controlled at various potentials, and to establish, where possible, the nature of the activation-controlled behaviour by working at high rotation speeds. Since a number of anodic oxidations, *e.g.*, of hydrocarbons, require elevated temperatures before they will proceed at conveniently measurable rates, and qualitative experiments indicate a role of diffusion control in the chemisorption and electro-oxidation of these molecules, it is necessary to study such oxidation processes at the rotating disc electrode where the mass-transport conditions can be controlled.

Descriptions or diagrams of rotating disc assemblies have been given in some previous publications<sup>6-8</sup> and details of the motor and speed control devices have been reported. However, it seems advantageous to give the engineering details more completely, particularly in regard to the design of an apparatus for operation at elevated temperatures, as a number of special problems arise under such conditions. Accordingly, we have considered that it may be of general usefulness to report in the present paper some details of the construction and operation of such an instrument for these conditions, and some tests of the apparatus in the oxidation of H<sub>2</sub>, and oxidation and reduction in the [Fe(CN)<sub>6</sub>]<sup>4-</sup>-[Fe(CN)<sub>6</sub>]<sup>3-</sup> system.

## DESIGN AND CONSTRUCTION

*(i) Requirements*

The apparatus developed was capable of being operated up to 10,000 rev./min which is sufficiently fast for the study of most anodic oxidation reactions involving organic substances. For hydrocarbon oxidations, a temperature of 120-150° is desirable so that an apparatus operating up to this temperature in, for example, strong H<sub>3</sub>PO<sub>4</sub> or HClO<sub>4</sub>, was required.

The following problems arise generally in the design of a rotating disc assembly

\* On leave of absence from the Technical University, Warsaw, Poland.

but become accentuated when a range of elevated temperatures is to be used in the electrode-kinetic studies (in particular, (c) and (d) below present special difficulties under these conditions): (a) insulation of the drive shaft or electrode holder from the solution; (b) corrosion of parts of the apparatus; (c) differential expansion of components of the disc and shaft as the temperature is changed and (d) evaporation of solvent into the bearing assembly of the rotating shaft.

The general design of the apparatus is shown in the detailed drawing (Fig. 1) and the whole assembly was mounted on a heavy drill stand with a 6-in. column bolted to the floor.

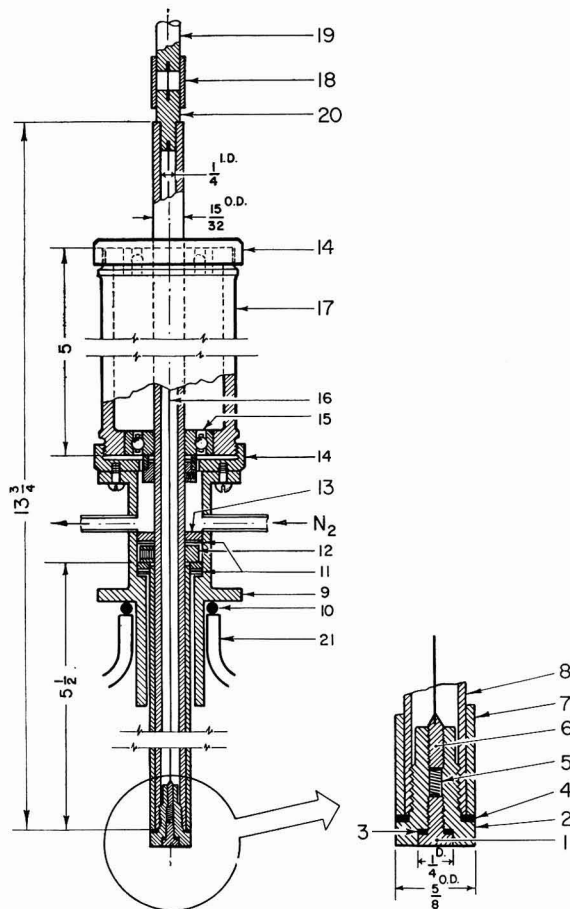


Fig. 1. Engineering drawing of the rotating electrode assembly.

### (ii) Electrode assembly

The disc itself was a solid platinum cylinder (1 in Fig. 1) 0.25 in. in diameter and about 6 mm in length, sunk into a Kelf guard ring insulator (2) threaded into the main shaft (8) which was constructed from stainless steel. The Pt electrode was sealed into (2) by means of a compressible gasket (3) and a tight fit was maintained by screwing the electrode tightly into (2) by means of a screwdriver operating in a channel at

the inner end of (1) inside the threaded region of (2), before the shaft and electrode were assembled. Contact to the external circuit was made by means of a spring seated on the upper end of (1) and communicating with a threaded brass pin (6) soldered to the connecting wire (16) which passed out through the top of the shaft (see below). The whole electrode assembly (see inset in Fig. 1) could be screwed into the shaft (7) and sealed by means of the Teflon or silicone-rubber washer at (4). The shaft (8) was protected by a 1-mm thick KelF sheath (7) which extended just above the cell into the gas-seal housing (9) at the region (11, 12).

The use of the sheath (7) around the main shaft is, of course, most necessary, as stainless steel suffers appreciable corrosion under conditions of highly acid media at elevated temperature, and it also serves for the general purpose of electrical insulation. Teflon was initially used and is satisfactory for room-temperature operations. However, this substance has an unusually high coefficient of expansion and becomes loose on the main shaft at 100°, admitting the electrolyte with resultant corrosion. KelF is more satisfactory and has a coefficient of expansion much more compatible with that of stainless steel. Use of a solid Teflon or KelF main shaft is unsatisfactory at elevated temperatures since thermal distortion tends to occur. The gasket (4) is also quite essential in order to prevent: (a) leakage into the electrode contact at (1, 5, 6) and consequent local short-circuit currents, and (b) leakage at the bottom of the stainless-steel shaft. The design shown in Fig. 1 for this part of the apparatus was found to be satisfactory for many days of operation at 100° in acid media but was the result of a number of trials of other less satisfactory arrangements.

A ring-disc<sup>6</sup> electrode assembly could also be used at the bottom of the shaft and in that case, a different commutator contact arrangement would be required.

### (iii) Gas seal

The design of a gas seal for speeds up to 10,000 rev./min and for use with solutions at 100–150° presented substantial problems. A seal is required (a) to prevent diffusion of oxygen into the apparatus (*cf.* ref. 9); (b) for maintenance of a reproducible atmosphere of N<sub>2</sub> or hydrocarbon gas (or mixtures thereof, *cf.* ref. 10) in the cell during kinetic runs, and (c) to prevent evaporation of solvent into the bearing housing in the region (14, 15), and thus to prevent corrosion of the bearing that otherwise soon occurs.

First, a seal to the cell is made between the Teflon plate and guide assembly (9) by means of an O-ring (10). A later modification uses a flange seal and O-ring at this point. The whole electrochemical cell, the top of which is shown as (21), can be raised to make a good seal at (10) by adjustment of (a) the three screwed legs on a base plate below the cell (not shown) and (b) the ring which holds the housing of the gas seals. The Teflon assembly (9) extends up to the bearing housing and is precisely and tightly screwed on to it at (14).

The gas seals (11) are thin Teflon discs mounted on the main shaft and located by the locking ring (12). A felt seal (13) is also used above the ring (12) together with another thin Teflon disc (indicated by the upper arrow of 11) which minimises friction between the felt seals (13), the ring (12) and the gas seal housing (9). The ring (12) is located above a thicker Teflon ring sealed to the sheath (7) below which the two thin Teflon washers at (11) are located to minimise friction between the Teflon ring and the base of the housing. This constitutes the main part of the seal.



The whole gas-seal housing is ventilated and an inlet and outlet for passage of dry  $N_2$  into it above the seals was provided, as shown, to prevent any traces of moisture reaching the high-speed bearings (15) or when complete absence of oxygen in the cell was desired. This part of the apparatus is most essential for satisfactory operation at elevated temperatures.

(iv) *Bearing assembly*

The remaining part of the assembly is more conventional. The two high-speed bearings (15) (type ND 20201) are mounted at the top and bottom of the bearing housing (17) and located by a ring similar to (12); they are locked and covered with (14) and (17) as shown. The ring (12) in (14) allows adjustment for tightness in the lower bearing. The upper bearing is mounted with a cap (14) to close off the bearing housing.

(v) *Electrode contact and drive motor*

The electrode contact wire (16) passes through the main shaft into a termination block (20) which can either be insulated from the main shaft — or connected to it (earthed condition, as normally used). Contact to the drive motor (not shown) is made by means of a wire passing through a flexible coupling (18) to the motor shaft (19). A magnetic clutch of the type described by IBL<sup>11</sup> could also be used here; (18) is about 1 in. long and must not be too rigid. Electrical contact continues through the motor shaft and the armature, and is taken off from the primary end of an 18:1 reduction gear. The motor shaft was machined to a 60°-bevel and contact was made *axially* to it by means of a spring-loaded graphite plate. This arrangement, which involves minimum linear contact velocity, was found to be superior to the use of a conventional "commutator" with slip rings or carbon brushes. In the latter case, the relatively high linear contact velocity introduces undesirable noise in potentiostatic and transient measurements, whereas the "point-contact" arrangement is entirely satisfactory in this regard.

Two separate detachable motors (Heller, Las Vegas, type GT21) were used to cover speed ranges up to 6000, and to 10,000 rev./min, respectively. The motors were operated with a Heller type 2T60 speed control. Constancy of speed, as indicated by measurements on an oscilloscope (see below), was better than 1% (*cf.* ref. 7) and during the period of any measurement, variations were usually undetectable.

(vi) *Rotation velocity*

The drive motor was provided with an 18:1 rigid (non-slip) reduction gear. A small commutator was fixed to the end of this "slow" shaft with a 180° on-off contact arrangement. A small e.m.f. was applied to the two brushes of this contact and the circuit completed through the Y-plates of an oscilloscope. A good square-wave pattern resulted, the frequency of which could be measured precisely on the oscilloscope with reference to a standard calibration frequency.

(vii) *Cell*

The all-glass electrochemical cell is shown schematically in Fig. 2. It is provided with counter-electrode and reference-electrode compartments with stopcock and gas-supply arrangements as in normal designs previously published. The working compartment should, however, be unusually large; the present cell was 6½ in. in

diameter and 8 in. high. It is desirable to have the rotating electrode mounted eccentrically in the cell in order to minimise vortices in the liquid during rotation.

Gases could be bubbled near the electrode to saturate the solution. The design of the cell shown in Fig. 2 allowed the use of an adjustable Luggin capillary which is mounted on a 7/10 standard joint inside the cell well below the disc. The capillary could be moved sideways across the electrode and its height could be varied by using different tips which were detachable. In this way, any effects of the tip leading to interference with the hydrodynamic flow lines could be checked\*.

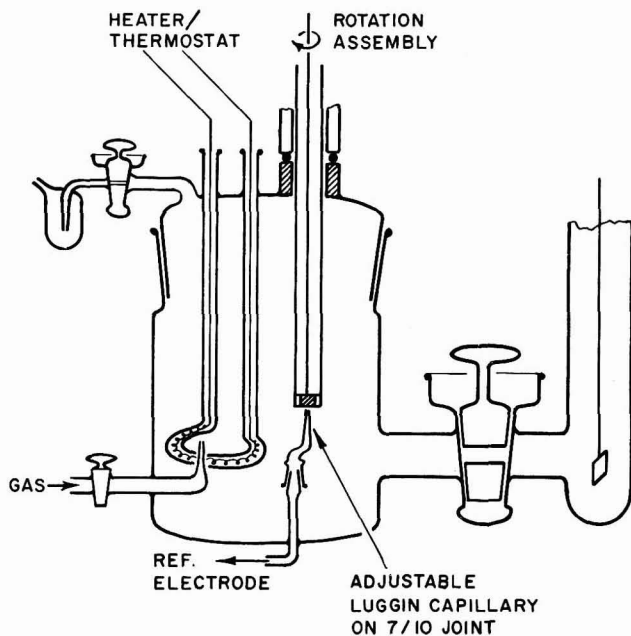


Fig. 2. Schematic diagram of the working electrode compartment of the cell.

Investigations of the effect of variation in the position of the capillary tip showed, however, that the slope of the current-(frequency)<sup>½</sup> relation was unaffected by the position of the tip except to a small extent at the highest frequency (9,600 rev./min) when the tip was only 0.5 mm from the electrode surface. Provided that current measurements are always made in a potential range where complete diffusion control obtains, and the current is thus independent of the potential, use of a Luggin capillary will usually be unnecessary. The present apparatus was, however, designed for the study of potentiostatic current-potential relations with systems where transitions from diffusion to activation control (or *vice versa*) were anticipated and under these conditions, the arrangement shown in Fig. 2 is desirable.

#### KINETIC RUNS

Tests of the apparatus were made by studying the oxidation of H<sub>2</sub> and the

\* The question of the effect of the shape of the end of the electrode shaft in regard to the flow pattern has recently been carefully investigated by BLURTON AND RIDDIFORD<sup>19</sup>.

oxidation-reduction behaviour of the  $[\text{Fe}(\text{CN})_6]^{3-}-[\text{Fe}(\text{CN})_6]^{4-}$  couple in aqueous NaOH solution (*cf.* ref. 12) up to  $90^\circ$ .

Potentials were controlled by means of a Wenking potentiostat and currents were measured on a Sensitive Research Instrument Co. micromillammeter. A platinized-Pt hydrogen reference electrode was used for the study of the oxidation of  $\text{H}_2$  and a plain Pt electrode for the redox system  $[\text{Fe}(\text{CN})_6]^{3-}-[\text{Fe}(\text{CN})_6]^{4-}$ . Well-known<sup>4</sup> general techniques were used for gas and solution purification including deoxygenation by  $\text{N}_2$ . The potassium ferrocyanide and ferricyanide salts were the analytical-grade materials.

(i) Oxidation-reduction with the  $[\text{Fe}(\text{CN})_6]^{4-}-[\text{Fe}(\text{CN})_6]^{3-}$  system

A log-log plot of current,  $i$ , as a function of rotation frequency, for  $[\text{Fe}(\text{CN})_6]^{3-}$  reduction, for example, gave a slope of  $0.5 \pm 0.01$  up to 6600 rev./min, indicating satisfactory operation of the disc. The overvoltage-log  $[i]$  curve gave the characteristic current plateau for diffusion control. The potential used was then set at  $-650$  mV *i.e.*, in the middle of the plateau between the limiting current for  $[\text{Fe}(\text{CN})_6]^{3-}$  reduction and the onset of  $\text{H}_2$  evolution.

The plots of current density,  $i$ , *vs.* (rotation frequency)<sup>1/2</sup> are shown in Figs. 3 and 4 for reduction of  $[\text{Fe}(\text{CN})_6]^{3-}$  and oxidation of  $[\text{Fe}(\text{CN})_6]^{4-}$ , respectively, for temperatures of 30, 50, 70 and  $90^\circ$  in 1.0 *N* aqueous NaOH and for rotation speeds up to 9300  $\text{min}^{-1}$ .

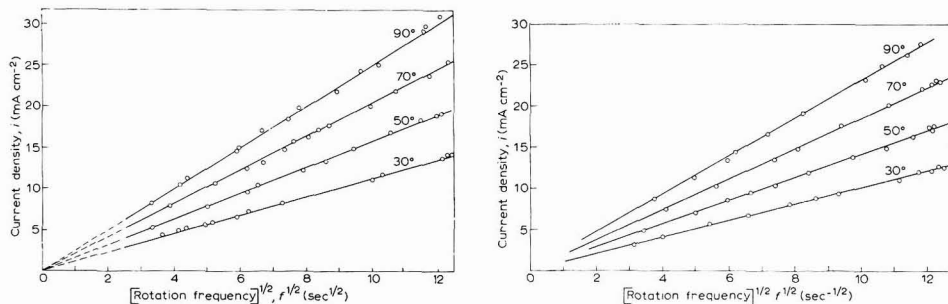


Fig. 3-4.  $i-f^{1/2}$  relations for: (3), ferricyanide reduction; (4), ferrocyanide oxidation.

Concentrations of 0.01 *N* were used in each case in order to be able to compare the results with those of BAZAN AND ARVIA<sup>12</sup>. The diffusion constants,  $D$ , were calculated from the lines shown in Figs. 3 and 4 using the relation

$$D = 0.54 \nu^{1/2} (\Gamma/\sqrt{2\pi f})^{2/3} \quad (1)$$

derived from the well-known Levich equation

$$i = 0.62 FC_0 D^{2/3} \nu^{-1/6} \omega^{1/2} \quad (2)$$

where  $\nu$  is the kinematic viscosity in  $\text{cm}^2 \text{sec}^{-1}$ ,  $\omega$  the angular rotation frequency in radians  $\text{sec}^{-1}$  ( $= 2\pi f$ ),  $F$  the Faraday,  $C_0$  the concentration of the electroactive ion in the bulk expressed in equivalent  $\text{cm}^{-3}$  and  $f$  the rotation in rev./sec. The derived data for  $D$ , together with other data required (see below) in the calculation, are given in Table I for  $[\text{Fe}(\text{CN})_6]^{3-}$  and  $[\text{Fe}(\text{CN})_6]^{4-}$ . Viscosities,  $\mu$ , and densities,  $d$ , of the solu-



TABLE 1

 DATA AND RESULTS FOR DIFFUSION-CONTROLLED OXIDATION AND REDUCTION IN THE  
 $[\text{Fe}(\text{CN})_6]^{4-}$ - $[\text{Fe}(\text{CN})_6]^{3-}$  SYSTEM IN 1 N NaOH

$t$ (°C)	$\mu \cdot 10^2$ ( $g\text{ cm}^{-1}\text{ sec}^{-1}$ )	$d$ ( $g\text{ cm}^{-3}$ )	$\nu^{\frac{1}{2}}$ ( $\text{cm}^{\frac{1}{2}}\text{ sec}^{-\frac{1}{2}}$ )	$[\text{Fe}(\text{CN})_6]^{3-}$		$[\text{Fe}(\text{CN})_6]^{4-}$	
				$(i/\nu^{\frac{1}{2}}) \cdot 10^3$ ( $A\text{ sec}^{\frac{1}{2}}\text{ cm}^{-2}$ )	$D \cdot 10^5$ ( $\text{cm}^2\text{ sec}^{-1}$ )	$(i/\nu^{\frac{1}{2}}) \cdot 10^3$ ( $A\text{ sec}^{\frac{1}{2}}\text{ cm}^{-2}$ )	$D \cdot 10^5$ ( $\text{cm}^2\text{ sec}^{-1}$ )
30	1.013	1.041	0.314	1.135	0.65	1.02	0.56
50	0.650	1.036	0.282	1.60	0.98	1.43	0.83
70	0.476	1.021	0.261	2.06	1.33	1.87	1.15
90	0.370	1.009	0.246	2.56	1.73	2.33	1.49

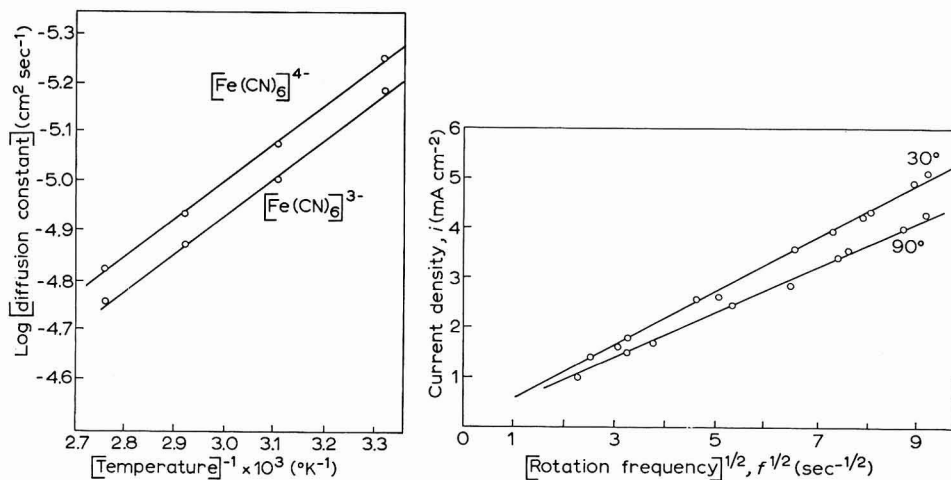

 Fig. 5. Arrhenius plots for the diffusion constants of  $[\text{Fe}(\text{CN})_6]^{3-}$  and  $[\text{Fe}(\text{CN})_6]^{4-}$  in 1 N aq. NaOH (30-90°).

 Fig. 6.  $i$ - $f^{\frac{1}{2}}$  relations for oxidation of  $\text{H}_2$  at 27° and 90° in aq. 1 M  $\text{HClO}_4$ , (apparent inversion of currents with temp. is due to the solubility and partial pressure effects).

tions were determined at the four temperatures by standard methods. The data of BAZAN AND ARVIA<sup>12</sup> for 25° are somewhat higher, *viz.*  $D = 6.77 \times 10^{-6} \text{ cm}^2 \text{ sec}^{-1}$  and  $5.81 \times 10^{-6} \text{ cm}^2 \text{ sec}^{-1}$  for  $[\text{Fe}(\text{CN})_6]^{3-}$  and  $[\text{Fe}(\text{CN})_6]^{4-}$ , respectively, with a quoted<sup>12</sup> accuracy of 3-10%. The activation energy for diffusion of both these ions is obtained from Fig. 5 as 3.6 kcal mole<sup>-1</sup>. Uncertainties in  $D$  have been estimated by statistical methods from the present results, and their standard errors are given in Table 2. Estimates of uncertainties in some other previously published data are included for comparison.

The diffusion constants of the ions may also be derived from the Nernst relation

$$D^0 = \frac{RT\lambda^0}{zF^2}$$

for infinite dilution conditions from the ionic mobility at infinite dilution,  $\lambda^0$ . In the present case,  $\lambda^0$  for  $[\text{Fe}(\text{CN})_6]^{4-}$  is 110.5 and  $\lambda^0$  for  $[\text{Fe}(\text{CN})_6]^{3-}$  is 101 at 25° so that

TABLE 2

UNCERTAINTIES IN SLOPES OF  $i$ - $\sqrt{f}$  RELATIONS\* AND DERIVED  $D$ -VALUES

Author	$H_2$ oxidation		$[Fe(CN)_6]^{4-}$ oxidation		$[Fe(CN)_6]^{3-}$ reduction	
	S.D. of slope (relative)	Max-error ( $p=0.95$ ) $\Delta D/D$ (%)	S.D. of slope (relative)	Max-error ( $p=0.95$ ) $\Delta D/D$ (%)	S.D. of slope (relative)	Max-error ( $p=0.95$ ) $\Delta D/D$ (%)
LEWIS AND RUETSCHI (up to $\sqrt{f}=9$ incl.)	0.78	2.3				
LEWIS AND RUETSCHI (up to $\sqrt{f}=11$ incl.)	1.79	5.25				
FRUMKIN AND AJKAZJAN 1.19		3.5				
BAZAN AND ARVIA			0.42	1.24	0.69	2.04
Present work, 30°	0.36	1.07	0.25	0.74	1.22	3.58
Present work, 90°	0.45	1.34	0.19	0.56	0.46	1.34

\* Note: these estimates are made from enlarged reproductions of the published graphs and may not represent exactly the error in the original results. However, the entries for the "present work" refer to our original data. Estimated errors are expressed for the 95% significance level ( $p = 0.95$ ) of the error.

$D^0 = 0.74 \times 10^{-5} \text{ cm}^2 \text{ sec}^{-1}$ , and  $0.89 \times 10^{-5} \text{ cm}^2 \text{ sec}^{-1}$ , respectively, for these two ions<sup>13</sup>. These figures compare satisfactorily with those in Table 1 bearing in mind that the latter are derived for a higher ionic strength and hence will tend to be smaller.

### (ii) Oxidation of $H_2$

The diffusion-controlled oxidation of  $H_2$  has been studied previously by FRUMKIN AND AJKAZJAN<sup>8</sup> and by LEWIS AND RUETSCHI<sup>18</sup>, and their work provides a basis for checking the results obtained with the present apparatus.

In the case of  $H_2$  oxidation<sup>8</sup>, the diffusion-limited currents were measured up to 4500 rev./min at 30° and 90°, at a finely platinized electrode in 1 *M* aqueous  $HClO_4$ . The anode potential was maintained constant at +100 mV ( $E_H$ ), and the current was found not to increase on raising the potential to *ca.* +600 mV ( $E_H$ ). Beyond a potential of *ca.* +900 mV passivation occurs. With the gas solute, allowance must be made in the calculations of  $D$  for (a) the salting-out of the gas by the electrolyte; (b) the dependence of the gas solubility on temperature and (c) the vapor pressure of the solvent.

The solubilities of  $H_2$  in 1 *M*  $HClO_4$  were calculated to be  $6.93 \times 10^{-7}$  and  $2.32 \times 10^{-7}$  mole  $\text{cm}^{-3}$  at 30° and 90°, respectively, from the published<sup>14</sup> Henry's law constants, *viz.*  $5.54 \times 10^7$  and  $5.71 \times 10^7$ , for these two temperatures, allowing for the difference of solubility of the gas in water and in the acid (salting-out effect), an effect which amounts to about 5% (*cf.* ref. 15). The water vapour partial pressure must be allowed for at each temperature; the data for pure water at 30° and 90°, give vapour pressures of 31.8 and 525.8 mm Hg, respectively. Correction for the vapour-pressure lowering due to the presence of  $HClO_4$  gives the actual partial pressures of water as 30.6 and 509 mm Hg at the respective two temperatures. This compares satisfactorily with the water vapour pressures over 1 *N*  $H_2SO_4$  and  $KCl$  solutions<sup>16</sup>. The equilibrium partial pressures\* of  $H_2$  are then approximately 729 mm Hg at 30° and 251 mm Hg at

90°. The corresponding measured slopes (*cf.* ref. 8) of the plots of  $i$  vs.  $(f)^{\frac{1}{2}}$  are  $0.545 \times 10^{-3}$  and  $0.46 \times 10^{-3} \text{ A sec}^{\frac{1}{2}} \text{ cm}^{-\frac{1}{2}}$  at 30° and 90° (Fig. 6). From the Levich equation, again, we obtain  $D_{30^\circ} = 4.24 \times 10^{-5}$  and  $D_{90^\circ} = 14.2 \times 10^{-5} \text{ cm}^2 \text{ sec}^{-1}$  with a *mean* activation energy for the two measurements of 4.35 kcal mole<sup>-1</sup>. The known diffusion constants for H<sub>2</sub> in water are<sup>17</sup>  $4.3 \times 10^{-5}$  (10°),  $4.7 \times 10^{-5}$  (16°) and  $5.2 \times 10^{-5} \text{ cm}^2 \text{ sec}^{-1}$  at 21°, which may be compared with the following data obtained by LEWIS AND RUETSCHI<sup>18</sup> in aqueous KOH:  $18.2 \times 10^{-5} \text{ cm}^2 \text{ sec}^{-1}$  (30°, 0.1 N KOH);  $4.0 \times 10^{-5} \text{ cm}^2 \text{ sec}^{-1}$  (30°, 5 N KOH);  $23.7 \times 10^{-5} \text{ cm}^2 \text{ sec}^{-1}$  (50°, 0.1 N KOH) and  $7.9 \times 10^{-5} \text{ cm}^2 \text{ sec}^{-1}$  (50°, 5 N KOH). These results differ substantially from those of ref. 17 and those from the present work; the discrepancies may arise on account of (a) the different electrolyte used and (b) because the dependence of current on (rotation frequency)<sup>½</sup> in ref. 18 was not linear at high frequencies.

A summary of the relevant solubility ( $c$ ) and kinematic viscosity ( $\nu$ ) data involved in the present work, together with the derived values of  $D$ , is given below:

$t$ (°C)	$c \cdot 10^7$ (mole cm <sup>-3</sup> )	$\nu \cdot 10^2$ (cm <sup>2</sup> sec <sup>-1</sup> )	$D \cdot 10^5$ (cm <sup>2</sup> sec <sup>-1</sup> )
30	6.93	1.02	4.24
90	2.32	0.49	14.2

The use of this apparatus in hydrocarbon oxidation studies at platinum will be described in a forthcoming publication.

#### ACKNOWLEDGEMENT

Grateful acknowledgement is made to the U.S. Army Engineer Research and Development Laboratories, Fort Belvoir, Va. for support of this work on Contract No. CP 70A1-63-4 in connection with fundamental studies on electrochemical hydrocarbon oxidation. We are indebted to Drs. G. R. FREYSINGER and M. SAVITZ for their interest in this work, and to Dr. P. STONEHART of the American Cyanamid Co., for suggestions concerning the design of the electrical contact arrangements.

Special acknowledgement is also made to the engineering staff at the National Research Council (Division of Pure Chemistry), for their patience and care in fabricating several versions of the apparatus.

#### SUMMARY

Factors in the design and construction of a rotating disc electrode apparatus for use at elevated temperatures are described and discussed. Tests of the apparatus in the study of oxidation and reduction of the ferrocyanide–ferricyanide couple, and in the oxidation of hydrogen up to 90°, are reported.

\* We assume that the equilibrium partial pressure of H<sub>2</sub> applies here. However, as bubbles of H<sub>2</sub> appear in the electrolyte, it is evident that H<sub>2</sub> must momentarily be somewhat above 1 atm in pressure. During passage of the bubble to the surface, presumably solvent vapour evaporates into it and H<sub>2</sub> diffuses into the solution across the interface. The situation for solubility seems nevertheless satisfactory since, in a closed vessel, the limiting diffusion current remains sensibly constant when bubbling is interrupted for short times, and the diffusion currents (see below) decrease with increasing temperature.



## REFERENCES

- 1 B. LEVICH, *Physicochemical Hydrodynamics*, Prentice Hall Inc., Englewood Cliffs, N.J., 1962 p. 69.
  - 2 J. O'M. BOCKRIS, *Modern Aspects of Electrochemistry*, Vol. I, edited by J. O'M. BOCKRIS, Butterworths, London, 1954, ch. IV.
  - 3 V. S. BAGOTSKII AND YU. B. VASILEV, *Electrochim. Acta*, 9 (1964) 869.
  - 4 B. E. CONWAY, D. GILROY, N. MARINCIC AND E. RUDD, *Proceedings of a Symposium on Electrode Processes*, The Electrochemical Society, Cleveland, 1966.
  - 5 D. GILROY AND B. E. CONWAY, *J. Phys. Chem.*, 69 (1965) 1259; see also B. E. CONWAY, *Theory and Principles of Electrode Processes*, Ronald Press, New York, 1965.
  - 6 A. N. FRUMKIN, L. NEKRASOV, B. LEVICH AND YU. IVANOV, *J. Electroanal. Chem.*, 1 (1959/60) 84.
  - 7 M. P. BELYANCHIKOV, YU. V. PLESKOV AND B. G. POMINOV, *Russ. J. Phys. Chem. English Transl.*, 34 (1960) 782.
  - 8 A. N. FRUMKIN AND E. A. AJKAZJAN, *Izv. Akad. Nauk SSSR Otd. Khim. Nauk*, No. 2 (1959) 202.
  - 9 A. M. AZZAM, J. O'M. BOCKRIS, B. E. CONWAY AND H. ROSENBERG, *Trans. Faraday Soc.*, 46 (1950) 918.
  - 10 H. WROBLOWA, B. J. PIERSMA AND J. O'M. BOCKRIS, *J. Electroanal. Chem.*, 6 (1963) 401.
  - 11 N. IBL, paper presented at the C.I.T.C.E. meeting, Rome, Italy 1962.
  - 12 J. C. BAZAN AND A. J. ARVIA, *Electrochim. Acta*, 10 (1965) 1025.
  - 13 J. J. LINGANE AND I. M. KOLTHOFF, *J. Am. Chem. Soc.*, 61 (1939) 825.
  - 14 *International Critical Tables*, N.Y. and London, 1929, 3, pp. 24, 256.
  - 15 B. E. CONWAY, J. E. DESNOYERS AND A. C. SMITH, *Phil. Trans. Roy. Soc. (London)*, A256 (1964) 389.
  - 16 B. E. CONWAY, *Electrochemical Data*, Elsevier, Amsterdam, 1952, p. 90.
  - 17 *International Critical Tables*, N.Y. and London, 1929, 5, pp. 12, 63.
  - 18 G. P. LEWIS AND P. RUETSCHI, *J. Phys. Chem.*, 67 (1965) 65.
  - 19 K. F. BLURTON AND A. C. RIDDIFORD, *J. Electroanal. Chem.*, 10 (1965) 457.
- J. Electroanal. Chem.*, 13 (1967) 333-342

## A STUDY OF THE ADSORPTION OF CADMIUM(II) ON MERCURY FROM THIOCYANATE SOLUTIONS BY DOUBLE POTENTIAL-STEP CHRONOCOULOMETRY

FRED. C. ANSON\*, JOSEPH H. CHRISTIE, AND ROBERT A. OSTERYOUNG

*North American Aviation Science Center, Thousand Oaks, California (U.S.A.)*

(Received February 25th, 1966; in revised form, May 20th, 1966)

### INTRODUCTION

The earliest applications of the chronocoulometric method to the study of the adsorption of electroactive substances at electrodes<sup>1-3</sup> suffered somewhat from the lack of an exact double-layer charging correction in the presence of adsorption, but the new double potential-step chronocoulometric method<sup>4-6</sup> allows an internal measure of the true double-layer charging correction to be obtained.

The previous paper<sup>6</sup> presented the theoretical treatment of *double* potential-step chronocoulometry applied to the study of reactant adsorption. This paper considers the application of this technique to the study of the adsorption of Cd(II) at mercury electrodes from thiocyanate solutions.

The solutions contained Cd(II) in the millimolar concentration range, sodium thiocyanate at varying concentrations from 0-1 *F*, and sufficient sodium nitrate to maintain an ionic strength of unity. The potential was potentiostatically controlled and adjusted to an initial potential,  $E_i$ , sufficiently anodic of the half-wave potential that no current flowed. At time  $t = 0$ , the potential was stepped to a value  $E_t$ , sufficiently cathodic of  $E_{\frac{1}{2}}$  that the concentration of Cd(II) at the electrode surface was instantaneously reduced to zero. After a time,  $\tau$ , the potential was stepped back to  $E_i$  which was sufficiently anodic that for  $t > \tau$ , the surface concentration of Cd(Hg) was zero. The measured parameter was  $Q$ , the total charge passed as a function of time.

### RESULTS AND DISCUSSION

In the absence of adsorption of either the reactants or products, the  $Q-t$  behavior that results when the double potential-step is applied is<sup>6</sup>

$$Q(t \leq \tau) = 2nFA * C_0 \sqrt{\frac{D_0 t}{\pi}} + Q_{dl} \quad (1)$$

$$Q_r = Q(\tau) - Q(t > \tau) = 2nFA * C_0 \sqrt{\frac{D_0}{\pi}} \Theta + Q_{dl} \quad (2)$$

where  $Q_{dl}$  is the charge consumed by the electrode-electrolyte double-layer capaci-

\* Permanent address: Division of Chemistry and Chemical Engineering, California Institute of Technology, Pasadena, California.

tance when the potential is changed from  $E_1$  to  $E_2$ ;  $Q$  is the charge that has passed at time  $t \leq \tau$ ,  $Q_r$  is the charge that passes in the opposite direction for  $t > \tau$ ,

$$\Theta = \tau^{\frac{1}{2}} + (t - \tau)^{\frac{1}{2}} - t^{\frac{1}{2}} \quad (3)$$

\* $C_0$  is the bulk concentration of the species  $O$ , and  $n$ ,  $F$ ,  $A$  and  $D_0$  have their usual significance. It has previously been pointed out<sup>4</sup> that, in the absence of reactant or product adsorption, plots of  $Q(t \leq \tau)$  vs.  $t^{\frac{1}{2}}$  and  $-Q_r$  vs.  $\Theta$  on the same graph give straight lines of equal and opposite slopes and equal  $Q$ -axis intercepts corresponding to  $Q_{dl}$ . This is the behavior that would be expected for the double potential-step

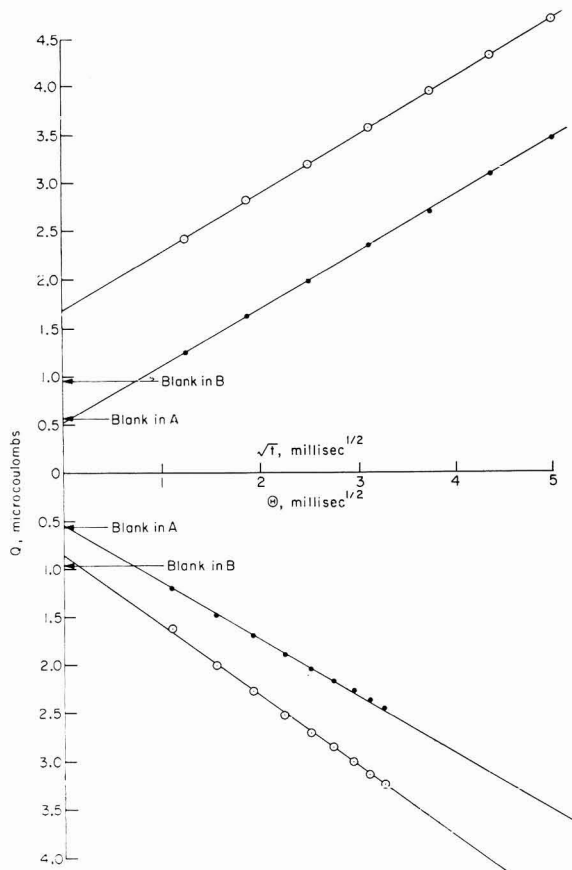


Fig. 1.  $Q$  vs.  $t^{\frac{1}{2}}$  and  $\Theta$  for double potential step from  $-200$  to  $-900$  to  $-200$  mV vs. S.C.E. A (●),  $1$  mM Cd(II) in  $1$  F NaNO<sub>3</sub>; B (○),  $1$  mM Cd(II) in  $0.2$  F NaSCN +  $0.8$  F NaNO<sub>3</sub>. Points labelled Blank in A and B refer to coulombs required to charge the double layer determined in the Cd-free base solns.

chronocoulometry of Cd(II) in a medium (e.g.,  $1$  F NaNO<sub>3</sub>) from which Cd(II) is not adsorbed.

The two lines labelled A in Fig. 1 are the  $Q-t^{\frac{1}{2}}$  and  $Q_r-\Theta$  plots for  $1.0$  mM Cd(II) in  $1$  F NaNO<sub>3</sub>. The equality of the intercepts ( $0.54$  and  $0.55$   $\mu$ C) and slopes ( $0.58$  and  $0.58$   $\mu$ C/msec<sup>1/2</sup>) demonstrates that Cd(II) is not adsorbed from this solution.



The value of the diffusion coefficient for Cd(II) calculated from the slope of the plots is  $6.7 \times 10^{-6}$  cm<sup>2</sup>/sec which agrees well with the polarographically-measured value ( $6.2 \times 10^{-6}$  cm<sup>2</sup>/sec).

If Cd(II) is adsorbed, a plot of  $Q(t < \tau)$  vs.  $t^{\frac{1}{2}}$  should have an intercept on the  $Q$ -axis corresponding to the charge required to charge the double layer plus the charge required to reduce the initially adsorbed Cd(II). Thus the expected effect of reactant adsorption is to increase the  $Q$ -axis intercept. The slope of  $Q-t^{\frac{1}{2}}$  plots should remain unchanged. The equation for the  $Q-t^{\frac{1}{2}}$  behavior in the presence of adsorption is<sup>6</sup>

$$Q(t \leq \tau) = 2nFA * C_0 \sqrt{\frac{D_0 t}{\pi}} + nFAG_0 + Q_{d1} \tag{4}$$

where  $G_0$  is the amount of reactant initially adsorbed in moles/cm<sup>2</sup>. The  $Q_r$  vs.  $\Theta$  plot is more seriously affected by adsorption because the concentration profile of the cadmium amalgam that results when the adsorbed cadmium ion is reduced, differs from the profile that corresponds to eqn. (2).

It was shown in the preceding paper<sup>6</sup> that under these conditions  $Q_r$  may be well approximated by a linear function of  $\Theta$ :

$$Q_r = 2nFA * C_0 \sqrt{\frac{D_0}{\pi}} \left[ 1 + \frac{a_1 nFAG_0}{Q_c} \right] \Theta + a_0 nFAG_0 + Q_{d1} \tag{5}$$

where  $Q_c$  is the charge arising from reduction of diffusing reactant during the first potential step ( $t \leq \tau$ ),

$$Q_c = 2nFA * C_0 \sqrt{\frac{D_0 \tau}{\pi}}$$

The values of  $a_1$  and  $a_0$  are about unity and zero, respectively. Their exact values are calculated from the particular experimental measurement times in the way already described<sup>6</sup>; for the experimental times used in the present experiments,  $a_1 = 0.97$  and  $a_0 = -0.069$ .

According to eqn. (5), the slope of the  $Q_r$  vs.  $\Theta$  plot is  $1 + a_1 nFAG_0/Q_c$  times as great in the presence of adsorption and the  $Q$ -axis intercept is smaller than  $Q_{d1}$  by an amount,  $a_0 nFAG_0$ . In order to measure  $G_0$  as accurately as possible, it is advantageous to choose  $\tau$  so that the ratio  $nFAG_0/Q_c$  is not too small.

The  $Q_{d1}$ -terms in eqns. (4) and (5) represent the change in charge in the double layer in the presence of adsorbed Cd(II). Note that the intercept of the  $Q_r-\Theta$  plot is, except for the small correction,  $a_0 nFAG_0$ , the proper double-layer blank. The true  $Q_{d1}$  may be calculated from the intercepts of the  $Q-t^{\frac{1}{2}}$  and  $Q_r-\Theta$  plots:

$$Q_{d1} = \frac{{}^0Q_r - a_0 {}^0Q}{1 - a_0} \tag{6}$$

where  ${}^0Q$  and  ${}^0Q_r$  are the  $Q$ -axis intercepts of the  $Q-t^{\frac{1}{2}}$  and  $Q_r-\Theta$  plots, respectively.

It is this feature of double potential-step chronocoulometry that makes it particularly useful for studying adsorbed reactants; the double-layer "blank" comes directly out of the experiment—it is not necessary to use the less reliable blank measured in supporting electrolyte free of reactant.

The amount of adsorbed cadmium can be determined from the intercepts of the  $Q-t^{\frac{1}{2}}$  and  $Q_r-\Theta$  plots:

$$nFA\Gamma_0 = \frac{^{\circ}Q - ^{\circ}Q_r}{1 - a_0} \quad (7)$$

It also follows from eqns. (4) and (5) that

$$\frac{S_r}{S_f} = 1 + \frac{a_1 nFA\Gamma_0}{Q_c} \quad (8)$$

where  $S_r$  and  $S_f$  are the slopes of the  $Q_r - \Theta$  and  $Q - t^{\frac{1}{2}}$  plots, respectively. This relationship may be used to check the internal consistency of the results.

The two lines labelled B in Fig. 1 are the  $Q - t^{\frac{1}{2}}$  and  $Q_r - \Theta$  plots for 1.0 mF Cd(II) in 0.8 F NaNO<sub>3</sub>-0.2 F NaSCN. Note that the slopes and intercepts of the two lines are no longer equal—specific adsorption of the cadmium has been produced by the addition of the thiocyanate. Although the two  $Q - t^{\frac{1}{2}}$  plots (A and B) have different intercepts, their slopes are about the same (0.58 vs. 0.60  $\mu\text{C}/\text{msec}^{\frac{1}{2}}$ ) as expected from eqns. (1) and (4) ( $D_0$  is no doubt somewhat different in the presence of SCN<sup>-</sup>). The value of  $\Gamma_0$  resulting from the B-plots in Fig. 1 is

$$nF\Gamma_0 = \frac{1}{A} \left( \frac{^{\circ}Q - ^{\circ}Q_r}{1 + 0.069} \right) = \frac{1}{0.032} \left( \frac{1.67 - 0.86}{1.069} \right) = 23.7 \mu\text{C}/\text{cm}^2.$$

The value of  $nF\Gamma_0$  obtained from the B-plots in Fig. 1, 23.7  $\mu\text{C}/\text{cm}^2$ , places a lower limit on the time after  $\tau$  at which useful data points may be taken, because this amount of cadmium ion must have been generated at the electrode surface or have diffused there from the solution in order for adsorption equilibrium at  $E_1$  to have been re-established. For the condition of Fig. 1 we calculate (eqns. (4) and (5) and much effort or Fig. 1, geometry, and less effort!) that this condition was achieved by the time  $\Theta$  reached about 0.7 msec <sup>$\frac{1}{2}$</sup>  ( $t = \tau + 0.6$  msec).

The points indicated as blanks in Fig. 1 were obtained by determining the step change in charge for a potential step between -200 and -900 mV in a 1 F NaNO<sub>3</sub> solution and for a solution 0.2 F NaSCN + 0.8 F NaNO<sub>3</sub>. In 1 F NaNO<sub>3</sub>, the blank agrees with the intercepts of both the  $Q - t^{\frac{1}{2}}$  and  $Q_r - \Theta$  plots. In the thiocyanate solution, there appears to be little change in the coulombs required to charge the double

TABLE 1

CHARGE ON EXTRUDED Hg DROPS IN 0.5 F NaSCN-0.5 F NaNO<sub>3</sub>

$E$ (mV vs. SCE)	[Cd(II)] (mF)				
	0	0.5	1.0	2.0	10
	$Q$ ( $\mu\text{C}/0.032 \text{ cm}^2$ change in area)				
-200	0.69	0.73	0.69	0.73	0.72
-300	0.43	0.48	0.47	0.54	0.52
-400	0.39	0.38	0.32	0.40	0.40

layer whether or not Cd(II) is present. This can be inferred from the fact that a blank in a pure thiocyanate solution is the same as the anodic intercept of the  $Q_r - \Theta$  plot for the thiocyanate solution containing cadmium, within experimental error. Thus, the electrical charge on the drop in the thiocyanate solution is unaffected by the presence of adsorbed cadmium. To check this point further, mercury-drop extrusion experi-

ments<sup>4</sup> were carried out. Data are presented in Table I. Within the experimental error of about  $\pm 0.05 \mu\text{C}/\text{drop}$ , the charge is seen to be independent of the cadmium ion in solution, in spite of the presence of adsorbed cadmium demonstrated by the chronocoulometric experiments for the same solutions. The electronic charge on the electrode thus appears to be determined by the amount of specifically adsorbed thiocyanate and the additional adsorption of cadmium ion produces too small a change in the net charge on the electrode, to be measured.

*Dependence of  $\Gamma_0$  on Cd(II) concentration*

A convenient way to present the data is as plots of  $Q^*$  vs.  $t^{1/2}$  where the  $Q^*$ 's are the measured values of  $Q$  during the cathodic step minus  $Q_{dl}$  (cf. eqn. (6)). The inter-

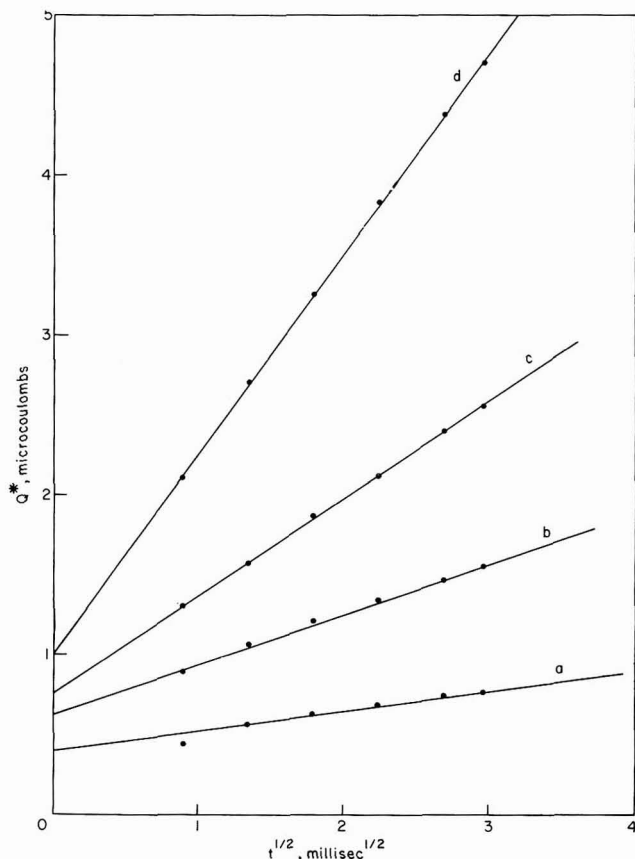


Fig. 2.  $Q^*$  vs.  $t^{1/2}$  for varying concns. of Cd(II) in 0.5 F NaSCN + 0.5 F NaNO<sub>3</sub>. [Cd(II)]: (a), 0.2; (b), 0.5; (c), 1.0; (d), 2.0 mF.

cepts of such plots are the values of  $nF\Gamma_0$ . Figure 2 contains a series of such plots at several Cd(II) concentrations for a constant supporting electrolyte composition of 0.5 F NaNO<sub>3</sub> + 0.5 F NaSCN. The increase in intercept with the Cd(II) concentration reflects the increasing adsorption of Cd(II). The slopes of the plots in Fig. 2 are



proportional to the Cd(II) concentrations as expected (the ratio of slope to concentration for the four curves is 18.7, 19.2, 18.8 and 19.3  $\mu\text{C}/\text{msec}^{1/2} \text{cm}^2 \text{mF}$ ).

#### Dependence of $\Gamma_0$ on thiocyanate concentration

A typical set of  $Q^*$  vs.  $t^{1/2}$  plots for 0.5 mF Cd(II) in various thiocyanate supporting electrolytes is presented in Fig. 3. The intercept reaches a maximum at a thiocyanate concentration of 0.2 F and then decreases with further increases in the thiocyanate concentration. Figure 4 shows the dependence of the intercepts on the concentration of thiocyanate.

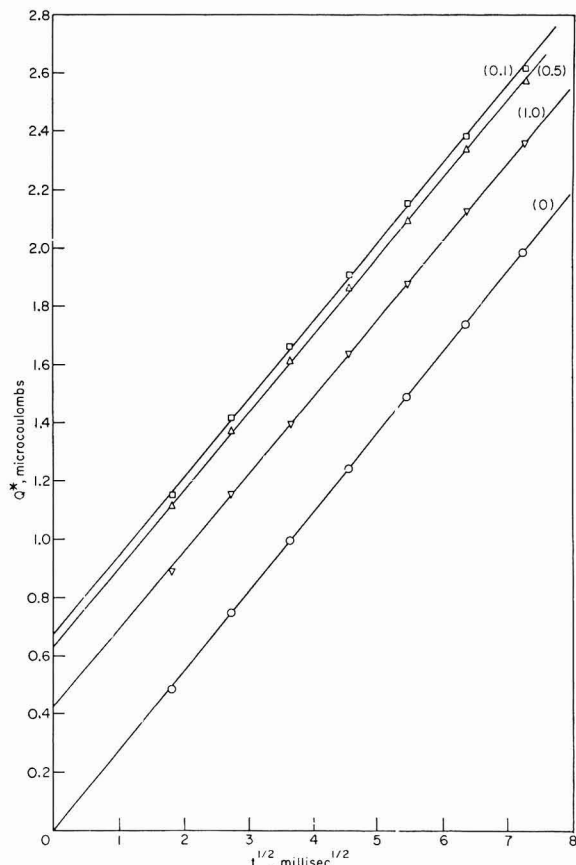


Fig. 3.  $Q^*$  vs.  $t^{1/2}$  for 0.5 mF Cd(II) in varying concns. of thiocyanate. Ionic strength maintained at 1 with  $\text{NaNO}_3$ ; the concentrations of thiocyanate are indicated.

#### Dependence of $\Gamma_0$ on potential

Figure 5 shows plots of  $Q^*$  for three different initial potentials,  $E_i$ . The intercepts increase as the electrode potential becomes more positive. The plots in Fig. 5 do not change if  $E_i$  is changed from  $-0.70$  to  $-1.00$  V vs. S.C.E. This is the expected result, since this potential range is within the diffusion plateau of the corresponding Cd(II) polarogram.

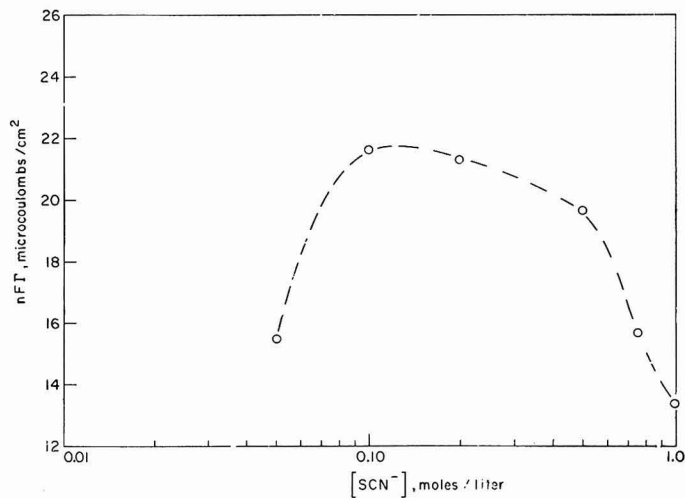


Fig. 4. Dependence of Cd(II) adsorption on the concn. of thiocyanate (potential step, -200 to -900 mV). 0.5 mF Cd(II), ionic strength maintained at 1 with NaNO<sub>3</sub>.

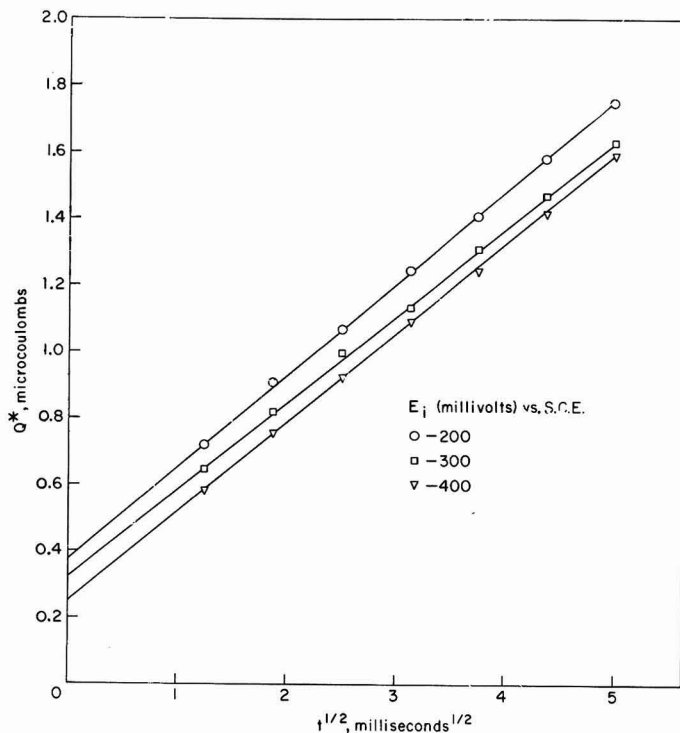


Fig. 5.  $Q^*$  vs.  $t^{1/2}$  for 0.5 mF Cd(II) in 1 F NaSCN. Potential steps are from initial values indicated on the figure to -900 mV and back to the initial potential.

TABLE 2  
CALCULATED AND OBSERVED VALUES OF RATIOS OF SLOPES FOR  $Q_c-t^{\frac{1}{2}}$  AND  $Q_p-t^{\frac{1}{2}}$  PLOTS

$(mF)$ [Cd(II)]	$E_t$						
	-200	-300	-400	-200	-300	-400	
	$Q_c(\mu C/cm^2)$	16.2	16.2	8.3	5.1	3.3	
0.2		17.0	16.2	8.3	5.1	3.3	
		41.3	40.1	12.7	10.1	8.0	
0.5		41.3	40.1	12.7	10.1	8.0	
		84.1	82.6	15.6	14.1	10.1	
1.0		84.1	82.6	15.6	14.1	10.1	
	$nFT_0(\mu C/cm^2)$						
		1.47	1.3	1.2	1.2	1.2	
	$(S_T/S_T)_{\text{estd.}}$	1.47	1.3	1.2	1.2	1.2	
	$(S_T/S_T)_{\text{obs.}}$	1.51	1.30	1.31	1.25	1.19	
		1.19	1.17	1.11	1.17	1.17	

TABLE 3  
DATA SUMMARY FOR ADSORPTION OF Cd(II) FROM THIOCYANATE SOLUTIONS  
 $nFT_0$ ,  $\mu C/cm^2$ . Potential steps from -200, -300 or -400 to -900 mV vs. S.C.E.

[SCN <sup>-</sup> ]	$E_t$					
	-200	-300	-400	-200	-300	-400
	0.05 F	0.1 F	0.2 F	0.5 F	0.75 F	1.0 F
	$[Cd(II)]$ (mF)					
0.2	~0	~0	~0	12.1	10.8	9.4
	13.9	11.2	5.8	18.4	14.2	9.8
0.5	21.2	17.1	9.3	24.4	16.1	13.4
1.0	21.2	17.1	9.3	24.4	16.1	13.4

### Adsorption isotherm

Figure 6 contains plots of  $nFT_0$  vs. Cd(II) concentration for three starting potentials. No data are reported for cadmium concentrations greater than 2 mF because above this concentration the uncompensated resistance present in the cell seriously degrades the effective response time of the potentiostat, introducing major errors. This problem and its partial solution have been discussed elsewhere<sup>8,9</sup>.

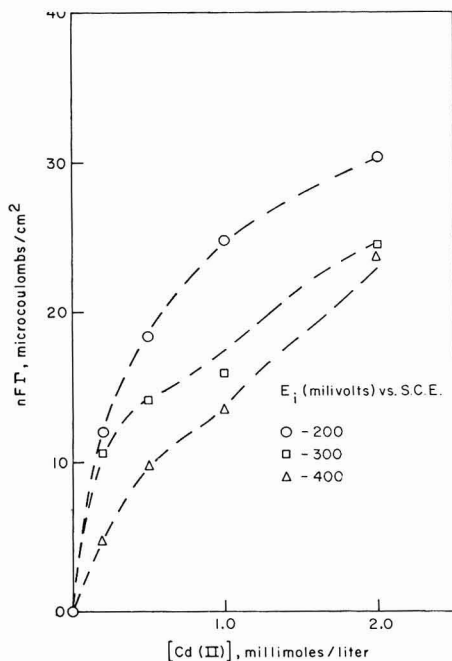
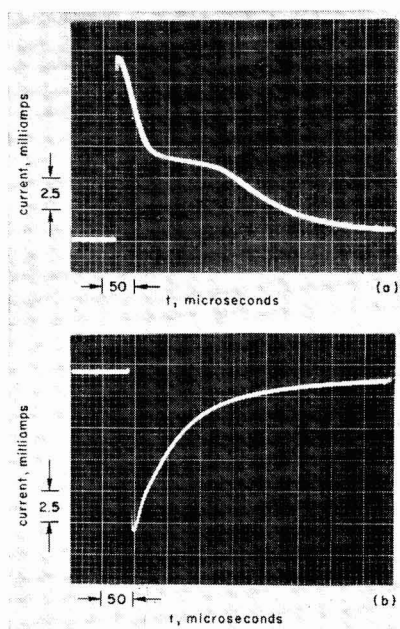


Fig. 6.  $nFT_0$  vs. [Cd(II)] for three initial potentials. Soln. is 0.5 F NaSCN + 0.5 F NaNO<sub>3</sub>.

Fig. 7. Current-time transients for (a) cathodic and (b) anodic portion of double potential-step from -200 to -900 to -200 mV vs. S.C.E. Solution is 1 mF in Cd(II) and 0.5 F NaSCN + 0.5 F NaNO<sub>3</sub>. Hanging mercury drop electrode area, 0.032 cm<sup>2</sup>.



### Internal consistency of the data

Table 2 shows examples of the calculated and observed values for ratios of the slopes of the  $Q-t^{1/2}$  and  $Q_r-\Theta$  plots in 1 F NaSCN. The calculated ratios were obtained from eqn. (8). The agreement between theory and experiment was quite good at all thiocyanate concentrations and helps to convince us of the soundness of the approach.

### Morphology of current-time transients

Figure 7 is typical of the initial portion of the current-time transients that result when a double potential-step is applied to a Cd(II) solution in the presence of sufficient thiocyanate to produce detectable Cd(II) adsorption. The unexpected "shoulder" on the cathodic transient in Fig. 7 was not observed in thiocyanate-free sodium nitrate supporting electrolytes. In these solutions, smooth current-time traces were observed for both anodic and cathodic steps, similar to the anodic trace in Fig. 7.



We believe that the abnormal shape of the cathodic current-time transients results from the presence of adsorbed Cd(II) and some unavoidable uncompensated resistance<sup>7,8</sup> in the electrolysis cell. The large current that flows initially to charge the double layer and reduce the adsorbed reactant, produces an ohmic drop across this uncompensated resistance that is large enough to keep the *actual* electrode potential from reaching the desired value (on the diffusion-limited plateau of the Cd(II) polarogram) until the large current transient has decayed substantially. Application of an electronic feed-back technique<sup>7</sup> which decreases the effective uncompensated resistance, results in an increase in the magnitude of the current on the "shoulder" together with a decrease in the length of time that the "shoulder" is visible. Thus, the "shoulder" arises from reactant adsorption, which in turn, gives rise to departure of the electrode reaction from pure diffusion control for the first 10–50  $\mu$ sec. This effect and its consequences have been discussed in greater detail elsewhere<sup>7</sup>.

The theoretical model used to derive eqn. 5 assumed that the excess of Cd(Hg) produced from reduction of the adsorbed Cd(II) is formed as a sharp concentration "spike". The observed current transient (Fig. 7) indicates that this "spike" is broadened by the effect of the uncompensated resistance. However, on the time scales used, the "spike" was still sharp enough to satisfy the assumptions used in the derivation.

#### CONCLUSIONS

The noteworthy points are the uniform potential dependence of the adsorption and the fact that maximum adsorption is reached at an intermediate thiocyanate concentration. The effect of changes in  $E_1$  on the adsorption of Cd(II) is in the direction to be expected if the adsorption of Cd(II) occurs by bonding with the already specifically adsorbed thiocyanate. Although a number of possibilities suggest themselves as candidates for the adsorbed species, calculations of the concentrations of the cadmium-thiocyanate complexes from the equilibrium constants did not lead to clear-cut correspondences with the amounts of adsorbed Cd(II). It seems to us fruitless to speculate further on the basis of the data presently available. Chronocoulometric studies of the adsorption of zinc and lead, which form analogous thiocyanate complexes, are under way in an effort to acquire enough data to justify generalizations about the fundamental processes involved.

The data in Table 3 demonstrate the power of the double potential-step chronocoulometric procedure to provide rather precise measurements of the quantity of adsorbed reactant at values well below the double-layer charge. No arbitrary model of the electrode reaction sequences is required in order to interpret the data, and an altogether appropriate double-layer charging "blank" is provided by the technique. The combination of these advantages convinces us that the double potential-step chronocoulometric technique is probably the best faradaic method presently available for studying adsorbed reactants.

#### EXPERIMENTAL

The electronic apparatus and multichannel analyzer data acquisition system used are described in detail elsewhere<sup>9</sup>. The basic circuitry was similar to that already described<sup>2,5</sup>. The potentiostat was a Wenking fast-rise model, having a rise

time of about  $2 \mu\text{sec}$ . The current-measuring and integrating amplifiers were Philbrick SP 656 operational amplifiers. The experiments were arranged so that the second potential step always occurred at a particular channel on the multichannel analyzer. This had the effect of maintaining the ratio  $\Theta/\tau$  constant, independent of the conversion factor relating channel number to real time. Thus, the correction terms,  $a_1$  and  $a_0$ , were the same for all experiments (see eqn. (20), ref. 6) and were equal to 0.97 and  $-0.069$ , respectively.

Solutions were prepared from reagent-grade materials using triple-distilled water. Stock solutions of 20 mF cadmium nitrate, 2 F NaSCN and 2 F NaNO<sub>3</sub> were prepared and the test solutions were prepared by appropriate dilution. A commercially-available hanging mercury drop electrode was used (Brinkmann Instruments, Inc.). The area of the hanging mercury drop was 0.032 cm<sup>2</sup> (determined by direct weighing).

All potentials are in millivolts *vs.* the S.C.E.

#### ACKNOWLEDGEMENTS

The advice and assistance of GEORGE LAUER with certain experimental problems and the aid of JOHN COOPER in preparing an almost endless number of solutions are appreciated.

#### SUMMARY

The adsorption of Cd(II) in thiocyanate solutions has been studied by a double potential-step chronocoulometric method. The amount of Cd(II) adsorbed decreases as the electrode potential is made increasingly cathodic. The amount of adsorbed Cd(II) was also studied as a function of the concentration of thiocyanate. The double potential-step chronocoulometric method permits an accurate double-layer capacity correction and appears to be the best faradaic method for the determination of adsorbed reactant.

#### REFERENCES

- 1 F. C. ANSON, *Anal. Chem.*, 36 (1964) 932.
- 2 J. H. CHRISTIE, G. LAUER AND R. A. OSTERYOUNG, *J. Electroanal. Chem.*, 7 (1964) 60.
- 3 R. A. OSTERYOUNG AND F. C. ANSON, *Anal. Chem.*, 36 (1964) 975.
- 4 F. C. ANSON, *Anal. Chem.*, 38 (1966) 54.
- 5 F. C. ANSON AND D. A. PAYNE, *J. Electroanal. Chem.*, 13 (1967) 35.
- 6 J. H. CHRISTIE, R. A. OSTERYOUNG AND F. C. ANSON, *J. Electroanal. Chem.*, 13 (1967) 236.
- 7 G. LAUER AND R. A. OSTERYOUNG, *Anal. Chem.*, 38 (1966) 1106.
- 8 K. B. OLDHAM, *J. Electroanal. Chem.*, 11 (1966) 171.
- 9 G. LAUER AND R. A. OSTERYOUNG, *Anal. Chem.*, 38 (1966) 1137.

## THE CHRONOPOTENTIOMETRIC DETERMINATION OF TRANSPORT NUMBERS

J. BROADHEAD AND G. J. HILLS

*Department of Chemistry, The University, Southampton, Hampshire (England)*

(Received March 26th, 1966; in revised form, May 5th, 1966)

## INTRODUCTION

Controlled electrolyses at a micro-electrode have almost invariably been carried out in the presence of excess supporting electrolyte. This major component serves three purposes, (i) the minimisation of ohmic overpotential by reduction of the cell resistance, (ii) the suppression of the migration current to simplify the theoretical interpretation of results, (iii) the stabilisation of the double-layer capacity, which in 0.1 *M* KCl, for example, is insensitive to the presence of minor constituents and to quite large voltage excursions.

The addition of supporting electrolyte also has a number of disadvantages. It often involves the simultaneous addition of electro-active trace impurities. It also incurs an additional uncertainty in the interpretation of results because of the inevitable involvement of its ions in the surface reaction, in interionic attraction etc. and it is normally not possible to extrapolate the measurements to a state of thermodynamic ideality. Nevertheless, under favourable circumstances, mass-transfer controlled electrolyses can be described for systems both with and without supporting electrolyte. In the latter case, the superposition of the potential gradient on the diffusive or osmotic force is appropriately related to the transport number of the consumable ion which can thus be evaluated for suitable boundary conditions. This is particularly true for the chronopotentiometric method and it is the purpose of this paper to explore the reliability and sensitivity of this method for the determination of transport numbers in aqueous and non-aqueous systems.

Chronopotentiometry is invariably traced back to SAND<sup>1</sup>. He was the first to note the enhancement of the transition time in the absence of supporting electrolyte, and to relate it to the transport number of the reducible ions.

Several other, less satisfactory investigations followed<sup>2-4</sup> and although both EUCKEN<sup>2</sup> and SLENDYK<sup>3</sup> made voltammetric measurements in the absence of supporting electrolyte, they failed to incorporate transport numbers into their theoretical interpretations. MACGILLAVRY<sup>5</sup> and KOLTHOFF AND LINGANE<sup>6</sup> drew attention to the fact that in the polarography of solutions containing no supporting electrolyte, the relevant diffusion coefficient is that of the salt and not that of the ion. LAITINEN<sup>7</sup>, using a chronoamperometric method, and DELAHAY, MATTAX AND BERZINS<sup>8</sup>, MORRIS AND LINGANE<sup>9</sup>, MORRIS<sup>10</sup> and BRO<sup>11</sup>, using chronopotentiometric procedures, all introduce transport numbers into their theoretical treatments.

Within a more general context, mass transfer in a combination of concentration and potential gradients has been considered in terms of irreversible thermodyna-

mics by BEARMAN<sup>13</sup>, and by LOPUSHANSKAYA, PAMFILOV AND TSISAR<sup>14</sup>. LAITY<sup>12</sup> has been particularly concerned to delineate in this way the diffusion coefficients obtained from chronopotentiometric measurements and MILLS<sup>15</sup> has recently reviewed the whole field. Even so, a recent experimental paper<sup>16</sup>, concerned with the measurement of diffusion currents at zero concentration of supporting electrolyte, apparently overlooks the migration current and the consequential distinction between ionic and salt diffusion coefficients.

In all the work referred to above, the object has been to eliminate the transport term, whereas here the object is to isolate and to determine the transport numbers of the constituent ions of a single electrolyte by *single-salt* chronopotentiometry. Since this work was completed, a paper by EMEL'YANENKO AND SIMULIN<sup>17</sup> has been published with the same aim, but it is a limited study of the problem which again overlooks the important distinction between salt- and ion-diffusion coefficients. This paper is further discussed below.

#### THEORETICAL RELATIONSHIPS

The relationship between current density, salt concentration and transition time has been reported previously in terms of linear diffusion. Since the experimental work here uses a small mercury drop, the essential equations have been re-derived for spherical diffusion and the limitations under which the effects of sphericity may be neglected, are stated.

The description of migration and diffusion in a spherically symmetrical potential gradient is given in detail elsewhere<sup>18</sup> and will only be outlined here. The primary assumption is made that the velocity,  $v_i$ , of a charged particle or ion in a solution is proportional to the force,  $X_i$ , exerted upon it<sup>19</sup>, *i.e.*,

$$v_i = h_i X_i \quad (1)$$

According to KIES<sup>20</sup>, if we consider  $X_i$  as the negative gradient of the electrochemical potential, relate the constant of proportionality  $u_i$  in eqn. (1) to the mobility of the ionic species, and hence to the diffusion coefficient of the ion, then the number of  $g$ -ions,  $dN_i$ , passing through the cross-sectional area,  $A$ , at a distance,  $x$ , from the electrode in the increment of time,  $dt$ , is given by:

$$x \left( \frac{\partial N_i}{\partial t} \right) = -AD_i \left( \text{grad } c_i + \frac{z_i F c_i}{RT} \text{ grad } V \right) \text{ mole sec}^{-1} \text{ cm}^{-2} \quad (2)$$

where  $D_i$  is the ionic diffusion coefficient,  $\text{grad } c_i$  is the concentration gradient,  $z_i$  is the valence or charge number,  $F$  the faraday,  $R$  the gas constant,  $T$  the absolute temperature and  $\text{grad } V$  the electric potential gradient.

From eqn. (2) it is possible to set up the time- and distance-dependent spherical diffusion equations analogous to those of MORRIS AND LINGANE<sup>9</sup> which describe linear diffusion. The solution of these equations<sup>8</sup> with the well-known chronopotentiometric boundary conditions is:

$$c_+(r,t) = c_+ - \frac{ir_0}{nFD_+ \left( \frac{1-z_+}{z_-} \right)} \left\{ 1 - \exp \left( \frac{D_s t}{r_0^2} \right) \text{erfc} \left[ \frac{(D_s t)^{\frac{1}{2}}}{r_0} \right] \right\} \quad (3)$$

where  $i$  is the current density and  $r_0$  is the radius of the spherical cathode.

This is the basic equation for single-salt chronopotentiometry at a spherical electrode. The transition time,  $\tau$ , is defined by  $c_{+(r_0, \tau)} = 0$  and when  $\tau$  is very small,  $D_s \tau / r_0^2 \ll 1$ , then

$$\exp(D_s \tau / r_0^2) \rightarrow 1 \quad (4)$$

and

$$\operatorname{erfc} \left[ \frac{(D_s \tau)^{\frac{1}{2}}}{r_0} \right] \rightarrow 1 - \left( \frac{2D_s^{\frac{1}{2}} \tau^{\frac{1}{2}}}{\pi^{\frac{1}{2}} r_0} \right) \quad (5)$$

By incorporation of approximations (4) and (5) in eqn. (3) together with progressive elimination of diffusion coefficients in terms of the Nernst–Einstein equation, we obtain the expression for single-salt chronopotentiometry

$$c_+ = \frac{2i \tau^{\frac{1}{2}}}{\pi^{\frac{1}{2}} n F D_s^{\frac{1}{2}}} t_- \quad (6)$$

where  $t_-$  is the anionic transport number ( $= 1 - t_+$ ).

$D_s$  can also be eliminated in a similar way, since

$$D_s = \frac{RT}{F^2} \left( \frac{\lambda_+ \lambda_-}{\lambda_- + \lambda_+} \right) \left( \frac{1}{z_+} - \frac{1}{z_-} \right) \quad (7)$$

$$= \frac{RT}{F^2} (t_+ t_- \Lambda) \left( \frac{1}{z_+} - \frac{1}{z_-} \right) \quad (8)$$

Squaring both sides of eqn. (6) and substituting for  $D_s$  then gives

$$c_+^2 = \frac{4i^2 \tau t_- (z_+ z_-)}{\pi n^2 RT t_+ \Lambda (z_+ - z_-)} \quad (9)$$

For a (1:1) electrolyte,

$$\frac{z_+ z_-}{z_+ - z_-} = \frac{1}{2}$$

and eqn. (9) may then be simplified and rearranged to

$$\frac{t_+}{1 - t_+} = \frac{2i^2 \tau}{RT \pi \Lambda c_+^2} \quad (10)$$

This equation is valid in so far as the Nernst–Einstein relation is applicable. It is likely to be valid for the low concentrations used in this type of experiment and it is certainly not a major source of error. Any residual uncertainty could be eliminated by extrapolation to infinite dilution where the Nernst–Einstein relation is strictly true. Under these circumstances,

$$\frac{t_+^0}{1 - t_+^0} = \frac{2}{RT \pi \Lambda_0} \left( \frac{i^2 \tau}{c_+^2} \right)_{c_+ \rightarrow 0} \quad (11)$$

and thus the transport numbers may be exactly obtained from the limiting slope of  $i^2 \tau$  vs.  $c_+^2$ .

#### EXPERIMENTAL

A series of chronopotentiograms was recorded at a hanging mercury drop of the

GERISCHER<sup>22</sup>-type. An apparatus was therefore required that would furnish a succession of mercury drops of known area and that would exclude spent mercury from subsequent reaction. Since the solutions to be used were dilute, it was necessary to exclude all traces of oxygen and other electro-reducible impurities. Moreover, since the mercury electrode was a stationary drop and perhaps in use for several minutes, it was also essential to exclude all traces of surface-active material.

#### *Apparatus and reagents*

The cell used (Fig. 1(a)) was adapted from a 500-ml flask. The electrodes were introduced and manipulated through ground-glass joints and syringe barrels. A

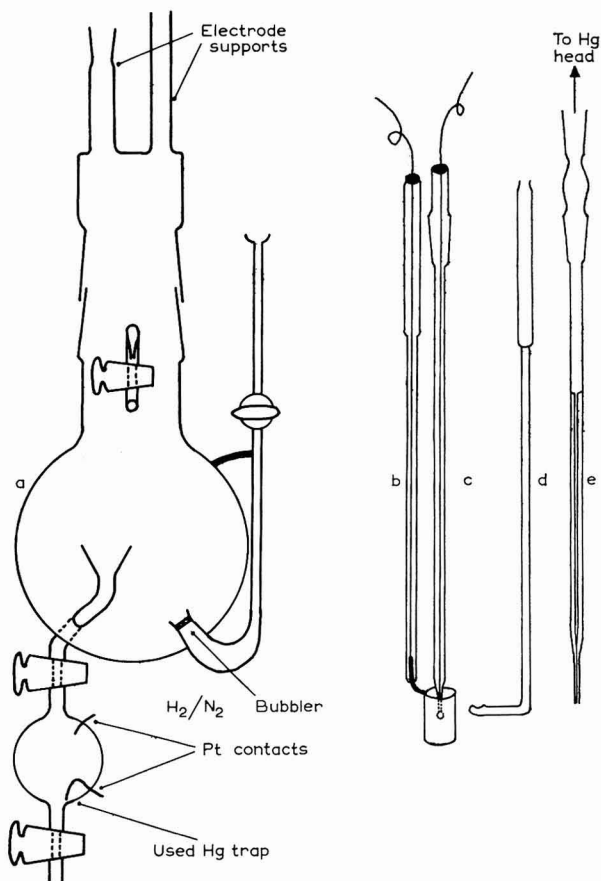


Fig. 1. Cell and electrodes: (a), cell; (b), cylindrical platinum anode; (c), mercury drop suspension; (d), spoon; (e), mercury capillary.

purified mixture of 75% hydrogen and 25% nitrogen introduced through a sintered-glass disc was used to deoxygenate the cell solution. A funnel, tap and 25-ml vessel assembly were sealed through the cell wall below the capillary to remove used and redundant mercury drops from the vicinity of the electrodes. Although two platinum wire contacts were also incorporated in the used mercury container to maintain

the pool at a small cathodic overpotential, they were found to be unnecessary since there was always a separation of the mercury from the main cell solution by a pocket of deoxygenating gas trapped below the upper tap.

The suspension for the hanging mercury drop electrode, Fig. 1(c), was constructed by sealing 0.2-mm diam. platinum wire into a soda-glass sheath of 0.4 mm external diam. When the tip had been carefully ground down and plated with mercury, successive mercury drops could be transferred to it by a glass spoon, Fig. 1(d), from under the capillary, Fig. 1(e). The anode, Fig. 1(b), was a platinum cylinder, 1 cm diam., 1-cm long, which could be raised to allow access to the indicator electrode. This electrode, in the presence of the partial pressure of hydrogen, was used both as the anode and as a stable, unpolarised reference for the working electrode. This arrangement had the advantages of simplicity, of avoiding the complications of distortion of the field symmetry around the micro-electrode (an important factor in dilute solutions) and of eliminating the possibility of ingress of foreign electrolyte from a salt bridge.

The temperature of the cell was controlled at  $25^{\circ} \pm 0.05^{\circ}$  by an air thermostat. The principal innovation of this thermostat was the inclusion of a simple but persistent source of cooling, in this case, a block of solid carbon dioxide. The filament heating then functioned normally and good control of temperature was readily maintained.

The constant current was supplied from a 120–300 V power pack placed in series with 1–10 M $\Omega$ , and the resulting chronopotentiograms were displayed on a D.C. Solarscope type AD557. Chronopotentiograms were recorded photographically (Polaroid camera type 405, using type-42 film) and the cell current was calculated from the p.d. across a standard 1000- $\Omega$  resistor in the constant-current circuit. A calibrated time base was supplied by an oscillator driving the intensity modulation of the oscilloscope to give time markers on each individual trace.

Analar reagents were used with the exception of "Specpure" TiCl (supplied by Johnson, Matthey, and Co., Ltd.) and TiClO<sub>4</sub> which had to be prepared. TiClO<sub>4</sub> was prepared<sup>23</sup> by neutralizing Ti<sub>2</sub>CO<sub>3</sub> with 60% A.R. HClO<sub>4</sub>, recrystallising three times from slightly acid solution and then drying for 8 h at 120–130°. All solutions were prepared from water redistilled from an alkaline solution of KMnO<sub>4</sub> through a 3-ft. "rod and disc" anti-splash column. N,N-dimethylformamide<sup>24</sup> (DMF) was dried for a week over 4A molecular sieves and then distilled under 5–10 mm of N<sub>2</sub> pressure. DMF so prepared had a density of 0.9440 g ml<sup>-1</sup> which was in good agreement with values reported by other workers (0.9439<sup>23</sup>, 0.9445<sup>25</sup>, 0.9442<sup>26</sup>, 0.9441<sup>27</sup>, 0.9443<sup>28</sup>). The 75% hydrogen–25% nitrogen deoxygenating mixture was passed over copper "flitters" maintained at 450°, over KOH pellets, through a liquid nitrogen trap, over 5A molecular sieves and finally through a pre-saturator. For the aqueous work, the gas was further deoxygenated by vanadous chloride solution<sup>29</sup>. Polarographic mercury was purified in the usual way<sup>30</sup>.

### *Procedure*

The glassware was cleaned in a boiling 10 : 1 mixture of perchloric and nitric acids<sup>31</sup>, rinsed with conductivity water and then steamed for 2 h. All solutions were made up by weight. The cell solution was deoxygenated and equilibrated to thermostat temperature over a period of 3 h. When the cell solution was at rest, a succession of mercury drops were caught and transferred to the cathode, a new drop being used for



each chronopotentiogram. The area of each mercury drop was calculated from the weight of a given number of mercury drops and a correction was made for the cross-sectional area of the wire that was used as the suspension.

#### RESULTS AND DISCUSSION

Typical chronopotentiograms of the two systems studied are shown in Fig. 2, (a) and (b); their shape calls for comment. Figure 2 (a) is a set of chronopotentiograms for a dilute aqueous solution of  $\text{TlCl}$  at one current density. The pre- and post-transition portions of the traces are different from those of classical chronopotentiograms. From the rest potential, the section of the trace corresponding to the charging of the double layer has a very steep slope. This is in accord with the lower interfacial capacity to be expected in the absence of supporting electrolyte; it may also be influenced by a greater degree of adsorption of surface-active materials.

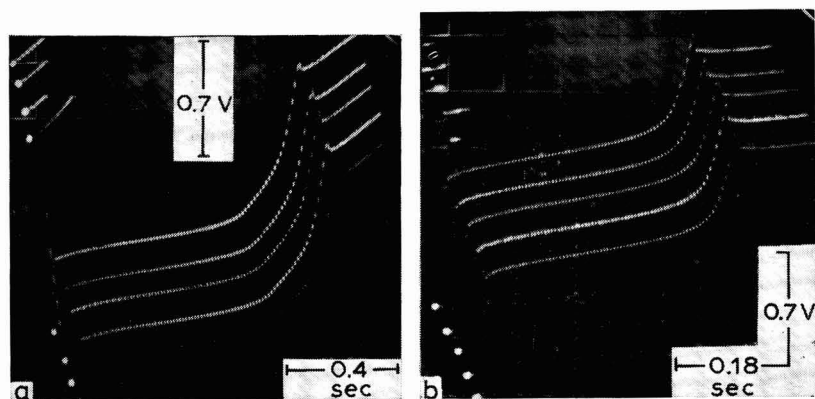


Fig. 2. Chronopotentiograms of: (a), 0.891 mM aq.  $\text{TlCl}$  at  $0.833 \text{ mA cm}^{-2}$ ; (b), 0.497(0) mM  $\text{TlClO}_4$  in DMF at  $0.420 \text{ mA cm}^{-2}$ .

At the end of the transition time, the potential rise is not sharply defined and two distinct slopes are seen. This distortion, which increases the uncertainty in the geometrical construction leading to the transition time, is almost certainly the result of a complex charging current. The double-layer capacity in dilute solutions is principally that of the diffuse layer and is potential dependent to a much greater degree than it is in the presence of supporting electrolyte. Moreover, the quarter-time potential of the thallos ion is close to the potential of zero charge for mercury in aqueous chloride solutions so that the voltage excursion at the end of the chronopotentiogram coincides with a sharply varying charging current.

The situation is complicated still further by the fact that the thallos ions are specifically adsorbed at the aqueous-mercury interface over the effective range of potentials of the chronopotentiogram<sup>36</sup>. This unforeseen factor exaggerates an otherwise negligible capacitance current in a manner that is not readily allowed for. DELAHAY<sup>35</sup> and BARD<sup>37</sup> have considered the effects of this and other contributions to the current density but have done so mainly in simple terms. Thus, the capacitative

contribution was regarded by BARD<sup>37</sup> as that of a fixed capacity of constant value related directly to the concentration and for which a simple correction could be made. He evolved a criterion for the absence of other than concentration-polarization, namely, the linearity of the plot of  $i\tau/c$  vs.  $\tau^{\frac{1}{2}}$ . In this work the relationship is a linear one (see Fig. 5), the slope of which ( $819 \text{ A ml cm}^{-2} \text{ sec}^{-1}$ ) is close to the more normal chronopotentiometric constant ( $809 \text{ A ml cm}^{-2} \text{ sec}^{-1}$ ) derived from the slope of  $i\tau^{\frac{1}{2}}$  vs.  $c$ .

#### Aqueous solutions

In spite of the distortion of the after-transition section, the magnitude of the transition time was not thought to be in serious error. The upper, perhaps pessimistic, limit of error was estimated to be  $\pm 5\%$ . Figure 3 shows a plot of  $i\tau^{\frac{1}{2}}$  vs.  $i$  for five concentrations of aqueous thallos chloride. They are summarised, together with

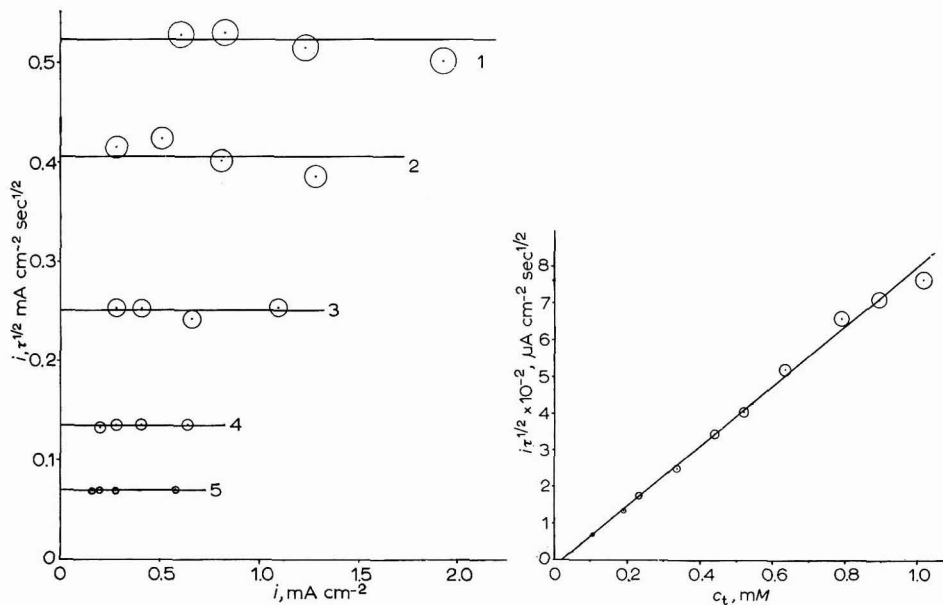


Fig. 3. Plots of  $i\tau^{\frac{1}{2}}$  vs.  $i$  for aq. TlCl.  $c_+$ : (1), 0.632; (2), 0.519; (3), 0.337; (4), 0.190; (5), 0.106 mM.

Fig. 4. Plot of  $i\tau^{\frac{1}{2}}$  vs.  $c_+$  for ten concns. of TlCl.

five more, in Fig. 4 which shows the linear dependence of  $i\tau^{\frac{1}{2}}$  vs.  $c$ . The slope of this line is, according to eqn. (6), equal to  $\frac{1}{2}\pi^{\frac{1}{2}}nFD_s^{\frac{1}{2}}/(1-t_+)$ . The value of  $D_s$  was found by KOLTHOFF AND LINGANE to be  $2.02 \cdot 10^{-5} \text{ cm sec}^{-1}$  and, thus, the cationic transport number in aqueous thallos chloride solutions is  $0.525 \pm 0.025$ . This is in reasonable agreement with the established value of 0.495. Alternatively, eqn. (10) can be used to evaluate the transport number, *i.e.*, in terms of the limiting equivalent conductance of thallos chloride ( $151.05 \text{ } \Omega^{-1} \text{ cm}^2 \text{ mole}^{-1}$ : taken from standard tables). This leads to a value for  $t_+$  of 0.527 which is virtually identical with that obtained from values of  $D_s$ .

Both values are slightly high though hardly more so than the estimated error

of the method. It could be concluded that the distortion at the end of the chronopotentiogram inevitably protracts the transition time and erroneously augments the transport number. Some evidence that this is so is seen in the following section which described the results obtained in DMF. Here, the chronopotentiograms were well shaped and gave transport numbers in excellent agreement with the established values.

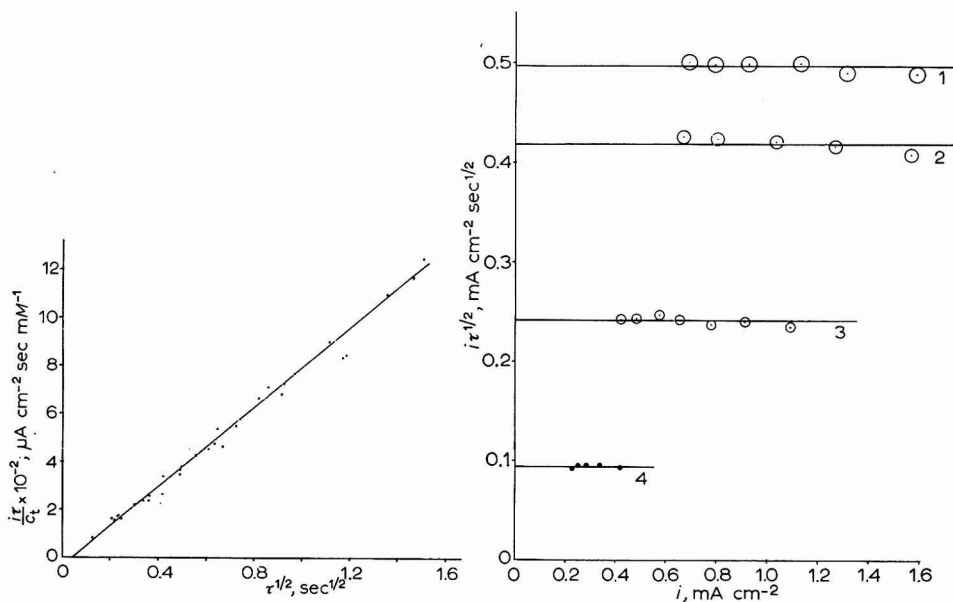


Fig. 5. Plot of  $i\tau/c_+$  vs.  $\tau^{1/2}$  for ten concs. of  $\text{TiCl}_4$ .

Fig. 6. Plots of  $i\tau^{1/2}$  vs.  $i$  for solns. of  $\text{TiClO}_4$  in DMF.  $c_+$ : (1), 1.01(6); (2), 0.848(5); (3), 0.497(0); (4), 0.204 (9) mM.

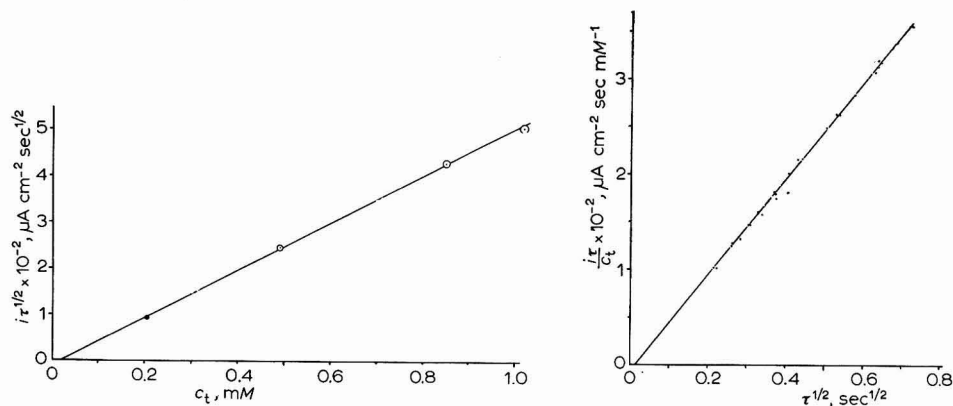


Fig. 7. Plot of  $i\tau^{1/2}$  vs.  $c_+$  for the four concs. of  $\text{TiClO}_4$  in DMF.

Fig. 8. Plot of  $i\tau/c_+$  vs.  $\tau^{1/2}$  from all the points in Fig. 6.

*DMF solutions*

Inspection of the chronopotentiograms of  $\text{TlClO}_4$  in DMF, Fig. 2 (b), shows that the transition time is very well defined. The results of the anhydrous solutions of  $\text{TlClO}_4$  in DMF are recorded graphically by plots of  $i\tau^{\frac{1}{2}}$  vs.  $i$ , Fig. 6, and analysed by plots of  $i\tau^{\frac{1}{2}}$  vs.  $c_+$ , Fig. 7, and  $i\tau/c_+$  vs.  $\tau^{\frac{1}{2}}$ , Fig. 8. The mean deviation in the graph of  $i\tau^{\frac{1}{2}}$  vs.  $c_+$  is less than  $\pm 2\%$  and the transport number for the thallos ion in this system was calculated from the plot of  $i\tau/c_+$  vs.  $\tau^{\frac{1}{2}}$ , which allows for specific adsorption and double-layer effects. The slope of this graph, Fig. 8, as calculated by the method of least squares, was  $510.1 \text{ A sec}^{\frac{1}{2}} \text{ cm mole}^{-1}$ . This was squared and inserted into eqn. (10) together with the equivalent conductivity of  $\text{TlClO}_4$  at infinite dilution as determined by PRUE AND SHERRINGTON<sup>23</sup>, and gave a value of  $0.423 \pm 0.009$  for the transport number of the thallos ion in a dilute solution of thallos perchlorate in DMF. This compares well with the value of 0.424 obtained from the data of PRUE AND SHERRINGTON<sup>23</sup>.

## CONCLUSION

It is evident that single-salt chronopotentiometry (and probably other voltametric procedures without supporting electrolyte) provides a rapid and general method for the determination of transport numbers in aqueous and non-aqueous solutions. A similar proposal has been made by EMEL'YANENKO AND SIMULIN<sup>17</sup> who quote transport numbers to  $\pm (5-7\%)$ . It must be noted, however, that they used the unmodified Sand equation which incorporates the ionic diffusion coefficient instead of that of the salt. They also used more concentrated solutions (0.025–0.12 *M*) of 2 : 2 electrolytes. These circumstances are not a fair test of the method which under the optimal conditions is capable of a higher precision ( $\pm 2\%$ ) and which for many purposes may therefore be adequate.

Certainly, under difficult experimental conditions of high or low temperatures or high pressures, where only small quantities of the system are available or where no obvious reversible electrode process is available for conventional procedures, this simple rapid method may well be the most suitable and perhaps even the only method that can be used.

## SUMMARY

The expression for the transport number of an ionic species has been derived from the chronopotentiometric transition time at a spherical micro-electrode in the absence of supporting electrolyte. The transport number is related to the transition time and to the diffusion coefficient of the salt, or alternatively, it is expressed in terms of the transition time and the equivalent conductivity of the salt at infinite dilution.

These expressions have been examined in relation to two types of system (i) dilute aqueous solutions of thallos chloride and (ii) anhydrous solutions of thallos perchlorate in *N,N*-dimethylformamide. In both cases, the experimental results conform to the proposed relationships and in each, transport numbers have been evaluated in good agreement with those obtained independently. The results confirm that "single-salt chronopotentiometry" is a rapid, satisfactory, albeit approximate, method of determination of transport numbers.

## REFERENCES

- 1 H. J. SAND, *Phil. Mag.*, 1 (1901) 45.
- 2 A. EUCKEN, *Z. Physik. Chem.*, 59 (1907) 72.
- 3 I. SLENDYK, *Coll. Czech. Chem. Commun.*, 3 (1931) 385.
- 4 W. S. SEBBORN, *Trans. Faraday Soc.*, 29 (1933) 825.
- 5 D. MACGILLAVRY, *Rec. Trav. Chim.*, 56 (1937) 1039.
- 6 I. M. KOLTHOFF AND J. J. LINGANE, *J. Am. Chem. Soc.*, 61 (1939) 1045; *Polarography*, Interscience Publishers, New York, 2nd ed., 1952, p. 122.
- 7 H. A. LAITINEN, *Trans. Electrochem. Soc.*, 82 (1942) 289.
- 8 P. DELAHAY, C. C. MATTAX AND T. BERZINS, *J. Am. Chem. Soc.*, 76 (1954) 5319.
- 9 M. D. MORRIS AND J. J. LINGANE, *J. Electroanal. Chem.*, 6 (1963) 300.
- 10 M. D. MORRIS, *ibid.*, 8 (1964) 1.
- 11 P. BRO, *J. Electrochem. Soc.*, 111 (1964) 1104.
- 12 R. W. LAITY, *J. Phys. Chem.*, 67 (1963) 671.
- 13 R. J. BEARMAN, *ibid.*, 66 (1962) 2072.
- 14 A. I. LOPUSHANSKAYA, A. V. PAMFILOV AND I. A. TSISAR, *Russ. J. Phys. Chem., English Transl.*, 37 (1963) 1193.
- 15 R. MILLS, *J. Electroanal. Chem.*, 9 (1965) 57.
- 16 D. S. TURNHAM, *ibid.*, 10 (1965) 19.
- 17 G. A. EMEL'YANENKO AND G. G. STULIN, *Russ. J. Phys. Chem., English Transl.*, 38 (1964) 1639.
- 18 J. BROADHEAD, M.Sc. Thesis, Southampton, 1965.
- 19 G. MILAZZO, *Electrochimie*, Springer, Vienna, 1952, p. 21.
- 20 H. L. KIES, *J. Electroanal. Chem.*, 4 (1962) 156.
- 21 I. M. KOLTHOFF AND J. J. LINGANE, *Polarography*, Interscience Publishers, New York, 2nd ed., 1952, p. 55.
- 22 H. GERISCHER, *Z. Physik. Chem. Leipzig*, 202 (1953) 302.
- 23 J. E. PRUE AND P. J. SHERRINGTON, *Trans. Faraday Soc.*, 57 (1961) 1795.
- 24 S. B. BRUMMER, *J. Chem. Phys.*, 42 (1965) 1636.
- 25 J. R. RUHOFF AND E. E. REID, *J. Am. Chem. Soc.*, 59 (1937) 401.
- 26 G. R. LEADER AND J. F. GORMLEY, *ibid.*, 73 (1951) 5731.
- 27 C. M. FRENCH AND K. H. GLOVER, *Trans. Faraday Soc.*, 51 (1955) 1418.
- 28 D. P. AMES AND P. G. SEARS, *J. Phys. Chem.*, 59 (1955) 16.
- 29 L. MEITES AND T. MEITES, *Anal. Chem.*, 20 (1948) 984.
- 30 D. J. G. IVES AND G. J. JANZ, *Reference Electrodes*, Academic Press, New York, 1961, p. 133.
- 31 E. O. SHERMAN, Ph.D. Thesis, Illinois, 1962.
- 32 P. DELAHAY AND T. BERZINS, *J. Am. Chem. Soc.*, 75 (1953) 2486.
- 33 D. C. GRAHAME, *Chem. Rev.*, 41 (1947) 441.
- 34 I. M. KOLTHOFF AND J. J. LINGANE, *Polarography*, Interscience Publishers, New York, 2nd ed., 1952, pp. 52, 55.
- 35 P. DELAHAY, *New Instrumental Methods in Electrochemistry*, Interscience Publishers, New York, 1954, p. 207.
- 36 M. SLUYTERS-REHBACH, Thesis, Utrecht, 1963.
- 37 A. J. BARD, *Anal. Chem.*, 35 (1963) 340.

## ADSORPTION ET IMPEDANCE FARADIQUE

### II. ÉTUDE EXPÉRIMENTALE

A. M. BATICLE ET F. PERDU

*Laboratoire d'Electrolyse du C.N.R.S., 1, Place A. Briand, Bellevue, Hauts de Seine (France)*  
(Reçu le 6 avril, 1966)

Nous avons montré, dans un article précédent<sup>1</sup>, les possibilités d'exploitation des mesures de l'impédance d'une électrode, en régime sinusoïdal, en présence d'adsorption des espèces réagissantes, en utilisant le schéma représentatif établi par SENDA ET DELAHAY<sup>2</sup>. Rappelons que l'établissement de ce schéma suppose trois hypothèses fondamentales. D'une part, les adsorptions des deux espèces réagissantes sont indépendantes l'une de l'autre. D'autre part, la variation du potentiel de l'électrode influe plus sur le processus de transfert de charges que sur le processus d'adsorption. De plus, le transfert de charges ne se fait que par l'intermédiaire des espèces adsorbées\*.

Nous avons utilisé ce calcul pour l'étude de la réaction  $Tl(Hg) \rightleftharpoons Tl^+ + e$ .

Les travaux de FRUMKIN et de ses collaborateurs<sup>3-7</sup>, ont mis en évidence l'adsorption du thallium, dans la double couche, sous les deux formes, atomique ou ionique, suivant que les potentiels considérés sont plus négatifs ou plus positifs que  $-517$  mV/ECN; l'adsorption des atomes correspondant à la formation de dipôles Tl-Hg.

BOGUSLAVSKII ET DAMASKIN<sup>8</sup>, RANDLES<sup>9</sup>, BARKER<sup>10</sup>, BUTLER<sup>20</sup>, ont mesuré les capacités de double couche du mercure dans différents électrolytes-supports, en présence de  $Tl^0$  ou de  $Tl^+$  et observé des variations de cette capacité dues à la présence du thallium.

SLUYTERS<sup>11</sup> a mesuré l'impédance d'une électrode à gouttes de mercure dans des solutions de sels de  $Tl^+$  en fonction du potentiel et rend compte de la variation d'impédance observée, dans un petit domaine de basses fréquences, par une capacité ajoutée à la capacité de double couche.

LORENZ ET SALIÉ<sup>12,13</sup> ont proposé une interprétation de l'impédance faradique mesurée, en présence d'adsorption, qui les conduit, dans le cas du système  $Tl(Hg)/Tl^+$ , à considérer un état adsorbé de charge  $+0.7$ , commun aux deux espèces, ions ou atomes.

TAMAMUSHI ET TANAKA<sup>14</sup> ont observé lors de la réduction de  $Tl^+$ , sur électrodes à gouttes de mercure, avec courant alternatif surimposé, des angles de phase supérieurs à  $45^\circ$ , dans un grand domaine de potentiel et attribuent ces résultats à l'adsorption de  $Tl^+$  sur le mercure, adsorption qui dépend des anions associés (comme l'ont montré également FRUMKIN et ses collaborateurs).

\* GERISCHER<sup>21</sup>, a établi, dans le cas d'un processus de réaction hétérogène, un schéma analogue à celui de SENDA ET DELAHAY.

I. APPAREILLAGE; SOLUTIONS ET AMALGAMES

Les mesures ont été faites en courant sinusoïdal, aux potentiels d'équilibre,  $E_e$ , des électrodes considérées, à l'aide d'un pont d'impédances dont la description a été donnée précédemment<sup>15</sup>. La précision du pont a été améliorée en utilisant des boîtes de capacités et résistances d'une meilleure qualité (General Radio, précision 0.05%). Le pont a été construit de façon à conserver, pour la précision globale, la précision de l'impédance d'équilibrage, entre 20 Hz et 50 kHz.

Nous avons utilisé des électrodes à gouttes d'amalgame, tombant en chute libre, la cadence des gouttes étant de l'ordre de 4 sec, et un dispositif antivibratoire de suspension du thermostat renfermant la cellule. Le pont est équilibré à la fin de la vie de chaque goutte. Les capillaires étaient étirés pour empêcher la formation d'un film de solution à l'intérieur du capillaire<sup>16</sup> et minimiser l'effet d'écran, et munis d'un contact de platine scellé dans le capillaire, pour diminuer la chute ohmique à l'intérieur du capillaire.

Nous avons ainsi obtenu des résultats expérimentaux beaucoup moins dispersés qu'avec un marteau magnétique et des capillaires siliconés. Les capillaires et le réservoir d'amalgame étaient remplis d'azote U avant l'utilisation. Le degré de pureté du mercure et du thallium utilisés pour la préparation des amalgames étaient, respectivement, 99.9999% et 99.999%. Les amalgames étaient préparés par dissolution directe du thallium métallique dans le mercure en atmosphère d'azote U.

L'eau des solutions était distillée trois fois en atmosphère d'azote U. L'électrolyte support,  $H_2SO_4$  0.5 M, et le sulfate de thallium étaient des produits Merck pour analyse. Solutions et amalgames étaient maintenus en atmosphère d'azote U.

Le thermostat à air était fixé à  $30 \pm 0.1^\circ$  et entièrement blindé, le blindage étant relié à la masse commune de l'appareillage.

L'électrode de référence au calomel saturé était reliée à la cellule par un pont électrolytique à robinets fermés, comportant une solution intermédiaire de  $H_2SO_4$  0.5 M. Les potentiels que nous indiquons ne sont pas corrigés pour les potentiels de jonction liquide.

II. RÉSULTATS EXPÉRIMENTAUX

Nous avons mesuré l'impédance des électrodes à leurs potentiels d'équilibre,  $E_e$ . Le seul moyen de faire varier le potentiel des électrodes étant de faire varier les concentrations relatives  $C_R$  et  $C_O$  des atomes dans les amalgames et des ions dans

TABLEAU 1

$C_R$ (%)	$C_O$ (mole. l <sup>-1</sup> )	$E_e$ (mV/ECS)	Expériences
5	$10^{-3}$	-686	I
5	$10^{-2}$	-626	V
1	$10^{-3}$	-635	II
0.09	$0.97 \times 10^{-3}$	-567	III
0.0074	$10^{-3}$	-503	IV
0.0057	$10^{-2}$	-436	VI



les solutions, nous avons exploré un domaine de potentiel limité, (Tableau 1). Les concentrations des amalgames sont données en grammes de thallium par grammes de mercure.

### 1. Calcul de l'impédance, $R_f - j/\omega C_f$

L'impédance globale,  $R_s - j/\omega C_s$ , étant mesurée, il faut tenir compte de la résistance,  $R_E^*$ , de la solution et des connexions, et de la capacité de la double couche,  $C_E$  (Fig. 1, a et b), pour obtenir l'impédance  $R_f - j/\omega C_f$  qui est équivalente<sup>1</sup> pour chaque fréquence, à l'ensemble des impédances d'adsorption (indice a), de transfert de charges (indice t) et de diffusion (indice d), (Fig. 1, A' et B'). Les indices O et R représentent respectivement, dans cette étude, les formes  $Tl^+$  et  $Tl^0$ .

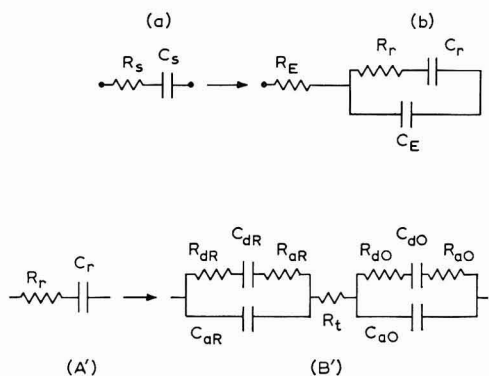


Fig. 1. (a), Impédance globale mesurée; (b), Impédance équivalente; (A'), Impédance faradique globale; (B'), éléments de l'impédance faradique.

L'examen du schéma représentatif de l'impédance globale montre que, lorsque  $\omega \rightarrow \infty$ ,  $R_s \rightarrow R_E$  et  $C_s \rightarrow C_E$ . Un calcul rigoureux a permis de l'établir en tenant compte de toutes les impédances.

Nous avons donc pris, pour effectuer nos calculs, les valeurs de  $R_E$  et  $C_E$  obtenues par extrapolation des valeurs  $R_s$  et  $C_s$  lorsque  $\omega \rightarrow \infty$ .

Les extrapolations de  $R_s$ , à fréquence infinie, ont été comparées aux valeurs de  $R_E$  mesurées directement sur des gouttes de mercure pur, de mêmes surfaces, dans l'acide sulfurique 0.5 M. Nous avons obtenu des écarts maximums de 1% entre les deux séries de valeurs, c'est-à-dire que nous retrouvons là l'écart sur la pesée des gouttes, puisque nous évaluons les surfaces à partir des poids des gouttes.

Nous n'avons pu contrôler les valeurs extrapolées de  $C_E$  puisqu'il est impossible de mesurer la capacité de double couche dans le domaine de potentiel où nous avons travaillé: que l'on prenne des amalgames et l'électrolyte support seul<sup>8</sup>, ou des solutions de  $Tl^+$  et le mercure pur<sup>9,10</sup>, la courbe  $C_E$  en fonction du potentiel est toujours déformée par l'apparition d'une impédance faradique (pseudo-capacité) due à la réaction  $Tl(Hg) \rightleftharpoons Tl^+ + e$ .

Remarquons toutefois que, dans les conditions de cette étude l'ensemble des

\*  $R_E$  = résistance de l'électrolyte,  $C_E$  = capacité de la double couche.  $R_{aR}$ ,  $R_{aO}$ ,  $C_{aR}$ ,  $C_{aO}$ , résistances et capacités d'adsorption des espèces Ox et Red.  $R_{dR}$ ,  $R_{dO}$ ,  $C_{dR}$ ,  $C_{dO}$ , résistances et capacités de diffusion des espèces Ox et Red.  $R_t$ , résistance de transfert de charges.

calculs est dominé par l'influence des résistances les variations des termes capacitifs ayant beaucoup moins de retentissement.

2. Examen des courbes,  $\cotg \theta/\omega^{\frac{1}{2}}$ ,  $R_r/\omega^{-\frac{1}{2}}$ ,  $(I/\omega C_r)/\omega^{-\frac{1}{2}}$

Ayant déterminé  $R_E$  et  $C_E$ , nous avons pu calculer, pour chaque fréquence les valeurs de  $R_r$ ,  $I/\omega C_r$  et  $\cotg \theta = \omega R_r C_r$ . En se référant à notre travail précédent<sup>1</sup>, la forme des courbes  $\cotg \theta/\omega^{\frac{1}{2}}$  (Fig. 2) met en évidence l'adsorption du thallium. Dans le domaine des basses fréquences, les angles de phase sont plus grands que  $45^\circ$ ,

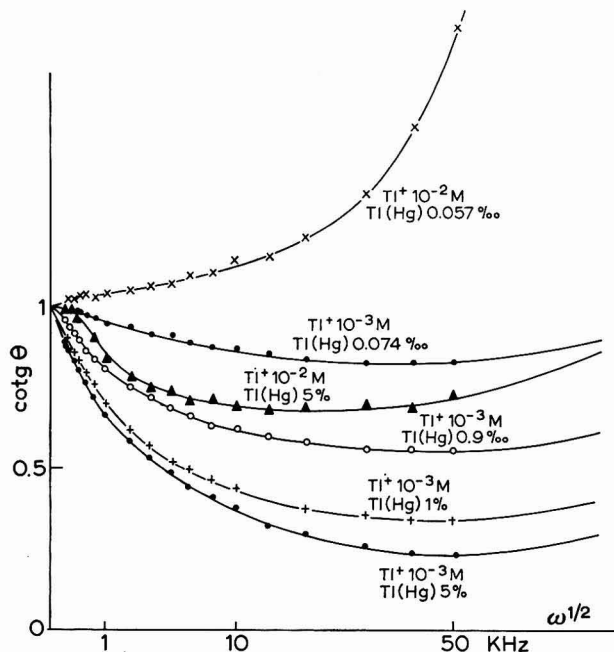


Fig. 2. Variations de  $\cotg \theta = \omega R_r C_r$  en fonction de  $\omega^{\frac{1}{2}}$  pour les différentes expériences.

augmentent puis diminuent lorsque la fréquence augmente. Nous voyons qu'une seule des pentes à l'origine est positive, donc l'angle de phase est inférieur à  $45^\circ$  mais  $\cotg \theta/\omega^{\frac{1}{2}}$  est une courbe et non une droite et là encore il faut conclure à l'adsorption.

Mais l'aspect de ces courbes ne permet pas de conclure à l'adsorption d'une seule ou des deux formes  $Tl^0$  et  $Tl^+$ . En effet, les limites pour  $\omega \rightarrow \infty$  ne sont pas encore atteintes, limites qui auraient pu permettre de répondre à cette question. Le domaine de fréquence dans lequel les extrapolations pour  $\omega \rightarrow \infty$  ou  $\omega \rightarrow 0$  sont valables dépend des valeurs relatives des différents paramètres. En particulier le domaine d'extrapolation à fréquences infinies sera d'autant plus repoussé vers les hautes fréquences que les résistances  $R_{a0}$ ,  $R_{aR}$  et  $R_t$  seront plus petites, c'est-à-dire que les vitesses d'adsorption et de transfert de charges seront plus grandes. C'est précisément le cas pour le thallium comme nous le verrons plus loin. Par contre, si ces vitesses étaient très faibles, ce serait le domaine d'extrapolation basse fréquence qui serait repoussé vers les fréquences très faibles.

Les courbes  $R_r$  et  $I/\omega C_r$  en fonction de  $\omega^{-\frac{1}{2}}$  (Figs. 3, 4, 5) ont un aspect égale-

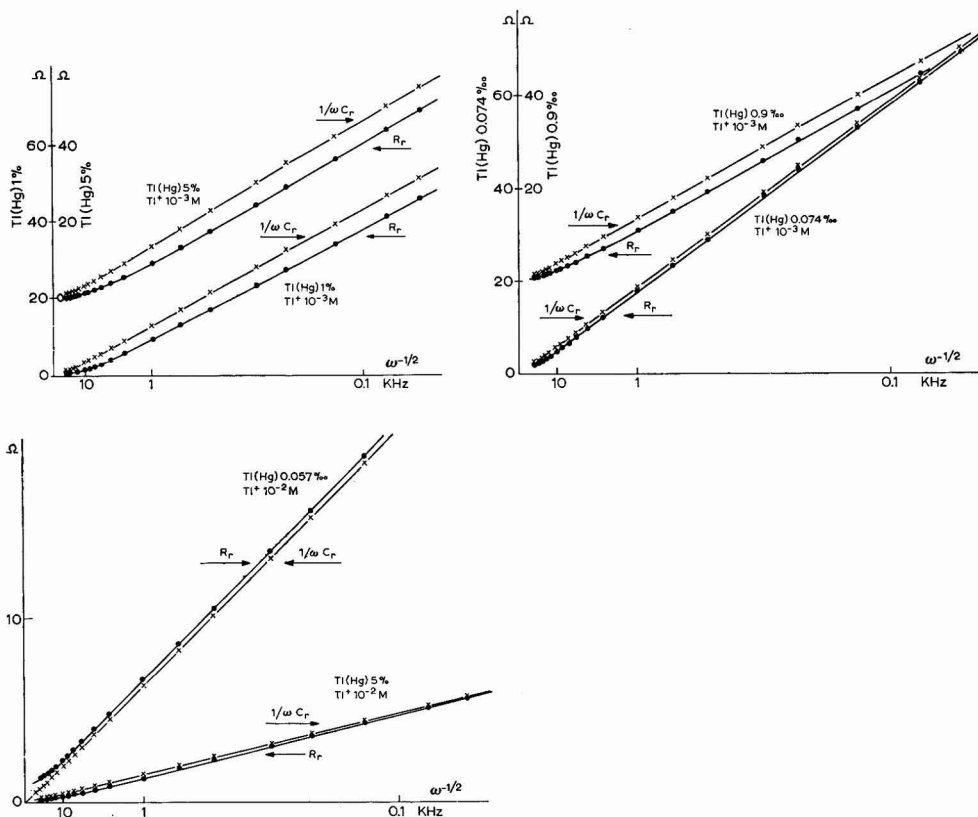
ment caractéristique de l'adsorption. Nous avons établi<sup>1</sup> en effet que, lorsque  $\omega \rightarrow 0$ ,

$$R_r - 1/\omega C_r \rightarrow R_t + \Sigma R_{ai} - 2 \Sigma C_{ai} \sigma_i^2 \tag{1}$$

Les signes  $\Sigma$  sont étendus aux espèces O et R. L'écart  $R_r - 1/\omega C_r$  peut donc être positif ou négatif suivant les valeurs relatives des différents paramètres. Pour tous les amalgames nous observons  $R_r > 1/\omega C_r$  sauf pour l'expérience No. VI, ce qui correspond aux signes des pentes à l'origine de  $\cotg \theta/\omega$  <sup>†</sup> données par :

$$d(\cotg \theta)/d(\omega^{\frac{1}{2}})_{\omega \rightarrow 0} = [R_t + \Sigma R_{ai} - 2 \Sigma C_{ai} \sigma_i^2] \cdot [1/\Sigma \sigma_i] \tag{2}$$

et qui sont toutes négatives sauf pour l'expérience VI.



Figs. 3-5. Variations de l'impédance faradique en fonction de  $\omega^{-\frac{1}{2}}$  pour les expériences: (3), I et II; (4), III et IV; (5), V et VI.

Remarquons que les valeurs de  $\cotg \theta$  semblent plus dispersées que celles de  $R_r$  et  $1/\omega C_r$ . En fait les erreurs s'ajoutent dans l'expression  $\cotg \theta = \omega R_r C_r$ . Les courbes  $R_r$  et  $1/\omega C_r$  en fonction de  $\omega^{-\frac{1}{2}}$  montrent que la diffusion est le phénomène prépondérant dans un grand domaine de basses fréquences\*.

\* Un autre système est actuellement à l'étude dans lequel l'adsorption est le phénomène prépondérant même aux très basses fréquences.

3. Calcul de la résistance de transfert de charges,  $R_t$

Nous avons montré<sup>1</sup> que lorsque  $\omega \rightarrow \infty$  :

$$R_r \rightarrow R_t + \omega^{-2} \Sigma [(1/R_{ai} C_{ai}^2) (1 - \sigma_i \omega^{-1/2} / R_{ai})] \tag{3}$$

Lorsque les vitesses d'adsorption sont assez faibles ( $R_{ai}$  grands), le terme,  $\sigma_i \omega^{-1/2} / R_{ai}$ , est négligeable devant 1 à fréquences élevées, et l'extrapolation de la droite  $R_r / \omega^{-2}$  est très précise. Ce n'est pas le cas du thallium dont les vitesses d'adsorption sont grandes et il faut extrapoler une courbe ce qui est moins précis. De plus la vitesse de transfert de charges est très grande<sup>9,10</sup>, et nous obtenons des valeurs de  $R_t$  très faibles. Pour les expériences à concentrations les plus faibles nous avons obtenu les valeurs du Tableau 2 en bon accord avec les valeurs connues<sup>9,10</sup> pour  $I_a^0$ .

4. Calcul des coefficients de diffusion

Nous avons montré<sup>1</sup>, que la pente des courbes  $R_r$  et  $1/\omega C_r$ , en fonction de  $\omega^{-1/2}$ , lorsque  $\omega \rightarrow 0$  est :

$$\sigma_0 + \sigma_R = \frac{RT}{n^2 F^2 \sqrt{2} A} \left[ \frac{1}{C_{O^0} D_{O^{\ddagger}}} + \frac{1}{C_{R^0} D_{R^{\ddagger}}} \right] \tag{4}$$

A partir des pentes expérimentales de ces courbes nous avons ainsi pu calculer les coefficients de diffusion  $D_O$  et  $D_R$  pour les deux espèces  $Tl^+$  et  $Tl^0$  dans l'acide sulfurique 0.5 M et, dans le mercure, respectivement (Tableau 2).

TABLEAU 2

Expé- riences	Amalgames (%)	$C_R$ (mole l <sup>-1</sup> )	$C_O$ (mole l <sup>-1</sup> )	$D_O$ (cm <sup>2</sup> sec <sup>-1</sup> · 10 <sup>6</sup> )	$D_R$ (cm <sup>2</sup> sec <sup>-1</sup> · 10 <sup>6</sup> )	$R_t$ ( $\Omega$ cm <sup>2</sup> )	$I_a^0$ (A cm <sup>-2</sup> )
I	5	5.45	10 <sup>-3</sup>	18.1		~ 0	
II	1	7.5 · 10 <sup>-1</sup>	10 <sup>-3</sup>	17.9		~ 0	
III	0.09	5.85 · 10 <sup>-2</sup>	10 <sup>-3</sup>	18.3	10.4	0.011	2.36
IV	0.0074	4.91 · 10 <sup>-3</sup>	0.97 · 10 <sup>-3</sup>	17.9	10.9	0.060	0.43
V	5	5.45	10 <sup>-2</sup>	18.0		~ 0	
VI	0.0057	3.77 · 10 <sup>-3</sup>	10 <sup>-2</sup>	17.7	10.6	0.033	0.67

$\bar{D}_O = 17.98 \quad \bar{D}_R = 10.63$

Pour les amalgames les plus concentrés les coefficients  $\sigma_R$ , inversement proportionnels à  $C_R^0$  sont négligeables devant  $\sigma_0$ . Les surfaces,  $A$ , ont été évaluées à partir du poids des gouttes, en supposant celles-ci sphériques, et en utilisant les valeurs de densités de RICHARDS ET DANIELS<sup>17</sup>.

5. Calcul des éléments de l'impédance d'adsorption

Nous avons vu plus haut que la forme des courbes  $\cotg \theta / \omega^{\ddagger}$  n'a pu nous permettre de déterminer si les deux formes  $Tl^0$  et  $Tl^+$ , ou une seule, étaient adsorbées. Un moyen de trancher cette question est d'utiliser le calcul que nous avons proposé<sup>1</sup>. Mais ce calcul utilise les éqns. (34) et (35) déterminées aux fréquences élevées. De même que les courbes  $\cotg \theta$  n'ont pas encore, dans le domaine de fréquences étudié, atteint leurs limites, par suite de la grande vitesse de l'adsorption et du transfert de charges ( $R_t$  et  $R_{ai}$  faibles), de même nous ne pouvons établir ces deux équations. Il est

impossible, pour autant, de négliger à priori les termes réels de l'impédance puisque l'ensemble dépend des valeurs relatives des éléments et que les admittances,  $j\omega C$ , varient en fonction de la fréquence.

Nous avons alors utilisé les éqns. (39) et (40) proposées dans<sup>1</sup> dans le cas d'une seule adsorption et cherché dans la constance des valeurs  $R_{ai}$  et  $C_{ai}$  obtenues en fonction de la fréquence, et la concordance des courbes expérimentales et calculées, une justification de notre calcul. Rappelons ces équations:

$$(1/\omega C_{ai})^2(\sigma_i\omega^{-\frac{1}{2}} - B) + (1/\omega C_{ai})(A^2 + B^2 - 2B\sigma_i\omega^{-\frac{1}{2}}) + \sigma_i\omega^{-\frac{1}{2}}(A^2 + B^2) = 0 \quad (5)$$

$$R_{ai} = [1/A] \cdot [(1/\omega C_{ai})(B - \sigma_i\omega^{-\frac{1}{2}}) + \sigma_i\omega^{-\frac{1}{2}}(B - A)] \quad (6)$$

$$A = R_r - R_t - \sigma'\omega^{-\frac{1}{2}} \quad (7)$$

$$B = 1/\omega C_r - \sigma'\omega^{-\frac{1}{2}} \quad (8)$$

L'indice,  $i$ , représente ici l'espèce adsorbée et l'exposant, ' $'$ , correspond à l'espèce non adsorbée.

L'existence des racines des éqns. (5) et (6) dépend de la condition:

$$A^2 + B^2 > 2A\sigma_i\omega^{-\frac{1}{2}} \quad (9)$$

Pour les expériences I-V, cette condition n'est réalisée qu'en posant l'adsorption des ions  $Tl^+$ , alors que pour l'expérience VI il faut poser l'adsorption des atomes  $Tl^0$ .

Dans toutes nos expériences les impédances d'adsorption et de transfert sont faibles, de sorte que, à des fréquences plus ou moins élevées selon les concentrations des espèces actives le terme réel ( $R_S - R_E$ ) de l'impédance globale mesurée est inférieur à  $1 \Omega$ , alors que la résistance de l'électrolyte est connue à  $0.1 \Omega$  près ( $1\%$  sur  $10 \Omega$ ). Aux fréquences élevées le calcul de  $R_{ai}$  et  $C_{ai}$  dépend donc étroitement du choix de  $R_E$ . Aux basses fréquences, l'impédance d'adsorption n'est plus qu'une petite part de l'impédance globale par suite de l'importance relative de l'impédance de diffusion. Nous avons retenu les valeurs de  $R_{ai}$  et  $C_{ai}$  calculées entre ces deux limites (Tableau 3, Figs. 6 et 7).

Rappelons que les termes  $\partial\Phi_i/\partial C_i$  et  $\partial\Gamma_i/\partial C_i$  du Tableau 3 sont calculés à l'aide des valeurs de  $C_{ai}$  et  $R_{ai}$  selon les équations suivantes<sup>2</sup>:

$$\partial\Phi_i/\partial C_i = \frac{RT}{n^2 F^2} \cdot \frac{1}{AR_{ai}} \cdot \frac{1}{C_i} \quad (10)$$

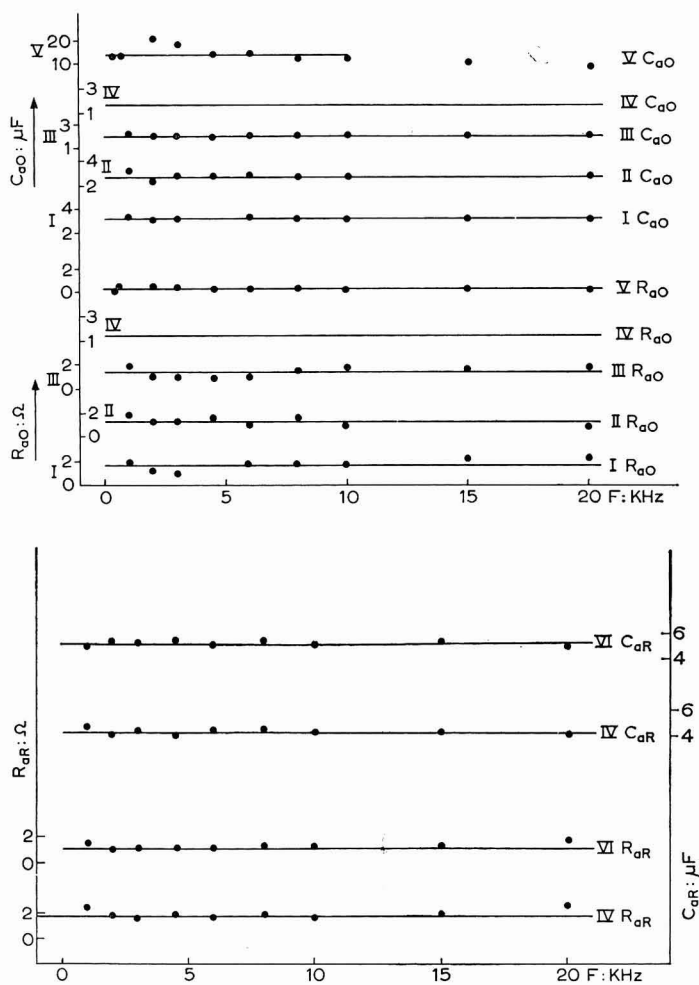
$$\partial\Gamma_i/\partial C_i = \frac{RT}{n^2 F^2} \cdot \frac{C_{ai}}{A} \cdot \frac{1}{C_i} \quad (11)$$

TABLEAU 3

No. expérience	$C_{aO}$ ( $\mu F cm^{-2}$ )	$R_{aO}$ ( $\Omega cm^2$ )	$\partial\Gamma_O/\partial C_O$ ( $cm \cdot 10^6$ )	$\partial\Phi_O/\partial C_O$ ( $cm sec^{-1}$ )	$C_{aR}$ ( $\mu F cm^{-2}$ )	$R_{aR}$ ( $\Omega cm^2$ )	$\partial\Gamma_R/\partial C_R$ ( $cm \cdot 10^6$ )	$\partial\Phi_R/\partial C_R$ ( $cm sec^{-1}$ )
I	82.4	0.066	22.3	4.2				
II	65	0.063	17.5	4.9				
III	50	0.064	13.6	4.2				
IV	43	0.060	11.9	4.7	107	0.064	5.9	0.87
VI					132	0.045	9.7	1.6

$\Phi_i$  et  $I_i$  sont, respectivement, le flux et l'excès superficiel de la substance adsorbée.

La résolution, aux différentes fréquences, des éqns. (5) et (6) donne, pour les expériences I, II, III et VI, des valeurs de  $R_{ai}$  et  $C_{ai}$  dispersées autour de valeurs moyennes, dispersion plus importante sur  $R_{ai}$  que sur  $C_{ai}$ . Les écarts expérimentaux sont responsables de cette dispersion, puisqu'ils se trouvent, par le mode de calcul, entièrement reversés sur l'impédance d'adsorption.



Figs. 6-7. Valeurs calculées aux différentes fréquences des résistances et capacités d'adsorption: (6), des ions  $Tl^+$  pour les expériences I, II, III, IV et V; (7), des atomes  $Tl^0$  pour les expériences IV et VI.

Pour l'expérience IV, les valeurs de  $R_{a0}$  et  $C_{a0}$  varient systématiquement avec la fréquence. En introduisant dans le calcul par approximations successives, l'adsorption simultanée des deux espèces  $Tl^0$  et  $Tl^+$ , nous avons obtenu pour des valeurs constantes de  $R_{a0}$  et  $C_{a0}$  des valeurs associées dispersées normalement pour  $R_{aR}$  et  $C_{aR}$ .

L'expérience V, dans laquelle les concentrations sont les plus élevées, conduit à de faibles valeurs de l'impédance globale mesurée particulièrement défavorable pour les calculs. Pour  $F > 2$  kHz nous avons mesuré  $R_S - R_E < 0.9 \Omega$  et les valeurs de  $R_{a0}$  et  $C_{a0}$  sont peu cohérentes aux fréquences élevées, les calculs ayant peu de signification sur ces valeurs mesurées trop faibles, pour lesquelles les écarts expérimentaux ont une valeur relative trop importante.

Les valeurs moyennes de  $R_{ai}$  et  $C_{ai}$  calculées pour les autres expériences ont été reportées dans les expressions de l'impédance globale et les courbes, ainsi recalculées, de  $R_r$  et  $1/\omega C_r$  en fonction de  $\omega^{-\frac{1}{2}}$ , coïncident avec les courbes expérimentales à la précision des écarts expérimentaux, écarts dont l'importance relative croit aux fréquences très élevées.

Les expériences I, II et III, ont mis en évidence l'adsorption des ions  $Tl^+$ , l'expérience VI celle des atomes  $Tl^0$ . L'expérience IV indique une adsorption simultanée des deux espèces.

À basses fréquences nous avons vu<sup>1</sup> que:

$$R_{r\omega \rightarrow 0} \rightarrow R_t + \sum R_{ai} - 2 \sum C_{ai} \sigma_i^2 + \sum \sigma_i \omega^{-\frac{1}{2}} \quad (I2)$$

$$(1/\omega C_r)_{\omega \rightarrow 0} \rightarrow \sum \sigma_i \omega^{-\frac{1}{2}} \quad (I3)$$

L'écart constant, à très basses fréquences, entre les portions linéaires des droites  $R_r$  et  $1/\omega C_r$  en fonction de  $\omega^{-\frac{1}{2}}$  sera donc:

$$K = R_t + \sum R_{ai} - 2 \sum C_{ai} \sigma_i^2 \quad (I4)$$

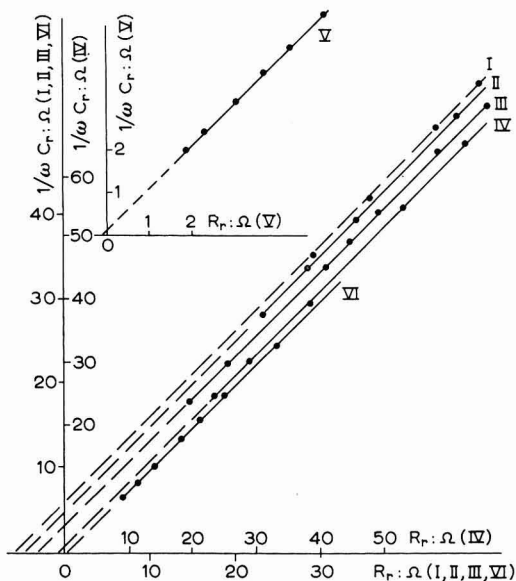


Fig. 8. Représentation des impédances faradiques dans le plan complexe, pour les différentes expériences, aux basses fréquences.

En utilisant la représentation de l'impédance  $R_r - j/\omega C_r$  dans le plan complexe, Fig. 8, comme l'a fait SLUYTERS<sup>19</sup> (pour l'impédance globale dans le cas d'une réaction simple) l'extrapolation à fréquence infinie de la droite à  $45^\circ$  obtenue à basse fréquence, coupe l'axe réel au point d'abscisse,  $K$ .



D'autre part, nous avons vu que lorsque  $\omega \rightarrow 0$  la pente à l'origine de la courbe  $\cotg \theta/\omega^{\frac{1}{2}}$  est donnée par :

$$P = \frac{R_t + \sum R_{ai} - 2 \sum C_{ai} \sigma_i}{\sum \sigma_i} \tag{15}$$

Nous avons donc calculé  $P$  et  $K$  à partir des paramètres déterminés ci-dessus et comparé les valeurs obtenues à celles déterminées graphiquement sur les Figs. 2 et 8 (Tableau 4). L'accord entre les deux séries de valeurs est réalisé sauf pour l'expé-

TABLEAU 4

	<i>K</i> calculé	<i>K</i> extrapolé	$R_r - 1/\omega C_r$	<i>P</i> calculé ( $\times 10^3$ )	<i>P</i> graphique ( $\times 10^3$ )
I	-6.6	< -6	< -6	-5.6	< -5.45
II	-4.93	-4.9	-4.9	-4.58	-4.51
III	-3.04	-3	-3	-2.76	-2.78
IV	-0.82	-0.8	-0.8	-0.56	-0.58
VI	0.35	$0.3 < K < 0.4$	0.35	0.69	+0.57

rience No. I. Pour celle-ci, à la fréquence du dernier point mesuré (0.070 kHz) nous n'avons pas encore atteint la droite à 45° (Fig. 6) et les valeurs de  $K$  et  $P$  sont obtenues par défaut. De même,  $R_r - 1/\omega C_r$  tend vers sa limite sans l'avoir encore atteinte.

III. DISCUSSION DES RÉSULTATS

En choisissant le système Tl(Hg)/Tl<sup>+</sup> pour exploiter le calcul proposé<sup>1</sup>, nous nous sommes placés aux limites d'utilisation de la méthode. En effet, comme toujours en cinétique, la mise en évidence des phénomènes rapides est délicate. Le calcul proposé serait d'autant plus aisé que les vitesses d'adsorption et de transfert seraient plus lentes, ramenant ainsi vers des fréquences moins élevées le domaine de prépondérance des termes cinétiques de l'impédance. Dans le cas du thallium, c'est la diffusion qui est le phénomène prépondérant. Remarquons, au passage, que dans l'ensemble des calculs les écarts expérimentaux ont peu de retentissement sur les valeurs des capacités alors que les valeurs des résistances dépendent étroitement de la précision des valeurs expérimentales.

Nous devons examiner les hypothèses que nous avons utilisées au long de ce travail.

Tout d'abord nous avons ramené l'impédance globale,  $Z$ , à la somme de deux impédances (Fig. 1), (abstraction faite de la résistance de l'électrolyte,  $R_E$ ):

$$\frac{1}{Z} = j\omega C_E + \frac{1}{R_r - j/\omega C_r} \tag{16}$$

La capacité,  $C_E$ , a été prise constante et égale à sa valeur extrapolée à haute fréquence.

Nous n'avons pas tenu compte de la variation possible de ce terme avec la fréquence. En effet, si l'on reprend le calcul de SENDA ET DELAHAY<sup>2</sup>, l'expression de l'impédance globale,  $Z$ , serait :

$$\frac{I}{Z} = j\omega \left( \frac{\partial q}{\partial E} \right)_{R_0} + \frac{I}{R_r - j/\omega C_r} \left[ I + j\omega \left( \frac{\partial q}{\partial \Gamma_0} \right)_E \left( \frac{\partial \Gamma_0}{\partial E} \right)_c (A - jB) \right] \quad (17)$$

dans laquelle A et B sont définis par les eqns. (7) et (8).

En plus de la capacité fixe,  $(\partial q/\partial E)_{R_0}$ , il faudrait tenir compte du terme variable avec la fréquence:

$$j\omega \left( \frac{\partial q}{\partial \Gamma_0} \right)_E \left( \frac{\partial \Gamma_0}{\partial E} \right)_c \left( \frac{A - jB}{R_r - j/\omega C_r} \right)$$

pour calculer l'impédance  $R_r - j/\omega C_r$ . N'ayant aucun moyen de calculer ce terme correctif nous l'avons supposé négligeable. Notre hypothèse se vérifie par les résultats obtenus. En effet les valeurs de  $R_{ai}$  et  $C_{ai}$  calculées à moyennes et hautes fréquences satisfont les relations de  $K$  et  $P$  obtenus lorsque  $\omega \rightarrow 0$ , ce qui ne serait pas possible si le terme correctif n'était pas négligeable, les valeurs de  $R_{ai}$  et  $C_{ai}$  varieraient alors avec la fréquence. De plus les grandeurs  $\sigma_i$  ainsi calculées dépendent elles aussi de ce terme correctif et s'il n'était pas négligeable, les coefficients de diffusion seraient variables d'une expérience à l'autre ce que nous n'observons pas dans les limites de la précision des calculs.

D'autre part la distribution d'impédances que nous avons utilisée a nécessité trois hypothèses rappelées au début de cet article.

Il est difficile de comparer les différentes valeurs des paramètres obtenus puisque les variations des concentrations et des potentiels sont liées. Néanmoins on peut voir que les deux premières hypothèses semblent justifiées. En effet la vitesse d'adsorption,  $\partial \Phi_0 / \partial C_0$ , ne varie pratiquement pas dans les expériences I, II, III et IV concernant une même solution et des amalgames différents et on peut considérer les deux adsorptions comme indépendantes l'une de l'autre.

Dans ces mêmes expériences les impédances d'adsorption calculées,  $R_{ai}$  et  $C_{ai}$ , restent du même ordre de grandeur alors que l'impédance de transfert de charges varie bien davantage: Tableaux 2 et 3. Donc la variation de potentiel amenée par la variation de concentration  $C_R$  influe plus sur le processus de transfert de charges que sur le processus d'adsorption.

Enfin le fait d'avoir pu décomposer l'impédance globale en éléments correspondant au schéma choisi peut justifier la troisième hypothèse: si le transfert de charges pouvait se faire par l'intermédiaire des espèces non adsorbées aussi bien que par celui des espèces adsorbées on aurait une répartition différente des impédances et l'utilisation du schéma de SENDA ET DELAHAY conduirait à des valeurs dépendant de la fréquence.

Ce double transfert de charges a cependant été supposé par LORENZ et ses collaborateurs<sup>12,13</sup> qui ont été amenés ainsi à définir un état d'adsorption commun aux deux espèces  $Tl^0$  et  $Tl^+$  de charge 0.7. Les auteurs ont travaillé dans un domaine de très faibles concentrations en thallium où la diffusion doit être encore plus prépondérante que dans nos conditions expérimentales et où leur hypothèse de linéarité des isothermes d'adsorption est probablement valable alors qu'elle ne le serait pas dans notre domaine de concentrations. Ils ont été amenés à supposer la résistance de transfert nulle alors que nous avons pu la déterminer pour les concentrations les moins élevées. Remarquons que ces auteurs ont été amenés à travailler sur des extra-

polations à  $\omega \rightarrow 0$  de formes analogues aux nôtres, mais partant d'hypothèses différentes leur interprétation est différente.

Nous avons cherché également à utiliser l'interprétation de l'impédance d'adsorption proposée par SLUYTERS et ses collaborateurs<sup>11</sup>. Ces auteurs ont supposé la résistance de transfert de charges négligeable et ramené l'impédance d'adsorption à une capacité  $\Delta C_E$  placée en parallèle sur la capacité de double couche :

$$\frac{I}{Z} = j\omega(C_E + \Delta C_E) + \frac{I}{R_d - j/\omega C_d} \tag{18}$$

et résolu graphiquement le problème dans le cas de mercure et de sels de thallium en superposant courant continu et courant alternatif.

En reprenant cette interprétation, mais sans faire d'hypothèses sur l'impédance de transfert de charges, nous pouvons écrire l'impédance globale mesurée sous la forme :

$$\frac{I}{R_S - R_E - j/\omega C_S} = j\omega(C_E + \Delta C_E) + \frac{I}{R_t + \Sigma(R_{di} - j/\omega C_{di})} \tag{19}$$

Nous pouvons déterminer les valeurs de  $R_t$  et  $C_E + \Delta C_E$  en utilisant<sup>1</sup> le système d'équations suivant, analogue au système (5), (6), (7) et (8) :

$$\begin{aligned} & (I/\omega C)^2[\sigma\omega^{-\frac{1}{2}} - I/\omega C_S] + (I/\omega C)[R^2 + I/\omega^2 C_S^2 - 2\sigma\omega^{-\frac{1}{2}}/\omega C_S] \\ & + \sigma\omega^{-\frac{1}{2}}(R^2 + I/\omega^2 C_S^2) = 0 \end{aligned} \tag{20}$$

$$R_t = (I/R) [I/\omega C (I/\omega C_S - \sigma\omega^{-\frac{1}{2}}) + \sigma\omega^{-\frac{1}{2}}(I/\omega C_S - R_S)] \tag{21}$$

en posant :

$$C_E + \Delta C_E = C \tag{22}$$

$$R_S - R_E = R \tag{23}$$

$$\sigma_O + \sigma_R = \sigma \tag{24}$$

Nos conditions expérimentales sont assez différentes puisque nous sommes partis de solutions de sulfate de thallium et non de nitrate + chlorure (adsorption moins forte dans notre cas<sup>6,14</sup>), et d'amalgames et non de mercure pur. D'autre part nous travaillons en courant sinusoïdal pur et non en courants continu et alternatif surimposés, et à des fréquences plus élevées.

La résolution des éqns. (20) et (21) n'est pas possible pour toutes les fréquences mesurées. Pour les expériences II, III et IV, elle n'est possible qu'aux basses fréquences, et aux fréquences élevées seulement pour les expériences I et VI.

Les valeurs obtenues de  $R_t$  restent du même ordre de grandeur, 0,5-3  $\Omega$  pour toutes les expériences sans suivre la loi du transfert de charges  $R_t \sim I/C_R^\alpha C_O^{1-\alpha}$ . Les capacités  $\Delta C_E$  varient systématiquement avec la fréquence.

Cette interprétation ne peut donc être retenue dans nos conditions expérimentales.

Une question se pose encore c'est celle de l'existence de l'adsorption de la 2<sup>o</sup> espèce dans les expériences I, II, III, V et VI. Nous avons examiné le jeu des impédances relatives de diffusion et d'adsorption. En effet, l'impédance d'adsorption n'apparaîtra que si elle est petite ou comparable à l'impédance de diffusion correspondante (Fig. 1). Elle apparaîtra donc plus facilement aux fréquences élevées où

TABLEAU 5

<i>Expérience</i>	$C_{aR}$ limite ( $\mu F\ cm^{-2}$ )	$\partial\Gamma_R/\partial C_R$ ( $cm \cdot 10^6$ )	$C_{aO}$ limite ( $\mu F\ cm^{-2}$ )	$\partial\Gamma_O/\partial C_O$ ( $cm \cdot 10^6$ )
I	154.000	7.7		
II	22.600	8.2		
III	1.960	8.9		
IV	156.000	7.7		
VI			440	11.9

effectivement nous obtenons des écarts ( $F > 20$  kHz) par rapport aux valeurs calculées aux fréquences plus basses. Mais dans ce domaine l'importance des erreurs expérimentales croît très rapidement. Nous avons essayé un calcul d'impédances relatives, (Tableau 5), pour tenter de répondre à la question.

Nous avons considéré isolément l'impédance correspondant à la diffusion et à l'adsorption hypothétique de l'espèce apparemment non adsorbée:  $R_{ai}$ ,  $C_{ai}$ ,  $R_{ai}$ ,  $C_{ai}$  et pris  $R_{ai} = 0$ . Pour que l'adsorption ait un effet non négligeable sur cette impédance il faut  $C_{ai} > 1/\sqrt{2\sigma_i\omega}$ . Si  $R_{ai}$  a une valeur non nulle la limite de  $C_{ai}$  sera plus élevée.

Nous avons ainsi calculé les termes  $\partial\Gamma_i/\partial C_i$  correspondants (Tableau 5). Nous avons fait ces calculs à 20 kHz, où l'impédance d'adsorption est relativement prépondérante.

Il faut ensuite comparer les impédances relatives O et R pour avoir la valeur de l'écart introduit dans les calculs par une deuxième adsorption hypothétique. Et là, le déséquilibre entre les deux grandeurs, amené par la dissymétrie des concentrations des deux espèces, fait que l'influence de la deuxième adsorption se trouve masquée.

En utilisant les résultats de FRUMKIN ET GORODETSKAIA<sup>3</sup>, nous avons calculé la valeur  $(\partial\Gamma_R/\partial C_R)_E$  pour l'amalgame à 1%, pour le potentiel  $-635$  mV/ECS et trouvé qu'elle correspondrait à une valeur de  $8.4 \cdot 10^{-7}$  cm soit  $C_{aR} = 2400 \mu F\ cm^{-2}$  pour notre expérience No. II. A 20 kHz, cette capacité amènerait un écart de 10% maximum sur la valeur de l'impédance R. Mais l'impédance O est alors 100 fois plus grande que l'impédance R et les variations de cette dernière ne peuvent être observées. L'adsorption R ne peut apparaître dans nos calculs.

En travaillant à des fréquences plus élevées l'importance relative de l'impédance d'adsorption augmente, mais dans les conditions de nos expériences, nous avons vu que l'impédance globale mesurée est si faible que les erreurs expérimentales amènent des écarts importants sur les valeurs calculées.

D'autre part, le domaine de potentiel dans lequel nous avons travaillé se situe autour du potentiel limite pour l'adsorption des deux espèces  $Tl^0$  et  $Tl^+$  déterminé par FRUMKIN<sup>7</sup>. Pour  $-E < 515$  mV (ECN) commence le domaine d'adsorption du  $Tl^+$  et pour  $-E > 515$  mV (ECN) celui du  $Tl^0$ . Or nous avons observé les adsorptions inverses pour les expériences I, II, III et VI et l'adsorption simultanée des deux espèces pour l'expérience IV.

Compte tenu des comparaisons d'impédance exposées plus haut, des travaux de FRUMKIN et des résultats de ce travail, il nous semble que ce domaine de potentiel autour du potentiel limite doit être un domaine de transition où les deux espèces sont probablement adsorbées, mais que l'adsorption n'est un frein cinétique que pour des concentrations peu élevées.

## BIBLIOGRAPHIE

- 1 A. M. BATICLE ET F. PERDU, *J. Electroanal. Chem.*, 12 (1966) 15.
- 2 M. SENDA ET P. DELAHAY, *J. Phys. Chem.*, 65 (1961) 1580.
- 3 A. N. FRUMKIN ET A. GORODETSKAIA, *Z. Physik. Chem.*, 136 (1928) 451.
- 4 A. N. FRUMKIN ET F. J. CIRVES, *J. Phys. Chem.*, 34 (1930) 74.
- 5 A. N. FRUMKIN ET A. S. TITEVSKAYA, *Zh. Fiz. Khim.*, 31 (1957) 485.
- 6 A. N. FRUMKIN ET N. S. POLYANOVSKAYA, *Zh. Fiz. Khim.*, 32 (1958) 157.
- 7 A. N. FRUMKIN, *Surface Phenomena in Chemistry and Biology*, edited by J. F. DANIELLI, K. G. A. PANKURST ET A. C. RIDDIFORD, Pergamon Press, Londres, 1958.
- 8 L. I. BOGUSLAVSKII ET B. B. DAMASKIN, *Zh. Fiz. Khim.*, 34 (1960) 2099.
- 9 J. E. B. RANGLES, *Transactions of the Symposium on Electrode Processes*, edited by E. YEAGER, John Wiley and Sons, New York, 1961, p. 209.
- 10 G. C. BARKER, *Transactions of the Symposium on Electrode Processes*, edited by E. YEAGER, John Wiley and Sons, New York, 1961, p. 325.
- 11 M. SLUYTERS-REHBACH, B. TIMMER ET J. H. SLUYTERS, *Rec. Trav. Chim.*, 82 (1963) 553.
- 12 W. LORENZ ET G. SALIE, *Z. Physik. Chem. Leipzig*, 218 (1961) 259.
- 13 G. SALIE ET W. LORENZ, *Z. Physik. Chem. Frankfurt*, 29 (1961) 408.
- 14 R. TAMAMUSHI ET N. TANAKA, *Z. Physik. Chem. Frankfurt*, 28 (1961) 158.
- 15 A. M. BATICLE, *Electrochim. Acta*, 8 (1963) 595.
- 16 G. C. BARKER ET I. L. JENKINS, *Analyst*, 77 (1952) 685.
- 17 T. W. RICHARDS ET F. DANIELS, *J. Am. Chem. Soc.*, 41 (1919) 1732.
- 18 G. N. LEWIS ET M. RANDALL, *J. Am. Chem. Soc.*, 43 (1921) 233.
- 19 J. H. SLUYTERS, *Rec. Trav. Chim.*, 79 (1960) 1092.
- 20 J. N. BUTLER, *J. Electroanal. Chem.*, 9 (1965) 149.
- 21 H. GERISCHER, *Z. Physik. Chem.*, 201 (1952) 55.

*J. Electroanal. Chem.*, 13 (1967) 364-377

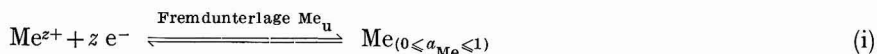
## CHRONOAMPEROMETRISCHE UNTERSUCHUNG VON BLEINIEDERSCHLÄGEN AUF GOLDELEKTRODEN

E. SCHMIDT UND H. R. GYGAX

*Institut für anorganische, analytische und physikalische Chemie der Universität Bern (Schweiz)*

(Eingegangen am 13. April, 1966)

Bei den in vorangegangenen Mitteilungen<sup>1-5</sup> beschriebenen chronoamperometrischen Versuchen zur Abscheidung bzw. Auflösung metallischer Niederschläge auf festen Fremdmetallelektroden gemäss



war die Auswahl des Depolarisators  $\text{Me}^{z+}$  und des Elektrodenmetalls  $\text{Me}_u$  so getroffen worden, dass in den binären Systemen  $\text{Me}-\text{Me}_u$  bei Zimmertemperatur weder intermetallische Verbindungen noch feste Lösungen nennenswerter Phasenbreite auftreten und ("ungesättigte")  $\text{Me}$ -Niederschläge der Aktivität  $a_{\text{Me}} < 1$  demnach (unter Ausschluss von Uebersättigungserscheinungen) nur in Form metallischer Monoschichten<sup>3</sup> vorliegen können. Nachfolgend wird am Beispiel der Reduktion von  $\text{Pb}^{2+}$  an Goldunterlagen das chronoamperometrische Verhalten einer  $\text{Me}-\text{Me}_u$ -Kombination ( $\text{Pb}-\text{Au}$ ) untersucht, die die genannten Mischbarkeitsbedingungen nicht erfüllt, und bei der deshalb die Möglichkeit einer Bildung von Legierungsphasen im Verlauf der elektrolytischen  $\text{Me}$ -Abscheidung nicht von der Hand zu weisen ist. Wie aus Tabelle 1

TABELLE 1

EIGENSCHAFTEN DES SYSTEMS  $\text{Au}-\text{Pb}$

<i>Nachgewiesene Verbindungen</i>	$\text{Au}_2\text{Pb}$ (34.44 Gew. % Pb)	$\text{AuPb}_2$ (67.76 Gew. % Pb)
<i>Gegenseitige Mischbarkeit der reinen Komponenten (25°)</i>	Au in Pb: 0%	Pb in Au: 0%
<i>Diffusionskoeffizienten</i>	extrapoliert nach ref. 17: $D_{25^\circ}(\text{Au in Pb}) \approx 2 \cdot 10^{-11} \text{ cm}^2\text{sec}^{-1}$ Bruttokoeffizient nach ref. 8: $D_{25^\circ}(\text{Au in Pb}) = 1.89 \cdot 10^{-14} \text{ cm}^2\text{sec}^{-1}$	

hervorgeht, sind im System  $\text{Pb}-\text{Au}$  auf thermoanalytischem und röntgenographischem Weg die Verbindungen  $\text{Au}_2\text{Pb}$  und  $\text{AuPb}_2$  nachgewiesen worden\*, die gegenseitige Mischbarkeit der reinen Komponenten ist verschwindend (vgl. ref. 7).

### EXPERIMENTELLES

Die Chronoamperogramme der untersuchten wässrigen Depolarisatorlösungen

\* Die Stabilität von  $\text{Au}_2\text{Pb}$  bei tiefen Temperaturen ist umstritten<sup>6</sup>.

(Bleikonzentration:  $0.275 \cdot 10^{-3} < m < 0.536 \cdot 10^{-3}$  mM cm<sup>-3</sup>; Leitelektrolyte: verschiedene, vgl. Tabellen 2 und 4) wurden unter Verwendung eines potentiostatisierten Gleichspannungspolarographen (Radiometer PO<sub>4</sub> mit Hilfspotentiostat) als Potential-Sweep-Kurven

$$i = i_{(t,E)} \quad (1a)$$

mit

$$E = {}_aE - \beta t, \quad 1.67 \leq |\beta| \leq 3.34 \text{ mV sec}^{-1} \quad (1b)$$

registriert, die sich unter Berücksichtigung von (1b) je nach Abscisseneichung in Zeit- oder Spannungseinheiten sowohl als Strom-Zeit-, wie auch als Strom-Spannungs-transienten auswerten lassen. Als polarisierte Goldunterlage diente eine Au-Elektrode

TABELLE 2

DATEN DER BLEIVORSTUFEN AN GOLDUNTERLAGEN (Peaks Nr. I<sub>a</sub> und I<sub>b</sub>)

Leitelektrolyt (0.5 M)	Depolarisator- konzentration (Mole l <sup>-1</sup> · 10 <sup>-4</sup> )	Peakpotentiale gegen ${}_rE_{Pb}$ (mV)				${}^s q$ (mA sec cm <sup>-2</sup> )
		I <sub>a</sub>		I <sub>b</sub>		
		cath	anod	cath	anod	
KCl (pH 4.5)	3.90-5.36	370 ± 10	385 ± 10	180 ± 5	205 ± 5	0.465 ± 0.025
KBr (pH 4.0)	2.75-5.36	300 ± 10	330 ± 15	120 ± 5	160 ± 5	0.420 ± 0.025
KI (pH 5.0)	5.36	300 ± 15	300 ± 15	165 ± 5	175 ± 10	0.435 ± 0.025
NH <sub>4</sub> ClO <sub>4</sub> (pH 4.5)	3.90	380 ± 15	420 ± 15	185 ± 5	210 ± 5	0.445 ± 0.025
HClO <sub>4</sub> (pH 0.5)	5.36	370 ± 10	390 ± 15	200 ± 3	220 ± 3	0.435 ± 0.025
NH <sub>2</sub> SO <sub>3</sub> H (pH 0.5)	3.90	400 ± 10	415 ± 10	200 ± 3	210 ± 3	0.450 ± 0.025
KOH (pH 13.5)	3.90-5.36	380 ± 10	405 ± 15	175 ± 5	210 ± 5	0.460 ± 0.025

vom Kammertyp mit zylindrischem Elektrodenraum (Querschnitt  $A = 0.785$  cm<sup>2</sup>, identisch mit der geometrischen Elektrodenoberfläche; Kammerhöhe  $\delta$  variabel,  $0 \leq \delta \leq 2 \cdot 10^{-2}$  cm). Detaillierte Angaben über Konstruktion und Handhabung der Messanordnung finden sich an anderer Stelle<sup>1,3</sup>. Die in der Elektrodenkammer eingeschlossene Depolarisatormenge  $N_{Me}$  lag in der Regel zwischen 1 und 10 Nanomolen und wurde während eines Einzelversuches jeweils zunächst mit kathodisch steigendem Potential auf der Unterlage abgeschieden ( $\beta > 0$ , kathodischer Durchlauf) und anschliessend, eventuell nach einer Wartezeit  $t_w$  von 1 bis 20 min, mit anodisch ansteigendem Spannungssignal wieder abgelöst ( $\beta < 0$ , anodischer Durchlauf). Die kathodischen und anodischen Teilkurven zeigen die für Kammerpolarogramme charakteristische Peakform (im vorliegenden Fall Mehrfachpeaks) mit

$$i \rightarrow 0 \quad \text{für } t = 0 \text{ und } t \rightarrow \infty^* \quad (2)$$

Ihre (grundstromkorrigierten) Stromintegrale stellen ein Mass für das umgesetzte Depolarisatorquantum dar; im kathodischen Durchlauf z.B. gilt

$$\lim_{t \rightarrow \infty} \int_0^t i dt \equiv q_{\text{cath}} = zFN_{Me} \quad (\text{vgl. ref. 1}) \quad (3)$$

(Vorzeichen von  $i$ : positiv für reduzierende Ströme).

Die Potentialangaben der Kurven und Tabellen beziehen sich entweder auf die gesättigte Kalomelektrode (SCE) oder aber auf das Ruhepotential  ${}_rE_{Me}$  der Messelek-

\* Unter  $i$  wird der durch die Reaktion (i) bedingte, d.h. grundstromkorrigierte Stromfluss verstanden.

trode.  $rE_{Me}$  gibt denjenigen Potentialwert an, bei welchem sich ein stromloses Gleichgewicht zwischen der Depolarisatorlösung der Anfangskonzentration  $m$  und einem ("gesättigten") Me-Niederschlag der Aktivität  $a_{Me} = 1$  auf der Elektrodenoberfläche einstellt:

$$rE_{Me} = {}_0E_{Me} + \frac{RT}{zF} \ln m \quad (4)$$

#### RESULTATE UND DISKUSSION

Diemit *kathodisch ansteigendem* Potential ( $\beta > 0$ ) aufgenommenen Teilkurven der Blei-Chronoamperogramme setzen sich aus drei deutlich getrennten, im Kurven-

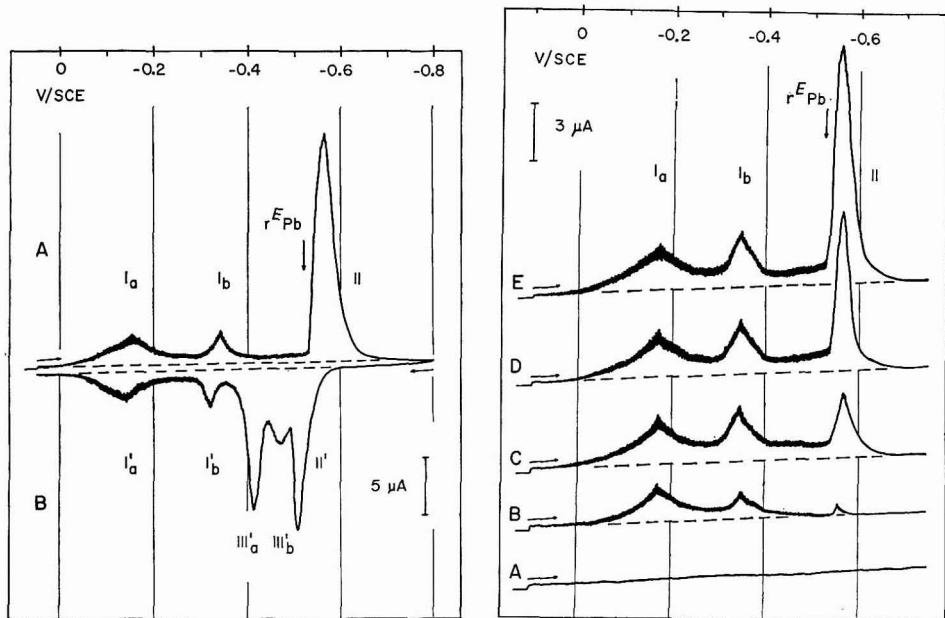


Fig. 1. Strom-Spannungskurve der Depolarisatorabscheidung bzw. Auflösung im System Au-Pb in KCl.

A, Potentialvorschub in kathodischer Richtung (Abscheidungskurve); B, Potentialvorschub in anodischer Richtung (Ablösekurve);  $I_a$ ,  $I_b$ , Kathodische Pb-Vorstufen an Au;  $I_a'$ ,  $I_b'$ , Anodische Pb-Vorstufen an Au; II, II', Kathodische bzw. anodische Pb-Hauptstufe; III $_a'$ , III $_b'$ , Anodische Legierungsstufen; (— — —), Grundstrom;  $rE_{Pb}$ , Ruhepotential einer reinen Pb-Elektrode. Depolarisator:  $3.90 \cdot 10^{-4} M Pb^{2+}$ ; Leitsalz:  $0.5 M KCl$ ; Elektrodenfläche:  $A = 0.785 cm^2$ ; Kammerhöhe:  $\delta = 1.20 \cdot 10^{-2} cm$ ; Durchlaufgeschwindigkeit:  $\beta = 0.1 V/min$ ; Widerstand im Leitkanal:  $R_K = 1100 \Omega$ .

Bei den angegebenen Potentialen wurde die Ohm'sche Spannungskorrektur nicht berücksichtigt.

Fig. 2. Strom-Spannungskurven der Abscheidung von Pb auf Au in Abhängigkeit von der Kammerhöhe  $\delta$  (Potentialvorschub in kathodischer Richtung).

$I_a$ ,  $I_b$ , II und  $rE_{Pb}$  wie in Fig. 1. A, Grundstrom; B,  $0 cm$ ; C,  $3.0 \cdot 10^{-3} cm$ ; D,  $6.0 \cdot 10^{-3} cm$ ; E,  $9.0 \cdot 10^{-3} cm$ . Bei Kurve B entspricht das Kammervolumen dem Restvolumen (vgl. ref. 1). Depolarisator,  $3.06 \cdot 10^{-4} M Pb^{2+}$ ; Widerstand im Leitkanal,  $R_K = 1000-1200 \Omega$ . Leitsalz, Elektrodenfläche und Durchlaufgeschwindigkeit wie in Fig. 1.

Bei den angegebenen Potentialen wurde die Ohm'sche Spannungskorrektur nicht berücksichtigt.



beispiel der Fig. 1 (Kurve A) als Peaks Nr. I<sub>a</sub>, I<sub>b</sub> und II gekennzeichneten Strommaxima zusammen, von denen Nr. I<sub>a</sub> und I<sub>b</sub> auf Grund ihrer Potentiallage gegenüber dem Ruhepotential  $rE_{Pb}$  ( $E > rE_{Pb}$ , vgl. (4)) als Abscheidepeaks einer ungesättigten Bleibedeckung ( $a_{Pb} < 1$ ) zu identifizieren sind und demgemäss in Analogie zur früher eingeführten Terminologie<sup>1,3</sup> als *Vorpeaks* bezeichnet werden, während das Maximum Nr. II in das Stabilitätsgebiet gesättigter Bleiniederschläge ( $a_{Pb} = 1$ ,  $E < rE_{Pb}$ ; *Hauptpeak*) fällt. Der Potentialabstand zwischen den Maxima I<sub>a</sub> bzw. I<sub>b</sub> und  $rE_{Pb}$  beträgt je nach Leitsatz 0.3–0.4 bzw. 0.1–0.2 V (Tabelle 2). Die Kurven lassen bezüglich der Verteilung des kathodischen Gesamtstromintegrals  $q_{cath}$  auf Haupt- und Vorstufen in Abhängigkeit von der Depolarisatormenge  $N_{Pb}$  ein ähnliches Verhalten erkennen wie die Abscheidendurchläufe legierungsfreier Systeme vom Vorstufentyp (vgl. System Tl–Au, ref. 3, Fig. 6). Die im Bereich der Vorpeaks I<sub>a</sub> und I<sub>b</sub> umgesetzte Stromsumme  $i q_{cath}$  strebt mit steigendem  $N_{Pb}$  einem Grenzwert  $s q$  zu, der gleichzeitig den für ein Auftreten des Hauptpeaks (Nr. II) erforderlichen Mindestwert von  $q_{cath}$  darstellt (Fig. 2). Zwischen  $q_{cath}$ ,  $i q_{cath}$  und dem Stromintegral des Hauptpeaks  $ii q_{cath}$  besteht die Beziehung

$$\begin{aligned} i q_{cath} &= q_{cath}, & ii q_{cath} &= 0 & \text{für } q_{cath} \leq s q \\ i q_{cath} &= s q, & ii q_{cath} &= q_{cath} - s q & \text{für } q_{cath} > s q \end{aligned} \quad (5)$$

(vgl. Fig. 3), wobei  $s q$  nach Tabelle 2 in der Grössenordnung des Sättigungsstrom-

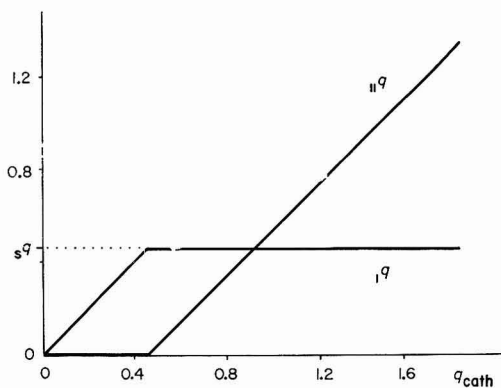


Fig. 3. Verteilung der kathodischen Strommenge auf die einzelnen Stufen des kathodischen Chronoamperogramms nach Gleichung (5).

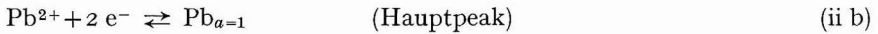
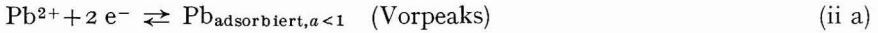
integrals monoatomarer Bleischichten in legierungsfreien Systemen liegt ( $0.42 \text{ mA sec cm}^{-2} \leq s q \leq 0.46 \text{ mA sec cm}^{-2}$ , vgl. ref. 3). Die aus Auftragungen von  $q_{cath}$  gegen  $\delta$  nach

$$z_{Pb} = \frac{d q_{cath}}{m_{Pb} F A d \delta} \quad (\text{vgl. ref. 3, Gl. (22)}) \quad (6)$$

ermittelte Ladungsaufnahme pro Bleiion weicht im gesamten Bedeckungsgebiet um höchstens  $\pm 5\%$  vom theoretischen Wert  $z_{Pb} = 2$  ab\*. Die beiden Vorpeaks werden daher der Ausbildung einer metallischen Monoschicht zugeordnet, und es wird angenommen, dass bei der Reduktion des  $Pb^{2+}$ , ähnlich wie bei der Bleiabscheidung auf Ag- und Cu-Unterlagen, an der Goldelektrode zunächst ein monoatomares Blei-

\* Ueberschusseffekte<sup>3,4</sup> wurden auch in Halogenidlösungen nicht beobachtet.

adsorbat entsteht, das nach Ueberschreiten des Ruhepotentials in eine Bedeckung der Aktivität  $a_{\text{Pb}} = 1$  übergeht:



Die aus Scheinaktivitätsmessungen<sup>3</sup> berechnete Aktivitätsisotherme der Monoschicht

$$\lg a_{\text{Pb}} = f(y/sy) \quad (7)$$

( $y$ : Oberflächenkonzentration des Pb-Adsorbats;  $sy$ : Sättigungswert von  $y$ ) hat die Form einer Doppelsigmoiden mit zwei verhältnismässig flachen Stufen bei  $\lg a_{\text{Pb}} \approx -6$  und  $\lg a_{\text{Pb}} \approx -13$ , die den Aktivitätsniveaus im Potentialintervall der Vorpeaks  $I_a$  und  $I_b$  entsprechen (Fig. 4).

Von den beiden genannten, in der kathodischen Teilkurve unterscheidbaren

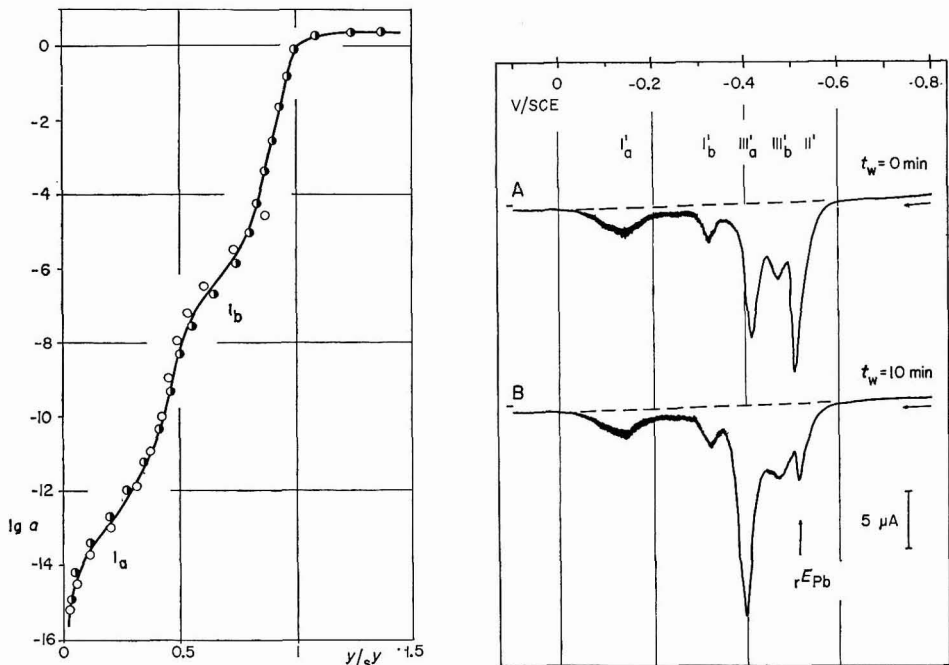


Fig. 4. Aktivitätsisotherme des Bleiniederschlags auf einer Goldelektrode als Funktion der Bedeckung.

(●), kathodische Scheinaktivität; (○), anodische Scheinaktivität (bis zum Beginn der Legierungsbildung, vgl. Fig. 1); (—), reversible Aktivität  $a_{\text{Pb}}$ . Messfehlerspanne:  $\pm 3 \text{ mV} \triangleq 0.2$  logarithmische Einheiten.  $sy = 2.34 \cdot 10^{-9} \text{ Mole} \cdot \text{cm}^{-2}$ ;  $\triangleq sq = 0.460 \text{ mA sec cm}^{-2}$ .  $I_a, I_b$ , Aktivitätsniveaus der Vorstufen  $I_a$  und  $I_b$ .

Die Aktivitätsisotherme wurde aus der Strom-Spannungskurve der Fig. 1 berechnet.

Fig. 5. Einfluss der Wartezeit  $t_w$  auf die Kurvenform des anodischen Durchlaufes.  $I_a', I_b'$ , anodische Pb-Vorstufen an Au;  $II'$ , anodische Pb-Hauptstufe;  $III_a', III_b'$ , Legierungsstufen;  $\rightarrow$ , Potentialvorschub; (— — —), Grundstrom;  $rE_{\text{Pb}}$ , Ruhepotential einer reinen Pb-Elektrode; Kurven A und B, frisch abgedrehte Elektrodenoberfläche. Experimentelle Bedingungen wie Fig. 1.

Bei den angegebenen Potentialen wurde die Ohm'sche Spannungskorrektur nicht berücksichtigt.

konsekutiven Abscheidungsformen  $Pb_{\text{adsorbiert}, a < 1}$  und  $Pb_{a=1}$  tritt bei der Ablösung der Bleibedeckung im *anodischen Potentialdurchlauf* ( $\beta < 0$ , Kurve B in Fig. 1) lediglich die Monoschicht mit unveränderter Aktivitätscharakteristik wieder in Erscheinung (vgl. die anodischen Scheinaktivitäten in Fig. 4). Ihr oxydativer Abbau nach (ii a) führt zur Ausbildung der anodischen Maxima  $I_a'$  und  $I_b'$ , die sich in Übereinstimmung mit dem durch die Theorie<sup>3</sup> geforderten Verhalten von Monoschichtvorstufen von den kathodischen Peaks  $I_a$  und  $I_b$  praktisch nur durch das Stromvorzeichen unterscheiden, während Peakpotential, Höhe und Absolutwert des Stromintegrals annähernd erhalten bleiben. Im Gegensatz dazu geht die gesättigte Bedeckung während oder nach der Abscheidung im kathodischen Hauptpeak teilweise in einen neuen ungesättigten, vom Monoschichtadsorbat jedoch verschiedenen Zustand der Aktivität  $a_{Pb} < 1$  über, da das anodische Gegenstück zum Maximum Nr. II als *anodischer Hauptpeak* (Nr. II' in Kurve B der Fig. 1) zwar nachgewiesen werden kann, bezüglich seines Stromintegrals  $IIq_{\text{anod}}$  aber wesentlich hinter dem entsprechenden kathodischen Wert  $IIq_{\text{cath}}$  zurückbleibt (Tabelle 3). Dafür treten eine Reihe

TABELLE 3

BEISPIEL FÜR DIE STROMINTEGRALAUFTEILUNG AUF DIE EINZELNEN PEAKS

	Peak Nr.	Stromintegral (mA sec cm <sup>-2</sup> )	Summe (mA sec cm <sup>-2</sup> )
Kathodischer Durchlauf	$I_a$	} $Iq_{\text{cath}} = 0.460$ $IIq_{\text{cath}} = 0.760$	} $q_{\text{cath}} = 1.220$
	$I_b$		
	II		
Anodischer Durchlauf	$I_a'$	} $Iq_{\text{anod}} = 0.400^a$ $IIq_{\text{anod}} = 0.350$ $IIIq_{\text{anod}} = 0.490$	} $q_{\text{anod}} = 1.240^b$ $\Sigma = 0.840$
	$I_b'$		
	II'		
	III <sub>a, b'</sub>		

<sup>a</sup> Der Unterschied von  $Iq_{\text{cath}}$  und  $Iq_{\text{anod}}$  ist auf Unsicherheiten in der Abgrenzung der anodischen Vorstufe zurückzuführen.

<sup>b</sup> Der Wert von  $q_{\text{anod}}$  liegt wegen Nachdiffusion von Depolarisator  $Pb^{2+}$  in die Kammer (vgl. ref. 1) etwas höher als derjenige von  $q_{\text{cath}}$ .

zusätzlicher, elektropositiverer Ablösepeaks auf (in der Regel zwei, Nr. III<sub>a'</sub> und III<sub>b'</sub> in Fig. 1), die das Potentialgebiet zwischen den Maxima  $I_b'$  und II' ausfüllen und in deren Bereich offenbar die neu entstandene ungesättigte Bedeckung wieder abgebaut wird. Diese Peaks haben folgende Eigenschaften:

1) Die Summe ihrer Stromintegrale  $IIIq_{\text{anod}}$  ist annähernd gleich der Differenz zwischen  $IIq_{\text{anod}}$  und  $IIq_{\text{cath}}$ :

$$|IIIq_{\text{anod}}| = |IIq_{\text{cath}}| - |IIq_{\text{anod}}| \quad (\text{vgl. Tab. 3}) \quad (8)$$

2) Mit zunehmender Wartezeit  $t_w$  zwischen der Aufnahme der kathodischen und anodischen Teilkurven wächst  $IIIq_{\text{anod}}$  auf Kosten von  $IIq_{\text{anod}}$  (Fig. 5).

3) Es existiert kein Sättigungswert für  $IIIq_{\text{anod}}$ .

Letzteres wird insbesondere durch Ablösedurchläufe nach extremer kathodischer Vorpolarisation in der offenen Kammer illustriert ( $\delta \rightarrow \infty$ ), bei denen die abgeschiedene Bleimenge 20–50 Monoschichten erreicht. Der im Bereich der Peaks

III<sub>a'</sub> und III<sub>b'</sub> umgesetzte Anteil der anodischen Gesamtstrommenge geht in KCl-Leitelektrolyt bei  $t_w$ -Werten um 5 min bis gegen 90% der Gesamtbedeckung, d.h. ca. 25 Monoschichten, ohne dass eine Sättigung zu beobachten wäre (Fig. 6).

Sowohl die zeitliche Veränderlichkeit der Peaks III<sub>a'</sub> und III<sub>b'</sub> als auch das Fehlen einer Sättigungsschranke legen den Schluss nahe, dass das durch die Strommenge III $q_{anod}$  anodisch abgelöste ungesättigte Umwandlungsprodukt der primären

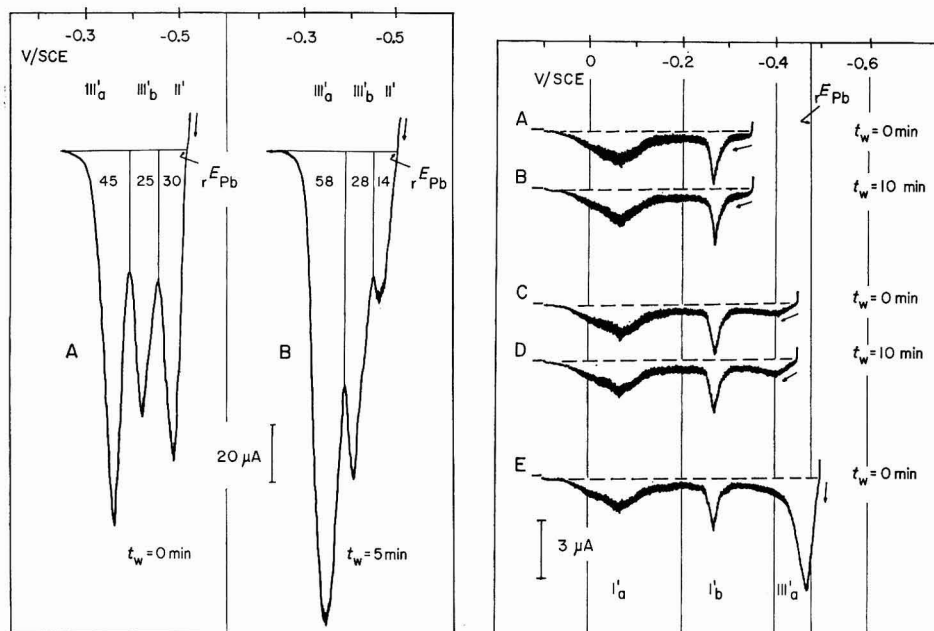


Fig. 6. Anodische Ablösekurven nach extremer Vorpolarisation in der offenen Kammer.

Legende vgl. Fig. 5.

Die in den Streifen innerhalb der Ablösefläche angegebenen Zahlen bezeichnen die prozentualen Anteile der gesamten Ablösefläche, welche auf die einzelnen Stufen entfallen. Stromintegrale der gesamten Ablösefläche,  $q_A = 8.9$  mC;  $q_B = 10.3$  mC. Depolarisator,  $5.3 \cdot 10^{-4}$  M Pb<sup>2+</sup>; Kammerhöhe,  $\delta \rightarrow \infty$ ; Widerstand, 30  $\Omega$ . Leitsalz, Elektrodenfläche und Durchlaufgeschwindigkeit wie in Fig. 1.

Fig. 7. Ablösekurven bei verschiedenen kathodischen Potentialen der Vorpolarisation und verschiedenen Wartezeiten  $t_w$ .

I<sub>a'</sub>, I<sub>b'</sub>, anodische Pb-Vorstufen an Au; III<sub>a'</sub>, positivere Legierungsstufe;  $\rightarrow$ , Potentialvorschub; (— — —), Grundstrom;  $r_{EPb}$ , Ruhepotential einer reinen Pb-Elektrode. Kurven A und B,  $_{pot}E = +0.130$  V vs.  $r_{EPb}$ ; Kurven C und D,  $+0.030$  V; Kurve E,  $-0.020$  V. Leitelektrolyt, 0.5 M NH<sub>2</sub>SO<sub>3</sub>H; Kammerhöhe,  $\delta = 5.0 \cdot 10^{-3}$  cm; Widerstand im Leitkanal,  $R_K = 400$   $\Omega$ . Depolarisator, Elektrodenfläche und Durchlaufgeschwindigkeit wie in Fig. 1.

kathodischen Hauptpeakabscheidung als *Legierungsschicht* vorliegt, die durch eine der Kationenentladung (ii b) nachgelagerte Reaktion mit der Goldunterlage entstanden ist:



Die Aufspaltung des zugehörigen Ablösepeaks in ein Doppelmaximum deutet auf die Existenz zweier diskreter Aktivitätsniveaus dieser Legierungsbedeckung hin, von denen das elektropositivere ( $\triangle$  Peak III<sub>a'</sub>) einer goldreicheren, das elektronega-

tivere ( $\triangle$  Peak III<sub>b'</sub>) einer bleireicheren Phase entsprechen sollte. Ob es sich dabei um die beiden Verbindungen Au<sub>2</sub>Pb und AuPb<sub>2</sub> handelt, kann bislang nicht entschieden werden, da eine röntgenographische Identifikation der Elektrodenbeläge bei Niederschlagsmengen um 50 Monoschichten durch die grosse Oxydationsempfindlichkeit solcher dünnster Bleiüberzüge sehr erschwert wird. Versuche einer Zuordnung der Peaks anhand ihrer Spitzenpotentiale (Tabelle 4) durch Vergleich mit Potentialmessungen an thermisch hergestellten Pb–Au-Legierungen sind im Gang. WEAVER UND BROWN<sup>8</sup> haben durch Elektronenbeugung nachgewiesen, dass sich kombinierte Pb–Au-Aufdampfschichten bei Zimmertemperatur in die Verbindung AuPb<sub>2</sub> umwandeln, wobei die Reaktionsgeschwindigkeit wahrscheinlich durch die relativ rasche Diffusion des Au in die Bleimatrix bzw. in die Au–Pb-Mischphase bestimmt wird (Bruttodiffusionskoeffizient<sup>8</sup> bei 20°:  $1.89 \cdot 10^{-14}$  cm<sup>2</sup> sec<sup>-1</sup>). Allem Anschein nach

TABELLE 4

POTENTIALDATEN DER LEGIERUNGSSTUFEN III<sub>a'</sub> UND III<sub>b'</sub> IN DER OFFENEN KAMMER GEGEN  $rE_{Pb}$ 

Leitelektrolyt (0.5 M)	$rE_{Pb}$ (mV vs. SCE)	Peakpotentiale (mV vs. $rE_{Pb}$ )	
		III <sub>b'</sub>	III <sub>a'</sub>
KCl	-520 ± 3	105 ± 5	175 ± 5
KBr	-535 ± 3	135 ± 5	185 ± 10
NH <sub>4</sub> ClO <sub>4</sub>	-475 ± 3	115 ± 5	170 ± 5
KNO <sub>3</sub>	-500 ± 3	100 ± 5	155 ± 5
HClO <sub>4</sub>	-470 ± 3	110 ± 5	190 ± 10
NH <sub>2</sub> SO <sub>3</sub> H	-480 ± 3	110 ± 5	190 ± 10
KOH	-830 ± 3	145 ± 5	200 ± 5

folgt die Legierungsbildung unter chronoamperometrischen Bedingungen einem ähnlichen Mechanismus; die Annahme einer Reaktion zwischen der Goldbasis und einer zumindest als wachstumsfähiger Keim vorhandenen Pb-Phase der Aktivität  $a_{Pb} = 1$  entsprechend der in (iii) gewählten Formulierung wird durch die Beobachtung gestützt, dass der Legierungsvorgang nur im Stabilitätsgebiet gesättigter Bleiniederschläge ( $a_{Pb} = 1$ ,  $E \leq rE_{Pb}$ ) mit messbarer Geschwindigkeit abläuft und Legierungsstufen im kathodischen Kurvendurchlauf durchweg fehlen. Auch eine länger andauernde kathodische Vorpolarisation bei Potentialen oberhalb des Blei-Ruhepotentials  $rE_{Pb}$  führt lediglich bis zur Monoschichtbedeckung; werden beispielsweise frische Goldelektroden bei konstantem Potential  $p_{01}E$  kathodisch vorpolarisiert, so treten in einer unmittelbar anschliessend aufgenommenen Ablösekurve die Legierungspeaks III<sub>a'</sub> und III<sub>b'</sub> nur dann in Erscheinung, wenn  $p_{01}E$  der Bedingung

$$p_{01}E < rE_{Pb} \quad (9)$$

entspricht. Andernfalls sind nur die Ablösestufen der Monoschicht (I<sub>a'</sub> und I<sub>b'</sub>) festzustellen (Fig. 7).

Die Umwandlungsgeschwindigkeit der primären Bleibedeckung wird bisherigen qualitativen Beobachtungen nach durch folgende Faktoren beeinflusst:

1) durch Stromstärke und Stromintegral bei der primären Bleiabscheidung (Geschwindigkeitserhöhung bei intensiverter kathodischer Belastung der Elektrodenoberfläche während des Abscheidevorganges),

TABELLE 5  
BEOBACHTUNGEN VERSCHIEDENER AUTOREN, WELCHE AUF LEGIERUNGSBILDUNG BEI DER METALLABSCHIEDUNG AUF FREMDMETALLELEKTRODEN HINWEISEN

System	Methode		Autoren	Beobachtete Erscheinungen	Bemerkungen
	Unterlage	Depolarisator-metalle			
Au, Pt	Ni	Chronoamperometrie	NICHOLSON <sup>11</sup>	Multiple Stripping-Peaks	—
Pt	Ag, Cu, Pb	Chronopotentiometrie	NICHOLSON <sup>12</sup>	Unterspannung bei der anodischen Ablösung	Als Monoschichten gedeutet
Pt	Pb	Voltammetrie	HEYNDRICKX <sup>13</sup>	Multiple Stripping-Peaks	—
Pt	Pb	Polarographie	SCHMIDT, MOSER UND RIESEN <sup>14</sup>	Multiple Stripping-Peaks	Metallische Monoschicht nicht nachgewiesen
Pt	Cd	Oszillographische Polarographie	BERZINS UND DELAHAY <sup>15</sup>	Abscheidungsunterspannungen	—
Pt	Cu	Zyklische Chronoamperometrie	KUBLIK <sup>16</sup>	Abscheidungsunterspannungen	Als Monoschichteffekt gedeutet

- 2) durch das Leitanion (Geschwindigkeitszunahme parallel der Anionenreihe  $\text{KCl} < \text{NH}_4\text{ClO}_4, \text{KNO}_3 < \text{KBr}, \text{HClO}_4 < \text{KI} < \text{NH}_2\text{SO}_3\text{H}, \text{KOH}$ ),  
 3) durch einen Memory-Effekt der Elektrodenoberfläche (Geschwindigkeitszunahme bei mehrmaliger Abscheidung auf der gleichen Goldelektrode ohne mechanische Zwischenreinigung, vgl. Fig. 8).

Diese Befunde können als Hinweis darauf angesehen werden, dass die Kinetik der Reaktion (iii) von den Bedingungen abhängt, unter denen innerhalb der fertig

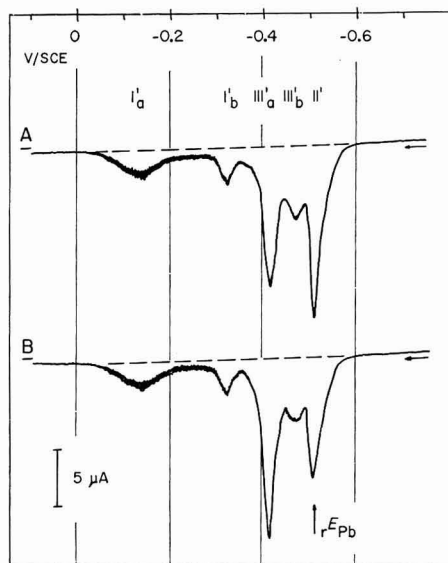


Fig. 8. Einfluss des Memory-Effektes auf die Form der Strom-Spannungskurve im Ablösedurchlauf.

$I'_a, I'_b$ , anodische Pb-Vorstufen an Au;  $II'$ , anodische Pb-Hauptstufe;  $III'_a, III'_b$ , Legierungsstufen;  $\rightarrow$ , Potentialvorschub; (— — —), Grundstrom;  $rE_{Pb}$ , Ruhepotential einer reinen Pb-Elektrode. A, 1. Durchlauf, Elektrodenoberfläche frisch abgedreht; B, 2. Durchlauf, ohne mechanische Zwischenbearbeitung der Goldoberfläche. Experimentelle Bedingungen wie Fig. 1.

Bei den angegebenen Potentialen wurde die Ohm'sche Spannungskorrektur nicht berücksichtigt.

ausgebildeten Blei-Monoschicht die Nukleation der primären Blei-Hauptpeakbedeckung erfolgt. Letztere liegt, vor allem bei Bruttobedeckungen in der Größenordnung weniger Monoschichten, kaum als kohärenter Metallfilm vor, sondern besteht aus isolierten Keimbezirken\*, deren Zahl (bei gegebener Gesamtbleimenge) die effektive Kontakt- und Reaktionsfläche zwischen Niederschlag und Unterlage bestimmt. Einflüsse, die eine Erhöhung der Keimzahl der Primärschicht zur Folge haben (Erhöhung der Abscheidungsüberspannung, Veränderungen in allfälligen Anionenadsorbaten, Restkeime früherer Bleibedeckungen), sollten daher eine beschleunigende Wirkung auf die Pb-Au-Legierungsreaktion ausüben, was durch die

\* Insuläre Strukturen in ultradünnen elektrolytischen Metallfilmen sind aus Untersuchungen von DICKSON, JACOBS UND PASHLEY am System Au-Ag bekannt<sup>9</sup>.

oben angeführten Beobachtungen bestätigt wird. Ueber quantitative Zusammenhänge wird bei späterer Gelegenheit berichtet.

Es stellt sich die Frage, ob die beschriebenen chronoamperometrischen Phänomene, nämlich die konsekutive Bildung von Metallmonoschichten und Legierungsphasen auf der gleichen Unterlage, auf das System Pb–Au beschränkt bleiben, oder ob analoge Erscheinungen unter vergleichbaren Versuchsbedingungen\* auch bei anderen Me–Me<sub>a</sub>-Kombinationen auftreten. Eine Reihe experimenteller Beobachtungen verschiedener Autoren, insbesondere das Auffinden multipler Stripping-Peaks ähnlich den Pb-Maxima II', III<sub>a</sub>' und III<sub>b</sub>' bei der anodischen Untersuchung von Metallniederschlägen, lässt sich durch eine Legierungsbildung während oder nach der Abscheidung erklären; in den meisten der in Tabelle 5 aufgeführten Fälle ist jedoch über die Existenz der Monoschichtstufe nichts Sicheres bekannt. Nach eigenen Versuchen führt die *Wismut*-Abscheidung auf Au (System Au–Bi mit Verbindung<sup>7</sup> Au<sub>2</sub>Bi, Existenz bei tiefen Temperaturen umstritten<sup>10</sup>) über eine Monoschicht, doch ist hier der Legierungspeak nur bei geringer Bruttobedeckung und grosser Wartezeit vor dem Ablösedurchlauf nachzuweisen.

Die Arbeit wurde mit Unterstützung des Schweizerischen Nationalfonds zur Förderung der Wissenschaftlichen Forschung durchgeführt. Wir danken Herrn Prof. K. HUBER für sein unseren Untersuchungen entgegengebrachtes Interesse.

#### SUMMARY

The reduction of lead from aqueous solutions on the surface of gold electrodes is studied chronoamperometrically using a thin-layer technique employing a chamber type cell. The current balance of the deposition or dissolution of lead on the electrode is verified by coulometrical evaluation of the chronoamperograms.

In the binary system Pb–Au there exist at room temperature two intermediate phases, namely Au<sub>2</sub>Pb and AuPb<sub>2</sub>.

The lead deposited on gold forms at first a metallic monolayer, defined as a layer of electrically neutral lead atoms at the electrode–electrolyte interface, the deposit having the appropriate thickness of one atomic diameter of lead. The activity isotherm of lead,  $a_{Pb}$ , depends upon the coverage of the electrode within the monolayer region. The existence of the unsaturated (submonoatomic) coverage of the gold electrode leads to the splitting of the cathodic current transient into a so-called prewave region, within which the activity of the metal is less than unity, and a main peak with unit activity of the electrodeposited depolarizer.

The formation of Au–Pb alloys only happens when the lead coverage reaches unit activity. The alloying of the lead deposited cathodically in the main peak gives rise during the anodic stripping to two new dissolution peaks of unsaturated lead layers, besides the current maxima of the main peak and the prewave region.

As opposed to the prewave peaks, the shape and current-integral values of these intermediate peaks are found to be functions of various experimental parameters, for instance of the time interval between cathodic deposition and anodic stripping of the lead deposit.

\* Es wird Zimmertemperatur vorausgesetzt; das Verhalten der Systeme bei höherer Arbeitstemperatur (Salzschmelzenpolarographie) bleibt hier ausser Betracht.



## LITERATUR

- 1 E. SCHMIDT UND H. R. GYGAX, *Helv. Chim. Acta*, 48 (1965) 1178.
- 2 E. SCHMIDT UND H. R. GYGAX, *Helv. Chim. Acta*, 48 (1965) 1584.
- 3 E. SCHMIDT UND H. R. GYGAX, *J. Electroanal. Chem.*, 12 (1966) 300.
- 4 E. SCHMIDT, H. R. GYGAX UND P. BOEHLER, *Helv. Chim. Acta*, 49 (1966) 733.
- 5 E. SCHMIDT UND H. R. GYGAX, *Helv. Chim. Acta*, 49 (1966) 1105.
- 6 O. J. KLEPPA UND D. F. CLIFTON, *Acta Cryst.*, 4 (1951) 74.
- 7 M. HANSEN UND K. ANDERKO, *Constitution of Binary Alloys*, McGraw-Hill, New York, 1958, S. 188 und 222.
- 8 C. WEAVER UND L. C. BROWN, *Phil. Mag.*, 8 (1963) 1379.
- 9 E. W. DICKSON, M. H. JACOBS UND D. W. PASHLEY, *Phil. Mag.*, 11 (1965) 575.
- 10 N. E. ALEKSEEVSKII, G. S. ZHDANOV UND N. N. ZHURAVLEV, zitiert nach *C.A.*, 49 (1955) 5050.
- 11 M. M. NICHOLSON, *Anal. Chem.*, 32 (1960) 1058.
- 12 M. M. NICHOLSON, *J. Am. Chem. Soc.*, 79 (1957) 7.
- 13 A. HEYDRICKX, *Bull. Soc. Chim. Belg.*, 63 (1954) 82.
- 14 E. SCHMIDT, P. MOSER UND W. RIESEN, *Helv. Chim. Acta*, 46 (1963) 2285.
- 15 T. BERZINS UND P. DELAHAY, *J. Am. Chem. Soc.*, 75 (1953) 555.
- 16 Z. KUBLIK, *J. Electroanal. Chem.*, 5 (1963) 450.
- 17 W. SEITH, *Diffusion in Metallen*, Springer Verlag, Berlin, 1955, S. 42.

*J. Electroanal. Chem.*, 13 (1967) 378-389

## INFLUENCE OF THE SOLVENT SYSTEM ON THE ORIENTATION OF 3-BUTENENITRILE AND 3-DIMETHYLAMINOPROPIONITRILE IN THE CO-ORDINATION SPHERE OF COPPER(I) AND SILVER IONS

FLOYD FARHA, JR. AND REYNOLD T. IWAMOTO

*Department of Chemistry, University of Kansas, Lawrence, Kansas (U.S.A.)*

(Received April 7th, 1966)

In a previous study<sup>1</sup>, it was shown that in solvents containing both hydroxy and the nitrile groups (hydracrylonitrile and alcohol-aliphatic nitrile mixtures) the particular functional group that co-ordinates to copper(II) ion is determined by the polar characteristic of the medium. The compatibility of the solvated species with the solvent appears to be an important factor in determining whether hydroxy groups or nitrile groups co-ordinate to the metal ion. In a polar medium, the mode of coordination favored is that which results in the formation of the more polar of the two possible solvated species. In a non-polar medium, the reverse is true.

In this regard, 3-butenitrile and 3-dimethylaminopropionitrile also are interesting solvents. They each contain two functional groups of markedly different polar characteristics but of closely similar co-ordinating ability for copper(I) and silver(I) ions. In this paper, we deal with the question of which functional group of 3-butenitrile and of 3-dimethylaminopropionitrile co-ordinates to these metal ions in a particular medium. For this study, use has been made of the potentials of the copper(I)-copper and the silver(I)-silver couples in the pure solvents and in mixed solvents of widely differing polar characteristics. The results of previous voltammetric studies on the solvation of copper(I) and silver ions in nitriles<sup>1-5</sup> and olefins<sup>1,6</sup> and of those on tertiary amines carried out in connection with this investigation also, have been used. From these studies of solutions of copper(I) and silver ions in nitriles, olefins, and tertiary amines, the relative solvation energies of copper(I) and silver ions in the three types of solvents appear to be tertiary amines > nitriles  $\gg$  olefins. Infrared and proton nuclear magnetic resonance studies have been carried out to substantiate and, in some cases, to clarify the information derived from the voltammetric data.

## EXPERIMENTAL

The organic solvents were purified by treatment with appropriate reagents followed by fractional distillation. Practical-grade propionitrile from Eastman Kodak Co. was distilled first from calcium hydride, then from a small amount of phosphorus(V) oxide. Propylene carbonate (practical grade, J. T. Baker Chemical Co.), 3-butenitrile (Eastman White Label), 3-dimethylaminopropionitrile (Eastman White Label), and  $\beta$ -dimethylaminoisopropyl acetate (purest available, Aldrich Chemical Co.) were purified by passage, first through a 2.5-cm (i.d.)  $\times$  55-cm column

of mixed acidic and basic Woelm chromatographic alumina, activity grade 1, then through a similar column of neutral Woelm chromatographic alumina, activity grade 1, and finally by fractional distillation under reduced pressure. The purest available 1,2-dichloroethane from Matheson, Coleman and Bell was purified by the same chromatographic procedure, followed by fractional distillation at atmospheric pressure.

Hexaaquocopper(II) perchlorate and anhydrous silver(I) perchlorate (both G. F. Smith Chemical Co.) were dried *in vacuo* at 70° and stored over anhydrous magnesium perchlorate. The dried copper salt was analysed and found to be, approximately, the trihydrate. Tetrakis(acetonitrile)copper(I) perchlorate was obtained by the reaction of copper metal with copper(II) perchlorate in acetonitrile. The solvated copper(I) salt was collected on a sintered-glass filter and dried in a vacuum oven at room temperature. Tetraethylammonium perchlorate ((C<sub>2</sub>H<sub>5</sub>)<sub>4</sub>NClO<sub>4</sub>) was prepared by the neutralization of 10% tetraethylammonium hydroxide solution (Eastman) with 70% reagent-grade perchloric acid. The salt was recrystallized six times from water, and dried *in vacuo* at 70°. Tetrabutylammonium perchlorate<sup>7</sup> and tris(4,7-dimethyl-1,10-phenanthroline)iron(II) perchlorate<sup>8</sup> were prepared as described previously. Ferrocene (Aldrich Chemical Co. product) was purified by sublimation<sup>9</sup>.

One-tenth formal (0.10 *F*) tetraethylammonium perchlorate solutions *ca.* 5 · 10<sup>-4</sup> *F* in copper(II) or silver(I) perchlorate were used in the electrochemical study. Tetrakis(acetonitrile)copper(I) perchlorate was substituted for copper(II) perchlorate in the tertiary amine solvents because of the insolubility of the copper(II) salt. All solutions were deoxygenated with purified nitrogen and protected from atmospheric oxygen and moisture during the course of measurement by passing nitrogen over the surface.

Current-voltage curves were obtained with a Kelley-Jones-Fisher<sup>10,11</sup> controlled-potential polarograph. The polarographic cell and electrodes are similar to those used previously<sup>1</sup>. All solutions were examined at 25 ± 1°.

The infrared spectral data were obtained with a Perkin-Elmer Model 421 spectrophotometer. The proton NMR studies were carried out with a Varian Model A-60 spectrophotometer with tetramethylsilane as the internal standard.

A calibration curve of dielectric constant *vs.* capacitance reading of a Sargent Model V chemical oscillator was used to obtain the dielectric constants of solvents for which no literature values are available.

## RESULTS

The pertinent electrochemical data on the behavior of copper and silver ions at the dropping mercury electrode and at the rotating platinum electrode, in 3-butenitrile, 3-dimethylaminopropionitrile, mixtures of each of these nitriles with propylene carbonate and with 1,2-dichloroethane, and several other solvents of importance in this study, are summarized in Table 1. Each potential has been adjusted to correct for differences in liquid-junction potential among the solvents<sup>8</sup>. Propionitrile 0.10 *F* in (C<sub>2</sub>H<sub>5</sub>)<sub>4</sub>NClO<sub>4</sub> has been selected as the reference solvent.  $E_{\text{corr.}} = E_{\frac{1}{2} \text{ oxid. of tris(4,7-dimethyl-1,10-phenanthroline)iron(II) (propionitrile 0.10 } F \text{ in (C}_2\text{H}_5)_4\text{NClO}_4) - E_{\frac{1}{2} \text{ oxid. of tris(4,7-dimethyl-1,10-phenanthroline)iron(II) (solvent) or } E_{\text{corr.}} = E_{\frac{1}{2} \text{ oxid. of ferrocene (propionitrile 0.10 } F \text{ in (C}_2\text{H}_5)_4\text{NClO}_4) - E_{\frac{1}{2} \text{ oxid. of ferrocene (solvent). Table 2 contains the half-$

TABLE 1  
ELECTROCHEMICAL BEHAVIOR OF COPPER IONS AND SILVER ION IN 3-BUTENENITRILE, 3-DIMETHYLAMINOPROPIONITRILE AND OTHER PERTINENT SOLVENTS<sup>a, b, c, d</sup>

$E^f$	Solvent <sup>e</sup>	$E_{\frac{1}{2}Cu(t), Cu(t)}^{m, o}$	$E_{Cu(t), Cu}^{m, p}$	$E_{\frac{1}{2}Cu(t), Cu(Hg)}^{n, q}$	$E_{Ag(t), Ag}^{m, r}$	$E_{\frac{1}{2}Ag(t), Cu(Hg)}^{n, s}$
27.2	Propionitrile (PrCN)	+1.00	-0.260	-0.270	+0.400	+0.470
52.3	50% PrCN-50% PrCO <sub>3</sub> <sup>g</sup>	+1.095	-0.177	-0.193	+0.473	+0.558
59.8	30% PrCN-70% PrCO <sub>3</sub>	+1.121	-0.100	-0.126	+0.507	+0.618
20.3	50% PrCN-50% DCE <sup>h</sup>	+1.051	-0.195	-0.224	+0.461	+0.496
16.3	30% PrCN-70% DCE	+1.009	-0.174	-0.200	+0.457	+0.513
25.3	3-Butenenitrile (BuCN)	+1.038	-0.250	-0.262	+0.438	+0.470
50.6	50% BuCN-50% PrCO <sub>3</sub>		-0.147	-0.140	+0.457	+0.582
59.8	30% BuCN-70% PrCO <sub>3</sub>		+0.111	+0.114	+0.570	>+0.661
18.4	50% BuCN-50% DCE		-0.101	-0.105	+0.467	+0.514
15.0	30% BuCN-70% DCE	+1.090	-0.181	-0.176	+0.445	+0.545
20.8	3-Dimethylaminopropionitrile (DMAP)		-0.452	-0.447	+0.116	>-0.111
49.2	50% DMAP-50% PrCO <sub>3</sub>		-0.302	-0.299	+0.256	>+0.161
58.8	30% DMAP-70% PrCO <sub>3</sub>		-0.268	-0.264	+0.283	>+0.161
17.0	50% DMAP-50% DCE		-0.291	-0.305	+0.254	>-0.061
14.5	30% DMAP-70% DCE <sup>1</sup>		-0.236	-0.225	+0.320	>-0.051
32.5	50% $\beta$ -Dimethylaminoisopropyl acetate-50% PrCO <sub>3</sub>		-0.302	-0.261	+0.277	>+0.191
69	PrCO <sub>3</sub>	+0.680 <sup>n</sup>		+0.585	+0.804	>+0.771
21.6	Allyl alcohol <sup>1, k</sup>			+0.030		+0.530

<sup>a</sup> 0.10 F (C<sub>2</sub>H<sub>5</sub>)<sub>4</sub>NClO<sub>4</sub> soln. <sup>b</sup> All  $E$ -values are *vs.* S.C.E. <sup>c</sup> All  $E$ -values are the average of two or more runs. <sup>d</sup> Each  $E$ -value has been corrected for junction p.d. between the solvent system *vs.* S.C.E. and propionitrile-0.10 F (C<sub>2</sub>H<sub>5</sub>)<sub>4</sub>NClO<sub>4</sub> *vs.* S.C.E. (see RESULTS). <sup>e</sup> % by volume. <sup>f</sup> Dielectric constant. <sup>g</sup> Propylene carbonate. <sup>h</sup> 1,2-Dichloroethane. <sup>i</sup>  $E$  dissolution of Hg. <sup>j</sup> Taken from ref. 6. <sup>k</sup> 0.10 F LiClO<sub>4</sub> soln. <sup>l</sup> 0.10 F (C<sub>4</sub>H<sub>9</sub>)<sub>4</sub>NClO<sub>4</sub> soln. <sup>m</sup> Obtained with the rotating platinum electrode. <sup>n</sup> Obtained with the dropping mercury electrode. <sup>o</sup>, <sup>p</sup>, <sup>q</sup>, <sup>r</sup>, <sup>s</sup> Slope of  $E$  *vs.*  $\log (i_a - i)/i$  or  $\log (i_a - i)$  plot: <sup>o</sup> 0.063  $\pm$  0.003, <sup>p</sup> 0.059  $\pm$  0.004, <sup>q</sup> 0.058  $\pm$  0.003, <sup>r</sup> 0.063  $\pm$  0.006, <sup>s</sup> 0.058  $\pm$  0.002.

TABLE 2

HALF-WAVE POTENTIALS FOR THE OXIDATION OF TRIS(4,7-DIMETHYL-1,10-PHENANTHROLINE) IRON(II) PERCHLORATE AND FERROCENE<sup>a, b</sup>

$\epsilon^d$	Solvent <sup>c</sup>	4,7-Dimethylferroin $E_{1/2}$ vs. S.C.E. <sup>j</sup>	Ferrocene $E_{1/2}$ vs. S.C.E. <sup>k</sup>
27.2	Propionitrile (PrCN)	+0.960	+0.444
52.3	50% PrCN-50% PrCO <sub>3</sub> <sup>e</sup>	+0.937	
59.8	30% PrCN-70% PrCO <sub>3</sub>	+0.909	
20.2	50% PrCN-50% DCE <sup>f</sup>	+0.966	
16.3	30% PrCN-70% DCE	+1.008	
25.3	3-Butenenitrile (BuCN)	+0.967	
50.6	50% BuCN-50% PrCO <sub>3</sub>	+0.950	
59.8	30% BuCN-70% PrCO <sub>3</sub>	+0.896	
18.4	50% BuCN-50% DCE	+0.983	
15.0	30% BuCN-70% DCE	+1.015	
20.8	3-Dimethylaminopropionitrile (DMAP)		+0.555
49.2	50% DMAP-50% PrCO <sub>3</sub>		+0.480
58.8	30% DMAP-70% PrCO <sub>3</sub>		+0.480
17.0	50% DMAP-50% DCE		+0.469
14.5	30% DMAP-70% DCE <sup>g</sup>		+0.455
32.5	50% $\beta$ -Dimethylaminoisopropyl acetate-50% PrCO <sub>3</sub>		+0.454
69	PrCO <sub>3</sub>	+0.890	
21.6	Allyl alcohol <sup>h, i</sup>	+0.890	

<sup>a</sup> 0.10 *F* (C<sub>2</sub>H<sub>5</sub>)<sub>4</sub>NClO<sub>4</sub> soln. <sup>b</sup> Obtained with the rotating platinum electrode. <sup>c</sup> % by volume, <sup>d</sup> Dielectric constant. <sup>e</sup> Propylene carbonate. <sup>f</sup> 1,2-Dichloroethane. <sup>g</sup> 0.10 *F* (C<sub>4</sub>H<sub>9</sub>)<sub>4</sub>NClO<sub>4</sub>. <sup>h</sup> Taken from ref. 8. <sup>i</sup> 0.10 *F* LiClO<sub>4</sub>. <sup>j, k</sup> Slope of *E* vs. log (*i*<sub>a</sub> - *i*)/*i* plot: <sup>j</sup> 0.062 ± 0.005, <sup>k</sup> 0.070 ± 0.008.

wave potentials for the oxidation of tris(4,7-dimethyl-1,10-phenanthroline)iron(II), and ferrocene in the solvents used in this investigation.

The infrared and proton NMR spectral data are summarized in Tables 3 and 4, respectively.

## DISCUSSION

### 3-Butenenitrile

3-Butenenitrile has two functional groups, an olefinic group and a nitrile group, both capable of co-ordinating to copper(I) and silver ions. Because the two groups do not differ markedly in their abilities to co-ordinate to these two ions, in a particular medium the polar characteristics of the solvent system should play an important role in determining which group co-ordinates to the metal ions and which makes up the outer sheath of the solvated species. Since the nitrile group is more polar than the olefinic group, in a polar medium the solvated ions will be expected to have olefinic groups co-ordinated to the metal ions and nitrile groups in the outer sheath. In a non-polar medium, the non-polar-like solvated species in which nitrile groups are co-ordinated to the metal ions and olefinic groups are in the outer sheath, should be favored.

Comparison of the potentials of the copper(I)-copper and silver(I)-silver couples in 3-butenitrile, with those in propionitrile and allyl alcohol (see Table 1) indicates that in 3-butenitrile, nitrile groups are co-ordinated to copper(I) and silver ions preferentially, *i.e.*, the less polar of the two possible solvated species is favored. In 3-butenitrile-1,2-dichloroethane mixtures, which are less polar in

TABLE 3  
 INFRARED DATA <sup>a, b</sup>

<i>Soln.</i>	<i>C≡N stretching</i>	<i>C=C stretching</i>	<i>C—N asymmetric stretching</i>
3-Butenenitrile (BuCN) BuCN, 0.5 <i>F</i> AgClO <sub>4</sub>	2220, 2250 2220 <i>ca.</i> 2238(bl.sh.) <i>ca.</i> 2250 <i>ca.</i> 2268(bl.sh.)	1625, 1635 1625 <i>ca.</i> 1635(rd.sh.)	
BuCN, 0.5 <i>F</i> CuClO <sub>4</sub>	2220 <i>ca.</i> 2238(bl.sh.) <i>ca.</i> 2250 <i>ca.</i> 2268(bl.sh.)	1625 <i>ca.</i> 1635(rd.sh.)	
30% BuCN–70% PrCO <sub>3</sub> <sup>c</sup> 30% BuCN–70% PrCO <sub>3</sub> , 0.5 <i>F</i> AgClO <sub>4</sub>	2218, 2248 2218 <i>ca.</i> 2238(bl.sh.) <i>ca.</i> 2248 <i>ca.</i> 2268(bl.sh.)	1625, 1635 1625 <i>ca.</i> 1635(rd.sh.) <i>ca.</i> 1565(bl.sh.)	
30% BuCN–70% DCE <sup>d</sup> 30% BuCN–70% DCE, 0.5 <i>F</i> AgClO <sub>4</sub>	2218, 2248 2218 <i>ca.</i> 2238(bl.sh.) <i>ca.</i> 2248 <i>ca.</i> 2268(bl.sh.)	1625, 1633 1625 <i>ca.</i> 1635(rd.sh.)	
3-Dimethylaminopropionitrile (DMAP) DMAP, 0.5 <i>F</i> AgClO <sub>4</sub>	2245 2245 <i>ca.</i> 2255(bl.sh.)		<i>ca.</i> 1050 <i>ca.</i> 1050 <sup>e</sup> 980(w.rd.sh.)
30% DMAP–70% PrCO <sub>3</sub> 30% DMAP–70% PrCO <sub>3</sub> , 0.5 <i>F</i> AgClO <sub>4</sub>	2243 2243		<i>ca.</i> 1050 <i>ca.</i> 1050 <sup>e</sup> 980
30% DMAP–70% DCE 30% DMAP–70% DCE, 0.5 <i>F</i> AgClO <sub>4</sub>	2243 2243 2255(bl.sh.)		<i>ca.</i> 1050 <i>ca.</i> 1050 <sup>e</sup> 980(w.rd.sh.)

<sup>a</sup> All frequencies in wave numbers (cm<sup>-1</sup>) with uncertainty of  $\pm 2$  cm<sup>-1</sup>. <sup>b</sup> Obtained in liquid cells with sodium chloride windows. <sup>c</sup> Propylene carbonate. <sup>d</sup> 1,2-Dichloroethane. <sup>e</sup> Interference due to absorption band of perchlorate.

character than 3-butenenitrile itself, it should follow that nitrile groups are again co-ordinated to the two metal ions. The similarity of the potentials of each couple in 3-butenenitrile–1,2-dichloroethane and propionitrile–1,2-dichloroethane mixtures indicates that this is indeed the situation. Because the potentials of the two couples are considerably more positive in propylene carbonate than in propionitrile or allyl alcohol and also more positive in the propionitrile–propylene carbonate mixtures than in propionitrile, it is difficult to attribute unequivocally the more positive values in 3-butenenitrile–propylene carbonate mixtures than in 3-butenenitrile to increase in olefinic co-ordination of the metal ions, although preferential co-ordination by olefinic groups leading to the formation of a polar solvated species (as explained previously) is expected in the polar propylene carbonate mixtures.

Infrared and proton NMR studies of copper(I), and silver solutions show clearly that in 3-butenenitrile–propylene carbonate mixtures there is increased participation of olefinic groups in the co-ordination of these ions. In the infrared

TABLE 4

PROTON NUCLEAR MAGNETIC RESONANCE DATA

Ligand	Soln.	Chemical shifts <sup>a</sup>		
		a	b	c
$\overset{\text{a}}{\text{CH}_3}\text{-}\overset{\text{b}}{\text{CH}_2}\text{-C}\equiv\text{N}$	30% PrCN-70% DCE <sup>f</sup>	1.17	2.24	
		1.28	2.37	
		1.41	2.48	
			2.59	
	30% PrCN-70% DCE, 0.5 F AgClO <sub>4</sub>	1.19	2.34	
		1.32	2.47	
		1.43	2.58	2.71
	30% PrCN-70% PrCO <sub>3</sub> <sup>g</sup>	— <sup>h</sup>	2.27	
			2.38	
			2.50	
			2.62	
	30% PrCN-70% PrCO <sub>3</sub> , 0.5 F AgClO <sub>4</sub>	— <sup>h</sup>	2.36	
		2.48		
		2.61		
		2.73		
$\overset{\text{a}}{\text{CH}_2}=\overset{\text{a}}{\text{CH}}\text{-}\overset{\text{b}}{\text{CH}_2}\text{-C}\equiv\text{N}$	3-Butenenitrile (BuCN)	5.48 <sup>i</sup>	3.18 <sup>i</sup>	
		5.63	3.20	3.27
	BuCN, 0.5 F AgClO <sub>4</sub>	5.48 <sup>i</sup>	3.23 <sup>i</sup>	
		5.63	3.25	3.31
	30% BuCN-70% DCE	5.55 <sup>i</sup>	3.18 <sup>i</sup>	
		5.68	3.22	3.25
	30% BuCN-70% DCE, 0.5 F AgClO <sub>4</sub>	5.52 <sup>i</sup>	3.32 <sup>i</sup>	
		5.69	3.35	3.38
	30% BuCN-70% PrCO <sub>3</sub>	5.47 <sup>i</sup>	3.23 <sup>i</sup>	
		5.63	3.25	3.29
			3.32	
	30% BuCN-70% PrCO <sub>3</sub> , 0.5 F AgClO <sub>4</sub>	5.68 <sup>i</sup>	3.31 <sup>i</sup>	
		5.88	3.33	3.37
		3.37	3.39	
$\begin{array}{l} \text{CH}_3^{\text{a}} \\ \diagdown \\ \text{N}-\overset{\text{b}}{\text{CH}_2}\text{-CH}_2\text{-C}\equiv\text{N} \\ \diagup \\ \text{CH}_3 \end{array}$	3-Dimethylaminopropionitrile (DMAP) DMAP, 0.5 F AgClO <sub>4</sub>	2.25	2.56	
		2.30	2.62	
	30% DMAP-70% DCE	2.29	2.53	
		2.58		
		2.63		

to be continued

TABLE 4 (Continued)

Ligand	Soln.	Chemical shifts <sup>d</sup>		
		a	b	c
	30% DMAP-70% DCE, 0.5 F AgClO <sub>4</sub>	2.30	2.58 2.63 2.68	
	30% DMAP-70% PrCO <sub>3</sub>	2.29	2.59	
	30% DMAP-70% PrCO <sub>3</sub> , 0.5 F AgClO <sub>4</sub>	2.43	2.72	
	30% β-Dimethylaminoisopropyl acetate-70% PrCO <sub>3</sub>	2.21	1.13 1.24	1.99
	30% β-Dimethylaminoisopropyl acetate-70% PrCO <sub>3</sub> , 0.5 F AgClO <sub>4</sub>	2.46	1.18 1.29	2.05

<sup>a, b, c</sup> See formulae above (methyl hydrogens, methylene hydrogens, etc.). <sup>d</sup> Chemical shifts are in parts per million (p.p.m.) *vs.* tetramethylsilane internal standard. <sup>e</sup> Propionitrile. <sup>f</sup> 1,2-Dichloroethane. <sup>g</sup> Propylene carbonate. <sup>h</sup> Methyl group on propylene carbonate interferes. <sup>i</sup> Complicated spectrum—only major peaks are reported.

study, consistent with the electrochemical results, the spectra of solutions of the two metal ions in 3-butenitrile and of silver ion in 30% 3-butenitrile-70% 1,2-dichloroethane show new bands in the 2220-2250 cm<sup>-1</sup> region for the C≡N stretching vibration, but no new bands in the 1630 cm<sup>-1</sup> region for the C=C stretching vibration. On the other hand, in polar 30% 3-butenitrile-70% propylene carbonate containing silver perchlorate, new bands are observed for both the C=C and C≡N stretching vibrations. Co-ordination of the lone pair of electrons on the nitrogen of the nitrile group has been shown to result in a high frequency (blue) shift of the nitrile stretching band<sup>12</sup>. Raman<sup>13</sup> and infrared<sup>14</sup> studies on silver-olefin complexes indicate that the stretching vibration of the double bond in the complex is shifted to a lower frequency, by about 50-70 cm<sup>-1</sup>, than that for the free ligand. In the 70%-propylene carbonate mixture, apparently, because of the stronger co-ordinating ability of the nitrile group than of the olefinic group for silver ion, orientation of all the butenenitrile molecules in the co-ordination sphere with the nitrile group in the outer sheath of the solvated species, is not possible.

The proton NMR spectrum of 3-butenitrile has absorption peaks at *ca.* 3.2 p.p.m. (*vs.* tetramethylsilane) for the methylene hydrogens, and at *ca.* 5.5 p.p.m. for the olefinic hydrogens. Owing to the complexity of the spectrum<sup>15</sup>, only the major peaks of this compound are reported in Table 4. In the spectra of 0.5 F solutions of silver perchlorate in 3-butenitrile, and in 30% 3-butenitrile-70% 1,2-dichloroethane, the absorption peaks of the methylene hydrogens are shifted to a lower field while those of the olefinic hydrogens remain unaltered. These results indicate, in agreement with the results of the electrochemical and infrared studies, that in these solutions only the nitrile groups of the 3-butenitrile molecules in the primary solvation sphere are co-ordinated to silver ion. A downfield chemical shift of the absorption peaks of the methyl hydrogens in acetonitrile and of the olefinic hydrogens in acrylonitrile upon co-ordination of the pair of electrons on the nitrile nitrogen, has previously been reported<sup>16</sup>. Similar data for propionitrile in 70% 1,2-dichloroethane and 70% propylene carbonate mixtures containing silver perchlorate are presented in Table 4. The absorption peaks of olefinic hydrogens have also been shown to be shifted downfield in olefin-silver complexes<sup>17,18</sup>. Definite downfield shifts of the



peaks of the olefinic hydrogens as well as of those for the methylene hydrogens of 3-butenitrile in the 70% propylene carbonate solution 0.5 *F* in silver perchlorate, support the infrared results that in this polar medium there is a degree of preferential orientation of 3-butenitrile molecules in the solvation sphere of silver ion with the polar nitrile groups in the outer sheath.

### *3-Dimethylaminopropionitrile*

The tertiary amine group of 3-dimethylaminopropionitrile is a non-polar-like functional group of greater co-ordinating ability for copper(I) and silver ions than the olefinic group. This is evident from the fact that the potentials of the copper(I)-copper and silver(I)-silver couples in 1 : 1 (by volume)  $\beta$ -dimethylaminoisopropyl acetate-propylene carbonate mixture are more negative than those in 1 : 1 propionitrile-propylene carbonate mixture, and the potentials of the copper and silver couples in propionitrile in turn are more negative than those in allyl alcohol. On this basis and since in a polar medium, 3-dimethylaminopropionitrile molecules in the solvation spheres of copper(I) and silver ions would very likely be preferentially oriented with the nitrile groups in the outer sheath, it is not surprising that the potentials for the two metal ion couples in 50% 3-dimethylaminopropionitrile-50% propylene carbonate and in 30% 3-dimethylaminopropionitrile-70% propylene carbonate are very similar to those in 50%  $\beta$ -dimethylaminoisopropyl acetate-50% propylene carbonate, indicating extensive co-ordination of the metal ions by tertiary amine groups. The considerably more negative potentials of the copper(I)-copper and silver(I)-silver couples in 3-dimethylaminopropionitrile than in propionitrile suggest a high degree of preferential co-ordination of copper(I) and silver ions by tertiary amine groups also in the substituted aminopropionitrile. The more positive potentials of the I,O couples of the two metal ions in each of the 3-dimethylaminopropionitrile-1,2-dichloroethane mixtures than in the corresponding 3-dimethylaminopropionitrile-propylene carbonate mixture and the more negative potentials in the former mixtures than in the corresponding propionitrile-1,2-dichloroethane mixtures mean that the polar character of the solutions in 3-dimethylaminopropionitrile-1,2-dichloroethane mixtures (although there is, as expected, increased nitrile co-ordination) is not low enough to overcome the stronger co-ordinating ability of the tertiary amine group to give completely nitrile-co-ordinated solvated species.

The infrared studies of solutions of silver perchlorate in 3-dimethylaminopropionitrile, 30% 3-dimethylaminopropionitrile-70% propylene carbonate, and 30% 3-dimethylaminopropionitrile-70% 1,2-dichloroethane give further information on the solvation phenomenon in solutions of this substituted nitrile. Here again, in the interpretation of the spectral data, use is made of the fact that co-ordination of the lone pair of electrons on the nitrogen of the nitrile group results in a high-frequency shift of the nitrile stretching band<sup>12</sup>. Co-ordination of the amine group to the metal ions is ascertained by examination of the asymmetric C-N stretching band at *ca.* 1050  $\text{cm}^{-1}$ . Previous infrared studies of trimethylamine<sup>19,20</sup> and trimethylamine-BX<sub>3</sub> complexes<sup>21,22,23</sup>, where X = H<sup>-</sup>, F<sup>-</sup>, Cl<sup>-</sup>, or Br<sup>-</sup>, indicate that when the amine co-ordinates to BX<sub>3</sub>, the asymmetric C-N stretching band of the free ligand (1043  $\text{cm}^{-1}$ ) shifts to lower frequencies ( $975 \pm 15 \text{ cm}^{-1}$ ).

In the case of 30% 3-dimethylaminopropionitrile-70% propylene carbonate containing silver perchlorate, the infrared spectrum not only confirms the electro-

chemical evidence that in this polar medium there is extensive co-ordination of silver ion by tertiary amine groups, but indicates that there is essentially no nitrile co-ordination. The spectrum has a new band at  $980\text{ cm}^{-1}$  for the C–N stretching vibration of the amino group, but no new  $\text{C}\equiv\text{N}$  band at  $2243\text{ cm}^{-1}$ . The fact that the non-polar-like tertiary amine group is a stronger co-ordinator of silver ion than the non-polar olefinic group, appears to be enough of a factor to give essentially amine-co-ordinated solvated silver ion in this polar medium instead of the partially nitrile-co-ordinated solvated silver ion that is obtained in the 3-butenenitrile-containing solution.

A clear indication of partial co-ordination of silver ion by tertiary amine groups in 3-dimethylaminopropionitrile, and 30% 3-dimethylaminopropionitrile–70% 1,2-dichloroethane is presented by the infrared spectra of these solutions. A new nitrile band at *ca.*  $2255\text{ cm}^{-1}$  and a weak C–N band at  $980\text{ cm}^{-1}$  characterize the spectra of the two solutions. Whereas the strong co-ordinating ability of the amino group for silver ion enabled essentially amine-co-ordinated solvated silver ion to be obtained in the polar propylene carbonate mixture, it prevents the formation in the 1,2-dichloroethane mixture of low polar characteristic, of the preferred non-polar-like solvated species.

The proton NMR spectrum of 3-dimethylaminopropionitrile exhibits only two absorption peaks, one at 2.56 p.p.m., attributable to four equivalent methylene hydrogens, and the other at 2.25 p.p.m., attributable to the six equivalent methyl hydrogens. The study of boron-containing addition compounds of Lewis bases, *e.g.*,  $(\text{C}_2\text{H}_5)_3\text{N}:\text{BH}_3$ ,  $(\text{C}_2\text{H}_5)_3\text{N}:\text{BF}_3$ ,  $(\text{CH}_3)_3\text{N}:\text{BH}_3$ , and  $(\text{CH}_3)_3\text{N}:\text{BF}_3$ , has shown that a downfield chemical shift of the absorption peaks of the hydrogens on the methyl- and ethyl-groups occurs upon co-ordination of the two free electrons on the base<sup>24</sup>.

The NMR studies provide a clearer picture than the infrared study of the difference in solvation of silver ion in 3-dimethylaminopropionitrile and in the 3-dimethylaminopropionitrile–1,2-dichloroethane mixture. The difference is consistent with that suggested by the electrochemical data. In pure 3-dimethylaminopropionitrile, the addition of silver perchlorate brings about a downfield chemical shift of the two absorption peaks, with the peak of the methylene hydrogens shifted a little more than that of the methyl hydrogens. The observed shifts indicate that both tertiary amine groups and nitrile groups are co-ordinated to silver ion in this medium. When diluted with 1,2-dichloroethane, 3-dimethylaminopropionitrile exhibits a singlet for the absorption peak of the methyl hydrogens and a triplet for the absorption peak of the methylene hydrogens. The latter hydrogens evidently become slightly nonequivalent in this medium. A very small downfield chemical shift of the absorption band of the methyl hydrogens and a substantial downfield shift of the absorption band of the methylene hydrogens in the spectrum of the 1,2-dichloroethane mixture containing silver perchlorate, clearly indicate that in this low polar medium there is, as expected, a high degree of preferential co-ordination of silver ion by nitrile groups. The proton NMR spectrum of the 3-dimethylaminopropionitrile–propylene carbonate mixture containing silver perchlorate shows large downfield shifts of the methyl and methylene hydrogen peaks consistent with the electrochemical and infrared picture of essentially complete co-ordination of silver ion in this medium by tertiary amine groups.

In summary, the combination of electrochemical, infrared, and proton NMR studies shows that in 3-butenenitrile–1,2-dichloroethane mixtures of low polar characteristic, there is essentially complete co-ordination of copper(I) and silver ions

by nitrile groups; however, in polar 3-butenitrile-propylene carbonate mixtures, olefinic *and* nitrile groups are co-ordinated to these ions. Complete co-ordination of olefinic groups is not possible in the latter media because of the stronger co-ordinating ability of the nitrile group for copper(I) and silver ions. In 3-butenitrile itself, the solvated ions appear to be completely nitrile co-ordinated. In the case of solutions of 3-dimethylaminopropionitrile, essentially complete co-ordination of copper(I) and silver ions by tertiary amine groups is observed in the polar propylene carbonate mixtures. Although the tertiary amine group has a stronger co-ordinating ability for copper(I) and silver ions than the nitrile group, in 1,2-dichloroethane mixtures there appears, nevertheless, to be a high degree of preferential co-ordination of the metal ions by nitrile groups. In 3-dimethylaminopropionitrile, both tertiary amine and nitrile groups are co-ordinated to copper(I) and silver ions.

## ACKNOWLEDGEMENT

We wish to acknowledge the generous support of the Directorate of Chemical Sciences, Air Force Office of Scientific Research (AFOSR Grant 220-63).

## SUMMARY

The influence of the solvent system on the orientation of 3-butenitrile and 3-dimethylaminopropionitrile in the co-ordination sphere of copper(I) and silver ion has been investigated by using propylene carbonate and 1,2-dichloroethane solutions and electrochemical, infrared, and proton NMR techniques.

## REFERENCES

- 1 F. FARHA, JR. AND R. T. IWAMOTO, *J. Electroanal. Chem.*, 8 (1964) 55.
- 2 I. M. KOLTHOFF AND J. F. COETZEE, *J. Am. Chem. Soc.*, 79 (1957) 870, 1825.
- 3 A. I. POPOV AND D. H. GESKE, *J. Am. Chem. Soc.*, 79 (1957) 2074.
- 4 R. C. LARSON AND R. T. IWAMOTO, *J. Am. Chem. Soc.*, 82 (1960) 3239, 3526.
- 5 J. F. COETZEE AND J. L. HEDRICK, *J. Phys. Chem.*, 67 (1963) 221.
- 6 I. V. NELSON, R. C. LARSON AND R. T. IWAMOTO, *J. Inorg. Nucl. Chem.*, 22 (1961) 279.
- 7 D. C. LUEHRS, R. T. IWAMOTO AND J. KLEINBERG, *Inorg. Chem.*, 4 (1965) 1739.
- 8 I. V. NELSON AND R. T. IWAMOTO, *Anal. Chem.*, 35 (1963) 867.
- 9 G. WILKENS, *Org. Syn.*, 36 (1956) 31.
- 10 M. T. KELLEY, H. C. JONES AND D. J. FISHER, *Anal. Chem.*, 31 (1959) 1475.
- 11 M. T. KELLEY, D. J. FISHER AND H. C. JONES, *Anal. Chem.*, 32 (1960) 1262.
- 12 See references such as: (a) H. J. COERVER AND C. CURRAN, *J. Am. Chem. Soc.*, 80 (1958) 3522; (b) T. L. BROWN AND M. KUBOTA, *J. Am. Chem. Soc.*, 83 (1961) 331, 4175; (c) V. N. FILIMONOV AND D. S. BYSTROV, *Opt. Spectry. USSR*, 12 (1962) 31. A review article by R. A. WALTON on this topic appears in *Quart. Rev. London*, 19 (1965) 126.
- 13 H. J. TAUFEN, M. J. MURRAY AND F. F. CLEVELAND, *J. Am. Chem. Soc.*, 63 (1941) 3500.
- 14 H. HOSOYA AND S. NAGAKURA, *Bull. Chem. Soc. Japan*, 37 (1964) 249.
- 15 *Varian N.M.R. spectra catalog (1962)*, spectrum no. 56.
- 16 B. L. ROSS, J. G. GRASSILLI, W. M. RICHEY AND H. D. KAESZ, *Inorg. Chem.*, 2 (1963) 1023.
- 17 J. C. SCHUG AND R. J. MARTIN, *J. Phys. Chem.*, 66 (1962) 1554.
- 18 M. AVRAM, H. P. FRITS, H. J. KELLER, C. G. KREITER, GH. MATESCU, J. F. W. McOMIE, N. SHEPPARD AND C. D. NENITZESCU, *Tetrahedron Letters*, 24 (1963) 1611.
- 19 E. J. ROSENBAUM, D. J. RUBIN AND C. R. SANDBERG, *J. Chem. Phys.*, 8 (1940) 366.
- 20 J. R. BARCELO AND J. BELLANATO, *Spectrochim. Acta*, 8 (1956) 27.
- 21 R. C. OSTHOFF, C. A. BROWN AND F. H. CLARKE, *J. Am. Chem. Soc.*, 73 (1951) 4045.
- 22 A. R. KATRITZKY, *J. Chem. Soc.*, (1959) 2049.
- 23 R. L. AMSTER AND R. C. TAYLOR, *Spectrochim. Acta*, 20 (1964) 1487.
- 24 T. D. COYLE AND F. G. A. STONE, *J. Am. Chem. Soc.*, 83 (1961) 4138.

## ELECTROREDUCTIONS OF BIS- AND TRIS-2,2'-BIPYRIDINE COMPLEXES OF CHROMIUM(III)

BEVERLY V. TUCKER\*, J. M. FITZGERALD\*\*, L. G. HARGIS\*\*\* AND L. B. ROGERS

*Chemistry Department, Purdue University, Lafayette, Indiana 47907 (U.S.A.)*

(Received March 21st, 1966)

## INTRODUCTION

One of the principal characteristics of chromium(III) is the ability to form a large number of relatively stable complexes. Because of their kinetic inertness, many complex species can be isolated as solids, and persist for relatively long periods of time in solution, even under conditions where they are thermodynamically unstable.

Chromium(III) complexes are generally reduced to chromium(II) complexes, which are further reduced to chromium metal with the destruction of the complex. However, complex formation with 2,2'-bipyridine stabilizes uncommon low-valence states of chromium such as chromium(I) and chromium(0). Tris-2,2'-bipyridine complexes of chromium(III), -(II), -(I), and -(0) in non-aqueous solvents have been reported<sup>1-3</sup>.

Using a commutator technique to obtain current-voltage curves, VLCEK<sup>4</sup> reported that tris(2,2'-bipyridine)chromium(III) ion was reduced at the dropping mercury electrode in three waves of approximately equal height both in water and in 50% ethanol. He reported half-wave potentials of  $-0.36$ ,  $-0.73$ , and  $-1.38$  V *vs.* S.C.E. in aqueous 0.5 M sodium chloride. Comparing these figures with the wave height of the hexamminechromium(III) ion, he concluded that each of the waves of  $\text{Cr}(\text{bipy})_3^{3+}$  corresponded to a reversible one-electron transfer, resulting finally in a tris(2,2'-bipyridine)chromium(0) complex. This reduced complex could be air-oxidized to the original tris-complex.

Such a series offered a possibility of extending the work of STREHLOW *et al.*<sup>5</sup> and NELSON AND IWAMOTO<sup>6</sup> on reference half-cells suitable for relating measurements of potentials in different solvents. Three oxidation-reduction pairs, all having the same chemical composition, would be available in the chromium system alone. Therefore, the original aim of the present study was to use the three one-electron steps of the  $\text{Cr}(\text{bipy})_3^{3+}$  ion to explore the effects of changes in charge and solvation on the relative positions of the half-wave potentials (and later the potentials of conventional half-cells).

Unfortunately, our attempts to reproduce the results of VLCEK, using conventional polarography, were unsuccessful. This was probably due to our using a different measuring technique, but it is possible that we had a different compound. The behaviour was sufficiently different, however, to make further study worthwhile.

---

\* Chevron Chemical Co., 940 Hensley St., Richmond, Calif.

\*\* Department of Chemistry, Seton Hall University, South Orange, N.J.

\*\*\* Department of Chemistry, Louisiana State University, New Orleans, La.

We found that the tris-complex readily converted to a bis-complex on reduction. Because two other bis-complexes could be prepared more easily than the tris and their polarographic behaviour proved to be very similar to that of the tris, they were selected for detailed study. Dichlorobis(2,2'-bipyridine)chromium(III) chloride,  $[\text{Cr}(\text{bipy})_2\text{Cl}_2]\text{Cl} \cdot 2 \text{H}_2\text{O}$ , and chloroaquobis(2,2'-bipyridine)chromium(III) perchlorate,  $[\text{Cr}(\text{bipy})_2\text{ClH}_2\text{O}](\text{ClO}_4)_2 \cdot 2 \text{H}_2\text{O}$  appeared to have nearly the same electrochemical behaviour in our preliminary electrochemical studies and were, in turn, similar to a bis(2,2'-bipyridine) chromium(III) complex produced from the tris-complex. For these reasons, one of the bis complexes,  $[\text{Cr}(\text{bipy})_2\text{Cl}_2]\text{Cl} \cdot 2 \text{H}_2\text{O}$ , was made the subject of an extensive study.

#### EXPERIMENTAL

##### *Apparatus*

An Oak Ridge National Laboratory Model Q-2005 controlled-potential coulometer<sup>7</sup> and a Model Q-1988 controlled-potential (and derivative) polarograph<sup>8</sup> were used to obtain the electrolytic and polarographic data. A Kintel digital voltmeter, Model 473A, was used for instrument calibration, and a Beckman Zeromatic pH-meter was used as the read-out device for the coulometer and for all pH measurements.

The cell used for both electrolytic and polarographic studies consisted of a 150-ml water-jacketed beaker fitted with a rubber stopper that contained a commercial reference electrode, a medium-porosity gas-dispersion tube, a dropping-mercury electrode for polarography, a platinum connecting lead for the mercury-pool cathode for coulometry, and one end of a 0.1 *M* potassium chloride salt bridge. The other end of the salt bridge was immersed in a 0.1 *M* potassium chloride solution containing a platinum counter electrode. The open-circuit *m*- and *t*-values of the capillary were 1.29 mg/sec and 4.83 sec in 0.1 *M* potassium chloride at 25°. This gave a capillary constant of 1.55  $\text{mg}^{2/3} \text{sec}^{1/6}$ .

Nitrogen, for de-aeration, was passed successively through vanadium(II) sulfate, sulfuric acid, anhydrous calcium sulfate, and pure solvent, prior to passage through the sample.

Absorption spectra were obtained using Perkin-Elmer Model 202 and Cary Model 11 recording spectrophotometers.

##### *Reagents*

All chemicals were reagent grade. Spectrophotometric-grade solvents were used for absorption spectra. Chloroform for extraction was washed with 1 *M* sodium hydroxide and then twice with distilled water immediately prior to use. The 2,2'-bipyridine was obtained from the G. Frederick Smith Chemical Company.

BURSTALL AND NYHOLM's<sup>1</sup> procedures were used to prepare  $\text{Cr}(\text{bipy})_3(\text{ClO}_4)_3 \cdot 3 \text{H}_2\text{O}$  and  $[\text{Cr}(\text{bipy})_2\text{Cl}_2]\text{Cl} \cdot 2 \text{H}_2\text{O}$ . The  $[\text{Cr}(\text{bipy})_2\text{ClH}_2\text{O}](\text{ClO}_4)_2 \cdot 2 \text{H}_2\text{O}$  was prepared without benefit of a previously-published procedure<sup>9</sup>.

*Analysis.* Calcd. for  $\text{Cr}(\text{bipy})_3(\text{ClO}_4)_3 \cdot 3 \text{H}_2\text{O}$ : C, 41.27; H, 3.46; N, 9.63. Found: C, 41.08; H, 3.70; N, 9.83%.

*Analysis.* Calcd. for  $[\text{Cr}(\text{bipy})_2\text{Cl}_2]\text{Cl} \cdot 2 \text{H}_2\text{O}$ : C, 47.39; H, 3.98; N, 11.09. Found: C, 47.65; H, 4.16; N, 10.92%.

*Analysis.* Calcd. for  $[\text{Cr}(\text{bipy})_2\text{ClH}_2\text{O}](\text{ClO}_4)_2 \cdot 2 \text{H}_2\text{O}$ : C, 36.79; H, 3.40; N, 8.58; Cl, 16.30; Cr, 7.97. Found: C, 36.74; H, 3.54; N, 8.53; Cl, 16.30; Cr, 8.10%.

After one week, less than 3% of the total 2,2'-bipyridine content could be extracted with chloroform from solutions of the complexes in 0.1 *M* potassium chloride. No major difference in electrochemical behaviour was observed between fresh solutions and week-old solutions. Nevertheless, fresh solutions were prepared every week.

### *Procedures*

Absorption spectra of reduced aqueous solutions were obtained by withdrawing 2–3 ml of the solution with a syringe and transferring through a rubber septum into a de-aerated 1-cm round-neck absorption cell.

The extraction studies involving reduced solutions were crucial and are, therefore, reported in detail. The extractions had to be carried out in the absence of even traces of oxygen. The following procedure was used for all chloroform extractions involving reduced solutions. A 2.00-ml aliquot was removed from the nitrogen-deaerated cell through a rubber septum by means of a 2-ml syringe and transferred to a 50-ml weighing bottle fitted with a one-hole stopper which, in turn, was fitted with a rubber septum. The weighing bottle contained 20.00 ml of chloroform which was continuously flushed, before and after addition of the de-aerated sample, with nitrogen that entered and left through syringe needles in the rubber septum. After two minutes of mixing, about 10 ml of the chloroform phase was transferred by means of a syringe to a stoppered bottle. Proper dilution of an aliquot of the chloroform phase was then made and an absorption spectrum obtained. A similar procedure was used for extraction and measurement of oxidized solutions except that no precautions were taken to eliminate air.

## RESULTS

### *Preliminary studies*

Strong acid or base destroyed the complexes, so reduction studies of the complexes were performed in weakly acidic and basic solutions. McIlvaine and acetate buffers covering the pH range from 2 to 9 were used in preliminary studies. Although the polarographic behaviour of the different complexes was fairly similar in a given buffer, the behaviour varied markedly at a given pH in buffers of different composition. This was not surprising in view of the report<sup>10</sup> that citrate, phosphate, and similar anions participate in catalytic electron-exchange reactions with chromium(II) to form chromium(III) complexes. Unbuffered solutions (between pH 5.0 and 5.5) were used, therefore, in the remainder of the experiments but selected pH measurements were made after electrolyses to determine if significant pH changes had occurred. In all cases, the changes were insignificant.

Figure 1 shows the polarograms of two chromium(III) complexes in 0.1 *M* potassium chloride. As discussed later, it was found that our data for the tris did not agree with that in the existing literature<sup>4</sup> (however, it does agree closely with the results published recently by BAKER AND DEV MEHTA<sup>11</sup>). We thought that loss of a molecule of 2,2'-bipyridine from the complex might be a source of the discrepancy. A brief examination of the ultraviolet spectra of the complexes (Fig. 2) and of 2,2'-

bipyridine indicated that it should be possible to detect free 2,2'-bipyridine in the presence of the complexes. This was checked and confirmed by adding free 2,2'-bipyridine to solutions of the individual complexes. The spectrophotometric technique for the detection of free 2,2'-bipyridine was so sensitive that, at the concentrations at

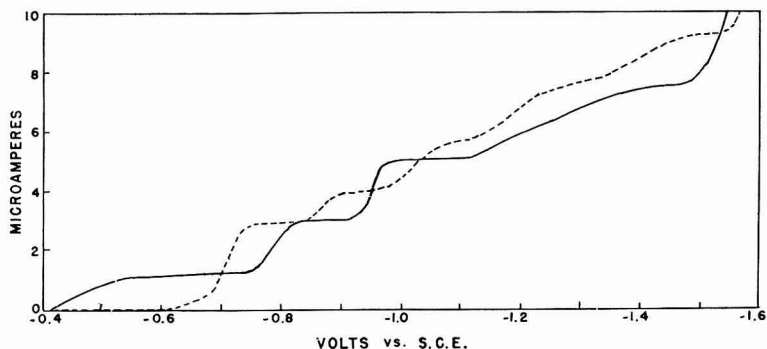


Fig. 1. Polarograms of 0.001 *M* chromium(III)-2,2'-bipyridine complexes in 0.1 *M* KCl. (—),  $\text{Cr}(\text{bipy})_3(\text{ClO}_4)_3 \cdot 3 \text{H}_2\text{O}$ ; (-----),  $[\text{Cr}(\text{bipy})_2\text{Cl}_2]\text{Cl} \cdot 2 \text{H}_2\text{O}$ .

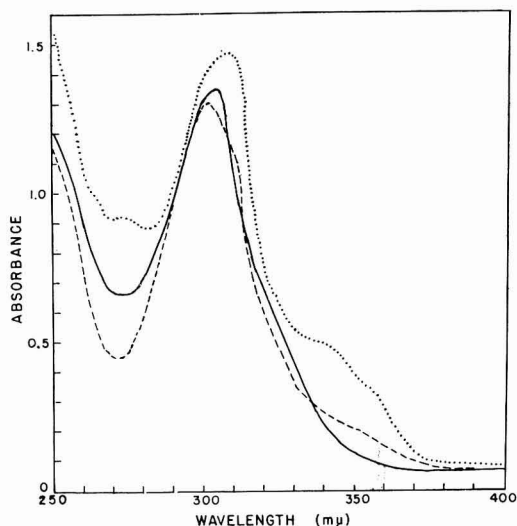


Fig. 2. Ultraviolet spectra of  $\text{Cr}(\text{bipy})_3(\text{ClO}_4)_3 \cdot 3 \text{H}_2\text{O}$  and of bis- and mono-complexes resulting therefrom. (.....),  $5 \cdot 10^{-5} \text{ M}$   $\text{Cr}(\text{bipy})_3(\text{ClO}_4)_3 \cdot 3 \text{H}_2\text{O}$ ; (—), bis-complex derived from the tris-complex; (-----), mono-complex derived from the tris-complex.

which we were working, dilutions were necessary prior to measurement. It was also established that neither the tris- nor bis-complexes were extractable into chloroform whereas free 2,2'-bipyridine was.

#### *Bis-complex*

In order to characterize the behaviour of  $[\text{Cr}(\text{bipy})_2\text{Cl}_2]\text{Cl} \cdot 2 \text{H}_2\text{O}$ , controlled-potential electrolyses were planned for a suitable potential on the plateau of each



polarographic wave. The reduced solutions were first examined polarographically. They were also examined spectrophotometrically, both before and after extraction with chloroform. In addition, the extracts were examined spectrophotometrically for 2,2'-bipyridine. The remainder of the reduced aqueous solution was oxidized and then re-examined in the same manner. Figure 3 shows the polarograms obtained for the products of controlled-potential reductions of the bis-complex at a series of progressively more negative potentials. The reduction appeared to be stepwise; however, evidence given below suggests that two different chromium(III) complexes were reduced and that the chromium(II) complex underwent a slow disproportionation to the chromium(III) complexes and a chromium(I) complex.

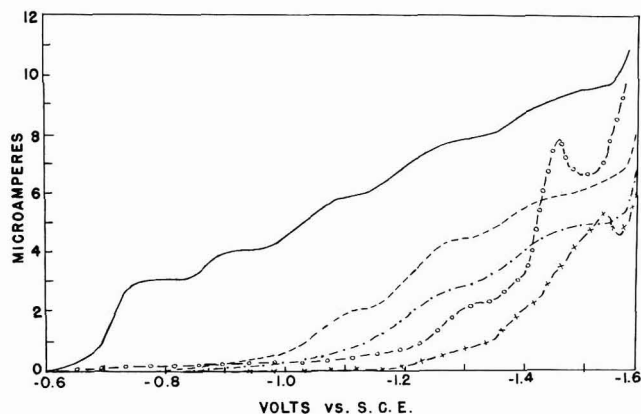


Fig. 3. Polarograms of the products of successive coulometric reductions of  $0.001 M$   $[\text{Cr}(\text{bipy})_2\text{Cl}_2] \cdot \text{Cl} \cdot 2 \text{H}_2\text{O}$  in  $0.1 M$  KCl. (—),  $[\text{Cr}(\text{bipy})_2\text{Cl}_2] \cdot \text{Cl} \cdot 2 \text{H}_2\text{O}$  (light yellow solution); (-----), after electrolysis at  $-0.78 \text{ V}$ ,  $n = 1.0$  (deep red solution); (-.-.-.-), after further electrolysis at  $-0.78 \text{ V}$ ,  $n = 1.0$  (total  $n = 2$ ; very slightly pink solution); (-x-x-x-x-), after further electrolysis at  $-1.26 \text{ V}$ ,  $n = 1.0$  (total  $n = 3$ ; black turbidity); (-o-o-o-o-), after air oxidation (light yellow turbidity).

When a solution of the bis-complex was electrolyzed at  $-0.78 \text{ V}$ , the solution first became intensely red and then decreased in intensity to a nearly colorless solution when significant current ceased to flow. The formation and disappearance of the red color was followed spectrophotometrically and found to reach maximum intensity at about 0.9 electrons/molecule. In going to the nearly colorless solution at the end of the electrolysis, another 1.1 electrons/molecule were passed. The fact that a total of 2.0 electrons was passed by electrolysis on the plateau of the first polarographic wave, and that a striking reversal of color appeared near the halfway point of the reduction, indicated that more than a simple one-step process was involved. Furthermore, it was noted that the rate of reduction, as indicated by the magnitude of the cell current, was quite fast until a coulometric  $n$ -value of about 0.9 had been obtained after which it slowed considerably so that the remainder of the reduction took four to five times longer.

When electrolyses are performed at a potential corresponding to the top of a polarographic wave, the polarogram of the reduced solution usually contains none of



the waves that occur at more positive potentials but all of the waves that occur at more negative potentials. In our experiments, however, polarograms obtained after electrolysis at  $-0.78$  V (corresponding to the top of the first wave) to a coulometric  $n$ -value of 1.0, showed that *two* waves instead of one had disappeared, including the second that had a half-wave potential of  $-0.88$  V. The manner of disappearance of the first two waves was investigated by performing other electrolyses on fresh aliquots and stopping at the intermediate coulometric  $n$ -values of 0.2 and 0.5. Polarograms of these showed that the heights of both waves had decreased proportionately, their relative heights thus remained the same. This strongly suggested the presence of two different species in slow equilibrium which reduced polarographically at different potentials. One possibility is that the waves corresponded to *cis*- and *trans*-isomers<sup>12</sup>.

If, instead of stopping at a coulometric  $n$ -value of 1.0, electrolysis at  $-0.78$  V was continued until significant current ceased to flow, a coulometric  $n$ -value of 2.0 was obtained. A polarogram of the final solution showed that the first *three* waves had disappeared and the fact that waves disappeared in regions of potential more negative than the reduction potential, was again very unusual. Furthermore, the marked difference in electrolysis rate between the reductions for  $n=1$  and  $n=2$  while electrolyzing at a potential on the first wave, the disappearance of the third wave, and the discrete color changes during electrolysis, all indicated that the chromium(II) complex—formed by the passage of one equivalent of electrons—was disproportionating slowly to chromium(III) complex(es) very much like the original one(s) and a chromium(I) complex. Thus, the chromium(II) complex ( $E_{\frac{1}{2}} = -1.03$  V) *was not* being reduced at  $-0.78$  V but appeared to be producing chromium(III) and chromium(I) by slow disproportionation. The chromium(III) produced by disproportionation was then reduced. The net effect was to produce chromium(I) from chromium(III). These conclusions were substantiated further by the following experiments.

A solution of the bis-complex, electrolyzed at  $-0.78$  V to the extent of only one electron/molecule (complete formation of the chromium(II) complex), was scanned polarographically at 30-min intervals while standing under nitrogen. The polarogram obtained immediately after reduction showed no evidence of the first two waves. However, the polarogram taken after the solution had aged for 60 min showed that both the waves, now attributed to chromium(III) complexes in the original solution, had grown to maximum values that were approximately one-half their initial heights. In other words, after standing 60 min, one-half the original amount of chromium(III) complexes had been reformed. Disproportionations of chromium(II) complexes of this sort have already been reported<sup>3,13,14</sup>.

Electrolyses were also performed at more negative potentials, thus permitting electron-transfer values greater than two to be examined. When a solution, which had previously been electrolyzed on the top of the first wave to a coulometric  $n$ -value of 2.0, was further electrolyzed at  $-1.26$  V, a black turbidity and a black film on the cell wall resulted. A coulometric  $n$ -value of 1.0 (or a total of 3.0) was obtained. This solution showed a polarographic wave at  $-1.40$  V followed by a sharp wave characteristic of hydrogen evolution. The fact that air oxidation of the solution resulted in a light yellow turbidity indicated that the black deposit was not chromium metal but a chromium(0) complex.

The discussion of redox behaviour has so far been limited to the electrochemical behaviour and the effects of reductions. A study of the solutions following an oxida-

tion step, led to other interesting and unusual results. It was noted that ligand lability was greater in the oxidized complexes than in the original complex. For example, although the 2,2'-bipyridine ligands in the original bis-complex were inert to chloroform extractions, a complex that had been reduced and then oxidized gave up 2,2'-bipyridine readily. A careful study was made to determine the conditions under which the 2,2'-bipyridine was made labile.

Solutions of the bis-complex were reduced at  $-0.78$  V to stages corresponding to 0.5, 1.0, 1.5, and 2.0 electrons/molecule and then extracted with chloroform. *In all cases*, the spectra of the extracts showed a small amount of residual absorption in the region of 2,2'-bipyridine absorption, but the shape of the curves and the low intensity of the absorption indicated that it was *not* due to free 2,2'-bipyridine or to reduced 2,2'-bipyridine. Since it is known that chloroform is sometimes reduced by lower-valent metal ions and complexes, the experiment was repeated using 1,2-dichloroethane as the extractant. Similar results were obtained, indicating that the chloroform extraction data were valid.

These experiments were then repeated except that each sample was oxidized prior to extraction. Ultraviolet spectra of the oxidized aqueous solutions prior to extraction *did not* show evidence of eliminated 2,2'-bipyridine, but, in all cases, the chloroform extract *did* show the presence of 2,2'-bipyridine. Apparently, 2,2'-bipyridine was not free in the aqueous solution of the complex but was labile because it was easily extractable.

Quantitative data regarding the number of extractable 2,2'-bipyridine molecules liberated/electron passed were difficult to obtain, especially for values of  $n$  less than unity. However, for solutions reduced to a total of 2.0 electrons/molecule, the amount of 2,2'-bipyridine extractable from the oxidized solution was close to one ligand/complex. This indicates that it was probably oxidation of chromium(I), not chromium(II), that led to lability of the 2,2'-bipyridine in the bis-2,2'-bipyridine complex of chromium(III) produced by oxidation.

Similar chloroform extractions made on samples that had been reduced at  $-1.26$  V, on the top of the fourth wave to the extent of 3.0 electrons/mole, gave almost identical results with those obtained for 2.0 electrons/mole. Only one equivalent of 2,2'-bipyridine could be extracted from the oxidized complex and the chemical change that made this ligand labile occurred during the oxidation of the reduced chromium complex.

The absorption spectrum of the mono-complex, derived from the bis-complex by reduction at  $-0.78$  V followed by air oxidation and successive chloroform extractions (to remove all labile 2,2'-bipyridine), showed an absorption maximum at a slightly shorter wavelength than that of the bis-complex (Fig. 2). This shift was in the expected direction.

The oxidation step was also interesting for another reason. Solutions of the bis-complex that had been reduced to the extent of 1.0 or 2.0 electrons/molecule gave polarograms that were *identical* with those obtained for the same solutions after oxidation by air (solutions were de-aerated again prior to the taking of polarograms). This unusual result indicates not only that the form of chromium(III) produced by air oxidation was not the same as that originally present, but also that the new oxidized form was no more easily reduced than the chromium(II) or (I) from which it had been produced. It has been reported that air oxidation of chromium(II) salts can result in

the formation of  $[\text{Cr}-\text{O}-\text{Cr}]$ - or  $[\text{Cr} \begin{array}{c} \diagup \text{O} \diagdown \\ \diagdown \text{O} \diagup \end{array} \text{Cr}]$ -type polymers<sup>15,16</sup>. The oxygen bonds in

these polymers appeared, from our polarographic studies, to be resistant to electron transfer. Only when the chromium(0) complex was air oxidized did the polarogram of the oxidized solution differ from that of the reduced solution (see Fig. 3).

Solutions of the bis-complex that had been reduced to the extent of 1.0 or 2.0 electrons/molecule and then oxidized with an equivalent amount of cerium(IV) sulfate (in a small volume of water adjusted to pH 2 with sulfuric acid and then de-aerated) gave polarograms that closely resembled the polarogram of the bis-complex containing a small amount of the oxidant (the excess cerium(IV) was probably reduced by chemical reaction with mercury from the D.M.E., and was present as cerium(III)). The positions of the waves in the polarogram of the bis-complex were the same with or without excess cerium but in the presence of excess cerium the diffusion current of the third wave was larger by an amount dependent upon the amount of cerium. Hence, oxidation by cerium(IV) generated an easily-reduced chromium(III) complex whereas air oxidation did not. Since the polarogram of the cerium(IV)-oxidized solution was very different from those of the reduced solutions but similar to that for the original bis-complex, it was evident that oxo-bridge polymers proposed for the air-oxidized solutions were not being formed to an appreciable extent. Nevertheless, the same changes in lability of 2,2'-bipyridine occurred upon treatment of reduced solutions with cerium(IV) as with air.

#### Tris-complex

Coulometric electrolyses were performed at controlled potential on tris(2,2'-bipyridine)chromium(III) perchlorate to elucidate the polarographic processes and to determine if the low-valent tris-complexes could be prepared electrochemically. Fig-

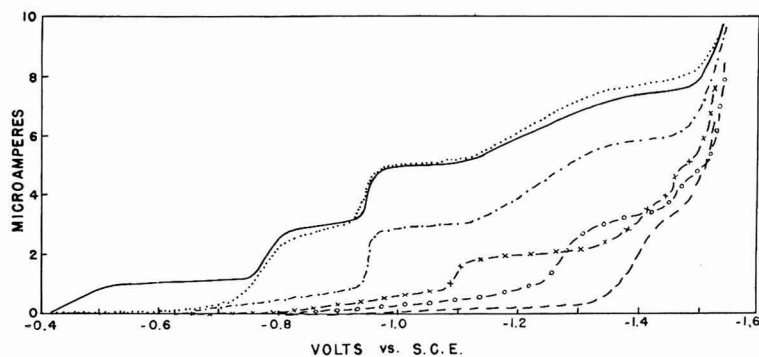


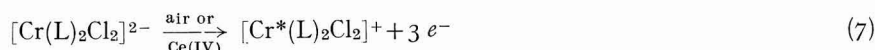
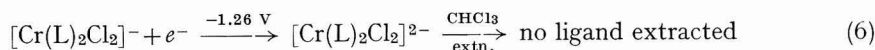
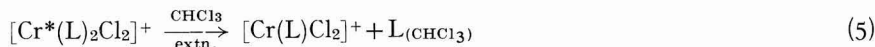
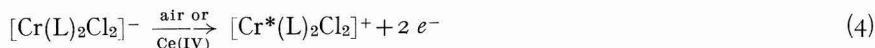
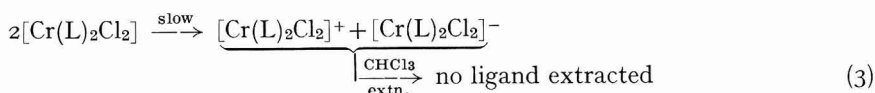
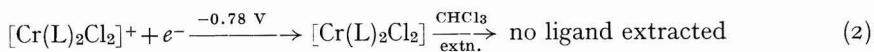
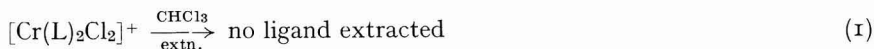
Fig. 4. Polarograms of the products of successive coulometric reductions of 0.001  $M$   $\text{Cr}(\text{bipy})_3(\text{ClO}_4)_3 \cdot 3 \text{H}_2\text{O}$  in 0.1  $M$   $\text{KCl}$ . (—),  $\text{Cr}(\text{bipy})_3(\text{ClO}_4)_3 \cdot 3 \text{H}_2\text{O}$  (deep yellow solution); (·····), after "electrolysis" at  $-0.64 \text{ V}$ ,  $n \sim 0$  (light yellow solution); (-·-·-·-), after further electrolysis at  $-0.82 \text{ V}$ ,  $n = 0.9$  (deep red solution); (-x-x-x-), after further electrolysis at  $-1.05 \text{ V}$ ,  $n = 1.1$  (total  $n = 2.0$ ; light blue solution); (-----), after further electrolysis at  $-1.30 \text{ V}$ ,  $n = 1.7$  (total  $n = 3.7$ , includes some hydrogen evolution; black turbidity); (-o-o-o-), after air oxidation (light yellow turbidity).

ure 4 shows the polarograms obtained for the products of controlled-potential reduction of the tris-complex at a series of progressively more negative potentials. The polarographic half-wave potentials for the original tris-complex agree quite well with those just reported by BAKER AND DEV MEHTA<sup>11</sup>. We, too, found that the first small wave disappeared after passing only a negligible amount of electricity. In fact, the wave also disappeared after several polarographic scans, indicating that a catalytic process was involved. At the same time, there was a marked change in color from a deep yellow to a very pale yellow. The ultraviolet spectrum of the aqueous solution showed that free 2,2'-bipyridine was present, and a chloroform extraction indicated that one molecule of 2,2'-bipyridine had been eliminated from the complex. It is clear that the elimination of 2,2'-bipyridine was catalyzed by chromium(II) produced during the brief electrolysis. This was not very unusual, considering that tris(2,2'-bipyridine)chromium(III) salts cannot be prepared directly but are made under rather forcing conditions in non-aqueous solvents.

Removal of the eliminated 2,2'-bipyridine by successive chloroform extractions left a bis-complex the polarographic, coulometric, extraction, and spectrophotometric behaviour of which was very similar to that discussed above for the bis-complex. Consequently, discussions of its characteristics will not be repeated here.

#### DISCUSSION

The reactions can be summarized as follows:



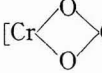
The asterisk denotes a chromium complex which appears to be stable but from which a bipyridine ligand could be extracted.

Two polarographic waves ( $E_{1/2} = -0.71$  and  $-0.88$  V) were associated with reaction (2) and their behaviour suggested the presence of two species, in equilibrium, which reduced polarographically at different potentials. It is likely that these result from cis- and trans-isomers<sup>13</sup>. Whether both forms existed together in the bulk of the solution or only at the electrode surface was not resolved in our study.

The disproportionation illustrated in reaction (3) was substantiated polarographically, coulometrically, and spectrophotometrically. Oxidation of the reduced complexes formed by reactions (4) and (7) gave a bis(2,2'-bipyridine)chromium(III) complex (indicated by asterisk) which differed, both polarographically and spectrophotometrically from the original bis-complex in that one molecule of 2,2'-bipyridine was labile and could be extracted with chloroform (eqn. (5)) (note that bipyridine was *not* extractable from the original bis-complex or at *any* stage of reduction, but only after oxidation to chromium(III)). After oxidation, although free bipyridine could not be detected spectrophotometrically in the aqueous phase, it must have become labile because one ligand could be extracted into chloroform. It would be of interest to check this unusual behaviour in future studies of other similar ligands.

Polarographic and spectrophotometric data indicated that, using either the tris- or bis-complex as the starting material, the same compound was formed by oxidation of the respective chromium(0) complexes. In both cases, a final oxidized species was produced which had one labile and one non-labile 2,2'-bipyridine. These reactions appear to offer a convenient preparation of a mono(2,2'-bipyridine)chromium(III) complex.

It is evident that the choice of oxidant is important in determining the nature of the final oxidation product. Although oxidation of the reduced complexes by air and cerium(IV) both produced bis-complexes containing one labile ligand, only cerium(IV) gave a product having virtually the same polarographic waves as those for the original solution prior to electrolysis. Although we have suggested that air oxidation of reduced complexes probably resulted in the formation of [Cr-O-Cr]- or

-type polymers, the exact structures of the oxidation products obtained

in the present study have yet to be elucidated.

The fact that the reactions occurring in oxidation steps were different from those in reductions, was revealed in another way. Although reduction of chromium(III) to chromium(II) produced a red solution, no red intermediate was visible in oxidations of chromium(0) or (I) by air to chromium(III) or in oxidations of chromium(I) by either one or two equivalents of cerium(IV). The absence of a red chromium(II) intermediate for the reaction of chromium(I) with oxygen can be rationalized on the basis of a two-electron transfer, but the reactions of chromium(0) with oxygen and chromium(I) with one equivalent of cerium(IV), cannot. Possibly, the chromium(II) species produced by oxidation disproportionated so rapidly that it escaped visual detection.

In all the above equations, two chloride ions have been shown in the coordination sphere on the assumption that the number did not change from that in the original complex. Preliminary experiments have been completed which show that one equivalent of chloride was liberated during the overall process of a two-electron reduction followed by air oxidation (Amperometric chloride titrations were performed on solutions of 1 mM [Cr(bipy)<sub>2</sub>Cl<sub>2</sub>]Cl in 1 mM KCl both before and after electrolysis at -0.78 V; the labile 2,2'-bipyridine molecule was found to interfere and was removed by successive chloroform extractions prior to the titration). Loss of chloride may have occurred in the oxidation step that led to one molecule of 2,2'-bipyridine becoming labile. A complete series of experiments comparable to those reported for the bipyri-

dine series would be necessary, however, in order to establish the exact conditions for the elimination.

As stated earlier, the original aim of the present study was to use the three one-electron steps of the  $\text{Cr}(\text{bipy})_3^{3+}$  ion to explore the effects of changes in charge and solvation on the relative positions of the half-wave potentials (and later the potentials of conventional half-cells). Although conventional polarography proved to be unsuitable, the earlier work of VLCEK<sup>4</sup> indicates that fast-scan techniques would make such a current-voltage study feasible. In that case, extension to related series involving different metal ions and/or different ligands would permit the generality of any conclusions to be tested.

Preliminary results<sup>9</sup> indicate that in some solvents bis-bipyridine complexes of chromium(III) are reduced directly to chromium(I).

#### ACKNOWLEDGEMENT

The polarograph and coulometer were assembled by J. W. AMY. Elemental analyses were performed by C. S. YEH. This research was supported in part by the United States Atomic Energy Commission under Contract AT(11-1)-1222.

#### SUMMARY

Dichlorobis(2,2'-bipyridine)chromium(III) chloride and tris(2,2'-bipyridine)-chromium(III) perchlorate have been investigated using polarography and controlled-potential coulometry. In aqueous medium, neither complex underwent three simple one-electron reductions to the corresponding chromium(0) complex; reductions were complicated and changes occurring on oxidation allowed 2,2'-bipyridine to be extracted from either complex. In one instance, reduction was complicated by a disproportionation reaction. Results indicated that, after reduction of either chromium(III) complex to the chromium(0) complex, the product of an oxidation by cerium(IV) or air was a bis(2,2'-bipyridine) chromium(III) complex from which one mole of 2,2'-bipyridine could be extracted. However, the polarographic and coulometric behaviour of the chromium(III) products from the two treatments differed considerably.

#### REFERENCES

- 1 F. H. BURSTALL AND R. S. NYHOLM, *J. Chem. Soc.*, (1952) 3570.
- 2 FR. VON HEIN AND S. HERZOG, *Z. Anorg. Allgem. Chem.*, 267 (1952) 337.
- 3 S. HERZOG, *J. Inorg. and Nucl. Chem.*, 8 (1958) 557.
- 4 A. A. VLCEK, *Nature*, 189 (1961) 393.
- 5 H. W. KOEPP, H. WENDT AND H. STREHLOW, *Z. Elektrochem.*, 64 (1960) 483.
- 6 I. V. NELSON AND R. T. IWAMOTO, *Anal. Chem.*, 33 (1961) 1795.
- 7 M. T. KELLEY, H. C. JONES AND J. D. FISHER, *Anal. Chem.*, 31 (1959) 488, 956.
- 8 *Ibid.*, 1475.
- 9 B. V. TUCKER, Ph.D. Thesis, Purdue Univ., 1964.
- 10 J. B. HUNT AND J. E. EARLEY, *J. Am. Chem. Soc.*, 82 (1960) 5312.
- 11 B. R. BAKER AND B. DEV MEHTA, *Inorg. Chem.*, 4 (1965) 848.
- 12 R. G. INSKEEP AND J. BJERRUM, *Acta Chem. Scand.*, 15 (1961) 62.
- 13 U. P. GEIGER AND E. CLASS, *Experientia*, 17 (1961) 444.
- 14 H. OBERENDER AND S. PAHL, *Z. Naturforsch.*, 18B (1963) 158.
- 15 M. ARDON AND R. A. PLANE, *J. Am. Chem. Soc.*, 81 (1959) 3197.
- 16 H. T. HALL AND H. EYRING, *ibid.*, 72 (1950) 782.

## CHLORO COMPLEXES OF COPPER(II) AND COPPER(I) IN METHANOL, ETHANOL, 2-PROPANOL, 2-BUTANOL AND ACETONE

STANLEY E. MANAHAN AND REYNOLD T. IWAMOTO

*Department of Chemistry, University of Kansas, Lawrence, Kansas (U.S.A.)*

(Received April 18th, 1966)

Comparison of the stepwise formation constants of the chloro complexes of copper(II) in acetonitrile<sup>1</sup> with the corresponding constants in water<sup>2</sup> illustrates the importance of the solvent in complex-ion stability. In water, the stepwise formation constants of  $\text{CuCl}^+$ ,  $\text{CuCl}_2$ ,  $\text{CuCl}_3^-$ , and  $\text{CuCl}_4^{2-}$  are 1, 0.2, 0.04 and 0.01, respectively, whereas in acetonitrile the values are  $5 \cdot 10^9$ ,  $8 \cdot 10^7$ ,  $1 \cdot 10^7$  and  $5 \cdot 10^3$ . In order to illustrate further the role of solvent in complex-ion stability and because of the considerable current interest in the chemistry of non-aqueous copper-halide solutions, we have determined the formation constants of the chloro complexes of copper(II) and of copper(I) in 0.10 *F* ( $\text{LiClO}_4 + \text{LiCl}$ ) solutions of methanol, ethanol, 2-propanol, 2-butanol and acetone. At this time, because of the understandable lack of quantitative supporting data, *e.g.*, ion-pair formation constants, a completely rigorous quantitative evaluation of the data obtained obviously is not possible. However, in spite of the slightly-larger-than-usual uncertainty of the constants obtained, a considerable understanding and appreciation of the nature and stability of the chloro complexes of copper(I) and copper(II) in the lower alcohols and in acetone have been realized.

## EXPERIMENTAL

Methanol and ethanol were purified and dried by treatment with Grignard reagent (prepared by refluxing 100 ml of alcohol containing 0.5 g of iodine and in contact with 5 g of magnesium—sufficient to dry 1 l of alcohol) followed by two distillations. 2-Butanol was refluxed over calcium hydride ( $\text{CaH}_2$ ) and a small quantity of sodium borohydride ( $\text{NaBH}_4$ ) prior to distillation. 2-Propanol and acetone were allowed to stand over Drierite for a week and were distilled after decantation. These procedures reduce the water content of the solvents, in general, to below  $10^{-2}$  *M*.

Lithium perchlorate was prepared by adding a slight excess of 70% reagent-grade perchloric acid to reagent-grade lithium carbonate, followed by three recrystallizations from water. The product was dried in an oven at 200° for several days. Reagent-grade lithium chloride was dried at a high temperature on a hot plate and ground to a powder in a dry box. Copper(II) perchlorate,  $\text{Cu}(\text{ClO}_4)_2 \cdot x\text{H}_2\text{O}$ , (G. F. Smith Co.) was dried *in vacuo* at 70° for 48 h. Copper(I) was added to the solvents as cuprous chloride (Fisher reagent-grade).

A controlled-potential polarograph of the type designed by Kelley, Jones and Fisher<sup>3</sup> was used to obtain the current-voltage curves. The copper amalgam data were obtained with a dropping copper amalgam electrode of special design<sup>4</sup>. The



TABLE 1

HALF-WAVE POTENTIALS FOR THE Cu(I), Cu(Hg) AND Cu(II), Cu(I) COUPLES IN METHANOL, ETHANOL, 2-PROPANOL, 2-BUTANOL, AND ACETONE AT VARIOUS CHLORIDE CONCENTRATIONS (V vs. S.C.E.)

Supporting electrolyte: 0.10 F (LiClO<sub>4</sub> + LiCl); temp. 25 ± 1°.

$-\log [Cl^-]$	<i>Cu(I), Cu(Hg)</i>	<i>Cu(II), Cu(I)</i>	$-\log [Cl^-]$	<i>Cu(I), Cu(Hg)</i>	<i>Cu(II), Cu(I)</i>
<i>Methanol</i> <sup>b</sup>			<i>2-Propanol (continued)</i>		
no chloride	+0.175	+0.210	1.99	-0.270	
3.12	-0.016	—	1.80		+0.536
3.03	—	+0.331	1.65	-0.304	
2.82	-0.045	—		$K_{Li^+, ClO_4^-} = 10^{1.5 g}$	
2.77	—	+0.340		$K_{Li^+, Cl^-} = 10^{2.2 g}$	
2.64	-0.066	+0.343			
2.42	-0.084	+0.355			
2.27	-0.105	+0.370			
2.12	-0.125	+0.375			
1.82	-0.161	+0.373			
1.41	-0.207	+0.368			
1.10	-0.242	+0.375			
	$K_{Li^+, ClO_4^-} = \text{strong electrolyte}^d$				
	$K_{Li^+, Cl^-} = 10^{0.5 e}$				
<i>Ethanol</i> <sup>a</sup>			<i>2-Butanol</i> <sup>e</sup>		
no chloride	+0.275	+0.360	no chloride	+0.345	+0.550
3.46	-0.058	+0.490	3.94	-0.035	+0.590
3.16	-0.085	+0.488	3.64	-0.073	+0.598
2.76	-0.130	+0.499	3.46	—	+0.597
2.40	-0.173	+0.469	3.46	-0.099	+0.586
2.08	-0.209	+0.480	3.34	-0.114	-0.588
1.67	-0.267	+0.490	3.16	—	+0.579
1.35	-0.318	+0.447	2.98	—	—
	$K_{Li^+, ClO_4^-} = 10^{0.80 d, f, g}$		2.93	-0.135	—
	$K_{Li^+, Cl^-} = 10^{1.43 d, g}$		2.89	—	+0.580
			2.60	-0.170	—
			2.58	—	+0.569
				$K_{Li^+, ClO_4^-} = 10^{1.6 g}$	
				$K_{Li^+, Cl^-} = 10^{2.3 g}$	
<i>2-Propanol</i> <sup>b</sup>			$-\log [LiCl]$		
no chloride	+0.286	+0.520	<i>Acetone</i> <sup>b</sup>		
4.12	-0.065	—	no chloride	+0.365	+0.520
3.89	-0.083	+0.580	3.22		+0.511
3.59	-0.108	+0.579	3.00	-0.408	—
3.42	-0.123	—	2.80		+0.480
3.41	—	+0.584	2.70	-0.444	—
3.29	-0.147	—	2.58		+0.469
3.19	—	+0.585	2.52	-0.463	—
3.12	-0.160	—	2.44		+0.462
3.03	—	+0.581	2.30	-0.475	—
2.86	-0.174	—	2.25		+0.453
2.82	—	+0.579	2.07		+0.444
2.68	-0.191	—	2.00	-0.504	—
2.52	—	+0.571	1.77	-0.528	—
2.43	-0.221	—	1.75		+0.422
2.33	—	+0.558	1.59	-0.539	—
2.22	-0.246	—	1.58		+0.408
2.08	—	+0.545	1.37	-0.550	—
			1.36		+0.402
			1.16	-0.556	+0.400
				$K_{Li^+, ClO_4^-} = 10^3 h$	
				$K_{Li^+, Cl^-} = 10^3 h$	

<sup>a</sup> Corrected for liquid-junction p. d. from 0.10 F LiClO<sub>4</sub> soln. by the use of the half-wave potentials for the oxidation of ferrocene in the chloride-containing soln. and in 0.10 F LiClO<sub>4</sub> soln.

<sup>b</sup> Not corrected for liquid-junction p. d. from 0.10 F LiClO<sub>4</sub> soln. because of less than 30-mV change in  $E_{1/2}$  oxidation of ferrocene from non chloride-containing soln. to highest chloride-containing soln. This difference in  $E_{1,j}$ , however, is taken into consideration in the analysis of the data.

<sup>c</sup> Not corrected for  $\Delta E_{1,j}$ , as max. LiCl concn. was only 0.02 F.



<sup>d</sup> Ref. 10.

<sup>e</sup> In a recent conductance study, KAY found no evidence for association between lithium and chloride ions in methanol<sup>11</sup>. The  $10^{0.5}$  value for the ion-pair formation constant of  $\text{Li}^+$ ,  $\text{Cl}^-$  in methanol was obtained by an extrapolation procedure involving the use of the ion-pair formation constants of  $\text{Na}^+$ ,  $\text{Cl}^-$  and  $\text{K}^+$ ,  $\text{Cl}^-$  in this solvent. The plot of ion-pair formation constants of  $\text{K}^+$ ,  $\text{Cl}^-$  and  $\text{Na}^+$ ,  $\text{Cl}^-$  in ethanol *vs.* the same information in methanol extrapolated to the ion-pair formation constant of  $\text{Li}^+$ ,  $\text{Cl}^-$  in ethanol gives  $10^{0.5}$  for  $K_{\text{Li}^+, \text{Cl}^-}$  in methanol. This extrapolation procedure is based on the observed, approx. linear relationship for plots of the ion-pair formation constants of  $\text{Li}^+$ ,  $\text{NO}_3^-$ ;  $\text{Na}^+$ ,  $\text{NO}_3^-$ ; and  $\text{K}^+$ ,  $\text{NO}_3^-$  in methanol and of the ion-pair formation constants of  $\text{Li}^+$ ,  $\text{Cl}^-$ ;  $\text{Na}^+$ ,  $\text{Cl}^-$ ; and  $\text{K}^+$ ,  $\text{Cl}^-$  in ethanol *vs.* the formation constants of the same salts in water (for details of this extrapolation method, see ref. 4). Assuming that  $\text{LiClO}_4$  is a strong electrolyte in methanol, one can determine the ion-pair formation constant of  $\text{Li}^+$ ,  $\text{Cl}^-$  that gives the most consistent value of  $\beta_{\text{CuCl}_2^-}$  in this solvent. The value of  $10^{0.5}$  for  $K_{\text{Li}^+, \text{Cl}^-}$ , which is identical with that obtained by the extrapolation procedure, best fits the copper(I) data in methanol.

<sup>f</sup> Ref. 12.

<sup>g</sup> Evaluated by an approximation method based on the value of  $a$  in the equation  $K = K_0 \exp(q^2/a DkT)$ , being approximately constant for a given salt in all four alcohols studied. The  $a$ -values used were crystal radii plus corrections for solvation (W. M. LATIMER, K. S. PITZER AND C. M. SLANSKY, *J. Chem. Phys.*, 7 (1939) 108) [For a detailed discussion of this approximation procedure see ref. 4].

<sup>h</sup> Evaluated by an approximation method similar to that referred to in footnote g.

supporting electrolyte was 0.10  $F$  ( $\text{LiClO}_4 + \text{LiCl}$ ). All determinations were carried out at  $25 \pm 1^\circ$ .

Changes in liquid-junction potential at high chloride concentrations were estimated from changes in the half-wave potential for the oxidation of ferrocene<sup>5</sup>.

The values for the chloride concentrations in Table 1 have been corrected for the formation of  $\text{Li}^+$ ,  $\text{ClO}_4^-$  and  $\text{Li}^+$ ,  $\text{Cl}^-$  ion-pairs in these solvents by the use of the formation constants given in Table 1. Because little information is available in the literature on the formation of these ion-pairs, approximation procedures (see footnotes in Table 1 and for a detailed discussion, ref. 4) were used to obtain the constants. The estimated values show the correct variation with solvent and are probably good to 0.3 of a log unit, certainly adequate for the purpose of (1) determining the nature of the copper(II)- and copper(I)-chloro complexes in these solutions, (2) estimating their formation constants, and (3) obtaining information on the effect of solvent on the nature and stability of these complexes.

## RESULTS AND DISCUSSION

### *Polarographic study of copper (I) complexes*

The copper(I) complex species in solution were studied by voltammetry at the dropping copper amalgam electrode (*ca.* 2 mF in copper metal). The dropping copper amalgam electrode (d.a.e.) has been found to have several advantages over the conventional dropping mercury electrode in the study of copper(I) complexes<sup>1</sup>.

The formulae and stepwise formation constants of the complexes of copper(I) ion with chloride ion in solution may be evaluated from the expression below for the dependence of the half-wave potential of the Cu(I), Cu(Hg) wave on the concentration of chloride:  $(E_{\frac{1}{2}})_c - (E_{\frac{1}{2}})_s = -0.059 \log (1 + \beta [\text{Cl}^-]_0 + \dots + \beta_p [\text{Cl}^-]_0^p)$ <sup>6</sup>. The  $\beta$ 's are the overall formation constants of the copper(I) complexes, and subscript zero denotes concentration at the electrode surface. The other terms have their usual significance<sup>7</sup>.

Data showing the observed half-wave potentials as a function of chloride ion concentration in 0.10  $F$  ( $\text{LiClO}_4 + \text{LiCl}$ ) solutions are given in Table 1. In the alcohols

and in acetone, the anodic copper(I), copper(0) polarograms were in all cases reversible or nearly reversible. Where the wave was drawn out, a model of a reversible wave was fitted to the foot of the experimental wave to obtain the half-wave potential<sup>1,8,9</sup> listed in Table 1. With the alcohols, the plots of  $(E_{1/2})_c - (E_{1/2})_s$  vs.  $-\log(\text{Cl}^-)$  are linear with slopes of *ca.* +0.12, indicating that  $\text{CuCl}_2^-$  is the copper(I) species in solution. The corresponding plots of the data for acetone solutions have slopes of +0.118 at chloride concentrations below *ca.*  $10^{-2} F$ , but at higher concentrations, the curves appear to be flattening out. Since this result is the opposite of what should be observed for the formation of complexes higher than  $\text{CuCl}_2^-$ , it is concluded that perhaps LiCl is precipitating in solutions of high chloride concentration. The data for chloride ion concentrations in excess of  $10^{-2} F$ , therefore, are suspect. The overall formation constants for  $\text{CuCl}_2^-$  in 0.10 *F* ( $\text{LiClO}_4 + \text{LiCl}$ ) solutions of the solvents investigated were calculated by standard procedure<sup>13</sup> and are given in Table 2. Values for  $\beta_{\text{CuCl}_2^-}$  in 1.0 *F* ( $\text{LiClO}_4 + \text{LiCl}$ ) solutions of some of the solvents are also included in the table. The uncertainty of the  $\beta_{\text{CuCl}_2^-}$  is within *ca.*  $10^{\pm 0.4}$ .

TABLE 2

FORMATION CONSTANTS OF THE CHLORO COMPLEXES OF COPPER(II) AND COPPER(I) IN METHANOL, ETHANOL, 2-PROPANOL, 2-BUTANOL, AND ACETONE  
0.10 *F* ( $\text{LiClO}_4 + \text{LiCl}$ ); temp.  $25 \pm 1^\circ$ .

	<i>Methanol</i>	<i>Ethanol</i>	<i>2-Propanol</i>	<i>2-Butanol</i>	<i>Acetone</i>
Copper(II)					
$\beta_{\text{CuCl}^+}$	$10^{4.2}$ ( $10^{4.1}$ ) <sup>a</sup> $10^{3.3}$ <sup>b</sup>	$< 10^{6.6}$ <sup>c</sup>	—	—	—
$\beta_{\text{CuCl}_2}$	$10^{6.5}$ ( $10^{6.3}$ ) <sup>a</sup> $10^{5.4}$ <sup>b</sup>	$10^{10.1}$ ( $10^{9.4}$ ) <sup>a</sup>	$10^{12.3}$ ( $10^{10.8}$ ) <sup>a</sup>	$10^{13.5}$ ( $10^{11.4}$ ) <sup>a</sup> $10^{11.0}$ <sup>b</sup>	$10^{19.9}$ <sup>b</sup>
$\beta_{\text{CuCl}_3^-}$	—	$< 10^{11.3}$ <sup>d</sup>	$10^{14.9}$ ( $10^{12.7}$ ) <sup>a</sup>	$10^{16.3}$ ( $10^{13.3}$ ) <sup>a</sup> $10^{15.1}$	$10^{25.1}$ ( $10^{22.3}$ ) <sup>a</sup> $10^{23.5}$ <sup>b</sup>
Copper(I)					
$\beta_{\text{CuCl}_2^-}$	$10^{9.3}$ ( $10^{9.1}$ ) <sup>a</sup> $10^{9.6}$ <sup>b</sup>	$10^{12.3}$ ( $10^{11.6}$ ) <sup>a</sup> $10^{12.5}$ <sup>b</sup>	$10^{13.4}$ ( $10^{11.9}$ ) <sup>a</sup>	$10^{14.1}$ ( $10^{12.2}$ ) <sup>a</sup> $10^{13.4}$ <sup>b</sup>	$10^{20.9}$ ( $10^{18.9}$ ) <sup>a</sup> $10^{19.2}$ <sup>b</sup>

<sup>a</sup> Formal constant, not corrected for ion-pairing.

<sup>b</sup> Value in 1.0 *F* ( $\text{LiClO}_4 + \text{LiCl}$ ).

<sup>c</sup> Max. value for  $\beta_{\text{CuCl}^+}$  if  $\text{CuCl}^+$  is obtainable.

<sup>d</sup> Max. value for  $\beta_{\text{CuCl}_3^-}$  if  $\text{CuCl}_3^-$  is obtainable.

### *Voltammetric study of the copper (II) complexes*

The copper(II), copper(I) polarographic wave cannot be observed at the dropping mercury electrode in the presence of chloride ion because of the relatively negative potential for the dissolution of mercury in chloride media. It is possible, however, to obtain current-voltage curves for this redox system at the rotating platinum electrode (r.p.e.). The methanol and ethanol solutions examined were *ca.*  $2 \cdot 10^{-4} F$  in copper(II). The current-voltage curves for 2-propanol, 2-butanol, and acetone solutions were obtained by the use of solutions containing both copper(I) and copper(II), each at *ca.*  $2 \cdot 10^{-4} F$  concentration. Such a system has the advantage that the half-wave potential occurs very near zero current, the current region in which, in this case, there nearly always appears to be reversible behavior.

The cathodic copper(II), copper(I) reduction waves in methanol and ethanol

at the r.p.e. were well-defined with "0.059/*n*"-values of 0.065–0.090 V. The waves were drawn-out for solutions of high chloride content. The half-wave potentials were evaluated, as in the copper(I), copper(Hg) case, by fitting a model of a reversible wave to the foot of each of the waves<sup>1,8,9</sup>. In 2-propanol, 2-butanol, and acetone, the half-wave potentials for the copper(II), copper(I) couple were evaluated from the continuous anodic-cathodic waves. The half-wave potentials coincided or very nearly coincided with the potentials at zero current.

The concentration regions of chloride examined were such that  $\text{CuCl}_2^-$  was the only copper(I) complex species in solution. Under this condition, the following equation holds:

$$(E_{\frac{1}{2}})_c - (E_{\frac{1}{2}})_s = 0.059 \log \frac{\beta_{\text{CuCl}_2^-} [\text{Cl}^-]^2}{1 + \beta_{\text{CuCl}^+} [\text{Cl}^-]_0 + \dots + \beta_{\text{CuCl}_4^{2-}} [\text{Cl}^-]_0^4}$$

The  $\beta$ 's represent the overall formation constants of the respective species, and subscript zero denotes concentration at the electrode surface. Examination of the above equation reveals that increasing chloride ion concentration shifts the half-wave potential positive, negative, or not at all, depending upon whether the primary copper(II) complex in solution has less than two, more than two, or exactly two chloride ligands, respectively.

The half-wave potential data at various chloride ion concentrations are given in Table I. For methanol, with increasing chloride ion concentration, the half-wave potential first shifts positive, then remains constant, showing that first  $\text{CuCl}^+$ , then  $\text{CuCl}_2$  are the main copper(II) species in solution. In the case of ethanol, the half-wave potential remains essentially constant throughout the region  $-3.5 < \log[\text{Cl}^-] < -1.5$ ;  $\text{CuCl}_2$ , therefore, must be the copper(II) species in solution. With 2-propanol, the plot of  $E_{\frac{1}{2}}$  vs.  $\log[\text{Cl}^-]$  shows first a zero slope, then a negative 0.059 slope, which indicate that both  $\text{CuCl}_2$  and  $\text{CuCl}_3^-$  are formed.

The analysis of the effect of varying chloride concentration on the half-wave potential of the Cu(II), Cu(I) couple in 2-butanol is not as clean cut as for the three previous alcohols. An effort, however, has been made to obtain a reasonable analysis, the results of which appear to be consistent with those reported for the other alcohols. At low chloride concentrations,  $(E_{\frac{1}{2}})_c$  does not appear to shift with increasing chloride concentration, whereas at higher chloride concentrations  $(E_{\frac{1}{2}})_c$  shifts to negative values consistent with a  $-0.059$  slope. This behavior indicates that below ca.  $10^{-3.2}$  M chloride concentration, the copper(II) species is  $\text{CuCl}_2$ , whereas above this concentration  $\text{CuCl}_3^-$  becomes the predominant species.

In acetone 0.1 *F* in supporting electrolyte in the concentration region for which the data are considered to be reliable ( $10^{-3}$ – $10^{-2}$  *F* chloride), the plot of the half-wave potential vs. the log of the formal chloride concentration is linear with a  $-0.059$  slope. Therefore, in this chloride concentration region the copper(II) species is  $\text{CuCl}_3^-$ . In the region  $10^{-1.6}$  for the formal chloride concentration, there is some indication of a steeper slope for the plot. This cannot be verified with certainty because, as explained under the discussion of the copper(I) results, the data taken at higher chloride concentrations are suspect. Nevertheless, in view of the large value of  $\beta_{\text{CuCl}_3^-}$  it does seem likely that  $\text{CuCl}_4^{2-}$  might become the predominant copper(II) species in solution. Spectrophotometric data<sup>14</sup> also indicate the existence of  $\text{CuCl}_4^{2-}$  in acetone solution.

The formation constants of the chloro complexes of copper(II) in the solvents

investigated calculated by standard procedure<sup>13</sup> are given in Table 2. Also included in Table 2 are formation constants in 1.0 *F* (LiClO<sub>4</sub>+LiCl) solutions of some of the solvents. The values are estimated to be good to within 10<sup>±0.6</sup>.

Absorbance measurements have been taken of alcohol solutions containing various ratios of chloride to copper(II). Although no attempt has been made to calculate formation constants from these data, they are consistent with the electrochemical data in regard to the species present at given chloride ion concentrations.

#### *Correlation of formation constants with solvent properties*

The polarographic half-wave potentials for the Cu(I), Cu(Hg) couple in various solvents in the absence of complexing agents indicate the degree of solvation of copper(I). An examination of these potentials (methanol, -0.04 V (*vs.* S.C.E.); ethanol, +0.02 V; 2-propanol, +0.00 V; 2-butanol, +0.06 V; acetone, +0.06 V —corrected for liquid-junction potential differences with aqueous 0.10 *M* lithium perchlorate as the reference solvent)<sup>4</sup> reveals that the degree of solvation of copper(I) ion is about the same in methanol, ethanol, 2-propanol, 2-butanol, and acetone, with a trend, as expected, to slightly weaker solvation in that order. The trend toward weaker solvation of copper(I) in passing through the alcohols from methanol to 2-butanol is reflected in a corresponding increase in the stability of CuCl<sub>2</sub><sup>-</sup>. Not all the increase in stability of CuCl<sub>2</sub><sup>-</sup>, however, can be attributed to decrease in solvation energy of copper(I) ion. The decreasing acid character of the OH group in the alcohols, through decrease in anion solvation, and the shift to solvents with lower dielectric constant also contribute to increase in stability of CuCl<sub>2</sub><sup>-</sup>. The value of  $\beta_{\text{CuCl}_2^-}$  in acetone is much higher than would be expected from the relatively weak solvation of copper(I) and from the dielectric constant of the medium. This situation may be explained on the basis that acetone, unlike the alcohols, is not a hydrogen-bonding solvent and chloride ion, therefore, is less strongly solvated in acetone than in the lower alcohols.

Half-wave potential data indicate that the solvation of copper(II) ion in the lower alcohols and acetone follows the same general trend as the solvation of copper(I). As expected, the stability of the chloro complexes of copper(II) in the alcohols reflects the solvating ability of the alcohols for copper(II) ions and chloride ion, *e.g.*, CuCl<sup>+</sup> can exist at moderately high chloride concentrations in methanol but not in ethanol, 2-propanol, or 2-butanol, and CuCl<sub>3</sub><sup>-</sup> is observed in 2-propanol and 2-butanol but not in methanol and ethanol. The increase in stability of the chloro complexes of copper(II) from methanol to 2-butanol also parallels the decrease in dielectric constant of the alcohols. As with the copper(I) complex, the extremely weak solvation of chloride ion in acetone accounts for the extremely high stabilities of the chloro complexes of copper(II) in this solvent as compared with the alcohols.

The constants reported are formal ones in the sense that no correction for the formation of ion-pair species such as Li<sup>+</sup> CuCl<sub>2</sub><sup>-</sup> and CuCl<sup>+</sup> ClO<sub>4</sub><sup>-</sup> has been made because the appropriate data are not available.

#### ACKNOWLEDGEMENT

This work was supported in part from a grant from the General Research Fund, University of Kansas.

## SUMMARY

The chloro complexes of copper(II) and copper(I) in methanol, ethanol, 2-propanol, 2-butanol, and acetone have been investigated by voltammetry. Log  $\beta_{\text{CuCl}_2^-}$  values in the solvents in the order listed above are: 9.3, 12.3, 13.4, 14.1, and 19.2. For the copper(II) complexes, log  $\beta_{\text{CuCl}^+}$  in methanol is 4.9 and in ethanol, < 6.6. Log  $\beta_{\text{CuCl}_2}$  in the alcohols starting with methanol are: 6.5, 10.1, 12.3, and 13.5, and log  $\beta_{\text{CuCl}_3^-}$  in ethanol, 2-propanol, 2-butanol, and acetone are: < 11.3, 14.9, 16.3 and 25.1.

## REFERENCES

- 1 S. E. MANAHAN AND R. T. IWAMOTO, *Inorg. Chem.*, 4 (1965) 1409.
- 2 J. BJERRUM, *Kem. Maanedstidsskrift*, 26 (1945) 24.
- 3 M. T. KELLEY, H. C. JONES AND D. J. FISHER, *Anal. Chem.*, 31 (1959) 1475.
- 4 S. E. MANAHAN, Ph.D. Thesis, University of Kansas, 1966.
- 5 I. V. NELSON AND R. T. IWAMOTO, *Anal. Chem.*, 35 (1963) 867.
- 6 H. A. LAITINEN, *Chemical Analysis*, McGraw-Hill, New York, N.Y., 1960, p. 286.
- 7 I. M. KOLTHOFF AND J. J. LINGANE, *Polarography*, Vol. 1, Interscience Publishers, New York, N.Y., 2nd ed., 1952, ch. 11, 12.
- 8 R. C. LARSON AND R. T. IWAMOTO, *Inorg. Chem.*, 1 (1962) 316.
- 9 I. M. KOLTHOFF AND F. G. THOMAS, *J. Phys. Chem.*, 69 (1965) 3054.
- 10 C. W. DAVIES, *Ion Association*, Butterworths, Washington, 1962, p. 90.
- 11 R. L. KAY, *U.S. At. Ener. Comm. NYO-10695 (1963)*; *Nucl. Sci. Abstr.*, 18 (L) (1964) No. 206.
- 12 R. L. KAY, *J. Am. Chem. Soc.*, 82 (1960) 2099.
- 13 I. M. KOLTHOFF AND J. J. LINGANE, *Polarography*, Vol. 1, Interscience Publishers, New York, N.Y., 2nd ed., 1952, ch. 12.
- 14 J. GAZO, *Chem. Zvesti*, 10 (1956) 509.

## ON THE INCREASE OF SENSITIVITY AND SPECIFICITY IN THE OSCILLOPOLAROGRAPHY OF URANIUM

ALFONSO MORALES AND FLORA GONZÁLEZ V.

*Central Department of Mathematics and Natural Science, University of Chile, Macul 774, Casilla 147, Santiago (Chile)*

(Received February 1st, 1966; revised March 26th, 1966)

## INTRODUCTION

The aim of the present paper is to investigate the oscillopolarographic activity and the specificity of the reaction for uranium and various metal ions. Recently, MATYSIK<sup>1</sup> has proposed a selective, semi-quantitative method for the rapid determination of uranium based on the high degree of oscillopolarographic selectivity of the compounds that uranium forms with phenols. Similarly, KALVODA AND JUAN<sup>2</sup> have observed that the oscillopolarographic sensitivity increases when the substance being studied is sparingly soluble or forms complexes with the supporting electrolyte.

The behaviour of uranium in both organic and inorganic supporting electrolytes is examined, and also the influence of complexing agents on the incision in the curve,  $dE/dt = f(E)$ .

## EXPERIMENTAL

Both the quantitative and qualitative determinations were made on a Krizick P576 Polaroscope. The curve,  $dE/dt = f(E)$ , is presented on the screen of the cathode-ray tube of this instrument. The position of the incisions is expressed<sup>3</sup> by means of the quantity,  $Q$ . The sensitivity of the qualitative test is expressed by means of the quantity,  $pD$ .

*Qualitative analysis and discussion*

The oscillopolarographic behaviour of U(VI) in both inorganic and organic supporting electrolytes is examined and in each case a study made of the conditions that make the reaction specific.

*Inorganic supporting electrolytes.* Both cathodic and anodic incisions are obtained in 0.1 *M* solutions of the inorganic acids, H<sub>3</sub>PO<sub>4</sub>, HCl, and HClO<sub>4</sub>; the anodic incisions ( $pD = 6.2$ ) are more sensitive than those of the cathodic branch ( $pD = 4.7$ ) (see Fig. 1).

In HClO<sub>4</sub>, the following cations form incisions: Cu(II), Cd(II), Pb(II), Bi(III), Zn(II), Fe(III), Sn(II), Mo(VI), V(V) and Cr(III). Table 1 shows that in the qualitative determination of U(VI) in 0.1 *M* HClO<sub>4</sub>, only Zn(II), V(V) and Cr(III) interfere; they are eliminated by using potassium ferrocyanide, urotropine and benzidine, respectively.

If these interfering elements are eliminated, perchloric acid can be used as a specific reagent for the detection of uranium at a concentration of  $0.02 \mu\text{g/ml}$ . This medium is unsuitable when quantitative results are required because the depth of the incision is not proportional to the concentration of uranium.

In  $0.1 M$  HCl, U(VI) produces two cathodic and one anodic incision, of which the anodic is more sensitive ( $pD = 5.7$ ). Many metallic ions, such as Zn(II), Cr(III) and V(V), act as depolarizers and interfere in the detection of U(VI). The effect of Zn can be eliminated with  $\text{K}_4\text{Fe}(\text{CN})_6$ , that of the other ions, with urotropine.

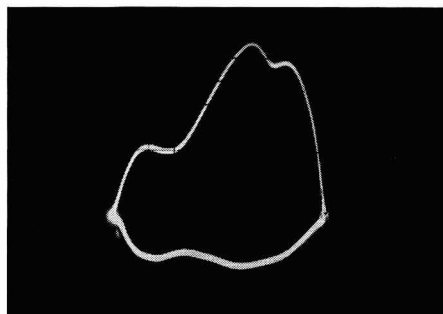
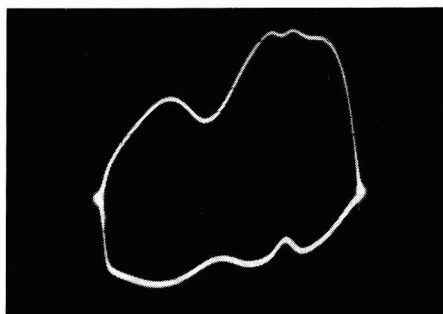


Fig. 1.  $0.05 \text{ ml } 10^{-2} M$  U(VI) in  $6 \text{ ml}$  of  $\text{HClO}_4$   $0.1 M$ ; d.c. =  $4 \text{ mA}$ ; a.c. =  $0.25 \text{ mA}$ .

Fig. 2.  $0.08 \text{ ml } 10^{-2} M$  U(VI) in  $6 \text{ ml}$  TEA ( $0.1 M$ )–HCl ( $0.1 M$ ) in  $1:5$  proportion ( $\text{pH} = 1$ ); d.c. =  $4 \text{ mA}$ ; a.c. =  $0.15 \text{ mA}$ .

TABLE 1

SUPPORTING ELECTROLYTE, PERCHLORIC ACID  $0.1 M$

	$Q_c$	$Q_a$	$pD$	Observations
U(VI)	—	0.63	6.2	
Pb(II)	0.45	0.41	5.4	
Cu(II)	—	0.18	5.9	
Cd(II)	—	0.40	5.7	
	0.54	—	5.4	
Bi(III)	—	0.12	5.4	
Zn(II)	—	0.67	5.9	Eliminated with $\text{K}_4\text{Fe}(\text{CN})_6$
	0.81	—	5.6	
Fe(III)	0.12	0.054	5.3	
Sn(II)	—	0.30	5.2	
	0.30	—	5.0	
Mo(VI)	0.30	—	4.4	
V(V)	0.83	—	5.0	Eliminated with urotropine
Cr(III)	0.81	—	5.7	Eliminated with benzidine
Ni, Al, La, Th	—	—	—	Inactive

Note: Besides the anodic incision,  $Q_a = 0.63$ , U(VI) produces two cathodic incisions ( $Q_c = 0.63$  and  $Q_c = 0.81$ ) of inferior sensitivity.

*Effect of complex-forming agents on inorganic supporting electrolytes.* When triethanolamine (TEA) is added to supporting electrolytes consisting of inorganic acids, it reduces the sensitivity but has the great advantage of eliminating interference due to other ions.

In a base solution of 0.1 *M* HCl and 0.1 *M* TEA in the proportion of 5 : 1, none of the 16 cations examined interferes in the detection of U(VI) (see Table 2 and Fig. 2).

*Organic supporting electrolytes.* Supporting electrolytes based on organic acids have a number of advantages in the detection of U(VI). The incision of the curve  $dE/dt = f(E)$  is ample and clear, and in general, the sensitivity is greater in organic supports. In media consisting of organic acids one anodic and two cathodic incisions are produced.

TABLE 2

SUPPORTING ELECTROLYTE, HYDROCHLORIC ACID (0.1 *M*)—TRIETHANOLAMINE (0.1 *M*)

	$Q_c$	$Q_a$	$pD$	Observations
U(VI)	0.76	—	4.4	
Pb(II)	0.34	0.34	5.4	
Cd(II)	0.36	0.34	5.4	
Bi(III)	0.10	0.14	5.4	
Cu(II)	—	0.20	5.6	
Zn(II)	0.69	—	5.6	
Mo(VI)	0.30	—	4.5	
Sn, V, Ni, Cr, Fe, Al, La, Zr, Th	—	—	—	No depolarizing activity

$Q_c$  = cathodic incision,  $Q_a$  = anodic incision.

In 0.1 *M* tartaric acid,  $10^{-2}$  *M* U(VI) produces two cathodic incisions and one anodic. At lower concentrations ( $10^{-3}$  *M*), only the anodic incision is formed. In this medium, Bi(III), Ni(II), Zn(II) and Cr(III) interfere. The interferences caused by these ions can be eliminated as described below. Other cations, although they may produce incisions, do not affect the detection of U(VI).

In 0.1 *M* citric acid also, are formed one anodic and two cathodic incisions, of which the anodic is the most sensitive ( $pD = 6.1$ ) (see Fig. 3). Table 3 shows that the following ions interfere in the detection of U(VI): Ni(II), Zn(II), Mo(VI) and Cr(III). The interferences caused by these ions can be eliminated by adding reagents of a strong complex-forming character.

In 0.1 *M* ascorbic acid, the following ions interfere in the detection of U(VI):

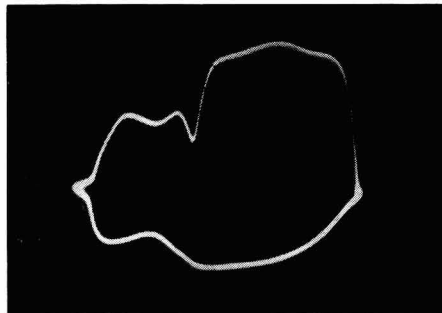
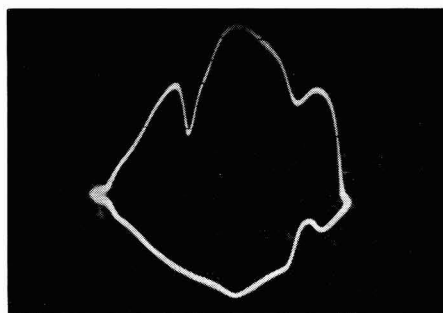


Fig. 3. 0.15 ml  $10^{-3}$  *M* U(VI) in 6 ml citric acid 0.1 *M*; d.c. = 2 mA; a.c. = 0.1 mA.

Fig. 4. 0.15 ml  $5 \cdot 10^{-3}$  *M* U(VI) in 6 ml TEA (0.1 *M*)—tartaric acid (0.1 *M*), pH = 5–8.



Pb(II), V(V), Al(III) and Zn(II). Other ions, although they may produce incisions, do not affect the determination of U(VI); Fe(III), Co(II), Cr(III), Mo(VI), La(III) and Zr(IV) are not reduced.

*Effect of complex-forming substances on organic supporting electrolytes.* In order to increase the specificity and sensitivity of the reaction being studied, triethanolamine (T.E.A.) was added to the organic supporting electrolytes. This increases the sensitivity and at the same time is an excellent reagent for eliminating interference caused by other ions.

TABLE 3  
SUPPORTING ELECTROLYTE, CITRIC ACID 0.1 M

	$Q_c$	$Q_a$	$pD$	Observations
U(VI)	—	0.75	6.1	
Cu(II)	0.21	0.21	5.3	
Pb(II)	0.42	0.44	5.4	
Ni(II)	0.78	—	5.5	
Bi(III)	0.32	—	5.4	
	—	0.23	5.1	
Zn(II)	0.74	0.73	5.6	
Cd(II)	—	0.52	5.7	
	0.49	—	5.4	
Fe(III)	0.09	—	5.3	
Mo(VI)	0.37	—	5.1	
Cr(III)	0.78	—	5.3	
Sb(V)	0.20	—	4.7	
Zr, La, Th	—	—	—	No depolarizing activity

*Note:* If the concn. of U(VI) is  $10^{-2}$ – $10^{-3}$  M, there are 2 cathodic and one anodic incisions ( $Q_c = 0.37$ ;  $Q_c = 0.78$  and  $Q_a = 0.75$ ) ( $pD = 5.7$ ). In more dilute solutions,  $10^{-4}$  M, only the anodic incision is produced.

In a mixture of 0.1 M tartaric acid and 0.1 M TEA in the proportion 2 : 4 at pH = 5–8, the specificity of the reaction is excellent. Only one clear, characteristic and sensitive cathodic incision is formed at  $-0.61$  V (S.C.E.),  $Q_c = 0.36$  and  $pD = 6.1$  (see Fig. 4). The addition of TEA eliminates the interferences caused by Zn(II), Ni(II) and Cr(III) that appear if pure tartaric acid is used. However, the pH must be higher than 4 or Pb(II) and Bi(III) begin to interfere. The interferences caused by these ions, even at pH 4, can be eliminated as shown in Table 4. The interferences caused by the Pb(II) incision disappears on the addition of 1 ml of a 0.1 M solution of EDTA + 1 ml of citric acid, to 6 ml of original solution. If too little EDTA is added, the Pb(II) incision is displaced to  $Q_c = 0.75$ . Similar results are obtained at pH = 4 by the addition of citrate, citric acid and EDTA.

The interference caused by Bi(III) can be eliminated by adding thiourea at pH = 5, or citric acid and EDTA, when the incision of Bi(III) is displaced to  $Q_c = 0.49$ , or citric acid and hydroxylamine, when the incision of Bi(III) is displaced to  $Q_c = 0.23$  and  $Q_a = 0.09$ . Under these experimental conditions using TEA with tartaric acid as supporting electrolyte U(VI) has been detected in the presence of 17 other ions.

In a mixture of 0.1 M citric acid and 0.1 M TEA in the proportion of 3 : 3 at pH = 4, only one cathodic incision is formed,  $Q_c = 0.41$  and  $pD = 5.6$  (see Fig. 5).

TABLE 4

SUPPORTING ELECTROLYTE, TARTARIC ACID (0.1 M)—TRIETHANOLAMINE (0.1 M)

	$Q_c$	$Q_a$	$pD$	Observations
U(VI)	0.36	—	6.1	pH = 1-4
	0.41	—		
	0.36	—		
Cu(II)	0.18	0.21	5.9	Suppressed with 1 ml EDTA, 0.1 M + 1 ml citric acid, 0.1 M
Pb(II)	0.36	—	5.1	
	—	0.29	5.0	
Zn(II)	—	0.47	5.6	
	0.72	—	5.1	
Bi(III)	0.40	0.12	5.4	Suppressed with thiourea
V(V)	0.16	—	6.0	
Sn, Mo, Fe, Al, Ni, Cr, La, Zr, Th	—	—	—	Inactive

Note: At pH values below 4, uranium produces two incisions of the same sensitivity which are very close to each other ( $Q_c = 0.36$  and  $Q_c = 0.41$ ); furthermore, Pb and Bi interfere. Between pH 5 and pH 8 there is only one incision ( $pD = 6.1$ ) and no interference.

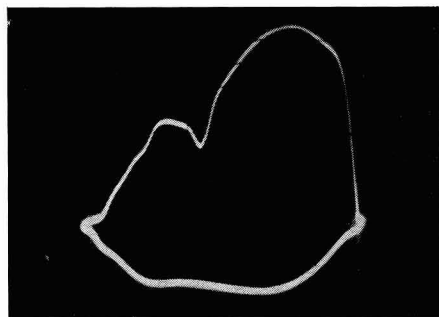


Fig. 5. 0.04 ml  $10^{-2}$  M U(VI) in 6 ml TEA (0.1 M)—citric acid (0.1 M) in 3 : 3 proportion (pH = 4); d.c. = 3 mA; a.c. = 0.15 mA.

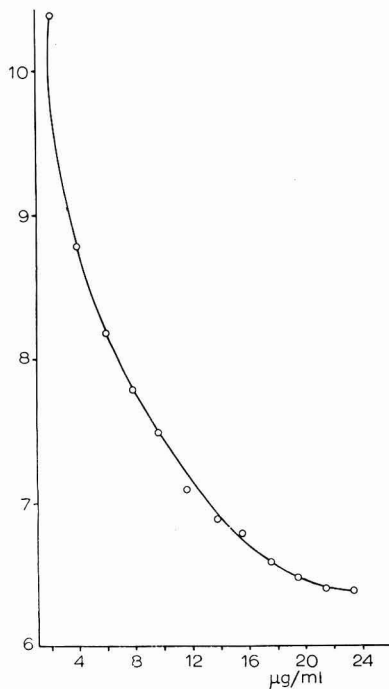


Fig. 6. Calibration curve for  $10^{-2}$  M U(VI) in TEA (0.1 M)—tartaric acid (0.1 M) medium at pH = 5-8; d.c. = 4 mA; a.c. = 0.05 mA.

The addition of TEA eliminates the interferences produced in a supporting electrolyte of citric acid alone but Pb(II) interferes and must be eliminated by EDTA.

In a mixture of 0.1 M ascorbic acid and 0.1 M TEA in the proportion of 3 : 4 at pH = 6, U(VI) produces only one cathodic incision:  $Q_c = 0.34$  and  $pD = 4.7$ .

The TEA eliminates the interferences that occur when ascorbic acid only is used except for the incision produced by Pb(II); this can be eliminated by adding  $10^{-1}$  M EDTA.

*Supporting electrolytes based on substances with a strong complex-forming nature.* Strongly complex-forming substances, EDTA, TEA, pyridine and TAN (tetra-acetic nitrile), afford a wide selection for dealing with the depolarizing activity of the metallic ions. A number of ions that in ordinary conditions produce marked incisions in the curve,  $dE/dt = f(E)$ , are made completely inactive in such supporting electrolytes. With supporting electrolytes of 0.1 M EDTA with 0.1 M TEA in the proportion of 5 : 1 and pH = 5, U(VI) can be detected in the presence of 16 other ions (see Table 5). In this medium, the only interfering ion is Cu(II), the incision of which is displaced to  $Q_c = 0.49$  by adding potassium ferrocyanide.

TABLE 5  
SUPPORTING ELECTROLYTE, EDTA (0.1 M)-TEA (0.1 M)

	$Q_c$	$Q_a$	$pD$	Observations
U(VI)	0.34	—	4.7	
Pb(II)	—	0.34	5.1	
Bi(III)	0.45	—	5.4	
Cr(III)	—	0.72	5.0	
*Cu(II)	0.34	0.18	5.2	Displaced with $K_4Fe(CN)_6$
Sb(V)	0.61	—	4.7	
Sn(II)	—	0.009	5.2	
V(V)	—	0.67	5.0	
Zn, Ni, Al, Fe, Mo, Co, Cd, La, Zr, Th	—	—	—	Inactive

\* = interfering

$Q_c$  = cathodic incision,  $Q_a$  = anodic incision

In pyridine with TAN, U(VI) forms only one cathodic incision:  $Q_c = 0.40$  and  $pD = 4.7$ . There are no interferences, although Cu(II), Pb(II), Cd(II) and Bi(III) ions produce incisions.

Both the TEA-EDTA mixture and the TAN-pyridine mixture have given excellent results in the detection of U(VI) in the presence of 17 other ions.

#### Quantitative results

The supporting electrolyte chosen from those studied, for the quantitative determination of uranium, was 0.1 M tartaric acid with 0.1 M triethanolamine.

The only interferences, which are caused by Pb(II) and Bi(III) ions, can be eliminated or displaced as described in the previous section, without disturbing the curve,  $dE/dt = f(E)$ . The depth of the incision is proportional to the concentration of uranium, as can be seen in the calibration curve (see Fig. 6). Determinations can be made between 2 and 24  $\mu\text{g/ml}$  of U(VI) in this support, with an error of  $\pm 1\%$ .

#### SUMMARY

The behaviour of uranium in both organic and inorganic supporting elec-

trolytes is examined, and also the influence of complexing agents on the incision in the curve,  $dE/dt = f(E)$ .

The addition of TEA to supporting electrolytes consisting of organic acids increases the sensitivity and the selectivity. The reaction becomes specific when the following are added to the supporting electrolyte: EDTA, thiourea, or substances that precipitate the interfering ions (*e.g.*,  $K_4Fe(CN)_6$ ). It has been possible to detect U(VI) in the presence of 16 different ions.

The behaviour of uranium has also been studied in complex-forming media: EDTA-TEA, pyridine and tetra-acetic nitrile. Specific reduction of uranium was obtained in these media in the presence of 17 other ions. In every case, the incision corresponds to the reduction of a complex absorbed on the surface of the electrode.

#### REFERENCES

- 1 J. MATYSIK, *Ann. Univ. Mariae Curie-Skłodowska, Lublin-Polonia*, AA 16 (1961) 37.
- 2 R. KALVODA AND A.-C. JUAN, *J. Electroanal. Chem.*, 8 (1964) 378.
- 3 R. KALVODA, *Techniques of Oscillographic Polarography*, Elsevier Publishing Co., Amsterdam, 1965.

*J. Electroanal. Chem.*, 13 (1967) 418-424

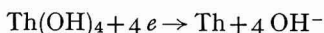
AMPEROMETRIC DETERMINATION OF THORIUM AND LANTHANUM  
IN PRESENCE OF NITRATE

ANIL K. MUKHERJI

*Department of Chemistry, Drexel Institute of Technology, Philadelphia, Pennsylvania 19104 (U.S.A.)*

(Received March 13th, 1966)

The standard electrode reduction potential of thorium ion to metal<sup>1</sup> is  $-1.90$  V and the polarographic reduction wave is masked by the larger reduction wave of hydrogen preceding it. In alkaline solutions, the reduction potential of the reaction



is  $-2.48$  V which makes the direct polarographic estimation of thorium by reduction, or its application to amperometry, virtually impossible.

Several indirect methods have been recommended for the amperometric determination of thorium. SMALES AND AIREY<sup>2</sup> proposed molybdate as a reagent. The titrations are carried out at an applied voltage of  $-0.9$  V and no diffusion current is obtained until after the end-point, when excess molybdate ions are reduced resulting in a reversed L-type titration graph. The experimental error for 5–25 mg of thorium is reported to be 3%.

KOLTHOFF AND JOHNSON<sup>3</sup> have recommended *m*-nitrophenylarsonic acid for thorium and uranium determinations. The pH is adjusted to 2.5, and on applying  $-0.3$  V, no diffusion current is produced until after the end-point, when the excess titrant undergoes a four-electron reduction to hydroxylamine.

SUNDERASAN AND KARKHANVALA<sup>4</sup> have titrated thorium with standardized sodium fluoride using ferric iron as indicator. A voltage of zero volts *vs.* S.C.E. is applied to the dropping mercury electrode, and at the end-point the diffusion current rapidly becomes zero.

LANGER<sup>5</sup> reported that thorium ions have the ability to carry nitrate ions to the mercury cathode and that these are then reduced at a potential of  $-1.3$  V. It seemed interesting to investigate further the possibility of utilizing nitrate reduction as an indicator for thorium titrations. The titrants examined were EDTA, and benzenephosphonic acid.

## EXPERIMENTAL

*Apparatus*

All polarograms were taken with a Sargent Model XV polarograph. The same capillary was used throughout the study. Measurements were made in an H-cell and oxygen was removed by bubbling purified nitrogen through the solution.

All pH-measurements were made with a glass electrode and a Beckman Zero-matic pH-meter.

*Thorium chloride solution*

A 0.05-*M* stock solution was prepared by dissolving reagent-grade thorium chloride (J. T. Baker); the solution was standardized by EDTA titration using thordin as indicator.

*Benzenephosphonic acid and EDTA solutions*

0.1-*M* stock solutions of benzenephosphonic acid (BPO), (Victor Chemicals), and the disodium salt of EDTA (J. T. Baker), were prepared by dissolving the appropriate amount of the reagent in distilled water.

All other chemicals used were reagent grade.

*The reduction of nitrate in the presence of thorium ions*

The reduction of nitrate was studied by adding 1 ml of 0.0811 *M* thorium

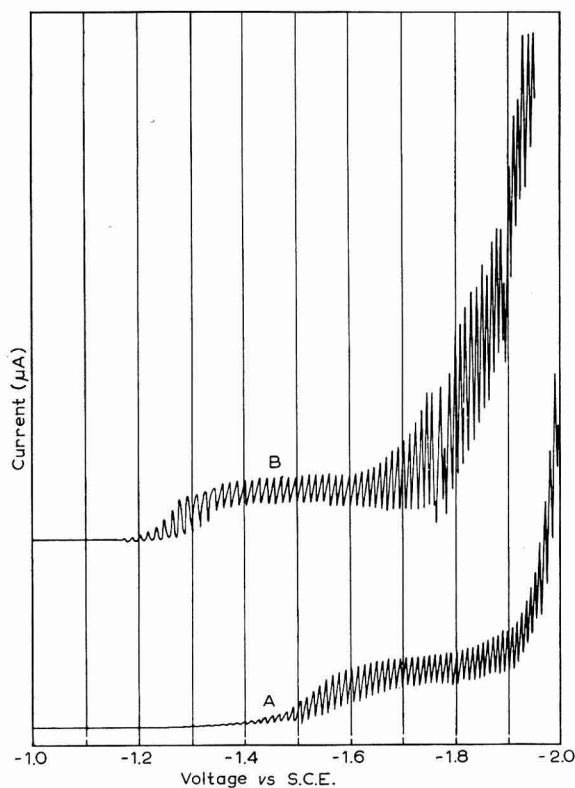


Fig. 1. Reduction of nitrate in the presence of thorium. (A), 0.95 mM ThCl<sub>4</sub> in 1 *M* NaCl; (B), as (A), +5 mM NaNO<sub>3</sub>.

chloride to 20 ml of 1 *M* NaCl to which 10 drops of 0.2% Triton X-100 had been added. The polarograms were scanned between -1 and -2 V vs. S.C.E., at a current sensitivity of 0.15 µA/mm. To the solution was then added 0.1 ml of 1 *M* NaNO<sub>3</sub>. The results are shown in Fig. 1. A polarographic reduction wave occurred at -1.25 to -1.30 V in the presence of nitrate ions (Curve B). Thorium chloride solutions without

nitrate, show a reduction wave at  $-1.55$  V due to the reduction of hydrogen (curve A). The diffusion current due to nitrate reduction is not affected by increasing the nitrate concentration and seems to be proportional to the concentration of thorium ions over a limited range.

#### Titration of thorium

To a few millilitre of thorium solution were added 2–3 ml of 1 M  $\text{NaNO}_3$ ; the solution was made up to 100 ml by the addition of 1 M  $\text{NaCl}$  as supporting electrolyte. The mixture was placed in a 250-ml beaker and the solution connected to the saturated calomel electrode by an agar bridge. Nitrogen was bubbled through the solution and the titrant for 5–10 min for de-aeration. The dropping electrode was set up in the usual manner and changes in diffusion currents were noted on the Sargent Model XV polarograph. A plot of scale deflection *vs.* volume of titrant was made to locate the end-point. Two typical titration curves are presented in Figs. 2 and 3.

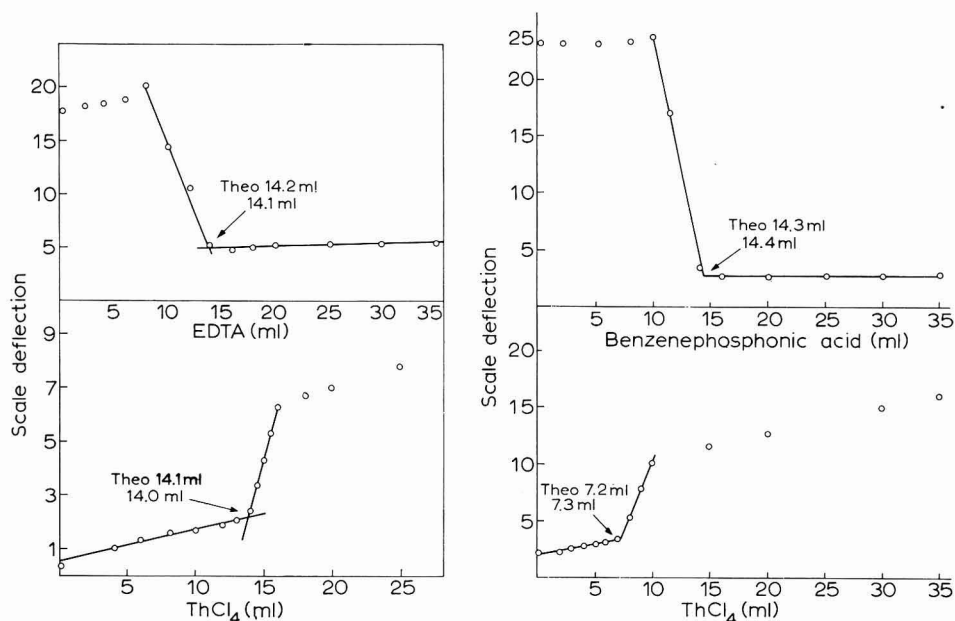


Fig. 2. Titration of thorium with EDTA.

Fig. 3. Titration of thorium with benzenephosphonic acid.

#### Effect of voltage

Although nitrate reduction takes place between  $-1.25$  and  $-1.30$  V, the titration of thorium is accurate only at  $-1.50$  V.

#### Effect of nitrate ion concentration

The nitrate: thorium ratio was varied between 1 : 0.2 and 1 : 50 for various titrations. The best results were obtained when the ratio was kept between 1 : 0.6 and 1 : 20 as shown in Table 1.

*Effect of pH*

No adjustment of pH was necessary when benzenephosphonic acid was used as a titrant. The EDTA titration, however, seems to be sensitive to pH changes. The most accurate results were obtained by maintaining a pH of 3 for thorium and EDTA solutions.

TABLE 1

EFFECT OF NITRATE IONS ON THE DETERMINATION OF THORIUM

<i>Ratio</i> $\text{NO}_3^- : \text{Th}^{4+}$	<i>Th</i> <sup>4+</sup> <i>present</i> (mg)	<i>Th</i> <sup>4+</sup> <i>found</i> (mg)	<i>Difference</i> (mg)
0.2	42.0	41.1	0.9
0.4	42.0	41.2	0.8
0.6	42.0	41.8	0.2
5	42.0	42.1	0.1
10	42.0	41.9	0.1
15	42.0	42.2	0.2
20	42.0	42.1	0.1
30	42.0	42.9	0.9
50	42.0	43.0	1.0

*Concentration range*

10–200 mg in 100 ml of solution can be titrated by either titrant with an accuracy of  $\pm 1.5\%$ . Outside this concentration range, the method is less accurate and the endpoints are not very sharp.

*Recommended procedure for the titration of thorium*

To an aliquot containing 10–200 mg of thorium add 2–3 ml of 1 M NaNO<sub>3</sub> and 1 ml of 0.2% Triton X-100. Make up the solution to 100 ml with 1 M NaCl solution. When the titration is carried out with EDTA, adjust the solution and the titrant to pH<sub>3</sub> with dilute HCl and check with a pH-meter. Bubble nitrogen through the solution for about 5 min. Adjust the voltage across the cell to  $-1.5$  V vs. S.C.E. and titrate with 0.01–0.001 M solutions of EDTA or benzenephosphonic acid. Stir the mixture after each addition of titrant, note the scale deflections and plot them against the volume of titrant to locate the endpoint.

Figures 2 and 3 show titration curves for EDTA and benzenephosphonic acid titrations. The range of accuracy is almost the same for both titrations. For EDTA titrations, the end-point occurs at a ratio of thorium : titrant of 1 : 1, as expected. With benzenephosphonic acid titrations, the end-point occurs at a ratio of 1 : 2 for thorium : titrant. This agrees with the composition of the thorium benzenephosphonate precipitate reported by BANKS AND DAVIS<sup>6</sup>. Representative results for both titrations are presented in Tables 2 and 3.

*Interference studies*

Interference studies were carried out by taking an aliquot of the thorium solution, adding a 5–10-fold excess of the foreign ion and titrating as described above. Except for the alkali metals, NH<sub>4</sub><sup>+</sup>, Mg<sup>2+</sup>, Ca<sup>2+</sup>, Ba<sup>2+</sup> and Sr<sup>2+</sup>, most common cations interfere. Among the anions, sulfate, acetate, bromate and iodate interfere with the analysis.



TABLE 2

AMPEROMETRIC DETERMINATION OF THORIUM WITH EDTA

<i>Th</i> <sup>4+</sup> present (mg)	<i>Th</i> <sup>4+</sup> found (mg)	Difference (mg)	<i>Th</i> <sup>4+</sup> present (mg)*	<i>Th</i> <sup>4+</sup> found (mg)	Difference (mg)
42.0	41.8	0.2	47.5	47.1	0.4
32.3	32.9	0.6	7.2	7.1	0.1
16.8	16.8	0.0	71.4	72.0	0.6
101.0	102.1	1.1	59.5	61.2	1.7
202.0	204.2	2.2			
8.4	8.3	0.1			

\* Reverse titrations

TABLE 3

AMPEROMETRIC DETERMINATION OF THORIUM WITH BENZENEPHOSPHONIC ACID

<i>Th</i> <sup>4+</sup> present (mg)	<i>Th</i> <sup>4+</sup> found (mg)	Difference (mg)	<i>Th</i> <sup>4+</sup> present (mg)*	<i>Th</i> <sup>4+</sup> found (mg)	Difference (mg)
229.0	231.0	2.0	7.2	7.3	0.1
22.9	21.7	1.2	33.7	34.3	0.6
23.4	22.0	1.4	14.3	14.4	0.1
42.0	41.7	0.3	28.8	29.0	0.1

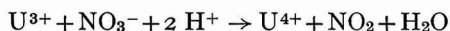
\* Reverse titrations

## DISCUSSION

It is evident from Figs. 2 and 3 that for the direct titration of thorium with EDTA and BPA, there is a large flow of current through the cell in the early part of the titration. This is due to the reduction of nitrate in the presence of thorium. However, as the end-point approaches, there is a sharp depletion in the thorium concentration and, therefore, a sharp drop in the reduction of nitrate ions and hence, a drop in current flowing through the cell. After the end-point, the amount of current flowing through the cell remains unchanged.

For reverse titrations, a small amount of current flows through the cell at the beginning, and the current rises slowly as the end-point is approached. As soon as the end-point is crossed, the smallest excess of thorium aids in the reduction of nitrate ions and hence, a large flow of current. As the reduction is not quantitatively proportional to thorium concentrations, the initial jump in the value of current flow is followed by a slower rise in current values.

The polarographic reduction of nitrate ions in the presence of cations such as UO<sub>2</sub><sup>2+</sup>, La<sup>3+</sup>, Zr<sup>4+</sup> and Th<sup>4+</sup> has been a subject of several investigations. In the case of UO<sub>2</sub><sup>2+</sup>, a catalytic mechanism is postulated<sup>7</sup>. The UO<sub>2</sub><sup>2+</sup> is first reduced to the 5+ and then to the 3+ state. During the second stage of reduction, nitrate ions are reduced according to the following:



The irreversible reduction of nitrate in the presence of 0.1 M Zr<sup>4+</sup> as supporting electrolyte has been studied by WHARTON<sup>8</sup>. He concludes that the reduction is not catalytic and involves the reduction of distinct Zr-NO<sub>3</sub> complexes.

It appears that the reduction of nitrate in the presence of thorium involves the reduction of Th-NO<sub>3</sub> complexes that are formed and reduced near the electrode. Since thorium ion does not exhibit any other valency than 4+, a catalytic mechanism is difficult to explain.

#### DETERMINATION OF LANTHANUM

NODDACK AND BRUCKL<sup>9</sup> first studied the polarographic reduction of lanthanum and reported two reduction waves at -1.90 and -2.00 V. They concluded that the reduction proceeded first to the 2+ state and finally to the metal. From other studies, it is now well established that, among the lanthanoids, the reduction to the 2+ state occurs only with Sm<sup>3+</sup>, Eu<sup>3+</sup> and Yb<sup>3+</sup>. For other members, the reduction wave corresponds to only one reduction step, to the metal, and is masked by the hydrogen wave. TOKUOKA AND RUZICKA<sup>10</sup> reported the reduction of nitrate in the presence of lanthanum and cerium ions. This reduction has been investigated for the amperometric determination of lanthanum.

#### *Reduction of nitrate in the presence of lanthanum*

The polarographic reduction of nitrate in the presence of LaCl<sub>3</sub> and 1 M NaCl as supporting electrolyte was studied as described earlier. The results are shown in Fig. 4. One of the characteristics of the nitrate wave is the abruptness with which the current increases (curve B). Instead of the usual exponential increase, the

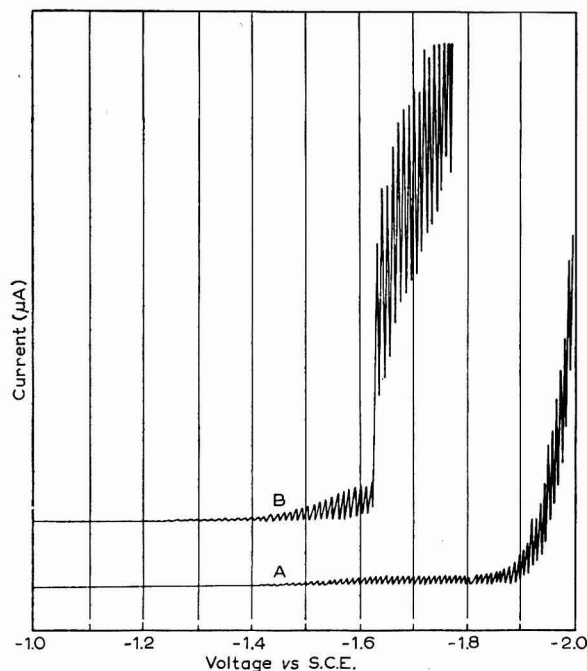


Fig. 4. Reduction of nitrate in presence of lanthanum. (A), 1 mM NaCl<sub>3</sub> in 1 M NaCl; (B), as (A) + 1 mM NaNO<sub>3</sub>.

current remains perfectly constant until the reduction potential is reached ( $-1.5$  to  $-1.6$  V) and then increases sharply.

*Recommended procedure for the titration of lanthanum*

To an aliquot containing 10–200 mg of lanthanum add 2–3 ml of 1 M NaNO<sub>3</sub> and 1 ml of 0.2% Triton X-100. Make up the solution to 100 ml with 1 M NaCl solution. Adjust the pH to pH3 with dilute HCl and check with a pH-meter. Bubble purified nitrogen through the solution for about 5 min for de-aeration. Adjust the voltage across the cell to  $-1.5$  V vs. S.C.E. and titrate with 0.01–0.001 M EDTA solution, stirring after each addition of titrant. Plot scale deflections against volume of EDTA to locate the end-point. Figure 5 shows representative titration curves and Table 4 presents some results. The method gives an experimental error of  $\pm(0.5-3\%)$ . Titrations using benzenephosphonic acid as titrant gave erratic results.

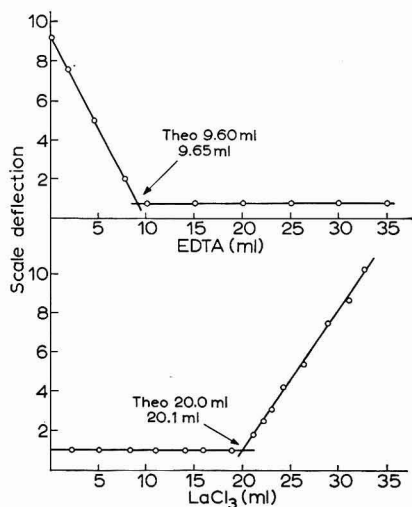


Fig. 5. Titration of lanthanum with EDTA.

TABLE 4  
AMPEROMETRIC DETERMINATION OF LANTHANUM WITH EDTA

<i>La</i> <sup>3+</sup> present (mg)	<i>La</i> <sup>3+</sup> found (mg)	Difference (mg)	<i>La</i> <sup>3+</sup> present (mg)*	<i>La</i> <sup>3+</sup> found (mg)	Difference (mg)
12.2	12.8	0.6	9.8	9.6	0.2
24.4	24.6	0.2	19.6	20.1	0.5
36.6	36.9	0.3	28.4	28.8	0.4
48.8	50.0	0.2	37.2	37.3	0.1
61.0	60.2	0.8	49.0	48.8	0.2

\* Reverse titrations

DISCUSSION

All the cations and anions mentioned earlier as interfering in the determination of thorium also interfere with the lanthanum titration *i.e.*, only the alkali metal and alkaline-earth metal ions are tolerated in this determination.

The diffusion current due to nitrate reduction is not affected by increase in nitrate ion concentration and is proportional to lanthanum concentrations only over a limited range. The reduction of nitrate may involve La-NO<sub>3</sub> type complexes.

#### SUMMARY

The reduction of nitrate ions in the presence of thorium and lanthanum is utilized for the amperometric determination of these two metal ions. Thorium can be titrated with EDTA or benzenephosphonic acid at a voltage of  $-1.5$  V vs. S.C.E. Lanthanum titrations are carried out at the same voltage using EDTA as a titrant. It is possible that M-NO<sub>3</sub> (where M = Th<sup>4+</sup> or La<sup>3+</sup>)-type complexes are reduced near the electrode. The effect of variation in experimental conditions and metal concentration, and the accuracy of determinations are discussed.

#### REFERENCES

- 1 R. PARSONS, *Handbook of Electrochemical Constants*, Butterworth, London, 1959, p. 69, 72.
- 2 A. A. SMALES AND L. AIREY, *Atomic Energy Research Establishment, Harwell, Chemical Division Memorandum, No. 131*.
- 3 I. M. KOLTHOFF AND R. A. JOHNSON, *J. Electrochem. Soc.*, 98 (1951) 138.
- 4 M. SUNDERASAN AND M. D. KARKHANVALA, *Current Sci., (India)*, 23 (1954) 258.
- 5 A. LANGER, *Ind. Eng. Chem., Anal. Ed.*, 12 (1940) 511.
- 6 C. V. BANKS AND R. J. DAVIS, *Anal. Chim. Acta*, 12 (1955) 418.
- 7 I. M. KOLTHOFF, W. E. HARRIS AND G. MATSUYAMA, *J. Am. Chem. Soc.*, 66 (1944) 1782.
- 8 H. W. WHARTON, *J. Electroanal. Chem.*, 9 (1965) 134.
- 9 W. NODDACK AND A. BRUCKL, *Angew. Chem.*, 50 (1937) 362.
- 10 M. TOKUOKA AND J. RUZICKA, *Collection Czech. Chem. Commun.*, 6 (1934) 339.

*J. Electroanal. Chem.*, 13 (1967) 425-432

## EVALUATION OF THE CHARACTERISTICS OF EXCHANGE REACTIONS I. EXCHANGE REACTION AT A SOLID ZINC ELECTRODE IN ALKALI

J. P. G. FARR\*

*Department of Industrial Metallurgy, University of Birmingham (England)*

N. A. HAMPSON

*Chemistry Department, Loughborough University of Technology, Leicestershire (England)*

(Received April, 15th, 1966)

For the zinc exchange at solid zinc electrodes in alkali, a.c. impedance measurements<sup>1,2</sup> have indicated that in the frequency range below 1 kc/sec the reaction is controlled by adatom diffusion. Furthermore, there is considerable evidence to suggest that intermediates are strongly adsorbed at the electrode interphase. Accordingly, it was decided to investigate the charge transfer reaction in the micro-second time range

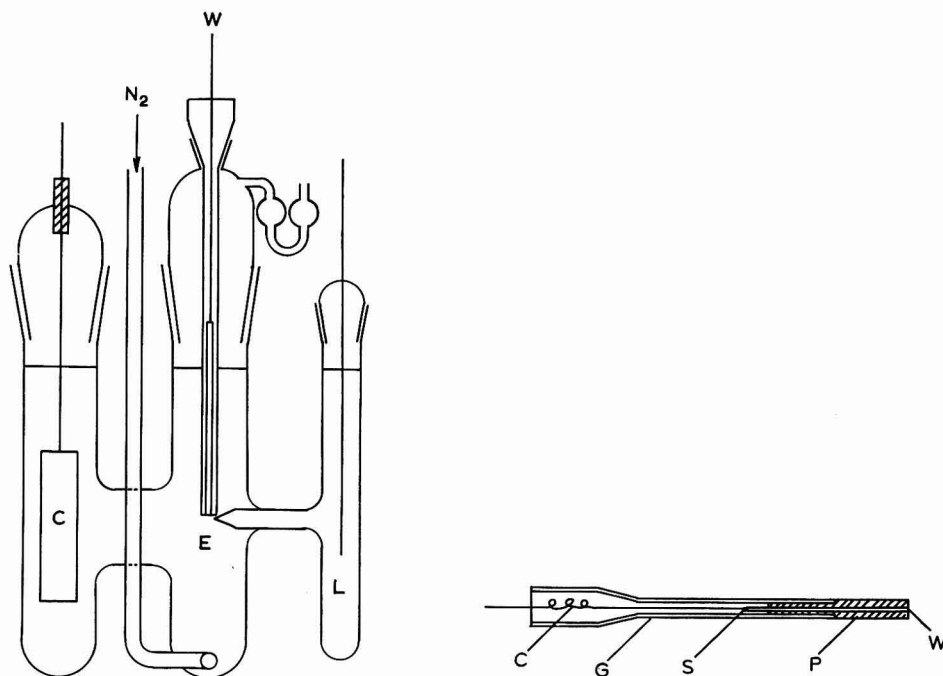


Fig. 1. Cell. (C), counter electrode; (E), test electrode compartment; (L), Luggin reference system; (W), test electrode.

Fig. 2. Microelectrode. (C), copper wire; (G), glass support; (S), soldered joint; (P), polyethylene sheath; (W), working face of electrode.

\* Joseph Lucas Fellow in Electrometallurgy.

using the double-impulse method<sup>3</sup> whereby adatom diffusion effects would not interfere.

## EXPERIMENTAL

### *Electrolytic system*

The cell is shown in Fig. 1 and a typical electrode is shown in Fig. 2. Electrodes were prepared from pure zinc (99.9999% supplied by Société de la Vieille Montagne), polycrystalline by melting under nitrogen, single crystal by the method of zone melting followed by cleaving (to give a (0001) face), heavily cold worked by swaging down polycrystalline material to at least a four-fold reduction in diameter. Electrolytes were generally maintained at high ionic strength. All materials used were of A.R. quality, water was bidistilled from deionised stock. Nitrogen for circulation was purified by passage over copper at 400°.

Additional purification by shaking electrolytes with purified charcoal was a convenient method of removing surface active impurities.

### *Electrical circuit*

The L-shaped pulse was obtained from two generators (Solatron, Type GO 1005).

The pre-pulse from one generator, triggered both the other generator and the oscilloscope (Hewlett-Packard, type 130C or Tektronix 545A). The delay units were adjusted so that the oscilloscope fired just before the complex pulse rose. From this arrangement, a complex negative pulse falling from zero (with the rise time less than 0.3  $\mu$ sec) was obtained, either step of the function was continually variable within the range 0.5  $\mu$ sec–0.1 sec. The output of the pulse generator combination was continuously variable; each was capable of delivering 80 mA at 100 V into 2500  $\Omega$  so that with microelectrodes a load resistance was included to limit the current amplitude. Current measurements were made by observing the potential developed across a low resistance.

Since both counter electrode and test electrode were initially and finally at earth potential, they were made of identical material. The reference electrode was also of material identical with the test electrode and was combined with a Luggin system.

### *Electrical adjustments*

Figure 3 shows a typical trace obtained with a single pulse. Figure 4 shows balanced double impulse traces with increasing double-layer charging pulse duration. 0.5, 1.0 and 1.5  $\mu$ sec pulses were satisfactory, overpotential increasing linearly with time as required for the non-faradaic process; 2- and 3  $\mu$ sec transients were curved during the initial pulse indicating faradaic current in addition to the capacitive component. Overpotentials were constant at the end of the shorter capacitive pulses (extrapolation not necessary in order to obtain  $\eta_D$ , the activation overpotential) some increase was observed with the longer initial pulses.

A 0.5  $\mu$ sec initial pulse in conjunction with a 7  $\mu$ sec faradaic pulse was generally used.

### *Measurements*

The value of the overpotential was determined for a range of anodic and catho-

dic faradaic currents. After a series of measurements had been completed, readings were checked at the highest and lowest faradaic current. If checks were not satisfactory this was due to either

- (i) electrode obscured by a bubble of nitrogen,
- (ii) thermal instability,
- (iii) insufficient electrode pretreatment.

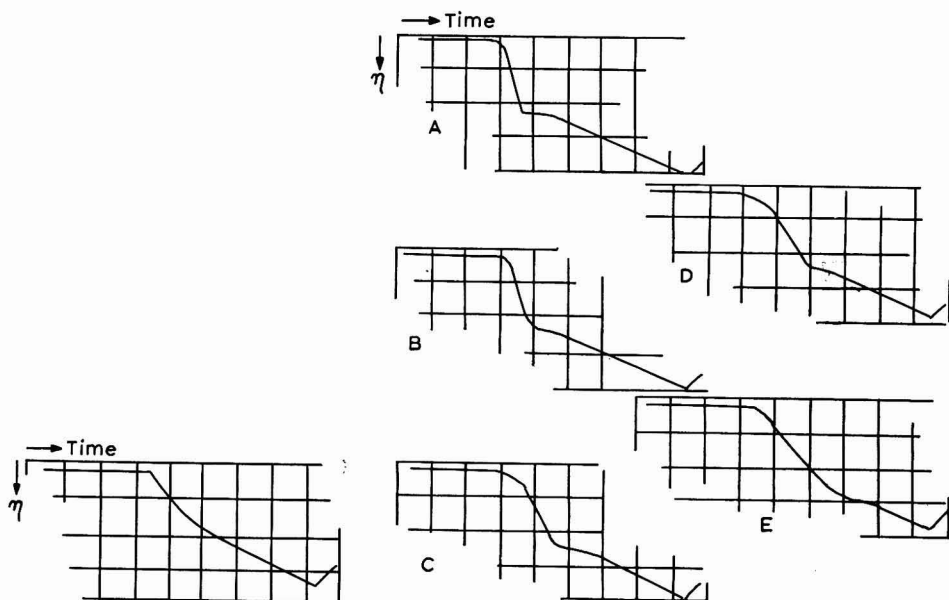


Fig. 3. Typical trace using a single pulse. Time base,  $1 \mu\text{sec cm}^{-1}$ ; sensitivity,  $1 \text{ mV cm}^{-1}$ ;  $25^\circ$ ; electrolyte,  $7 \text{ M KOH} + 0.015 \text{ M Zn}^{2+}$ .

Fig. 4. Typical "balanced" traces from double impulse expts. Time base,  $1 \mu\text{sec cm}^{-1}$ ; sensitivity,  $1 \text{ mV cm}^{-1}$ ;  $25^\circ$ ; electrolyte,  $7 \text{ M KOH} + 0.015 \text{ M Zn}^{2+}$ . Initial pulse: (A), 0.5; (B), 1.0; (C), 1.5; (D), 2.0; (E), 3.0  $\mu\text{sec}$ .

#### Accuracy of measurements

Electrode potentials could be read to  $\pm 0.01 \text{ mV}$  in the range up to  $2 \text{ mV}$ , and  $\pm 0.05 \text{ mV}$  in the range up to  $10 \text{ mV}$ . Current measurements were only as accurate as the oscilloscopes used for the potential measurement across the standard resistance,  $\pm 3\%$ . Temperature control was  $\pm 1^\circ$  at  $0^\circ$  and  $\pm 0.3^\circ$  throughout the experimental range. The maximum error in the determinations was about  $\pm 10\%$ .

#### Electrode pretreatment

The electrode was either mechanically or electrolytically polished, and chemically etched before assembly into the circuit. About 1000 atomic layers were removed from the surface by a charge of  $1 \text{ C cm}^{-2}$  at a rate insufficient to cause passivation. Experiments were commenced after an open circuit period of 5 min.

## RESULTS

*Polycrystalline zinc electrodes*

Typical faradaic current-overpotential data are shown in Fig. 5a. Increase of temperature reduced the overpotential at any applied current density.

Values of  $i_0$  and  $\alpha$  calculated using an iterative technique (see subsequent note) are shown in Table 1 together with values of  $i_0$  estimated geometrically; the agreement was satisfactory.

*Variation of exchange current with zinc ion concentration.* Table 2 shows exchange currents at 25° in electrolytes of low ionic strength. Table 3 shows similar determinations in electrolytes of high ionic strength. The exchange current was independent of the zinc ion concentration.

TABLE 1

EXCHANGE CURRENTS AND CHARGE TRANSFER COEFFICIENTS CALCULATED

(a) Geometrically, (b) iteratively

$T$	$Zn^{2+}$ ( $M$ )	$NaOH$ ( $M$ )	$i_0(a)$ ( $A\ cm^{-2}$ )	$i_0(b)$ ( $A\ cm^{-2}$ )	$\alpha$ ( $b$ )
25°	0.047	0.7	0.084	0.081	0.50
		1.4	0.092	0.091	0.50
		2.1	0.104	0.102	0.51
	0.009	0.50	0.087	0.086	0.50
		1.05	0.092	0.092	0.50
		2.60	0.108	0.092	0.50
40°	0.047	0.7	0.110	0.110	0.50
		1.4	0.124	0.121	0.54
		2.1	0.132	0.138	0.46
	0.009	0.50	0.119	0.116	0.53
		1.05	0.130	0.125	0.57
		2.60	0.147	0.145	0.53
55°	0.047	0.7	0.142	0.139	0.54
		1.4	0.157	0.152	0.61
		2.1	0.160	0.166	0.50
	0.009	0.50	0.144	0.141	0.53
		1.05	0.159	0.157	0.50
		2.60	0.178	0.178	0.50

TABLE 2

EXCHANGE CURRENTS AT 25° IN 1  $M$  TOTAL ELECTROLYTE CONCENTRATION(added  $NaClO_4$ )

$[NaOH]$ ( $M$ )	$[Zn^{2+}]$ ( $M$ )	$i_0$ ( $A\ cm^{-2}$ )	$[NaOH]$ ( $M$ )	$[Zn^{2+}]$ ( $M$ )	$i_0$ ( $A\ cm^{-2}$ )
0.1	Nil	0.049	0.2	Nil	0.054
0.1	0.00025	0.041	0.2	0.00075	0.045
0.1	0.0005	0.042	0.2	0.0015	0.052



TABLE 3

EXCHANGE CURRENTS AT 25° IN HIGH ELECTROLYTE CONCENTRATION

NaOH (M)	[Zn <sup>2+</sup> ] (M)	<i>i</i> <sub>0</sub> (A cm <sup>-2</sup> )	[KOH] (M)	[Zn <sup>2+</sup> ] (M)	<i>i</i> <sub>0</sub> (A cm <sup>-2</sup> )	[LiOH] (M)	[Zn <sup>2+</sup> ] (M)	<i>i</i> <sub>0</sub> (A cm <sup>-2</sup> )
7.0	Nil	0.140	7.0	0.016	0.238	4.95	Nil	0.185
7.0	0.0014	0.160	7.0	0.040	0.241	4.95	0.056	0.167
7.0	0.0047	0.120	7.0	0.080	0.231	4.95	0.140	0.175
7.0	0.0094	0.130	7.0	0.64	0.224	4.95	0.280	0.166
7.0	0.470	0.138						

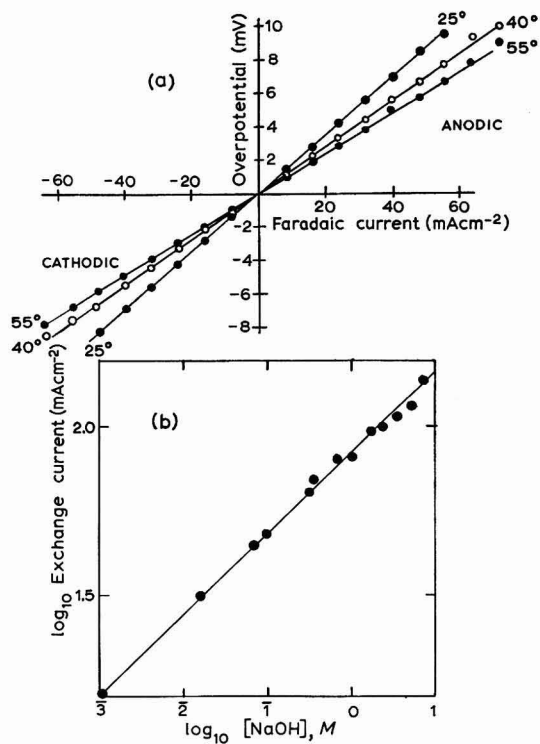


Fig. 5. Results of double impulse expts. Polycrystalline zinc electrode; electrolyte at const. ionic strength 7 (with NaClO<sub>4</sub>). (a), Typical faradaic current-overpotential curves at 0.35 M NaOH + 0.001 M Zn<sup>2+</sup>; (b), Variation of exchange current with hydroxide concn., 25°.

*Variation of exchange current with hydroxide concentration.* Figure 5b shows the variation of exchange current with sodium hydroxide content in a solution of ionic strength 7. Table 4 shows the slopes ( $\partial \log i_0 / \partial \log [\text{OH}^-]$ ) for the systems tested.

*Temperature dependence of exchange current.* Figure 6 shows the variation of exchange current with temperature in mixtures of sodium hydroxide and perchlorate; Fig. 7 shows the dependence in electrolytes based on other cations. For sodium ion solutions, the temperature variation corresponded to an enthalpy of 3.1 kcal.mole<sup>-1</sup>; for potassium and lithium, enthalpies were 2.9 and 2.65 kcal.mole<sup>-1</sup>, respectively.

TABLE 4

THE VARIATION OF EXCHANGE CURRENT WITH TEMPERATURE

Ionic strength (M)	[Zn <sup>2+</sup> ] (M)	Cation	$\partial(\log i_0)/\partial(\log [OH^-])$		
			25°	40°	55°
1.0	0.00025	Na	0.15		
7.0	Nil	Na	0.25		
7.0	0.0014	Na	0.23	0.23	0.23
7.0	0.0094	Na	0.15	0.16	0.16
7.0	0.047	Na	0.15	0.16	0.16
1.0-7.0	0.08	K	0.27		
1.0-7.0	0.056	Li	0.30	0.29	0.27

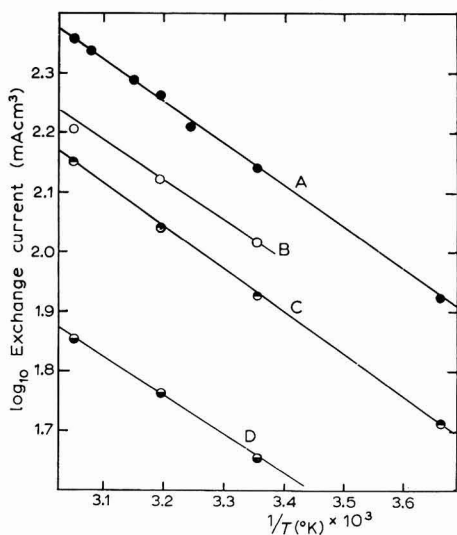


Fig. 6. Temp. dependence of exchange current. Polycrystalline zinc electrode; electrolyte, ionic strength (NaClO<sub>4</sub>) 7 M. (A), 7; (B), 2.1; (C), 0.7; (D), 0.07 M OH<sup>-</sup>.

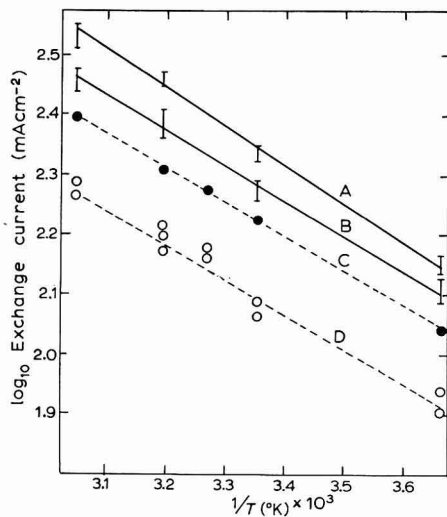


Fig. 7. Temp. dependence of exchange current. Polycrystalline zinc electrode. (A), 7.0 M KOH; (B), 3.5 M KOH; (C), 5.0 M LiOH; (D), 2.1 M LiOH. Electrolytes contained 0.05 M Zn<sup>2+</sup>. KOH electrolytes were at 7 M ionic strength with KF.

*Single crystal (surface orientation (0001) and heavily cold worked electrodes)*

Figure 8 shows the results of measurements on a single crystal electrode. The exchange current was about one-third of its value on a polycrystalline electrode; the activation enthalpy was 3.4 kcal.mole<sup>-1</sup>.

Figure 9 shows results of typical measurements on heavily cold worked electrodes. The exchange current and activation enthalpy were approximately those of the polycrystalline surface.

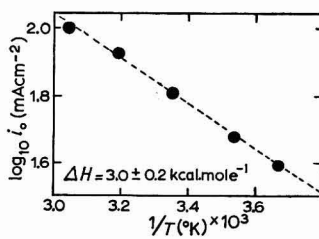
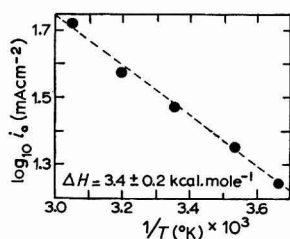
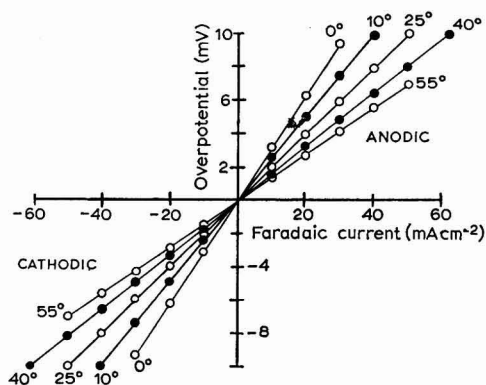
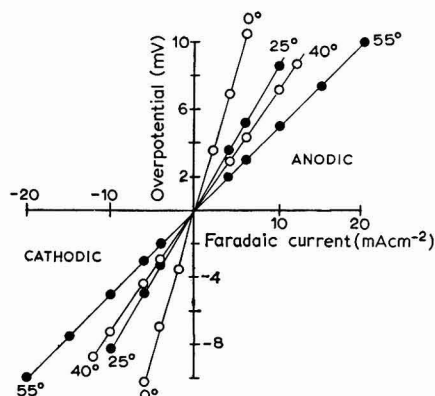


Fig. 8. Results of expts. with single crystal zinc. Electrolyte, 1.4 *M* NaOH, 0.047 *M* Zn<sup>2+</sup>; ionic strength, 7 *M* (with NaClO<sub>4</sub>).

Fig. 9. Results of expts. with heavily cold worked zinc. Electrolyte, 0.35 *M* NaOH, 0.001 *M* Zn<sup>2+</sup>; ionic strength, 7 *M* (with NaClO<sub>4</sub>).

## DISCUSSION OF RESULTS

### *Cleanliness of the system*

The double impulse method resembles experiments with a dropping mercury electrode in that the electrode is constantly being renewed. In a well-purified electrolyte, the stability requirement is reduced to a few seconds by repeat determinations; satisfactory reproducibility confirmed that impurities were below the level required to interfere with the experimental results.

### *The magnitude of the exchange current*

*Polycrystalline and single crystal electrodes.* The exchange currents observed are much larger than the values of adatom fluxes observed in a.c. experiments<sup>1,2</sup>. The exchange current on a polycrystalline electrode in 1 *M* sodium hydroxide is about 100 mA cm<sup>-2</sup>. The magnitude of the exchange current on single crystal electrodes, approximately one-third of the value on polycrystalline electrodes, indicates that the charge transfer rate is about the same on both types of surface, the apparent reduction being offset by the greater roughness factor for the polycrystals (2–3 times). This factor agrees well with pseudo-capacities observed at polycrystalline and single crystal surfaces<sup>1,2</sup>.

From a.c. measurements<sup>1,2</sup>, increases in exchange current in passing from single crystal to polycrystals are proportionately less than changes in adatom flux,

in agreement with the differences between the two processes. The enthalpy obtained for the activation energy plots compares well with corresponding values on polycrystals and confirms the relative unimportance of the surface orientation on the exchange reaction.

*Heavily cold worked electrodes.* The exchange current observed with these electrodes is slightly less than for polycrystalline electrodes, and indicates that the true area is similar per unit of superficial area in the two cases.

*The charge transfer reaction.* The dependence of exchange current on hydroxide ion concentration only indicates considerable interaction between that ion and the electrode surface, either as a strong physical adsorption or as an intermediate. Two possibilities may be considered for the occurrence of the exchange current dependence observed,

$$i_0 = ZFk^* C_{\text{OH}^-}^{0.2} \quad (\text{where } k^* \text{ involves a } k^0) \quad (1)$$

involving either a one- or two-step charge transfer.

*Two-electron charge transfer mechanism.* The charge transfer reaction



connects the exchange current,  $i_0$ , with the standard rate constant and the reactant concentration by the equation

$$(i_0)_i = 2 F k_{(i)}^0 C_{\text{OH}^-}^{\alpha(i)} C_{\text{Zn}(\text{OH})_2}^{2\alpha(i)} C_{\text{Zn}}^{(1-\alpha(i))} \quad (3)$$

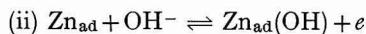
The concentration of  $\text{Zn}(\text{OH})_2$  at the electrode must be independent of zincate in solution; this implies a complete or almost complete adsorbed layer of  $\text{Zn}(\text{OH})_2$ .

Without postulating adsorption of  $\text{OH}^-$ , the charge transfer coefficient is 0.1. If  $\text{OH}^-$  is adsorbed and follows an equation of the form

$$[\text{OH}_{\text{ad}}^-] = A[\text{OH}^-]^{1/n} \quad (4)$$

which often describes adsorption from solution (but for which there is no theoretical justification),  $\alpha$  may be considerably greater than 0.1

*Successive electron transfer.* For the successive electron transfer process



followed by



(where the oxidised species may contain more or less  $\text{OH}^-$  than shown) we can write

$$(i_0)_{ii} = F k_{(ii)}^0 C_{\text{Zn}}^{\alpha(ii)} C_{\text{OH}^-}^{\alpha(ii)} C_{\text{Zn}(\text{OH})}^{(1-\alpha(ii))} \quad (5)$$

and

$$(i_0)_{iii} = F k_{(iii)}^0 C_{\text{Zn}(\text{OH})\text{OH}^-}^{\alpha(iii)} C_{\text{Zn}(\text{OH})_2}^{\alpha(iii)} C_{\text{Zn}}^{(1-\alpha(iii))} \quad (6)$$

For the whole process, the charge transfer resistance is given by

$$R_D = \left( \frac{-\partial \eta}{\partial i} \right)_{\eta=0} = \frac{RT}{4F} \left( \frac{1}{(i_0)_{(ii)}} + \frac{1}{(i_0)_{(iii)}} \right) \quad (7)$$

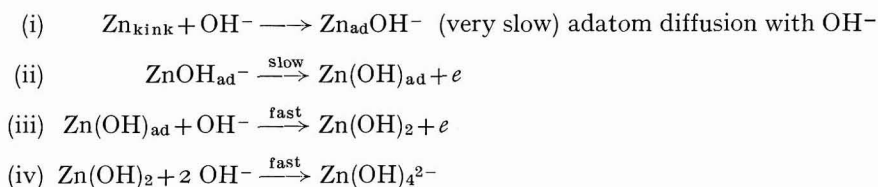
and the slowest process clearly dominates the value of  $R_D$ .

If (ii) is slow, an equation of form (1) will be the result of a constant concentration of Zn(OH) at the electrode surface.

If (iii) is the slow step in addition to a constant concentration of the intermediates represented by Zn(OH), the concentration of Zn(OH)<sub>2</sub> will require to be independent of zincate concentration by adsorption.

Both (ii) and (iii) may involve the adsorption of hydroxide, in which case the change transfer coefficient will be in excess of 0.2.

*Choice of the mechanism.* Of these possibilities, the two-step charge transfer process with (iii) faster than (ii) so that to some extent (iii) is obscured, is the most attractive since the postulation of a complete adsorption layer of the soluble product Zn(OH)<sub>2</sub> is avoided. Adsorption of hydroxide is indicated as the result of impedance measurements<sup>1,2</sup>; the transfer coefficient is likely therefore to be in excess of 0.2 as indicated by the mathematical analysis of overpotential-current data. The following reaction sequence is indicated.



*Activation enthalpy.* Values of the activation energy were very much lower than that obtained by HUSH AND BLACKLEDGE<sup>4</sup>, 10 kcal.mole<sup>-1</sup>, on an amalgam surface. Activation energies were smaller with lithium cations than with either sodium or potassium.

#### ACKNOWLEDGEMENT

The authors wish to thank Professors R. F. PHILLIPS and E. C. ROLLASON for provision of facilities and for the interest they have taken in the progress of this work.

#### SUMMARY

The exchange reaction at a solid zinc electrode in alkali has been investigated using polycrystalline, single crystal, and heavily cold worked zinc. Exchange currents have been measured. The dependence of the exchange current on the reactant concentration of the electrolyte indicated adsorption of intermediates at the electrodes; to some extent this was confirmed by calculation of the electron transfer coefficient using an iterative method. Various mechanisms are discussed, the most attractive is a two-step charge transfer process.

Enthalpies of activation for the transfer process are reported.

#### REFERENCES

- 1 N. A. HAMPSON, Ph.D. Thesis, University of London, 1966.
- 2 J. P. G. FARR AND N. A. HAMPSON, in press.
- 3 H. GERISCHER AND M. KRAUSE, *Z. Physik. Chem.*, Frankfurt, 10 (1957) 264.
- 4 N. S. HUSH AND J. BLACKLEDGE, *J. Electroanal. Chem.*, 5 (1963) 420.

## REVIEW

---

### ELEKTRISCHE METHODEN ZUM STUDIUM DER ELEKTRODENKINETIK

P. MAZUREK

*Institut für Elektrochemie und physikalische Chemie der Technischen Universität, Dresden*

(Eingegangen am 22. Dezember 1965, revidiert am 1. Juni, 1966)

#### EINLEITUNG

Informationen über einen elektrochemischen Prozess werden hauptsächlich aus Messungen elektrischer Größen gewonnen, die an der Elektrode, an der der Prozess abläuft, vorgenommen werden. Jahrzehntlang waren die Stromdichte-Potential-Messungen stationärer Zustände der einzige Weg zu diesem Ziel; heutzutage kann dagegen, dank der Entwicklung in den letzten fünfzehn Jahren, zwischen mehreren Wegen gewählt werden. Diesem Fortschritt steht allerdings der Nachteil einer Nomenklatur, die keineswegs als glücklich bezeichnet werden kann, gegenüber. So lässt sich beim Studium der Literatur feststellen, dass es für eine bestimmte Methode mehrere Namen gibt und dass umgekehrt für mehrere, völlig verschiedene Methoden ein einziger Name in Gebrauch ist. Das stört besonders bei Literaturzusammenstellungen (z.B. bei Lit. 1), wo es demzufolge notwendig wird, sich bei jeder zitierten Arbeit zu vergewissern, ob tatsächlich die interessierende Methode angewendet wurde oder nicht.

Diese Schwierigkeiten waren der Anlass zu vorliegender Arbeit; einerseits ist es ihr Ziel, zu zeigen, wodurch sich die einzelnen, für die Praxis bedeutungsvollen Methoden voneinander unterscheiden, andererseits, sie im Hinblick auf Leistungsfähigkeit und vorteilhaftesten Einsatz untereinander zu vergleichen. Der erste Gesichtspunkt schliesst den Versuch einer Systematisierung ein, der zweite dürfte das Interesse des Praktikers besitzen, der, um sein Problem zu bewältigen, zwischen den verschiedenen Lösungswegen wählen muss.

#### SYSTEMATISIERUNG DER METHODEN

Bekanntlich werden aus der Schar der Variablen, die das System charakterisieren, zwei ausgewählt, von denen die eine willkürlich verändert und die andere in Abhängigkeit von diesen Veränderungen gemessen wird; dabei wird dafür Sorge getragen, dass alle weiteren Variablen konstant bleiben. Stets ist ein Gleichgewichtszustand des Systems der Ausgangspunkt der Untersuchung; eine Störung\* wird

---

\* Obwohl die Störung des elektrochemischen Gleichgewichts auch auf nichtelektrischem Wege erfolgen kann (z.B. mit Ultraschall<sup>2</sup> oder mit UV-Strahlung bzw. sichtbarem Licht<sup>3</sup>), haben nur die Methoden Bedeutung erlangt, bei denen die Störung auf elektrischem Wege vorgenommen wird.

dadurch verursacht, dass die unabhängige Variable in definierter, gewünschter Weise verändert wird.

Es ist zweckmässig, unabhängige und abhängige Variable durch Zeitfunktionen zu beschreiben. Alle hierbei infrage kommenden Zeitfunktionen bestehen aus drei Teilen, aus zwei konstanten, die das Verhalten vor und nach der Störung wiedergeben, und aus einem veränderlichen Teil dazwischen, der den Übergang beschreibt. Dieser letztgenannte Teil, nach der Nomenklatur der Regelungstechnik die Führungsgrösse, bildet in Verbindung mit der unabhängigen Variablen die Grundlage der vorgenommenen Einteilung (Abb. 1).

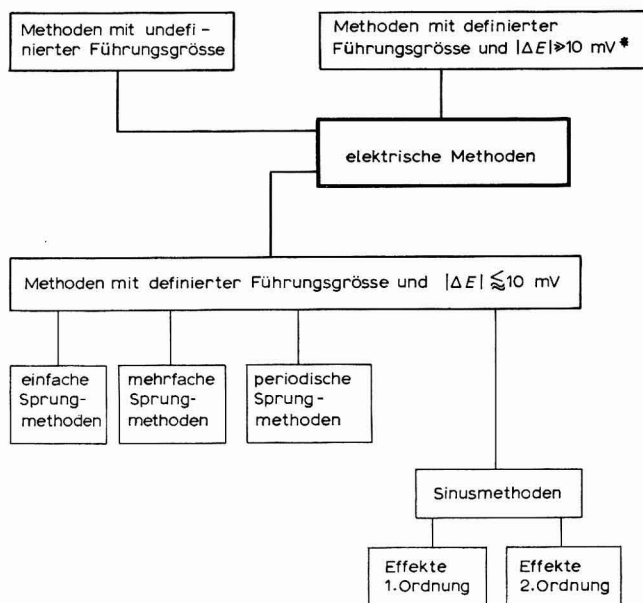


Abb. 1.

#### METHODEN MIT UNDEFINIERTER FÜHRUNGSGRÖSSE

Der Messvorgang verläuft folgendermassen: Man stellt die unabhängige Variable, ausgehend von einem stationären Gleichgewicht, nach einer völlig belanglosen Zeitfunktion auf einen neuen Wert ein. Nachdem dieser Wert erreicht ist, wartet man eine frei gewählte Zeit und bestimmt danach den Wert der abhängigen Variablen (entweder direkt oder indirekt mit Hilfe eines Unterbrechers). Im allgemeinen wartet man so lange, bis sich ein neues stationäres Gleichgewicht eingestellt hat. Wie weit man sich diesem Zustand tatsächlich nähert, hängt sehr von den jeweiligen Umständen ab, denn erfahrungsgemäss ändert sich die abhängige Variable oft noch Stunden nach der Störung. Daher wartet man in Anbetracht des Zeitaufwandes und der Fraglichkeit des erzielbaren stationären Gleichgewichts oft nur eine gewisse kurze Zeit, bis man die abhängige Variable bestimmt.

Man gewinnt also einzelne Wertepaare, die stationären Gleichgewichten zugeordnet werden. Um zu quantitativen Aussagen über die Durchtrittsreaktion zu

\* Maximal 1 bis 2 V; die absolute Änderung des Elektrodenpotentials  $|\Delta E|$  spielt aus theoretischen Gründen eine Rolle.

TABELLE 1

Unabhängige Variable, Führungsgrösse	Gemessene Grösse	Bezeichnung der Methode	Bestimmung des Austauschstromdichte	Bestimmung des Durchtrittsfaktors
$E$ , undefiniert	$I(t \rightarrow +\infty)$	potentiostatische Methode (potentiostatic method; méthode potentiostatique)	$j_0$ aus $\ln j(\eta \rightarrow 0)$ ( $\eta > 0.1$ V) (Tafelsche Geraden)	$\alpha$ aus $\partial \ln j / \partial \eta$ *
$I$ , undefiniert	$E(t \rightarrow +\infty)$	amperostatische (auch: galvanostatische) Methode (galvanostatic method; méthode galvanostatique)	oder $j_0$ aus $\ln \zeta(\eta \rightarrow 0)^5$ ; $\zeta = j / (1 - \exp(\eta f \eta))$ ( $\eta$ beliebig); $k_s < 0.1$ cm sec <sup>-1</sup>	oder $\alpha$ aus $\partial \ln \zeta / \partial \eta$ *

\* Grundsätzlich kann man den Durchtrittsfaktor aus der Konzentrationsabhängigkeit der Austauschstromdichte nach  $\partial \ln j_0 / \partial \ln C_{O(R)}$  (siehe z.B. Lit. 4) bestimmen, wobei aber nur eine Konzentration variiert werden darf. Einige Methoden erlauben es aber, den Durchtrittsfaktor ohne eine solche Konzentrationsvariation zu bestimmen. Für diese Fälle wird nur der andere Weg in den Tabellen angegeben.

gelangen, werden die Wertepaare auf zweierlei Weise halblogarithmisch aufgetragen. Das eine Verfahren ist nur für grosse Überspannungen gültig (es liefert die Tafelschen Geraden), das andere<sup>5</sup> gilt für beliebige Überspannungen und liefert ebenfalls einen linearen Zusammenhang zwischen der Überspannung und dem Logarithmus der Stromdichte, aus dem man die kinetischen Parameter ermitteln kann. Je schneller allerdings die Durchtrittsreaktion verläuft, desto mehr versagt das skizzierte Vorgehen, weil die Reaktionsgeschwindigkeit durch den Transport der Reaktionspartner bestimmt wird. Nimmt man als quantitatives Mass die Geschwindigkeitskonstante der Durchtrittsreaktion beim Standardpotential,  $k_s$ , so liegt die obere Leistungsgrenze dieser Methoden bei etwa  $k_s \lesssim 0.01$  cm sec<sup>-1</sup> (ruhender Elektrolyt) bzw.  $k_s \lesssim 0.1$  cm sec<sup>-1</sup> (rotierende Scheibenelektrode).

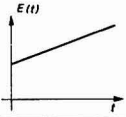
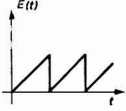
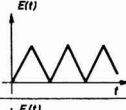
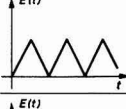
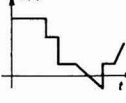
#### METHODEN MIT DEFINIERTER FÜHRUNGSGRÖSSE UND $|\Delta E| \gg 10$ mV

Verkürzt man die Wartezeit immer weiter, so gelangt man in letzter Konsequenz zur Wartezeit null. Dann misst man die abhängige Variable gleichzeitig, während die unabhängige (mit einer Ausnahme) kontinuierlich und nach einer definierten Zeitfunktion ein vorgegebenes Intervall durchläuft. Infolge der definierten Zeitfunktion kann jedem Zeitpunkt der Messung ein Wertepaar zugeordnet werden, das allerdings eine andere Bedeutung besitzt als das der Methoden mit undefinierter Führungsgrösse. Wegen des gerade erwähnten Zusammenhanges kann man die abhängige Variable entweder als Funktion der Zeit oder der unabhängigen Variablen darstellen.

Es ist natürlich möglich, die halblogarithmische Darstellung der Wertepaare zu versuchen. Allerdings erhebt sich die Frage, was die Geraden (falls sie existieren) bedeuten, m.a.W., wie sie zu interpretieren sind. Daher haben diese Methoden nur für qualitative Aussagen Bedeutung. Sie gestatten es nämlich, Einblicke qualitativer Art in das Reaktionsgeschehen zu erlangen. Welche Einsatzmöglichkeiten sich im ein-



TABELLE 2

Unabhängige Variable, Führungsgrösse	Gemessene Grösse	Bezeichnung der Methode	Einsatzmöglichkeiten der Methode
	$I = I(t)$	Chronoamperometrie (chronoamperometry; chronoampérométrie linéaire <sup>6)</sup> )	Analytik <sup>7</sup> *
 <p>z.B. Lit. 8</p>	} $I = I(E)$	oszillographische Polarographie mit vorgegebenem Spannungsverlauf <sup>9</sup> (cathode ray polarography <sup>8</sup> ; polarographie oscillographique à tension en dents de scie <sup>6)</sup> )	} Analytik <sup>7</sup> * Reversibilität einer Reaktion; Adsorptionsprozesse; Verhalten von Mischelektroden
 <p>z.B. Lit. 10, 11</p>			
			
			
		potentiostatische Dreieckspannungsmethode <sup>12,13</sup>	
		multipulse potentiodynamic method <sup>14,15</sup>	Adsorptionsprozesse

\* Dass bei der Systematisierung die Analytik gestreift wird, liegt in der Natur der Sache. Alle Methoden können nämlich prinzipiell auch für analytische Zwecke verwendet werden; ob und mit welchem Erfolg sich die Analytik ihrer bedient, hängt von den jeweiligen Umständen ab. Dadurch gibt es aber für wesensgleiche Methoden sowohl "kinetische" als auch "analytische" Bezeichnungen, wie z.B. "potentiostatische Dreieckspannungsmethode" (Verwendung von Festkörperelektroden) und "oszillographische Polarographie mit vorgegebenem Spannungsverlauf" (Verwendung von Quecksilbertropfelektroden).

zeln ergeben, ist in den Tabellen 2 und 3 angedeutet; eine ausführlichere Besprechung verbietet der Umfang dieser Arbeit.

Von Einfluss auf das Ergebnis ist die Geschwindigkeit, mit der die unabhängige Variable das gewählte Intervall durchläuft. Einerseits kann man, wenn man sie variiert, stationäre und instationäre Vorgänge unterscheiden, andererseits tritt bei sehr grossen Geschwindigkeiten, zumindest zu Beginn der Messung, der parasitäre Auf- bzw. Entladungsstrom der Doppelschichtkapazität störend in Erscheinung.

Wie aus Tabelle 2 hervorgeht, ist für die dort aufgeführten Methoden jedesmal die zeitproportionale Änderung der unabhängigen Variablen, des Elektrodenpotentials also, charakteristisch; das gilt unabhängig davon, ob sie periodisch oder nichtperiodisch erfolgt. Die diskontinuierlichen Sprünge der "multipulse potentiodynamic method" stellen keinen Widerspruch zu dieser Feststellung dar, denn nur die zeitproportionalen Stücke der Zeitfunktion werden für die Messung herangezogen; die diskontinuierlichen Stufen dienen der Vorbehandlung der Elektrode—sie liefern eine ungewöhnlich gute Reproduzierbarkeit der Oberflächenaktivität. Der Zeitpropor-

TABELLE 3

Unabhängige Variable, Führungsgrösse	Gemessene Grösse	Bezeichnung der Methode	Einsatzmöglichkeiten der Methode
Einzelimpulse des Zellstroms, beliebige Form <sup>16</sup>	Transitionszeiten aus $E = E(t)$	Chronopotentiometrie (chronopotentiometry; chronopotentiométrie)	Analytik <sup>7</sup> * Untersuchung instabiler Zwischenprodukte; Lebensdauer von Komplexionen <sup>17,18</sup> . Geschwindigkeitskonstanten gekoppelter chemischer Reaktionen <sup>18</sup> ; Bestimmung von Diffusionskoeffizienten
Doppelimpulse des Zellstroms, beliebige Form, jedoch mit Richtungs-umkehr		Chronopotentiometrie mit Stromumkehr (chronopotentiometry with current reversal; chronopotentiométrie avec inversement de courant)	
Einzelimpuls des Zellstromes beliebiger Form, dem Sinus-Wechselstrom niedriger Frequenz und kleiner Amplitude überlagert ist	Transitionszeiten aus $E_{\sim} = E_{\sim}(t)$	Wechselstromchronopotentiometrie (alternating current chronopotentiometry <sup>19</sup> ; chronopotentiométrie à courant alternatif surimposée)	
Sinus-Wechselstrom so grosser Amplitude, dass die Potentialänderung 1 bis 2 V beträgt	Elektrodenpotential $E_{\sim} = E_{\sim}(t)$ bzw. $(dE_{\sim}/dt) = \text{sinusoidal}$ $(dE_{\sim}/dt) (E_{\sim})$	oszillographische Polarographie nach Heyrovsky und Forejt <sup>9</sup> (alternating current oscillographic polarography; polarographie oscillographique à courant sinusoidal)	Analytik <sup>7</sup> * Reversibilität einer Reaktion; Adsorptionsprozesse

\* Vgl. Fussnote zu Tabelle 2.

tionalität wegen gehören alle Methoden in Tabelle 2 zu den "potentiodynamischen Methoden"\*.

Für die in Tabelle 3 zusammengestellten Methoden, deren unabhängige Variable der Zellstrom ist, gilt im wesentlichen das bereits Gesagte. Die Änderung der unabhängigen Variablen erfolgt mit einer, schon eingangs erwähnten Ausnahme wieder kontinuierlich, jedoch nicht unbedingt proportional zur Zeit\*\*; eine Periodizität der Zeitfunktion ist belanglos. Die Ausnahme bildet die Chronopotentiometrie, die oft einen rechteckigen Sprung des Zellstromes verwendet; um in der Nomenklatur der Regelungstechnik zu sprechen: in diesem Fall ist die Führungsgrösse eine  $\theta$ -Funktion der Zeit. Fast genau dieselbe Führungsgrösse besitzt eine einfache Sprungmethode, allerdings ist dort die Sprunghöhe wesentlich kleiner. Während man sich hier für die Transitionszeiten interessiert, interessiert man sich dort für den Kurvenverlauf  $E = E(t)$ . Im übrigen ist die spezielle Gestalt der Führungsgrösse natürlich eine Frage der experimentellen Realisierbarkeit.

#### METHODEN MIT DEFINIERTER FÜHRUNGSGRÖSSE UND $|\Delta E| \lesssim 10 \text{ mV}$

Zwei Gründe lassen sich dafür anführen, dass die so charakterisierten Methoden in den letzten Jahren in steigendem Masse zum Studium der Elektrodenkinetik, insbesondere zur Bestimmung der kinetischen Parameter, herangezogen wurden. Einerseits vermögen sie, den Einfluss der Konzentrationsüberspannung auf ein

\* Statt "potentiodynamisch" wird auch "potentiokinetisch" gesagt<sup>20</sup>.

\*\* Im zeitproportionalen Fall spricht man von "amperodynamischen Methoden".

Minimum zu reduzieren, andererseits gelingt es, mit ihnen noch solche Elektrodenreaktionen quantitativ zu erfassen, die wegen ihrer relativ hohen Geschwindigkeit den Methoden mit undefinierter Führungsgrösse nicht mehr zugänglich sind.

Diese Methoden zeichnen sich alle dadurch aus, dass sie den zu untersuchenden Prozess auf ein Modell übertragen, in dem der Reaktionsmechanismus, der Transport der Reaktanten im Elektrolyten und gewisse elektrische Grössen festgelegt werden. Das Ergebnis der mathematischen Analyse des Modells wird dann mit dem Ergebnis des Versuches verglichen. Der Grad der erzielbaren Übereinstimmung hängt in allererster Linie davon ab, inwieweit man das System dem gewählten Modell anpassen kann. Im Prinzip kann diese Relation umgekehrt werden, nur scheitert die Anpassung des Modells an die Versuchsanordnung sehr bald an den mathematischen Schwierigkeiten. So wird stets vorausgesetzt, dass die Durchtrittsreaktion von erster Ordnung ist und nur eine geschwindigkeitsbestimmende Stufe enthält. Das schränkt die Anwendbarkeit der Methoden bereits beträchtlich ein. Eine weitere Schwierigkeit bildet die Berücksichtigung der Doppelschicht sowohl im Hinblick auf den Kapazitätsstrom als auch bezüglich des Transportes der Reaktanten. Entweder wird ihre Existenz in den Modellen überhaupt negiert oder sie wird als unabhängig vom Elektrodenpotential und von den Reaktanten angesehen. Beide Voraussetzungen brauchen durchaus nicht von der Versuchsanordnung erfüllt zu werden.

Der Kapazitätsstrom spielt vor allem bei den Methoden eine Rolle, die mit dem Zellstrom als unabhängiger Variabler arbeiten. In diesen Fällen besteht der Hauptteil des unmittelbar nach einer Störung fliessenden Stromes aus dem Kapazitäts- und nicht aus dem Faradayschen Strom. Wie bereits darauf hingewiesen wurde, verschiebt sich das Verhältnis um so mehr zugunsten des Kapazitätsstromes, je rascher die Störung erfolgt; der Effekt ist also ganz besonders bei unendlich schneller Störung, d.h. bei einer  $\theta$ -Funktion als Führungsgrösse, ausgeprägt. Bei den Methoden, die das Elektrodenpotential zur unabhängigen Variablen haben, spielt dagegen der Kapazitätsstrom im Prinzip keine Rolle, sofern man über einen Potentiostaten genügender Leistungsfähigkeit verfügt. Ist das nicht der Fall, so nähert sich das Potential mehr oder weniger schnell seinem Sollwert; der Potentiostat besitzt mithin eine endliche Einstellzeit, wodurch die Messung erst längere Zeit nach dem Beginn der Störung auswertbar wird\*.

Eine weitere Schwierigkeit bei der mathematischen Behandlung bereitet die absolute Grösse der Störung. Während der Zellstrom und die Konzentrationen bei einer Reaktion  $n$ . Ordnung über lineare algebraische Gleichungen bzw. über lineare partielle Differentialgleichungen miteinander verknüpft sind, bestehen zwischen dem Elektrodenpotential und den Konzentrationen bzw. zwischen dem Elektrodenpotential und dem Faradayschen Strom exponentielle Beziehungen. Kleine Argumente erlauben die Linearisierung der Exponentialfunktionen, wodurch sich die mathematische Behandlung vereinfacht; so lassen sich verhältnismässig komplizierte Reaktionsschemata berechnen. Im Gegensatz dazu ist die Theorie, die beliebig grosse Störungen (oder m.a.W. Änderungen der unabhängigen Variablen) zulässt, schwer zu bewältigen. Nur die einfachsten Probleme und die Methoden, deren unabhängige Variable das Elektrodenpotential ist, bilden eine Ausnahme\*\*.

\* Es sei an dieser Stelle ausdrücklich darauf hingewiesen, dass in den Tabellen die ideale Gestalt der Führungsgrösse angegeben ist und keinerlei Vorzeichen beachtet werden.

\*\* Das ist der Grund für die Bemerkung zu Abb. 1.

In diesem Zusammenhang muss auf einen möglichen Trugschluss aufmerksam gemacht werden. Die Möglichkeit, komplizierte Reaktionsschemata berechnen zu können, bedeutet für die Praxis nicht in jedem Fall, dass man diese mit Hilfe kleiner Störungen auch aufklären kann. So ist es mitunter sehr schwierig, gekoppelte chemische Reaktionen bei nur kleinen Störungen geschwindigkeitsbestimmend werden zu lassen, wie es zu ihrer Untersuchung notwendig ist. Das erreicht man aber mit Hilfe grosser Störungen.

An dieser Stelle ist noch eine Bemerkung über die Methoden mit dem Zellstrom als unabhängiger Variabler notwendig. Die Grundgleichung der Elektrodenkinetik gibt den Faradayschen Strom als Funktion des Elektrodenpotentials an. Diese exponentielle Beziehung lässt sich umkehren<sup>21</sup>; sie liefert dann das Elektrodenpotential als Funktion des Faradayschen Stromes und erlaubt höhere Näherungen, die wichtig sind, wenn die Grenze der Leistungsfähigkeit verschoben werden soll. Auch die Berücksichtigung des Kapazitätsstromes in der mathematischen Behandlung verschiebt diese Grenze nicht, solange man sich auf lineare Näherungen beschränkt.

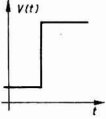
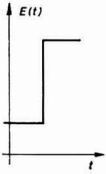
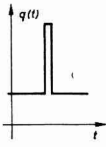
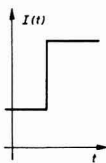
### *Einfache Sprungmethoden*

Die unabhängige Variable wird bei den einfachen Sprungmethoden nach einer  $\theta$ -Funktion der Zeit verändert. Man misst einen Teil der Zeitfunktion, die den Übergang der abhängigen Variablen von dem Ausgangs- in das Endgleichgewicht beschreibt. Das interessierende Zeitintervall erstreckt sich von etwa  $10^{-5}$  bis 1 sec (vom Beginn der Störung an gerechnet). Infolge dieser sehr kurzen Zeiten ist man auf die oszillographische Aufzeichnung und die Photographie angewiesen.

Einen Sonderfall stellt die Ladungssprung-Methode dar. Während bei den drei anderen Methoden die Stufe unendlich lang ist, die unabhängige Variable m.a.W. nach dem Sprung konstant bleibt, bleibt die Ladung der Doppelschicht nach dem Sprung nicht konstant. Nachdem nämlich eine definierte Ladungsmenge innerhalb sehr kurzer Zeit auf die im Gleichgewicht befindliche Elektrode gebracht wurde, wird der Elektrolysekreis sofort unterbrochen. Die in der Doppelschicht gespeicherte Ladung fliesst über einen Faradayschen Strom und einen entgegengesetzt gleich grossen Kapazitätsstrom ab. Beide Ströme heben einander auf; der Faradaysche Strom wird indirekt über die Potentialänderung  $E = E(t)$  bestimmt. Die Ladung der Doppelschicht ändert sich also näherungsweise nach einer Diracschen  $\delta$ -Funktion, der Ableitung der  $\theta$ -Funktion. Aus diesem Grunde ist die Potential-Zeit-Kurve der Ladungssprung-Methode, unabhängig vom speziellen Reaktionsmechanismus, gleich der Ableitung der Potential-Zeit-Kurve der Stromsprung-Methode<sup>41</sup>, dasselbe System vorausgesetzt. Die Ladungssprung-Methode besitzt gewisse Beziehungen zu den klassischen Unterbrechermethoden. Während jene aber bei stationären Bedingungen arbeiten, ist diese insofern anders, als sie eine gegen null gehende Elektrolysedauer vor dem Unterbrechen des Stromkreises besitzt.

Wie bereits erwähnt, darf die Störung bei der Potentialsprung-Methode prinzipiell beliebig gross sein. Für alle anderen Methoden müssen die Störungen so klein sein, dass sich das Elektrodenpotential nur um wenige Millivolt ändert. So kleine Störungen verursachen neue Schwierigkeiten. Sie bestehen darin, dass die Kurven, die das Zeitverhalten der abhängigen Variablen wiedergeben, unabhängig vom speziellen Reaktionsmechanismus einander sehr ähnlich sehen und nur schwer eine Entscheidung darüber zulassen, ob das gewählte Modell und das untersuchte System

TABELLE 4

Unabhängige Variable, Führungsgrösse	Gemessene Grösse	Bezeichnung der Methode	Bestimmung der Austauschstromdichte	Bestimmung des Durchtrittsfaktors
	$I(t)$	Spannungssprung-Methode (voltage-step method <sup>4,22,25</sup> ; voltostatic method <sup>23,24</sup> ; potentiostatic method <sup>4,22</sup> )	$j_0$ aus $I(t^{\frac{1}{2}} \rightarrow 0)$ <sup>25</sup> ; $k_s < 0.1 \text{ cm sec}^{-1}$	$\alpha$ aus $\partial \ln j_0 / \partial \ln C_{O(R)}$ (siehe z.B. Lit. 4)
	$I(t)$	Potentialsprung-Methode (potential-step method <sup>4,22,24</sup> ; potentiostatic method <sup>4,22-24</sup> ; méthode potentiostatique <sup>26</sup> )	$j_0$ aus* $I(t^{\frac{1}{2}} \rightarrow 0)$ <sup>4,27,28</sup> $k_s < 1 \text{ cm sec}^{-1}$ *	$\alpha$ aus $\partial \ln j_0 / \partial \ln C_{O(R)}$ (siehe z.B. Lit. 4)
	$Q(t)$	Potentialsprung-Integral-Methode (potential-step-integral method <sup>29,30</sup> ; integral potentiostatic method <sup>24</sup> )	$j_0$ aus $Q(t^{\frac{1}{2}})$ <sup>29</sup> ; $k_s < 1 \text{ cm sec}^{-1}$	$\alpha$ aus $Q(t^{\frac{1}{2}})$ <sup>29</sup>
	$E(t)$	Ladungssprung-Methode (charge-step method <sup>31,32</sup> ; charge-pulse method <sup>33</sup> ; coulometric impulse method <sup>24,34,35</sup> ; méthode coulométrique <sup>36</sup> )	$j_0$ aus $\log E(t)$ <sup>31</sup> ; $k_s < 1 \text{ cm sec}^{-1}$	$\alpha$ aus $\partial \ln j_0 / \partial \ln C_{O(R)}$ (siehe z.B. Lit. 4)
	$E(t)$	Stromsprung-Methode (current-step method <sup>22</sup> ; single pulse galvanostatic method <sup>4</sup> ; galvanostatic transient method <sup>37</sup> ; galvanostatic method <sup>4,23,37,38</sup> )	$j_0$ aus $E(t^{\frac{1}{2}} \rightarrow 0)$ <sup>39</sup> (1. Näherung mit Doppelschicht; höhere Näherungen ohne Doppelschicht <sup>40</sup> ); $k_s < 1 \text{ cm sec}^{-1}$	$\alpha$ aus $\partial \ln j_0 / \partial \ln C_{O(R)}$ (siehe z.B. Lit. 4)

\* Für grosse Potentialsprünge werden auch Anfangsstromdichte-Potential-Kurven gezeichnet, die wie in Tabelle 1 ausgewertet werden.

in Einklang stehen oder nicht. Die Einstellzeit des Potentiostaten verbietet im allgemeinen jedoch auch bei der Potentialsprung-Methode beliebig grosse Störungen.

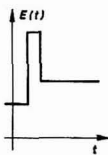
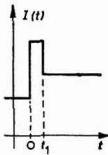
Der Bedeutung des Wortes nach sind nur die einfachen Sprungmethoden "Relaxationsmethoden". In Lit. 23 wurden auch nur diese Methoden dazu gezählt, inzwischen scheint sich die Bezeichnung jedoch für alle Methoden eingebürgert zu haben,

die die kinetischen Parameter nicht mit Hilfe halblogarithmischer Stromdichte-Potential-Kurven ermitteln (vgl. dazu Lit. 24 und 4).

### Mehrfache Sprungmethoden

Der Wunsch, die Leistungsfähigkeit der einfachen Sprungmethoden zu erhöhen, d.h. noch schneller verlaufende Durchtrittsreaktionen quantitativ zu erfassen, lässt sich nur dadurch verwirklichen, dass man zu immer kürzeren Messzeiten übergeht. Auf diesem Wege wird sehr bald eine Grenze erreicht, die von der Aufladung der Doppelschicht gesteckt ist. So wurde der Gedanke entwickelt, ihre relativ langsame Aufladung mit einem zusätzlichen Hilfsimpuls abzukürzen.

TABELLE 5

Unabhängige Variable, Führungsgrösse	Gemessene Grösse	Bezeichnung der Methode	Bestimmung der Austauschstromdichte	Bestimmung des Durchtrittsfaktors
	$I(t)$	potentiostatische Doppelimpuls-methode	$j_0$ wie bei der Potentialsprung-Methode $k_s < 10 \text{ cm sec}^{-1}$	$\alpha$ aus $\partial \ln j_0 / \partial \ln C_{O(R)}$ (siehe z.B. Lit. 4)
	$E(t)^{**}$	amperostatische (galvanostatische) Doppelimpuls-methode <sup>42, 43</sup> (double pulse (galvanostatic) method <sup>4, 24</sup> ; double impulsion galvanostatique <sup>44</sup> )	$j_0$ aus $E(t \rightarrow 0)$ <sup>45</sup> * $k_s < 10 \text{ cm sec}^{-1}$	$\alpha$ aus $\partial \ln j_0 / \partial \ln C_{O(R)}$ (siehe z.B. Lit. 4)

\* Im Zeitpunkt  $t'$  liegt für den eingestellten Strom reine Durchtrittsüberspannung vor; der Strom selbst wird nur für die Elektrodenreaktion verbraucht. Daher kann man aus den Wertepaaren, für die die Abgleichbedingung in  $t'$  erfüllt ist, eine Stromdichte-Potential-Kurve konstruieren, die der reinen Durchtrittsreaktion entspricht. Die Auswertung dieser Kurve erfolgt wie in Tabelle 1 angegeben.

\*\* Man bestimmt den Potentialverlauf  $E(t)$  zu Beginn des zweiten Impulses, d.h. zur Zeit  $t_1 + dt = t'$ , wenn  $t_1$  die Dauer des ersten Impulses ist.

Das Prinzip der Doppelimpulsmethoden sei anhand der zuerst entwickelten amperostatischen Variante<sup>42</sup> erläutert. Der erste Impuls, sehr kurz und gross, lädt praktisch nur die Doppelschicht auf, der zweite Impuls, länger und kleiner als der erste\*, liefert den Faradayschen Strom für die Elektrodenreaktion. Beide Impulse folgen unmittelbar aufeinander; sie müssen in einem bestimmten Verhältnis zueinander stehen, wenn der zweite Impuls gerade den Faradayschen Strom liefern soll. Dieses Verhältnis kann experimentell bestimmt werden. Nur wenn sich an die  $E(t)$ -Kurve zu Beginn des zweiten Impulses eine horizontale Tangente legen lässt, entsprechen der eingestellte Strom und das erhaltene Elektrodenpotential der reinen

\* Er muss so klein sein, dass sich das Elektrodenpotential nur um wenige Millivolt ändert<sup>45</sup>.

Durchtrittsreaktion. Der Abgleichbedingung wegen ist die amperostatische Doppelimpulsmethode einer Nullbestimmung äquivalent.

Die potentiostatische Doppelimpulsmethode ist der amperostatischen ähnlich. Mit Hilfe eines Vorimpulses hoher Amplitude und kurzer Dauer ist es möglich, die Einstellzeit des Potentiostaten um etwa eine Grössenordnung zu erniedrigen<sup>46</sup>. Man kann das Verfahren so weit treiben, dass die Einstellzeit der Dauer des ersten Impulses gleich wird<sup>44</sup>. Man nimmt bei dieser Methode keinen Nullabgleich vor, sondern bedient sich der Auswertung, die bei der Potentialsprung-Methode angegeben ist.

### *Periodische Methoden*

Alle im weiteren besprochenen Methoden zeichnen sich dadurch aus, dass die Führungsgrösse mindestens eine periodische Komponente besitzt. Es lassen sich der Führungsgrösse nach vier Fälle unterscheiden: 1) die Führungsgrösse besteht aus einer periodischen Komponente; 2) sie besteht aus einer periodischen Komponente, die einer zweiten, nichtperiodischen überlagert ist; 3) sie besteht aus einer periodischen Komponente, die einer zweiten, ebenfalls periodischen Komponente überlagert ist; 4) sie besteht aus zwei periodischen Komponenten, die einer dritten, nichtperiodischen Komponente überlagert sind.

Im ersten Fall wartet man, bis sich ein quasistationäres Gleichgewicht, d.h. ein von der Zahl der vorangegangenen Perioden unabhängiger Zustand eingestellt hat. Entweder misst man die Zeitfunktion der abhängigen Variablen oder ihren Wert als Funktion einer bestimmten Zeit. Im zweiten Fall untersucht man nicht bei allen zugehörigen Methoden ein quasistationäres Gleichgewicht, jedoch immer die abhängige Variable als Funktion der nichtperiodischen Komponente (die Frequenz der periodischen Komponente geht natürlich in das Ergebnis ein, sie wird aber im Gegensatz zur nichtperiodischen Komponente nicht verändert). Im dritten Fall liegen bei den Messungen wieder quasistationäre Gleichgewichte vor. Man arbeitet hier aber mit mittleren Werten (z.B. des Elektrodenpotentials) als abhängiger Variabler, die man dadurch einzuhalten sucht, dass man gewisse Veränderungen einer der beiden periodischen Komponenten (z.B. der Amplitude) vornimmt. Im vierten Fall schliesslich, bei dem ebenfalls quasistationäre Gleichgewichte vorliegen, interessieren Resultierende der beiden periodischen Komponenten und deren Abhängigkeit von der nichtperiodischen Komponente.

Die Ausführungen lassen erkennen, dass eine Systematisierung auf dieser Grundlage schwer zu überblicken sein wird; in der Tat wäre sie sehr verworren. Klarere Verhältnisse erhält man auf folgende Weise: Die periodischen Methoden werden in zwei Gruppen geschieden, je nachdem ob sie eine sinusförmige Komponente in der Führungsgrösse aufweisen oder nicht. Die Methoden mit sinusförmiger Komponente werden wiederum geteilt, nämlich in die, die Effekte 1. Ordnung benutzen, und in die, die Effekte 2. Ordnung benutzen. Diese Unterscheidung ist auf das Impedanzverhalten der Phasengrenze Elektrode-Elektrolyt zurückzuführen: Man kann die Phasengrenze, an der ja der Elektrodenprozess abläuft, als ein Schaltelement des elektrischen Messkreises ansehen. Dieses Schaltelement zeichnet sich gegenüber den anderen des Kreises durch seine nichtlineare Strom-Spannungs-Kennlinie aus. In kleinen Bereichen kann die Krümmung dieser Kennlinie vernachlässigt und also die Kennlinie selbst durch eine Gerade ersetzt werden. Beschränkt man sich auf solche Näherungen, so untersucht man Effekte 1. Ordnung. Kann man dagegen die Krüm-



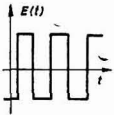
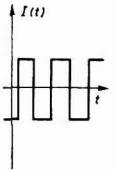
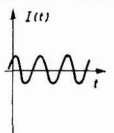
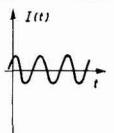
mung nicht mehr vernachlässigen, weil die nichtlineare Kennlinie zu weit ausgesteuert wird, so muss man nichtlineare Näherungen berücksichtigen; man studiert dann Effekte 2. bzw. höherer Ordnung\*.

Zunächst seien die Methoden ohne sinusförmige Komponente behandelt.

*Periodische Sprungmethoden*

Die logische Fortsetzung der einfachen und mehrfachen Sprungmethoden sind die periodischen Sprungmethoden, bei denen die unabhängige Variable periodisch nach  $\theta$ -Funktionen verändert wird. In jeder Halbperiode finden ebensolche Einschwingvorgänge wie bei den einfachen Sprungmethoden statt, allerdings sind sie hier im obigen Sinne quasistationär.

TABELLE 6

Unabhängige Variable, Führungsgrösse	Gemessene Grösse	Bezeichnung der Methode	Bestimmung der Austauschstromdichte	Bestimmung des Durchtrittsfaktors
	$I(t)$ (Vergleich mit Eichkurven)	periodische Potentialsprung-Methode (cyclic potential-step method <sup>47</sup> )	$j_0$ aus Eichkurven <sup>47, 48</sup> ; $k_s < 1 \text{ cm sec}^{-1}$	$\alpha$ durch Variation der positiven und negativen Sprunghöhe bei konstanter Konzentration <sup>47, 48</sup>
	$\delta E(\theta)^*$  $E(0.18 T)$	periodische Stromsprung-Methode (cyclic current-step method <sup>49</sup> )	1. Möglichkeit: $j_0$ aus $\delta E(\theta; \omega)$ <sup>49</sup>	$\alpha$ aus $\partial \ln j_0 / \partial \ln C_{O(R)}$ (siehe z.B. Lit. 4)
	$E(0.25 T)$	direkte oszillographische Methode	2. Möglichkeit: $j_0$ aus $E(0.18 T)$ (Vorliegen reiner Durchtrittsüberspannung) <sup>49</sup> $k_s < 1 \text{ cm sec}^{-1}$	
	$E(0.25 T)$		$j_0$ aus $E(0.25 T)$ (Vorliegen reiner Durchtrittsüberspannung) <sup>50</sup> $k_s < 1 \text{ cm sec}^{-1}$	$\alpha$ aus $\partial \ln j_0 / \partial \ln C_{O(R)}$ (siehe z.B. Lit. 4)

\* Es wird die Differenz  $\delta E(\theta)$  des Elektrodenpotentials in einem bestimmten Zeitpunkt  $\theta$  zweier benachbarter Halbperioden gemessen; die erste Halbperiode muss ungeradzahlig, die zweite geradzahlig sein.

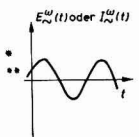
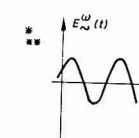
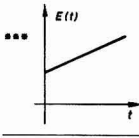
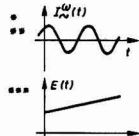
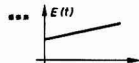
Ist das Elektrodenpotential die unabhängige Variable, so misst man die Zeitfunktion der abhängigen Variablen über die ganze Halbperiode. Um quantitative Aussagen zu erzielen, gleicht man die experimentell erhaltenen Zeitfunktionen in

\* Es erhebt sich hier natürlich die Frage, weshalb bei den zuvor besprochenen Methoden nicht von Effekten 1. bzw. 2. Ordnung gesprochen wurde. Tatsächlich treten aber diese Effekte nur bei periodischer Führungsgrösse in Erscheinung. Die Ursache dafür ist, dass nichtperiodische Signale ein kontinuierliches, periodische Signale dagegen ein diskretes Frequenzspektrum haben.



ihrer gesamten Länge an berechnete Eichkurven an. Daher kann man auch hier von einer Nullbestimmung sprechen. Werden dagegen unabhängige und abhängige Variable miteinander vertauscht, so misst man nicht mehr die Zeitfunktion der abhängigen Variablen, sondern ihren Wert in einem definierten Zeitpunkt der Halbperiode. Einerseits benötigt man für quantitative Aussagen eine Messreihe, bei der die Frequenz variiert wird, andererseits benutzt man die Tatsache, dass für alle periodischen Wechselströme in einem bestimmten Zeitpunkt der Halbperiode reine Durchtrittsüberspannung vorliegt, sofern der Ohmsche Spannungsabfall eliminiert wird. Dieser Zeitpunkt kann berechnet werden, so dass man aus der gemessenen reinen Durchtrittsüberspannung ohne weiteres die Austauschstromdichte errechnen kann.

TABELLE 7

Unabhängige Variable, Führungsgröße	Gemessene Größe	Bezeichnung der Methode	Bestimmung der Austauschstromdichte	Bestimmung des Durchtrittsfaktors
	$Z(\omega)$	Faradaysche Impedanz (faradaic impedance; impédance faradique)	$j_0$ aus dem gewählten Ersatzschaltbild (Überblick bei Lit. 4, 52) mit Hilfe der Vektorrechnung <sup>53, 54</sup> oder der komplexen Ebene <sup>9, 55-58</sup> oder unter Vernachlässigung des Imaginärteils der Warburg-Impedanz <sup>59</sup> (siehe dazu auch Lit. 60) $k_s < 1 \text{ cm sec}^{-1}$	$\alpha$ aus $\partial \ln j_0 / \partial \ln C_{O(R)}$ (siehe z.B. Lit. 4)
$E_{\text{ges}} = E + E_{\omega}$ 	$Z(E; \omega)$	Faradaysche Impedanz <sup>56, 61</sup> bzw. Faradaysche Admittanz <sup>61</sup>		
	$\varphi(E)$	Faradaysche Admittanz (faradaic admittance <sup>62, 63</sup> )	$j_0$ aus $\varphi_{\text{max}}(E)$ entsprechend der Theorie <sup>64</sup> $k_s < 1 \text{ cm sec}^{-1}$	$\alpha$ ohne Konzentrationsvariation <sup>64</sup>
	$I_{\omega}(E)$	Wechselstrompolarographie (i. Harmonische)	analytische Methoden	
	$E_{\omega}(E)$	Wechselspannungspolarographie (i. Harmonische) (siehe dazu Lit. 65, 66)		

\*  $\omega \leq 2\pi \cdot 500 \text{ Hz}$

\*\* kleine Amplitude (siehe Text)

\*\*\*  $E(t)$  wird so langsam geändert, dass quasistationäre Gleichgewichte vorliegen.

In praxi empfiehlt es sich, mit möglichst kleinen Frequenzen zu arbeiten, um den parasitären Kapazitätsstrom klein zu halten. Da ein Redoxsystem den Kapazitätsstrom relativ zum Faradayschen Strom steigert, wenn es irreversibler wird, muss eine Frequenzgrenze zu erwarten sein, oberhalb der die Geschwindigkeitskonstante der Durchtrittsreaktion ihren Wert verändert. Tatsächlich lässt sich dieser Effekt beobachten<sup>51</sup>.

Die im folgenden aufgeführten Methoden enthalten sämtlich sinusförmige Komponenten in der Führungsgrösse.

#### *Sinusmethoden: Effekte 1. Ordnung*

Während bei den polarographischen Methoden und der Faradayschen Admittanz die Führungsgrösse zusätzlich zur sinusförmigen Komponente eine nicht-periodische Komponente enthält, die so langsam variiert wird, dass sich quasi-stationäre Gleichgewichte einstellen, besteht die Führungsgrösse bei der Methode der Faradayschen Impedanz nur aus einer sinusförmigen Komponente; es werden ebenfalls quasistationäre Gleichgewichte untersucht. Das Interesse an der letztgenannten Methode dürfte sich in der letzten Zeit verstärkt haben, weil die Darstellung der Zellimpedanz in der komplexen Ebene ausser den kinetischen Parametern die Doppelschichtkapazität als Funktion des Elektrodenpotentials und der Konzentration der Reaktanten liefert. Darin ist diese Methode allen anderen überlegen.

#### *Sinusmethoden: Effekte 2. Ordnung*

Es wurde bereits darauf hingewiesen, dass die Doppelschicht das eigentliche Hemmnis ist, wenn man immer schnellere Durchtrittsreaktionen untersuchen will. Man muss dazu zu immer kürzeren Messzeiten bzw. zu höheren Frequenzen übergehen. Die Messzeit kann nicht beliebig verkürzt werden, da die Auf- bzw. Entladung der Doppelschicht eine gewisse Zeit benötigt. Einer Erhöhung der Frequenzen geht eine Verminderung des elektrischen Widerstandes der Doppelschicht parallel, so dass dann der Hauptteil des messbaren Gesamtstromes nicht mehr über die Faradaysche Impedanz, sondern über die Doppelschichtkapazität fliesst. Nun wurde gerade betont, dass die Methode der Faradayschen Impedanz die Doppelschichtkapazität zusätzlich liefert; wegen der Aussage des vorigen Satzes kommt man damit trotzdem nicht weiter. Um das gewünschte Ziel zu erreichen, muss man den durch die Doppelschicht bedingten Kapazitätsstrom von vornherein auszuschalten suchen. Das gelingt mit den Effekten 2. Ordnung, denn die Doppelschichtkapazität ist in weit geringerem Masse ein nichtlineares Schaltelement als die Faradaysche Impedanz; daher liefert sie keinen Beitrag zu den gemessenen Grössen.

Es gibt drei Effekte zweiter Ordnung: die Faradaysche Verzerrung, die Faradaysche Gleichrichtung und die Intermodulationsverzerrung. Sie lassen sich folgendermassen beschreiben: Wird der Messzelle eine sinusförmige Wechselspannung aufgeprägt, so enthält der resultierende Wechselstrom Oberwellen der angelegten Grundfrequenz; durch die nichtlineare Faradaysche Impedanz entstehen Verzerrungen, die allgemein mit "Faradaysche Verzerrung" bezeichnet werden. Die Amplituden der Oberwellen nehmen schnell mit der Amplitude der angelegten Grundfrequenz sowie mit steigender Ordnung ab. Daher beträgt die angelegte Amplitude mindestens 10 mV (dieser Wert ist natürlich von der Empfindlichkeit des Messgerätes abhängig), und man beschränkt sich auf die 1. Oberschwingung, die sogenannte 2. Harmonische.

TABELLE 8

<i>Effekt 2. Ordnung</i>	<i>Bezeichnung der Methode</i>	<i>Hinweise zur Bestimmung der kinetischen Parameter</i>
Faradaysche Verzerrung (faradaic distortion)* $k_s < 10-20 \text{ cm sec}^{-1}$	Faradaysche Verzerrung unter wechselstrompolarographischen Bedingungen	kinetische Parameter entsprechend der Theorie <sup>67</sup> aus Höhe und Abstand der Maxima; $\alpha$ ohne Konzentrationsvariation
	analytische Methode: Wechselstrompolarographie (2. Harmonische)	
	Faradaysche Verzerrung unter wechsellspannungspolarographischen Bedingungen	kinetische Parameter entsprechend der Theorie <sup>68</sup> analog dem obigen Fall
	analytische Methode: Wechsellspannungspolarographie (2. Harmonische)	
Faradaysche Gleichrichtung (faradaic rectification <sup>84</sup> )* $k_s < 10-20 \text{ cmsec}^{-1}$	Gleichrichtungsspannung (redoxokinetik potential <sup>69</sup> )	kinetische Parameter auf verschiedene Weise (siehe Text); $\alpha$ ohne Konzentrationsvariation
	Gleichrichtungsstrom (Fournier effect) <sup>67b,70</sup>	kinetische Parameter auf verschiedene Weise (siehe Text); $\alpha$ ohne Konzentrationsvariation
Intermodulationsverzerrung $k_s < 10-20 \text{ cm sec}^{-1}$	Intermodulationspolarographie <sup>71</sup> ; Doppeltonpolarographie <sup>72</sup> ; Hochfrequenzpolarographie <sup>9</sup> (r.f. polarography <sup>73</sup> ) (das sind "analytische" Bezeichnungen)	bzgl. der Bestimmung der kinetischen Parameter siehe Lit. 9, 24, 73, 74

\* Während bei der Faradayschen Verzerrung die Regelung der alternierenden Komponente das Ergebnis bestimmt, bestimmt bei der Faradayschen Gleichrichtung die Regelung der mittleren Komponente das Ergebnis.

Legt man an die Zelle statt einer Wechsellspannung einen Wechselstrom an, so tritt derselbe Effekt auf. Die Methoden, die sich seiner bedienen, haben auch als empfindliche Analysenmethoden Bedeutung.

Hält man unter genau denselben Versuchsbedingungen entweder die mittlere Grösse des Faradayschen Stromes oder die mittlere Grösse des Elektrodenpotentials konstant\*, so kommt es, weil die Oberwellen kompensiert werden müssen, zu einer Verschiebung des mittleren Elektrodenpotentials (mittlere Grösse des Faradayschen Stromes auf null eingestellt) oder des mittleren Faradayschen Stromes (mittlere Grösse des Elektrodenpotentials auf den Gleichgewichtswert eingestellt). Allgemein spricht man von Faradayscher Gleichrichtung. Diese Verschiebungen sind unabhängig davon, ob die Elektrode mit einem Wechselstrom oder einer Wechsellspannung polarisiert wird. Da bei einem Faradayschen Strom null kein chemischer Umsatz stattfindet, hat die erste Möglichkeit besondere Bedeutung erlangt. Die Gleichrichtungsspannung ist infolge der Aufladung der Doppelschichtkapazität zeitabhängig; man kann sie direkt messen, indem man die Verschiebung des mittleren Elektrodenpotentials nach dem Einschalten der hochfrequenten Sinusvariablen ver-

\* Geregelt wird, das sei wiederholt, der zeitliche Mittelwert, nicht etwa irgendeine Komponente, die zu ihm beiträgt.

folgt<sup>75,76\*</sup> oder die Gleichrichtungsspannung durch eine Spannungsstufe kompensiert<sup>74,77,78\*\*</sup>. Bei der Kompensation wurde sogar in Analogie zur amperostatischen Doppelimpulsmethode die Zeitabhängigkeit der Gleichrichtungsspannung eliminiert, indem die Sinusvariable mit einem Doppelimpuls "moduliert" wurde<sup>78\*\*</sup>. Alle vorstehend genannten Verfahren erlauben die Untersuchung der Änderung der Gleichrichtungsspannung mit der Frequenz; sie haben aber den Nachteil, quantitative Aussagen über die kinetischen Parameter erst nach der Bestimmung der über der Faradayschen Impedanz abfallenden Spannung zu ermöglichen. Diese Bestimmung ist bei den hohen Frequenzen ( $\approx 1$  MHz) nicht leicht. Es besteht aber auch die Möglichkeit, mit Hilfe der Frequenz, bei der die Gleichrichtungsspannung null wird, die gewünschten quantitativen Aussagen zu treffen<sup>79</sup>. Die Messung der über der Faradayschen Impedanz abfallenden Spannung wird damit unnötig.

Superponiert man der Messzelle gleichzeitig zwei periodische Komponenten, die sich in den Frequenzen unterscheiden und i.a. sinusförmig sind, so treten in der abhängigen Variablen ausser den Eingangsfrequenzen und deren Oberwellen noch Komponenten mit den Kombinationsfrequenzen (d.h. Summen- und Differenzfrequenzen der Eingangsfrequenzen und Oberwellen sowohl untereinander als auch miteinander) auf. Haben die beiden Komponenten unterschiedliche Amplituden und einen gewissen Abstand der Einzelfrequenzen, so spricht man (bei Überlagerung auf eine nichtperiodische Komponente wie bei den polarographischen Methoden) von Intermodulationspolarographie<sup>71</sup>, bei (meist) gleicher Amplitude und geringem Abstand der Frequenzen von Doppeltonpolarographie<sup>72</sup>. Die Polarogramme sind naturgemäss sehr kompliziert, da alle Seitenbänder mitgemessen werden. In der Regel bestimmt man daher mit frequenzselektiven Anordnungen nur bestimmte Komponenten der Intermodulationsverzerrungen.

Eine Methode, die gewissermassen einen Sonderfall der Intermodulationspolarographie darstellt, ist die Hochfrequenz-Polarographie<sup>73</sup>. Der Zelle wird ein hochfrequenter Sinusstrom (0.1 bis 6.4 MHz) überlagert, der mit einer Rechteckwelle von 225 Hz amplitudenmoduliert ist. Man misst mit Hilfe eines konventionellen Rechteckwellenpolarographen die Komponente, die durch die Intermodulation des hochfrequenten Trägers und seiner Seitenbänder entsteht. Da die Seitenbänder um 225 Hz von der Trägerfrequenz entfernt liegen und da man die Komponente misst, die durch Summen- bzw. Differenzbildung von Träger und Seitenband entsteht, misst man mit dem Rechteckwellenpolarographen den rechteckigen Wechselstrom von 225 Hz, den man der Elektrode zuführen muss, um ihr mittleres Potential konstant zu halten. Obwohl die Hochfrequenz-Polarographie aus diesem Grunde theoretisch mit Hilfe der Faradayschen Gleichrichtung erklärt werden kann<sup>9,73</sup>, ist sie experimentell zur Intermodulations-Polarographie zu zählen<sup>24</sup>.

#### VERGLEICH DER METHODEN

In praxi wird man die Methoden nach ganz bestimmten und unterschiedlichen Gesichtspunkten beurteilen. So wird wohl als erstes die Frage gestellt werden, welche Methode eine für das Problem ausreichende Leistungsfähigkeit besitzt. Die Geschwin-

\* Hier untersucht man also einen Einschwingvorgang.

\*\* In diesem Fall nimmt man einen Nullabgleich vor.

digkeitskonstante  $k_s$ , ein quantitatives Mass dafür, ist in den Tabellen angegeben. Wie man sieht, besitzen die Methoden der Tabelle 8 die grösste Leistungsfähigkeit. Seit dem Erscheinen der ersten Arbeiten ist aber gerade bzgl. der darin angegebenen Leistungsfähigkeiten Kritik an diesen Methoden geübt worden<sup>23</sup>; auch hat es bisher den Anschein, dass diese Methoden weniger zur Klärung von Problemen beigetragen als vielmehr Fragen aufgeworfen haben (z.B. Lit. 80), da sie Ergebnisse lieferten, die durchaus nicht mit denen anderer Methoden übereinstimmen.

Ein weiterer Gesichtspunkt dürfte der apparative Aufwand der Methoden sein. Diesbezüglich sind die Spannungssprung-Methode und die Ladungssprung-Methode die einfachsten. Beide Methoden besitzen aber Nachteile, die den anderen wiederum nicht zu eigen ist. So wird die Spannungssprung-Methode als einzige der einfachen Sprungmethoden vom Gesamtwiderstand des elektrischen Kreises beeinflusst. Überwiegt dieser Widerstand den Durchtrittswiderstand, so wird die Bestimmung der Austauschstromdichte unmöglich. Bei der Ladungssprung-Methode ist der Einfluss der Doppelschicht am augenfälligsten: man setzt nicht nur voraus, dass die Doppelschichtkapazität in dem interessierenden Intervall vom Elektrodenpotential unabhängig ist, sondern nimmt auch an, dass sie dort von anderen Faktoren (wie z.B. der Adsorption oberflächenaktiver Verunreinigungen) nicht beeinflusst wird. Daher ist eine gewisse Vorsicht bei der Anwendung dieser Methode geboten. Relativ grösser ist der apparative Aufwand bei den Methoden mit dem Elektrodenpotential bzw. dem Zellstrom als unabhängiger Variabler, doch ist die moderne Elektrochemie ohne Potentiostaten nicht denkbar\*. Die Potentialsprung-Methode ist den anderen einfachen Sprungmethoden nicht nur wegen der prinzipiell beliebig grossen Sprünge überlegen (die, wie schon erwähnt, Geschwindigkeitskonstanten gekoppelter chemischer Reaktionen zu bestimmen gestattet), sondern auch dann, wenn mehrere Elektrodenreaktionen gleichzeitig ablaufen. Der beobachtete Strom ist dann nämlich einfach die Summe der Einzelströme; im Fall der Ladungssprung-Methode konkurrieren die Reaktionen um die verfügbare Ladung, und das beobachtete Verhalten des Elektrodenpotential ist sehr viel komplizierter. Gleiches gilt für die Stromsprung-Methode. Weiterhin ist die Potentialsprung-Methode (für den Idealfall des rechteckigen Sprunges) im Gegensatz zu der Stromsprung- und Ladungssprung-Methode von der Kenntnis der Doppelschichtkapazität unabhängig. Bei der Potentialsprung-Integral-Methode erhöht sich der apparative Aufwand etwas. Während man bei der Potentialsprung-Methode wie auch bei den anderen einfachen Sprungmethoden die Zeitfunktion der abhängigen Variablen auf einem Oszillographenschirm sichtbar macht, misst man bei der Potentialsprung-Integral-Methode das Integral des fliessenden Stromes mit einem elektronischen Integrator. Der Vorteil, der auf Kosten des erhöhten apparativen Aufwandes geht, besteht darin, dass sich die Messzeit um den Faktor 2500 verlängert und das mühsame punktweise Umzeichnen der photographierten Kurve entfällt. Einen vielleicht geringeren Aufwand besitzen die Doppelimpulsmethoden. Das Problem für diese Methoden besteht nicht so sehr darin, den zweiten Impuls unmittelbar an den ersten anschliessen zu lassen, als vielmehr darin, dass natürlich während des "Aufladeimpulses" die Elektrodenreaktion bereits in Gang kommt. Besonders bei niedrigen Konzentrationen der Reaktanten kann eine beträchtliche

\* Bekanntlich kann man mit einem Potentiostaten sowohl das Elektrodenpotential als auch den Zellstrom regeln.

Konzentrationsüberspannung die Folge sein (vgl. dazu neben Lit. 45 auch 81). Den vergleichsweise höchsten Aufwand besitzen die Methoden der Tabelle 8; auch bzgl. der Theorie sind diese Methoden am aufwendigsten.

Die potentiostatische und die amperostatische Methode, die klassischen Methoden der Elektrodenkinetik, haben durch die neu geschaffenen Methoden keineswegs an Bedeutung verloren. Für Elektrodenreaktionen höherer als 1. Ordnung sind sie den neuen Methoden sogar überlegen, da auch für die einfachsten Varianten die mathematische Analyse des Modells an den nichtlinearen Gleichungen (insbesondere an den Differentialgleichungen) scheitert. In Verbindung mit der Theorie ist die Frage, wie die Messergebnisse erhalten und ausgewertet werden, interessant. Am attraktivsten sind i.a. Methoden, bei denen eine Nullbestimmung erfolgt. Sie besitzen auch vergleichsweise einen kleineren Messfehler. Eine solche Methode ist die amperostatische Doppelpulsmethode, bei der der genaue Verlauf der Elektrodenpotential-Zeit-Kurve uninteressant ist. Daher braucht man nicht das Schirmbild des Oszillographen zu photographieren und später die Kurve mühsam punktweise auszuwerten. Ein Beispiel für den Fall einer wenig attraktiven Nullbestimmung ist die Faradaysche Impedanz. Der Nullabgleich mit einer Brückenschaltung ist schwierig und zeitraubend, eleganter dürfte es sein, mit einer Apparatur nach dem Prinzip der phasempfindlichen Gleichrichtung (z.B. Lit. 82, 83) zu arbeiten.

Berücksichtigt man schliesslich noch, dass die meisten Methoden den Nachteil haben, den Durchtrittsfaktor aus der Konzentrationsabhängigkeit der Austauschstromdichte bestimmen zu müssen, so sieht man, dass eine beliebige Methode von einem Gesichtspunkt aus vorteilhaft, von einem anderen dagegen wenig vorteilhaft erscheinen kann. Die Wahl zwischen den Methoden hängt daher sehr von der jeweiligen Aufgabenstellung und den verfügbaren Hilfsmitteln ab; eine allgemeingültige Regel gibt es nicht. Theoretisch müssten die Methoden unter denselben Bedingungen übereinstimmende Ergebnisse liefern; differieren diese, so ist das wahrscheinlich eine Folge davon, dass die Versuchsanordnung mit dem Modell nicht übereinstimmt, möglicherweise im Reaktionsmechanismus.

Herrn Prof. K. SCHWABE möchte ich auch an dieser Stelle sehr herzlich für seine Unterstützung und Förderung bei der Arbeit danken.

#### ZUSAMMENFASSUNG

Um eine Zusammenstellung der im Titel bezeichneten Methoden zur Verfügung zu haben, wurden diese systematisiert und in Tabellen angeordnet. Grundlage der Systematisierung waren die unabhängige Variable und ihre vom Experimentator vorgegebene Zeitabhängigkeit. Die Tabellen enthalten folgende Angaben: die Bezeichnung der Methode, die unabhängige Variable und ihre Zeitabhängigkeit, die gemessene Grösse, die Aussagemöglichkeiten der Methode, die Wege zur Bestimmung der kinetischen Parameter sowie Hinweise auf die Literatur über die theoretischen Grundlagen der Methode. Vor- und Nachteile der Methoden werden, soweit das möglich ist, beschrieben.

## SUMMARY

Electrical methods for the study of the kinetics of electrode reactions were systematized and tabulated. The independent variable and its time dependence predetermined by the experimentalist were the base of the systematization. The tables contain the following items: the name of the method, the independent variable and its time dependence, the measured quantity, the capabilities of the method, the route which must be taken to determine the kinetic parameters, and references to literature dealing with the theoretical fundamentals of the method. Reference is also made to advantages and disadvantages of the methods so far as it is possible.

## VERWENDETE SYMBOLE

$C_O$	analytische Konzentration der oxydierten Form
$C_R$	analytische Konzentration der reduzierten Form
$E$	Elektrodenpotential
$E_{\sim}^{\nu}$	sinusförmige Komponente des Elektrodenpotentials der Frequenz $\nu$
$E_{\text{ges}}$	aus mehreren Komponenten bestehendes Elektrodenpotential
$F$	Faradaysche Konstante
$f$	$F/RT^*$
$I$	Zellstrom
$I_{\sim}^{\nu}$	sinusförmige Komponente des Zellstroms der Frequenz $\nu$
$j_0$	Austauschstromdichte (bzgl. der Doppelschicht nicht korrigiert)
$k_s$	Geschwindigkeitskonstante der Durchtrittsreaktion beim Standardpotential
$n$	Zahl der in der Durchtrittsreaktion ausgetauschten Elektronen
$Q$	vom elektronischen Integrator gespeicherte Ladung $\int dt \cdot I(t)$
$q$	Ladungsdichte der Elektrode
$R$	Gaskonstante
$T$	Periodendauer
$T^*$	absolute Temperatur
$t$	Zeit
$V$	Zellspannung
$Z$	Impedanz der Zelle
$\alpha$	Durchtrittsfaktor
$\eta$	Überspannung
$\theta$	$t/T$
$\varphi$	Phasenwinkel zwischen $E_{\sim}$ und $I_{\sim}$
$\varphi_{\text{max}}$	Maximalwert des Phasenwinkels
$\omega$	$2\pi/T$ , Kreisfrequenz

## LITERATUR

- 1 N. TANAKA UND R. TAMAMUSHI, *Electrochim. Acta*, 9 (1964) 963.
- 2 E. YEAGER, *Transactions of the Symposium on Electrode Processes, Philadelphia, 1959*, Wiley, New York, 1961, S. 145.
- 3 H. BERG, *Naturwissenschaften*, 47 (1960) 320; 49 (1962) 11.
- 4 P. DELAHAY, *Advan. Electrochem. Electrochem. Eng.*, 1 (1961) 233.
- 5 P. L. ALLEN UND A. HICKLING, *Trans. Faraday Soc.*, 53 (1957) 1626.
- 6 G. CHARLOT, J. BADOZ-LAMBLING UND B. TRÉMILLON, *Les réactions électrochimiques*, Masson, Paris, 1959.



- 7 K. SCHWABE, H. J. BÄR UND H. STEINHAUER, *Chem. Ingr.-Tech.*, 37 (1965) 483.
- 8 G. F. REYNOLDS, *Z. Chem.*, 5 (1965) 410.
- 9 H. SCHMIDT UND M. VON STACKELBERG, *Die neuartigen polarographischen Methoden*, Verlag Chemie, Weinheim/Bergstr., 1962.
- 10 P. DELAHAY, *J. Am. Chem. Soc.*, 75 (1953) 1190.
- 11 A. SEVČÍK, *Collection Czech. Chem. Commun.*, 13 (1948) 349.
- 12 W. VIELSTICH, *Z. Instrumentenk.*, 71 (1963) 29.
- 13 F. G. WILL UND C. A. KNORR, *Z. Elektrochem.*, 64 (1960) 258, 270.
- 14 S. GILMAN, *J. Phys. Chem.*, 66 (1962) 2657; 67 (1963) 78.
- 15 S. GILMAN, *J. Electroanal. Chem.*, 7 (1964) 382.
- 16 R. W. MURRAY UND C. N. REILLEY, *J. Electroanal. Chem.*, 3 (1962) 64, 182.
- 17 J. O'M. BOCKRIS, D. INMAN, A. K. N. REDDY UND S. SRINIVASAN, *J. Electroanal. Chem.*, 5 (1963) 476.
- 18 H. HOFFMANN UND W. JAENICKE, *Z. Elektrochem.*, 66 (1962) 7; *Z. Anal. Chem.*, 186 (1962) 93.
- 19 Y. TAKEMORI, T. KAMBARA, M. SENDA UND I. TACHI, *J. Phys. Chem.*, 61 (1957) 968.
- 20 I. EPELBOIN, *Z. Physik. Chem. (Leipzig)*, 226 (1964) 175.
- 21 P. J. GELLINGS, *Z. Elektrochem.*, 66 (1962) 477.
- 22 P. DELAHAY, *Ann. Rev. Phys. Chem.*, 8 (1957) 229.
- 23 W. H. REINMUTH, *Advan. Anal. Chem. Instr.*, 1 (1960) 241.
- 24 W. H. REINMUTH, *Anal. Chem.*, 36 (1964) 211R.
- 25 W. VIELSTICH UND P. DELAHAY, *J. Am. Chem. Soc.*, 79 (1957) 1874.
- 26 P. DELAHAY, *J. Chim. Phys.*, 54 (1957) 369.
- 27 H. GERISCHER UND W. VIELSTICH, *Z. Physik. Chem. (Frankfurt)*, 3 (1955) 16.
- 28 W. VIELSTICH UND H. GERISCHER, *Z. Physik. Chem. (Frankfurt)*, 4 (1955) 10.
- 29 J. H. CHRISTIE, G. LAUER UND R. A. OSTERYOUNG, *J. Electroanal. Chem.*, 7 (1964) 60.
- 30 R. A. OSTERYOUNG, G. LAUER UND F. C. ANSON, *Anal. Chem.*, 34 (1962) 1833.
- 31 P. DELAHAY, *J. Phys. Chem.*, 66 (1962) 2204.
- 32 P. DELAHAY UND A. ARAMATA, *J. Phys. Chem.*, 66 (1962) 2208.
- 33 P. DELAHAY, *Anal. Chem.*, 34 (1962) 1267.
- 34 P. DELAHAY UND W. H. REINMUTH, *Anal. Chem.*, 34 (1962) 1344.
- 35 W. H. REINMUTH, *Anal. Chem.*, 34 (1962) 1272.
- 36 A. HAMELIN, *Electrochim. Acta*, 9 (1964) 289.
- 37 H. GERISCHER, *Ann. Rev. Phys. Chem.*, 12 (1961) 227.
- 38 R. L. BIRKE UND D. K. ROE, *Anal. Chem.*, 37 (1965) 450.
- 39 T. BERZINS UND P. DELAHAY, *J. Am. Chem. Soc.*, 77 (1955) 6448.
- 40 P. J. GELLINGS, *Z. Elektrochem.*, 66 (1962) 481.
- 41 W. H. REINMUTH UND C. E. WILSON, *Anal. Chem.*, 34 (1962) 1159.
- 42 H. GERISCHER UND M. KRAUSE, *Z. Physik. Chem. (Frankfurt)*, 10 (1957) 264.
- 43 H. GERISCHER UND M. KRAUSE, *Z. Physik. Chem. (Frankfurt)*, 14 (1958) 184.
- 44 M. BONNEMAY, E. LEVART, A. A. PILLA UND E. POIRIER D'ANGÉ D'ORSAY, *Electrochim. Acta.*, 8 (1963) 805.
- 45 H. MATSUDA, S. OKA UND P. DELAHAY, *J. Am. Chem. Soc.*, 81 (1959) 5077.
- 46 M. BONNEMAY, E. LEVART, A. A. PILLA UND E. POIRIER D'ANGÉ D'ORSAY, *Compt. Rend.*, 256 (1963) 4008.
- 47 W. M. SMIT UND M. D. WIJNEN, *Rec. Trav. Chim.*, 79 (1960) 5.
- 48 M. D. WIJNEN UND W. M. SMIT, *Rec. Trav. Chim.*, 79 (1960) 203.
- 49 M. D. WIJNEN UND W. M. SMIT, *Rec. Trav. Chim.*, 79 (1960) 22.
- 50 J. H. SLUYTERS, *Rec. Trav. Chim.*, 81 (1962) 297.
- 51 M. D. WIJNEN UND W. M. SMIT, *Rec. Trav. Chim.*, 79 (1960) 289.
- 52 D. C. GRAHAME, *J. Electrochem. Soc.*, 99 (1952) C370.
- 53 P. DELAHAY UND T. J. ADAMS, *J. Am. Chem. Soc.*, 74 (1952) 5740.
- 54 J. E. B. RANGLES, *Discussions Faraday Soc.*, 1 (1947) 11.
- 55 J. H. SLUYTERS, *Rec. Trav. Chim.*, 79 (1960) 1092.
- 56 M. SLUYTERS-REHBACH UND J. H. SLUYTERS, *Rec. Trav. Chim.*, 82 (1963) 525, 535.
- 57 M. SLUYTERS-REHBACH UND J. H. SLUYTERS, *Rec. Trav. Chim.*, 83 (1964) 217, 581, 967.
- 58 M. SLUYTERS-REHBACH, B. TIMMER UND J. H. SLUYTERS, *Rec. Trav. Chim.*, 82 (1963) 553.
- 59 H. GERISCHER, *Z. Physik. Chem. (Leipzig)*, 198 (1951) 286; 201 (1952) 55; 202 (1953) 302; *Z. Physik. Chem. (Frankfurt)*, 1 (1954) 278.
- 60 R. DE LEVIE, *Electrochim. Acta*, 10 (1965) 395.
- 61 M. REHBACH UND J. H. SLUYTERS, *Rec. Trav. Chim.*, 80 (1961) 469; 81 (1962) 301.
- 62 H. H. BAUER UND P. J. ELVING, *J. Am. Chem. Soc.*, 82 (1960) 2091; H. H. BAUER, D. L. SMITH UND P. J. ELVING, *J. Am. Chem. Soc.*, 82 (1960) 2094.
- 63 R. TAMAMUSHI UND N. TANAKA, *Z. Physik. Chem. (Frankfurt)*, 21 (1959) 89.
- 64 H. MATSUDA, *Z. Elektrochem.*, 62 (1958) 977.
- 65 H. H. BAUER, *Rev. Polarog. (Kyoto)*, 11 (1963) 58.



- 66 B. BREYER UND H. H. BAUER, *Alternating Current Polarography and Tensammetry*, Wiley, New York, 1963.
- 67 H. H. BAUER, *Australian J. Chem.*, 17 (1964) 591, 715.
- 68 K. B. OLDHAM, *J. Electrochem. Soc.*, 107 (1960) 766.
- 69 K. S. G. DOSS UND H. P. AGARWAL, *J. Sci. Ind. Res. India*, 9B (1950) 280; *Proc. Indian Acad. Sci.*, 34A (1951) 263; 35A (1952) 45.
- 70 M. FOURNIER, *Compt. Rend.*, 232 (1951) 1673.
- 71 R. NEEB, *Naturwissenschaften*, 49 (1962) 447.
- 72 R. NEEB, *Z. Anal. Chem.*, 208 (1965) 168.
- 73 G. C. BARKER, R. L. FAIRCLOTH UND A. W. GARDNER, *Nature*, 181 (1958) 247.
- 74 G. C. BARKER, in E. YEAGER (Herausg.), *Transactions of the Symposium on Electrode Processes, Philadelphia, 1959*, Wiley, 1961, S. 325.
- 75 P. DELAHAY, M. SENDA UND C. H. WEIS, *J. Am. Chem. Soc.*, 83 (1961) 312.
- 76 H. IMAI UND P. DELAHAY, *J. Phys. Chem.*, 66 (1962) 1108.
- 77 H. IMAI UND P. DELAHAY, *J. Phys. Chem.*, 66 (1962) 1683.
- 78 M. SENDA, H. IMAI UND P. DELAHAY, *J. Phys. Chem.*, 65 (1961) 1253.
- 79 H. IMAI, *J. Phys. Chem.*, 66 (1962) 1744.
- 80 M. SLUYTERS-REHBACH UND J. H. SLUYTERS, *Rec. Trav. Chim.*, 83 (1964) 983.
- 81 P. DELAHAY, *Electrochim. Acta*, 2 (1960) 19.
- 82 H. GOBRECHT UND O. MEINHARDT, *Phys. Letters*, 11 (1964) 103.
- 83 J. H. SLUYTERS UND J. J. C. OOMEN, *Rec. Trav. Chim.*, 79 (1960) 1101.
- 84 K. B. OLDHAM, *Trans. Faraday Soc.*, 53 (1957) 80.

## NACHTRAG BEI DER KORREKTUR

Von den seit dem Abschluss der vorliegenden Arbeit erschienenen Veröffentlichungen ist besonders die als Fortsetzung zu Lit. 24 erschienene Übersicht<sup>85</sup> hervorzuheben. Inzwischen haben sich auch mehrere Autoren (siehe z.B. Lit. 86) mit der Leistungsfähigkeit der potentiodynamischen Methoden (Tabelle 2) im Hinblick auf quantitative Ergebnisse beschäftigt, so dass also diese Methoden nicht mehr ausschliesslich zu qualitativen Untersuchungen eingesetzt werden.

85 W. H. REINMUTH, *Anal. Chem.*, 38 (1966) 270R.

86 R. S. NICHOLSON, *Anal. Chem.*, 37 (1965) 1351.

## SHORT COMMUNICATION

### Evaluation of the characteristics of exchange reactions.

#### 2. Evaluation of data from double impulse experiments

L-Shaped pulses of current are of direct application to the study of fast electrode reactions using the method of GERISCHER AND KRAUSE<sup>1</sup>. The first part of the pulse prevails for a very short time (usually 1  $\mu$ sec or less) and charges the double layer to the overpotential,  $\eta_D$ , required to drive the electrode reaction at a rate determined by the amplitude of the second part (faradaic current). The condition where the double layer capacity is charged is given by

$$\left(\frac{\partial \eta}{\partial t}\right)_t = 0 \quad (1)$$

where  $t$  is time immediately at the end of the first part of the current pulse. The complex pulse may be regarded, and is often obtained, as two overlapping pulses—a brief “charging” pulse, and a “driving” pulse (see Part I<sup>2</sup>).

In the initial work of GERISCHER AND KRAUSE<sup>1</sup> it was assumed that the value of the overpotential at the end of the first pulse was  $\eta_D$ , the overpotential due to charge transfer. MATSUDA, OKA AND DELAHAY<sup>3</sup> have shown that for very fast reactions (standard rate constant,  $k^0 > 1$  cm sec<sup>-1</sup>),  $\eta_D$  must be obtained from an extrapolation to zero duration of the charging pulse, making conventional use of the  $t^{1/2}$  diffusion law. For slower reactions, for example the zinc or copper exchanges, the treatment of GERISCHER AND KRAUSE is adequate.

#### *Evaluation of experimental data*

For small overpotentials ( $\eta_D \ll RT/ZF$ , *i.e.*, about 6 mV) the faradaic current,  $i$ , is proportional to the overpotential for charge transfer,

$$-\eta_D = \frac{RT}{ZF} \cdot \frac{i}{i_0} \quad (2)$$

where  $i_0$  is the exchange current and  $R$ ,  $T$ ,  $Z$  and  $F$  have their usual meanings.

Consider a simple reaction of the type



where  $R$  and  $O$  are reduced and oxidised species, respectively, and for which the charge transfer rate equation

$$i = i_0 (\exp -\alpha ZF\eta_D/RT - \exp (1-\alpha)ZF\eta_D/RT) \quad (4)$$

describes the relationship between faradaic current and overpotential.

It is relatively simple to obtain the value of the exchange current,  $i_0$ , by measuring the slope of the  $\eta_D$ - $i$  curves as  $\eta_D \rightarrow 0$  when

$$i_0 = -\frac{RT}{ZF} \left(\frac{\partial i}{\partial \eta_D}\right)_{\eta_D=0} \quad (5)$$

The value of the charge transfer coefficient,  $\alpha$ , can be calculated from the expression,

$$i_0 = ZFk^0C_R^\alpha C_O^{(1-\alpha)} \quad (6)$$

by observing the dependence of the exchange current on reactant concentrations (this equation defines  $i_0$  in terms of concentrations since activities are not generally known;  $k^0$  is defined accordingly.)

For overpotentials greater than about 7 mV, the faradaic current – overpotential relationship tends to the familiar Tafel exponential law

$$\eta_D = a + b \log_{10} i \quad (7)$$

where  $a$  and  $b$  are constants.  $i_0$  and  $\alpha$  also follow from intercept and slope of Tafel plots.

This method is subject to considerably more error than “low overpotential” methods since the ohmic drop at large faradaic currents becomes appreciable. It is also possible that the mechanism might change with increased overpotential.

Another method for the calculation of the charge transfer parameters in the region where the deviation of the faradaic current–overpotential data from the linear law is small, involves using a computer. The best values of  $i_0$  and  $\alpha$  are obtained as the result of correlating  $i-\eta_D$  data in the form of eqn. (4) using an iterative technique.

#### Programme format

The programme used computes the optimum value of the charge transfer coefficient ( $\alpha$ ) by minimising the root-mean-square deviation about the mean of the

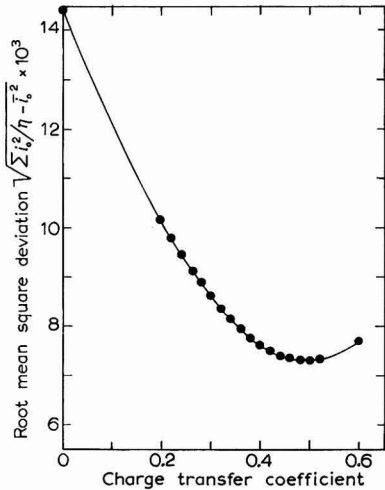


Fig. 1. Minimisation of r.m.s. deviation of  $i_0$ . Solid zinc electrode in 7 M NaOH containing  $Zn^{2+}$  at 25°.

calculated exchange current ( $i_0$ ) using eqn. (4). The value of  $\alpha$  is varied until the computed root-mean-square deviation reaches a minimum as shown in Fig. 1.

Error arising from ohmic factors can be examined using the programme. Successive values ( $i-\eta_D$ ) are “dropped off” at the highest overpotential allowing  $\alpha$  to be calculated as a function of overpotential range.

In Part I, Table 1, values of  $i_0$  obtained by the "low potential" method are compared with those by this iterative technique. Satisfactory agreement is demonstrated.

Copies of a computer programme written in Fortran II-D may be obtained from the authors (M.E.W.)

#### Summary

An iterative method for determining the best values of the exchange current and charge transfer coefficient from data obtained in simple double impulse experiments, is described.

#### Acknowledgement

The authors wish to thank Professors R. F. PHILLIPS AND E. C. ROLLASON for the provision of laboratory facilities and for the interest they have taken in the progress of this work.

*Department of Industrial Metallurgy,  
University of Birmingham,  
Great Britain, and  
Loughborough University of Technology,  
Leicestersh., Great Britain*

J. P. G. FARR

N. A. HAMPSON

Miss M. E. WILLIAMSON

1 H. GERISCHER AND M. KRAUSE, *Z. Physik. Chem., Frankfurt*, 10 (1957) 264.

2 J. P. G. FARR AND N. A. HAMPSON, *J. Electroanal. Chem.*, 13 (1967) 433.

3 H. MATSUDA, S. OKA AND P. DELAHAY, *J. Am. Chem. Soc.*, 81 (1959) 5077.

Received April 15th, 1966.

*J. Electroanal. Chem.*, 13 (1967) 462-464

## BOOK REVIEWS

---

*Research in Surface Forces*, edited by B. V. DERYAGIN, Consultants Bureau, New York, 1963, 190 pages, \$27.50.

Russian workers have contributed a great deal in recent years to the fundamental understanding of surface and colloid chemistry and it is particularly welcome to have available in English translation a collection of reviews by some of their foremost workers in this field. The original Russian publication in 1961 was produced to commemorate the 25th anniversary (in 1960) of the founding of the Laboratory of Surface Phenomena of the Institute of Physical Chemistry of the Academy of Sciences of the U.S.S.R. The Laboratory was initiated in 1935 as an offshoot from the Colloid-Electrochemical Institute in order to study the properties of thin liquid films. The permanent Director is Professor B. V. DERYAGIN who is also the Editor of this volume. The principal interest of the Laboratory is the study of surface forces and the rôle that these forces play in colloidal dispersions, aerosols and other polydispersed heterogeneous systems.

The book is divided into five parts, which are devoted in turn to general problems in surface forces, polymer adhesion, surface forces in thin liquid films, surface effects in dispersed systems and surface forces in aerosols. Twenty-eight papers in all are included, prefaced by an introduction which describes the evolution of the Laboratory from its inception until 1960. The reviews demonstrate clearly the Russian interest both in fundamental and applied science. For example, on the fundamental side, such problems as: diffusional surface forces in the neighbourhood of a liquid interface, the rôle of surface forces in Mica crystals, the measurement of the true density of the electrical double layer at a metal dielectric interface, the effect of electrolyte concentration on the height of the force barrier for adhesion of platinum wires and the theory of coagulation of lyophobic sols by mixtures of electrolytes, are discussed. On the applied side, topics such as: the state of connate water in oil reservoirs, a radioisotope study of the movement of moisture in peats, and surface effects in soil mechanics, are considered.

This is an extremely useful book, giving as it does an insight into the themes, theories and experimental methods of the Russian workers. It should undoubtedly be studied in detail by anyone interested in this field of work. Regrettably, the price of the translation is so high at \$27.50 (*ca.* £10) that it will prevent many workers from adding a personal copy to their bookshelves. Moreover, for such an expensive book the binding is of poor quality and clearly will not stand the test of continuous use.

R. H. OTTEWILL, University of Bristol

*Treatise on Electrochemistry* by G. KORTÜM, 2nd English edition, Elsevier Publishing Company, Amsterdam, London and New York, 1965, xxii + 637 pages, £ 8.10.0.

Electrochemistry has now become such a large subject that it is a formidable task for one man to attempt a comprehensive book that will give a balanced overall view. It is greatly to Professor KORTÜM's credit that he has succeeded so well in giving a general account of electrochemistry in a single volume. The excellent layout of the original text is clearly discernible but, in fact, the book has been completely rewritten since the first English edition (1951) and somewhat revised since the third German edition (1962) so that the author can claim with much justification that it is "now up to date".

The broad changes from the previous edition comprise the expansion of the original twelve basic chapters to thirteen, the omission of the chapter on gases and the introduction of two new chapters: *VI. Association and Incomplete Dissociation of Strong Electrolytes*, and *XIII. Applications of Electrochemical Processes*. The emphasis remains on the theoretical basis and physical interpretation of electrochemical phenomena, with little or no description of experimental methods. Each chapter has a useful list of references, and most sections end with a helpful bibliography in which there is perhaps a higher proportion of German texts than most English-speaking students would welcome.

In a work of this type it would be impossible to satisfy everyone. My own reservations concern some of the material on e.m.f.'s, double layers, and electrode reactions. Labelling the electrodes in a reversible cell as "anode" and "cathode" (p. 286) is undesirable although the situation is clearly explained later (p. 307). The footnote on p. 277 is misleading; there is no analogy between a real gas at its Boyle point and the hypothetical unit molal ideal solution. The device of introducing the activity of electrons in solution (p. 298) does not seem a helpful one, any more than the idea of free  $\text{CO}_2$  in solid  $\text{CaCO}_3$ . The impression given (p. 320) that there is a thermodynamically exact value of pH is unfortunate. It is not correct "that a zero charge density on the surface of the electrode is no longer realizable" when specific adsorption occurs (p. 397). The section on electrokinetic phenomena would be greatly improved by a reference to Onsager's reciprocal relations and the unity which they bring to the various effects. The derivation of the basic equation for "transition" overpotential is not as clear as it should be: in eqns. (71) and (72) (p. 464) the quantities  $k_+$  and  $k_-$  are not defined and the  $\Delta G$ 's are called energies of activation while eqn. (78) (p. 446) is derived from (75) ignoring  $\Delta G_+ - \Delta G_-$ . Also, the activity coefficient ratio will not approach unity in an excess of supporting electrolyte (p. 466) since O and R in eqn. (69) must have different charges. It is not at all clear how Fig. 105 relates to a reaction of the type of eqn. (69). Equations (88) are valid, not at constant overpotential, but at constant potential,  $\epsilon_i$ . It must be emphasized, however, that these criticisms are minor and that the book as a whole is admirably clear.

The translation into English has been well done and there are few traces of the original language. Some of the technical terms could be improved: "partial integration" for integration by parts (p. 178), "constant current polarography" for chronopotentiometry (p. 569). The claim to be up to date has had one unfortunate result in the discussion of the structure of water (p. 129) where the octahedral (*sic*) structure is preferred to the tetrahedral on recent (1957) evidence now known to be incorrect. The

description of the moving boundary method as "recent" (p. 31) does not give a correct idea of the modernity of the book.

The book is well printed and bound; eqn. (99) (p. 137) contains one of the very few misprints. It is a pleasure to welcome Professor KORTÜM's new edition and to know that it can be recommended unhesitatingly to students.

ROGER PARSONS, University of Bristol

*J. Electroanal. Chem.*, 13 (1967) 466-467

*Image Furnace Techniques* by TIBOR S. LASZLO, *Techniques of Inorganic Chemistry*, Vol. V, Interscience Publishers, Inc., New York, 1965, x+195 pages, 90s.

Image furnaces have found considerable use because they are unique in providing a method of reaching high temperatures, in the complete absence of contaminants, in any desired atmosphere. Their chief disadvantages are that the temperature distribution in the sample is not uniform and that, in all but the largest solar furnaces, which are very expensive, the sample size is restricted. They are invaluable for the preparation and study of highly refractory materials in which field they have found their main use.

The equipment is highly specialised and this book provides an excellent and up-to-date source of information on all aspects of construction and application. Sources of power, concentrators, flux measurement and calculations, and sample-handling are all covered, in about two thirds of the book, in sufficient detail to permit the intelligent selection and design of equipment by workers with no previous experience in the field. The last third of the book describes a very wide spectrum of problems to which image furnace techniques have been applied. Those of particular interest to electrochemists include: conductance measurements on solid and liquid refractory materials; the preparation of single crystal materials for use as containers for corrosive melts and the preparation of specialised ceramic materials *e.g.*, solid oxide electrolytes. A comprehensive bibliography of 244 references gives access to the bulk of published work and a tabulated list of image furnace facilities throughout the world provides a valuable means of contacting existing workers in the field.

The book can be recommended as a useful contribution to the documentation of the specialised techniques of inorganic chemistry, and electrochemists, particularly those concerned with high-temperature systems, may find it a valuable work of reference.

J. W. TOMLINSON Imperial College, London

*J. Electroanal. Chem.*, 13 (1967) 467

*Advances in Analytical Chemistry and Instrumentation*, Vol. 4, edited by C. N. REILLEY, Interscience, New York, 1965, 513 pp., \$16.00.

The title adequately describes this book, it being the fourth volume of the series, and it can be said that the high standard of the series is maintained. The book is composed of seven chapters, each on some aspect of analytical chemistry.

The topics covered are: (a) advances in precipitation from homogeneous solution, (b) differential dialysis, (c) the oxygen-flask method, (d) phase-solubility techniques, (e) the electrochemistry of cation sensitive glass electrodes, (f) recent advances in time-of-flight mass spectrometry, and (g) organic analysis with ultra-violet absorption spectroscopy. As can be seen, these chapters cover a wide range of analytical techniques. Each chapter is well documented and presented, although for the reviewer the highlight of the book is EISENMAN'S chapter on the glass electrodes. There are about 160 pages in this chapter; it is a masterly survey of this field and shows how far the analytical chemist must delve into physical chemistry to seek an understanding of the processes involved. Many lines of research are suggested but obviously they are not for those of us who wish "quick returns", perhaps a review of the "membrane electrodes" available for this work is also desirable.

For the other chapters, some of them have dated already because of the very active nature of research in these fields, but mention must be made of the excellent tables for the results of phase-solubility techniques, given in the chapter by HIGUCHI AND CONNORS.

A complete index for both subject and authors, and a cumulative index for all four volumes make for easier reference and greater usefulness.

Thus one may say of this book that it is a very useful addition to the analytical chemist's book shelf, although some chapters will be of more interest than others. To those of us interested in electroanalytical techniques, one chapter is a "must".

G. NICKLESS, University of Bristol

*J. Electroanal. Chem.*, 13 (1967) 468

*Computer Programming For Chemists*, by K. B. WIBERG, Benjamin, New York, Amsterdam, 1965, pages viii + 269, \$12.50 in U.S., \$13.75 elsewhere.

Rapid expansion in the use of computers in the physical sciences has shown the need for the average scientist to acquire some knowledge of programming. Many good books on programming have been published and these in general are designed for a wide range of readers. The present volume is designed explicitly for chemists in that the examples are drawn mainly from the field of organic chemistry. It should be pointed out that the title of this volume is somewhat misleading in that the author considers only Fortran (Algol is not even mentioned in the text) and the 7090 and 7094 Assembly language. If this definition of computer programming is accepted, the book provides a well-written introduction to the subject, with sections on input-output, matrices and arrays, iterative programs, subroutines and functions. Of particular value are the examples of complete computer programs which the author presents in the final chapter.

M. H. ROGERS, Computer Unit, University of Bristol

*J. Electroanal. Chem.*, 13 (1967) 468



*The Molecules of Nature* by JAMES B. HENDRICKSON, Benjamin, New York, 1965, 192 pp., \$7.00 (for the U.S.A.) or \$7.70; paperback \$3.95.

The enormous progress made over the past fifteen years, in our understanding of biosynthetic processes, allows natural products to be viewed simply and instructively on a biosynthetic basis. The author takes this as his starting point and sets the ambitious target of presenting to first-year students a brief scan of the field of natural products with the obvious hope that it will serve as a base for further reading and exploration.

A survey of the important biosynthetic pathways forms the first part of the book and this will inevitably be compared with BU'LOCK's recent account, but the present work is less successful since there are some errors, and fact and hypothesis are too often not distinguished. This section is followed by a brief account of the structure determination and chemistry of many natural products. The author comments, "In an attempt to reveal the whole skeleton of natural products studies we must cut close to the bone and dispense with much of the meat." Such a treatment has its dangers, not the least being that the reader will gain quite a false impression of the problem presented, for example, by the structure of strychnine (two pages). In the main, the later sections of this book have successfully avoided many such pitfalls and the presentation of numerous examples as problems is a valuable feature.

In summary, this book is a useful one although it is probably more suitable for widening the view of those who have a moderate knowledge of biosynthetic processes and natural products than for the complete beginner.

A. R. BATTERSBY, University of Liverpool

*J. Electroanal. Chem.*, 13 (1967) 469

*Les Séparations par les Résines Echangeuses d'Ions*, by B. TRÉMILLON, Gauthier-Villars, Paris, 1965, 400 pages, 90 NF.

This book is in French. In common with a large number of European books, the content pages are at the back of the book, beyond the index. The book is divided into two parts; Part I discusses in detail the fundamental properties of ion-exchange resins (152 pages) and Part II, the operation and applications of ion-exchange columns. One noteworthy feature of Part I, besides the section on equilibria and kinetics of exchange in aqueous solutions is the lucid discussion of the exchange of ions in solvents other than water. A large section also describes the influence of complexing chemical reactions on the ion-exchange resins, and their use in separation procedures.

Part II is also unconventional since it covers break-through volume concepts (including the theoretical background), frontal analysis, ion-exclusion. A chapter discusses separation by elution procedures together with examples. A novel feature is a complete and detailed chapter on the principles of ion-exchange operated in a counter-current manner. Finally, there is a short chapter on electro-migration in ion-exchange resins and membranes. An appendix gives in graphical form the experimental values of distribution coefficients for a large number of ions in a variety of media.

This book is to be recommended for libraries, but its high cost and language difficulty will probably deter its usage in English-speaking countries.

G. NICKLESS, University of Bristol

*J. Electroanal. Chem.*, 13 (1967) 469

*Titrations in non-aqueous solvents*, by KUCHARSKÝ AND ŠAFARÍK, Elsevier Publishing Company, Amsterdam, London, New York, 286 pp., Dfl. 35.— or 70s., 1964.

The first edition of this work appeared in 1961 in the Czech language, and the present edition is a translation of the first edition with a certain amount of revision to include some fifty more recent literature references extending into 1962, with some four references to the Authors' own work dating from 1963. The first half of the book is introductory and deals with general and theoretical matters. This excellent survey covers acid-base theories, solvents, end-point location, titrants and primary standards, factors affecting the course of the titration and titration methodology. The second half is devoted to practical procedures. This is almost entirely concerned with neutralisation titrations of 21 types of compounds, but includes four pages on oxidation-reduction reactions and five pages on the determination of equivalent weights: precipitation and complexation reactions are not mentioned. This is a fair reflection of the current situation in non-aqueous titrimetry. The book concludes with a useful tabulation of physical constants of non-aqueous solvents and good author and subject indexes.

A special word of praise is due to the translator, KAREL ŠUMBERA: seldom has so excellent a job been done. The authors give a well balanced, accurate account of their subject with adequate detail and good coverage. Anyone taking up non-aqueous titrimetry can confidently turn to this book for both theoretical and practical guidance in all aspects, and those already using these techniques will welcome this collected account, which admirably fills a long-felt want.

E. BISHOP, University of Exeter

*J. Electroanal. Chem.*, 13 (1967) 470

*Fuel Cells, Their Electrochemical Kinetics*, edited by V. S. BAGOTSKII AND YU. B. VASILEV, Consultants Bureau, New York, 1966, viii + 121 pages, \$15.00.

The title of this collection of papers is something of a misnomer. Of the ten papers collected here, seven are concerned with the basic theory of porous electrodes, two describe research on the mechanism of the oxidation of organic compounds at platinum electrodes, and one very short paper makes a point about solid electrolytes. There is no doubt that these are interesting papers, but only those on porous electrodes seem to form a group worthy of publication as a symposium, since the two on oxidation are both by the joint editors and inevitably present one point of view even if very consistently developed. Inclusion of the discussion at the Second Fuel Cell Conference in Moscow when these papers were presented would have added greatly to the value of this volume and provided a convincing reason for publication in this form rather than in normal journals.

The translated form is quite satisfactory and will undoubtedly be of value to those working in these subjects.

ROGER PARSONS, University of Bristol

*J. Electroanal. Chem.*, 13 (1967) 470

*Brennstoffelemente*, by WOLF VIELSTICH, Verlag Chemie GmbH, Weinheim/Bergstrasse, 1965, xv + 388 pages, DM 54.

This is a thorough and careful introduction to the problems of fuel cells, covering both the fundamental nature of electrode reactions and the practical difficulties of harnessing them in a workable fuel cell. The information available for deriving the mechanism of each of the possible electrode reactions is lucidly discussed with many illustrations of results from the author's own work as well as that of others. Besides the study of the classical current-voltage curve, which of course provides the most direct information on the practical use of an electrode, stress is also laid on the triangular potentiostatic sweep method.

In addition to the description of the more conventional types of fuel cell, which occupies the bulk of the book, there are chapters (by Dr. G. GRÜNEBERG) on electrochemical methods of converting heat and nuclear energy into electricity. Dr. VIELSTICH then discusses electrochemical methods of energy storage and, somewhat irrelevantly, the electrochemical separation of deuterium and tritium. In the final chapter he discusses the "state of the art" in 1964. It is inevitable that a chapter of this type will date and the photographs (among them — p. 368 — one of a well-known exponent of the art whose name does not even appear in the index) will find their place in some future Science Museum. However, the rest of the book is likely to remain useful for a longer period to those who wish to gain an understanding of the basic working of fuel cells.

The book is well printed and attractively laid out. A useful feature is the summary at the beginning of each chapter. The author index is reasonably full but the subject index could well have been expanded.

ROGER PARSONS, University of Bristol

*J. Electroanal. Chem.*, 13 (1967) 471

*Atlas of Electrochemical Equilibria in Aqueous Solutions*, by MARCEL POURBAIX, Pergamon Press, Oxford etc., Cebelcor, Brussels, 1966, 644 pages, £12.

The French edition of this Atlas was reviewed in this Journal (7 {1964} 492) with qualified enthusiasm. Since the English edition is simply a translation with no revision, everything that was said of the former remains true of the latter except that the printing is even better — well up to Arrowsmith's usual high standard — and the binding more substantial. It must be a matter of regret that the opportunity was not taken to bring this massive survey up to date since little contained therein is less than 10 years old and much is a good deal older. The question of whether a translation was needed is a difficult one to answer. Much of the material is diagrammatic or in the form of equations, but presumably most English-speaking readers would be prepared to spend an extra 20% for the English text and a better binding.

ROGER PARSONS, University of Bristol

*J. Electroanal. Chem.*, 13 (1967) 471

*Double Layer and Electrode Kinetics*, by PAUL DELAHAY, Interscience Publishers, Inc., New York, London, Sydney, 1965, 321 pages, \$ 14.50.

Over the past decade Professor DELAHAY'S *New Instrumental Methods in Electrochemistry* has proved itself to be a first-rate introduction to the field of electrode kinetics and I would guess that it has been more widely and more intensively read than any other monograph on the subject. But it was primarily a book on methodology. In his new book, Professor DELAHAY looks at the other side of the coin and says little about techniques, being mainly concerned with the interpretation of the experimental data in the light of current views about the electrode/solution interface.

It is an excellent book, thorough, up-to-date, well arranged and logically developed. It can be warmly recommended and I do not doubt that it will prove at least as useful as *New Instrumental Methods*; but not in quite the same way. This is not a beginner's book and in spite of Professor DELAHAY'S exceptional skill as an expositor of difficult themes, it is not easy reading. In the first place, it is very heavily loaded with references to recent work, and although this is a valuable feature in many respects, it also means that much work is mentioned but not discussed or explained in sufficient detail. Quite apart from this, the fact remains that, except at an elementary level, the study of the double layer and the analysis of electrode kinetics are complicated and difficult topics. The basic experimental techniques are limited in number and in this respect compare unfavourably with what can be done in investigations of homogeneous equilibria and kinetics (*spectrophotometry* is indexed once in this book; *spectroscopy* not at all). Moreover, the methods are often indirect, which tends to introduce an uncomfortably oblique approach to some aspects of the subject. As propositions in thermodynamics, Gibbs' adsorption isotherm and its ramifications are magnificent, but some of their applications can only be described as magnificently tortuous.

Apart from an introductory chapter, which gives an excellent survey of the whole field, the book is divided about equally between *Double Layer* and *Electrode Kinetics*, five chapters being devoted to each. Naturally a large proportion of both sections is concerned with mercury surfaces in aqueous solutions, but other systems are also discussed. Numerous well-chosen examples of electrode reactions are introduced and a large amount of experimental material is presented in graphical or tabular form.

Occasionally Professor DELAHAY does not quite hit the nail on the head and there are some fairly obvious misprints; but these are very trivial blemishes on a work that will surely come to be regarded as a major contribution to the subject.

J. N. AGAR, Cambridge University

JOURNAL OF ELECTROANALYTICAL CHEMISTRY AND INTERFACIAL  
ELECTROCHEMISTRY, VOL. 13 (1967)

AUTHOR INDEX

ADAMS, R. N. . . . .	184	LUCK, J. R. . . . .	149
ALEXANDER, W. A. . . . .	137, 181	MANAHAN, S. E. . . . .	411
ANSON, F. C. . . . .	35, 236, 343	MANN, C. K. . . . .	157, 163
ARIEL, M. . . . .	90	MARK, H. B. JR. . . . .	1
BARCLAY, D. J. . . . .	137, 181	MAZUREK, P. . . . .	442
BATICLE, A. M. . . . .	364	MAZZOCCHIN, G. A. . . . .	167
BELL, G. M. . . . .	280	MILLER, F. J. . . . .	193
BOMBI, G. G. . . . .	167	MILLS, F. . . . .	149
BONNEMAY, M. . . . .	44, 58	MINC, S. . . . .	189
BROADHEAD, J. . . . .	354	MINGINS, J. . . . .	280
BRONOËL, G. . . . .	44, 58	MIRON, C. . . . .	263
BRUMFIELD, A. . . . .	124	MOLINA, R. . . . .	144
BUCUR, R. V. . . . .	263	MORALES, A. . . . .	418
CHRISTIE, J. H. . . . .	79, 227, 236, 343	MUKHERJI, A. K. . . . .	425
CONWAY, B. E. . . . .	333	MÜLLER, L. . . . .	275
COULTER, P. D. T. . . . .	21, 28	MURRAY, R. W. . . . .	132
COVACI, I. . . . .	263	NELSON, R. F. . . . .	184
DĄBKOWSKI, J. . . . .	189	O'DONNELL, J. F. . . . .	157, 163
DMITRIEVA, A. . . . .	179	OSTERYOUNG, R. A. . . . .	236, 343
ELUARD, A. . . . .	208	PARRY, E. P. . . . .	177
FARHA, F. JR. . . . .	390	PAYNE, D. A. . . . .	35
FARR, J. P. G. . . . .	433, 462	PEOVER, M. E. . . . .	93
FARSANG, G. . . . .	73	PERDU, F. . . . .	364
FIORANI, M. . . . .	167	PERONE, S. P. . . . .	124
FITZGERALD, J. M. . . . .	400	PILLA, A. A. . . . .	44, 58
FRUMKIN, A. . . . .	179	RAO, S. B. . . . .	330
GOLDNER, H. J. . . . .	177	RINK, M. . . . .	10
GONZÁLEZ V., F. . . . .	418	ROGERS, L. B. . . . .	400
GROSS, D. I. . . . .	132	RUBY, W. R. . . . .	245
GYGAX, H. R. . . . .	378	SCHLITT, L. . . . .	10
HAMPSON, N. A. . . . .	433, 462	SCHMIDT, E. . . . .	378
HARGIS, L. G. . . . .	400	SESHAGIRI, V. . . . .	330
HICKLING, A. . . . .	100	SLUYTERS, J. H. . . . .	31, 152
HILLS, G. J. . . . .	354	SLUYTERS-REHBACH, M. . . . .	31
IWAMOTO, R. T. . . . .	21, 28, 390, 411	SOBOL, V. . . . .	179
JOHNSON, D. . . . .	100	SOHR, H. . . . .	107, 114
JOHNSTON, T. H. . . . .	177	STACKELBERG, M. VON . . . . .	10
KHASGIWALE, K. A. . . . .	144	TOMCSÁNYI, L. . . . .	73
KIROWA-EISNER, E. . . . .	90	TONG, L. K. J. . . . .	245
KOCZOROWSKI, Z. . . . .	189	TRÉMILLON, B. . . . .	208
KOOIJMAN, D. J. . . . .	152	TUCKER, B. V. . . . .	400
KRONENBERG, M. L. . . . .	120	VASSOS, B. H. . . . .	1
LANZA, P. . . . .	67	WHITE, B. S. . . . .	93
LEVART, E. . . . .	44, 58	WILLIAMSON, M. E. . . . .	462
LEVINE, S. . . . .	280	WOITTEZ, W. J. A. . . . .	31
LIANG, K. . . . .	245	WOJTOWICZ, J. . . . .	333
LINGANE, P. J. . . . .	227	ZITTEL, H. E. . . . .	193
LOHS, KH. . . . .	107, 114		

**JOURNAL OF ELECTROANALYTICAL CHEMISTRY AND INTERFACIAL  
ELECTROCHEMISTRY, VOL. 13 (1967)**

**SUBJECT INDEX**

- Acetic acid,  
voltammetry of metal ions in  
—— (COULTER, IWAMOTO) . . . 21
- Acetone,  
Cu-Cl complexes in ——  
(MANAHAN, IWAMOTO) . . . . . 411
- Acetonitrile,  
oxidation of polycyclic aromatics  
in —— (PEOVER, WHITE) . . . . . 93
- Acid-base titrations,  
twin mercury electrodes for  
—— (ARIEL, KIROWA-EISNER) . . . . . 90
- Acrylic acid,  
voltammetry of metal ions in  
—— (COULTER, IWAMOTO) . . . . . 28
- Adsorption,  
—— and faradaic impedance  
(BATICLE, PERDU) . . . . . 364
- Aliphatic amides,  
controlled-potential oxidation of  
—— (O'DONNELL, MANN) . . . . . 157  
determination of —— by controlled-potential coulometry  
(O'DONNELL, MANN) . . . . . 163
- Anodic stripping voltammetry,  
—— with Hg-plated graphite  
electrodes (PERONE, BRUMFIELD) . . . . . 124
- Bis-2,2'-bipyridine,  
electroreduction of Cr(III)-——  
complexes (ROGERS *et al.*) . . . . . 400
- 2-Butanol,  
Cl-Cu complexes in ——  
(MANAHAN, IWAMOTO) . . . . . 411
- 3-Butenenitrile,  
solvent and orientation of ——  
in Cu<sup>-</sup> and Ag<sup>-</sup> spheres (FARHA,  
IWAMOTO) . . . . . 390
- Cadmium,  
adsorption of ——(II) on Hg  
from SCN<sup>-</sup> solns. (ANSON,  
CHRISTIE, OSTERYOUNG) . . . . . 343  
determination of —— in  
Th(NO<sub>3</sub>)<sub>4</sub> by linear chronoamperometry  
(KHASGIWALE, MOLINA) . . . . . 144  
polarographic determination of  
—— in AgBr (PARRY, JOHN-  
STON, GOLDNER) . . . . . 177
- Catalytic reactions,  
double potential-step chronocoulometry  
for the study of ——  
(LINGANE, CHRISTIE) . . . . . 227
- Chloro complexes,  
—— of Cu in alcohols and  
acetone (MANAHAN, IWAMOTO) . . . . . 411
- Chromium,  
reduction of bis- and tris-2,2'-  
bipyridine complexes of ——  
(III) (ROGERS *et al.*) . . . . . 400
- Copper,  
Cl-complexes of —— in alcohols  
and acetone (MANAHAN,  
IWAMOTO) . . . . . 411  
dissolution of —— films from  
pyrolytic graphite (VASSOS,  
MARK) . . . . . 1  
orientation of 3-butenitrile and  
3-dimethylaminopropionitrile in  
——(I) spheres (FARHA, IWA-  
MOTO) . . . . . 390  
polarography of resacetophenone-  
oxime complex of —— (SESHA-  
GIRI, RAO) . . . . . 330
- Coulometric titrations,  
a potentiometric end-point in  
—— (ALEXANDER, BARCLAY) . . . . . 181
- Current-cessation chronopotentiometry,  
application of —— for qualitative  
analysis (ALEXANDER, BAR-  
CLAY) . . . . . 137
- Current distribution,  
—— at an electrode resulting  
from interfacial processes, diffu-  
sion and conduction (LEVART *et  
al.*) . . . . . 58
- Current-reversal chronopotentiometry,  
effects in —— at the HMDE  
(MURRAY, GROSS) . . . . . 132
- Cyanide complexes,  
formation of —— in molten  
KSCN (ELUARD, TRÉMILLON) . . . . . 208
- 3-Dimethylaminopropionitrile,  
influence of solvent on orientation  
of —— in Cu<sup>-</sup> and Ag<sup>-</sup> spheres  
(FARHA, IWAMOTO) . . . . . 390
- Discrete-ion effect,  
the —— in ionic double-layer  
theory (LEVINE, MINGINS, BELL) . . . . . 280
- Double-impulse experiments,  
characteristics of exchange reac-  
tions from —— (FARR, HAMP-  
SON) . . . . . 462
- Double-layer theory, see ionic d.l.t.
- Double potential-step chronocoulometry,  
—— and reactions following the  
electrode reaction (CHRISTIE) . . . . . 79  
—— and catalytic reactions  
(LINGANE, CHRISTIE) . . . . . 227  
—— and reactant adsorption  
(CHRISTIE, OSTERYOUNG, ANSON) . . . . . 236

— for adsorption studies (ANSON, CHRISTIE, OSTERYOUNG) . . . . .	343	soln. interface at high potentials (SLUYTERS-REHBACH, WOITTEZ, SLUYTERS) . . . . .	31
Electrical methods, — for the study of electrode reaction kinetics (MAZUREK) . . . . .	442	Iodine, chronopotentiometry of ——— at PGE and GCE (ZITTEL, MILLER) . . . . .	193
Electrocapillary maximum potentials, determination of ——— by the vibrating interphase method (KOCZOROWSKI, DABKOWSKI, MINC) . . . . .	189	Ionic double-layer theory, the discrete-ion effect in ——— (LEVINE, MINGINS, BELL) . . . . .	280
Electrode reaction kinetics, electrical methods for the study of — (MAZUREK) . . . . .	442	Isobutyric acid, voltammetry of metal ions in — (COULTER, IWAMOTO) . . . . .	28
Ethanol, Cl-Cu complexes in ——— (MANAHAN, IWAMOTO) . . . . .	411	Lanthanum, determination of Th and ——— in presence of NO <sub>3</sub> <sup>-</sup> (MUKHERJI) . . . . .	425
Exchange reactions, evaluation of characteristics of — (FARR, HAMPSON) . . . . .	433, 462	Lead depositions, study of ——— on Au electrodes (SCHMIDT, GYGAX) . . . . .	378
Faradaic impedance, adsorption and ——— (BATICLE, PERDU) . . . . .	364	Linear sweep voltammetry, — in a thin rigid layer (BUCUR, COVACI, MIRON) . . . . .	263
Following reactions, study of ——— by double poten- tial-step chronocoulometry (CHRISTIE) . . . . .	79	Mercury, SCN <sup>-</sup> adsorption on ——— (ANSON, PAYNE) . . . . .	35
Galvanostatic double-pulse method (KOOIJMAN, SLUYTERS) . . . . .	152	Mercury-drop synchronization device (LUCK, MILLS) . . . . .	149
Glassy-carbon electrode, chronopotentiometry of iodine at the ——— (ZITTEL, MILLER) . . . . .	193	Mercury-plated graphite electrodes, anodic stripping voltammetry with ——— (PERONE, BRUM- FIELD) . . . . .	124
Gold electrode, study of Pb-depositions on ——— (SCHMIDT, GYGAX) . . . . .	378	Metal ions, voltammetry of ——— in acetic acid (COULTER, IWAMOTO) . . . . .	21
Graphite electrodes, see mercury-plated g.e.		voltammetry of ——— in propionic, isobutyric and acrylic acids (COULTER, IWAMOTO) . . . . .	28
Hanging mercury-drop electrode, effects in current-reversal chrono- potentiometry at the ——— (MURRAY, GROSS) . . . . .	132	Methanol, Cl-Cu complexes in ——— (MANAHAN, IWAMOTO) . . . . .	411
Hydrazines, polarography of pharmaceutically important ——— (SCHLITT, RINK, VON STACKELBERG) . . . . .	10	Nickel oxide, measurements on thin layers of — (KRONENBERG) . . . . .	120
Hydrogen, oxidation of ——— dissolved in Pd in a stirred soln. (BUCUR, COVACI, MIRON) . . . . .	263	Nitrate, determination of Th and La in presence of ——— (MUKHERJI) . . . . .	425
oxidation of ——— on Pt (FRUM- KIN, SOBOL, DMITRIEVA) . . . . .	179	Oscillopolarography, sensitivity and specificity of — of U (MORALES, GONZALEZ) . . . . .	418
Hydroxylamine, the Ti(III)-—— reaction by double potential-step chrono- coulometry (LINGANE, CHRISTIE) . . . . .	227	Palladium, oxidation of H <sub>2</sub> dissolved in — (BUCUR, COVACI, MIRON) . . . . .	263
Hypophosphites, anodic behaviour of ——— (HICKLING, JOHNSON) . . . . .	100	Perchlorates, solubility products of AgHal in molten alkali ——— (FIORANI, BOMBI, MAZZOCCHIN) . . . . .	167
Interfacial tension, — of the Hg-I M HClO <sub>4</sub>		Persulfate ion, accelerating effect of Pt-oxides on the reduction of ——— on Pt electrodes in OH <sup>-</sup> milieu (MÜLLER) . . . . .	275

- p*-Phenylenediamines,  
study of reactions of ——— on the  
RDE (TONG, LIANG, RUBY) . . . . . 245
- pH-Meter,  
a multi-purpose recording ———  
(LANZA) . . . . . 67
- Phosphites,  
anodic behaviour of ———  
(HICKLING, JOHNSON) . . . . . 100
- Phosphoric compounds,  
pH-dependence of the inhibition  
in the polarography of ———  
(SOHR, LOHS) . . . . . 107
- complex formation in the ad-  
sorption layer by ——— (SOHR,  
LOHS) . . . . . 114
- Platinum,  
H<sub>2</sub> oxidation on ——— (FRUM-  
KIN, SOBOL, DMITRIEVA) . . . . . 179
- accelerating effect of ——— oxides  
on the reduction of S<sub>2</sub>O<sub>8</sub><sup>2-</sup> on the  
——— electrode in OH<sup>-</sup> milieu  
(MÜLLER) . . . . . 275
- Polycyclic aromatic hydrocarbons,  
oxidation of ——— in acetonitrile  
(PEOVER, WHITE) . . . . . 93
- Porous electrodes,  
reaction kinetics on ———  
LEVART *et al.*) . . . . . 44
- Potassium thiocyanate,  
molten ——— as a solvent; cyan-  
ide complex formation in ———  
(ELUARD, TRÉMILLON) . . . . . 208
- Potentiometric end-point,  
a ——— in coulometric titrations  
(ALEXANDER, BARCLAY) . . . . . 181
- 2-Propanol,  
Cl-Cu complexes in ———  
(MANAHAN, IWAMOTO) . . . . . 411
- Propionic acid,  
voltammetry of metal ions in  
——— (COULTER, IWAMOTO) . . . . . 28
- Propylene carbonate,  
——— as solvent for ERP  
(NELSON, ADAMS) . . . . . 184
- Pyrolytic graphite,  
dissolution of Cu films from  
——— (VASSOS, MARK) . . . . .  
chronopotentiometry of I<sub>2</sub> at the  
——— electrode (ZITTEL, MILLER) 193
- Reactant adsorption,  
double potential-step chrono-  
coulometry for the study of ———  
(CHRISTIE, OSTERYOUNG, ANSON) . 236
- Redox wave,  
recording of a polarographic  
——— on a stationary electrode  
(FARSANG, TOMCSÁNYI) . . . . . 73
- Resacetophenoneoxime,  
polarography of the ——— -Cu  
complex (SESHAGIRI, RAO) . . . . . 330
- Rotating disc electrode,  
a ——— for elevated temper-  
atures (WOJCIWICZ, CONWAY) . . . . . 333
- study of reactions of *p*-phenylene-  
diamines with the ——— (TONG,  
LIANG, RUBY) . . . . . 245
- Silver,  
orientation of 3-butenitrile and  
3-dimethylaminopropionitrile in  
——— spheres (FARHA, IWAMOTO) 390
- Silver bromide,  
polarographic determination of Cd  
in ——— (PARRY, JOHNSTON,  
GOLDNER) . . . . . 177
- Silver halides,  
solubility products of ——— in  
molten perchlorates (FIORANI,  
BOMBI, MAZZOCCHIN) . . . . . 167
- Solid zinc electrode,  
exchange reaction at a ——— in  
OH<sup>-</sup> milieu (FARR, HAMPSON) . . . . . 433
- Stationary electrode,  
recording of a polarographic redox  
wave on a ——— (FARSANG,  
TOMCSÁNYI) . . . . . 73
- Thiocyanate,  
——— ion adsorption on Hg  
(ANSON, PAYNE) . . . . . 35
- adsorption of Cd(III) on Hg from  
——— soln. (ANSON, CHRISTIE,  
OSTERYOUNG) . . . . . 343
- Thorium,  
determination of ——— and La in  
presence of NO<sub>3</sub><sup>-</sup> (MUKHERJI) . . . . . 425
- Thorium nitrate,  
determination of Cd in ——— by  
linear chronoamperometry  
(KHASGIWALE, MOLINA) . . . . . 144
- Titanium,  
study of the ———(III)-NH<sub>2</sub>OH  
reaction by double potential-step  
chronocoulometry (LINGANE,  
CHRISTIE) . . . . . 227
- Transport numbers,  
chronopotentiometric determina-  
tion of ——— (BROADHEAD,  
HILLS) . . . . . 354
- Tris-2,2'-bipyridine,  
electroreduction of Cr(III)-  
——— complexes (ROGERS *et al.*) 400
- Twin mercury electrodes,  
preparation and treatment of  
——— for acid-base titrations  
(ARIEL, KIROWA-EISNER) . . . . . 90
- Uranium,  
oscillopolarography of ———  
(MORALES, GONZALEZ) . . . . . 418
- Vibrating interphase method,  
determination of the electrocapil-  
lary maximum potentials by the  
——— (KOCZOROWSKI, DAB-  
KOWSKI, MINC) . . . . . 189



## CONTENTS

Construction and operation of a rotating disc electrode for elevated temperatures J. WOJCIOWICZ AND B. E. CONWAY (Ottawa, Canada) . . . . .	333
A study of the adsorption of cadmium(II) on mercury from thiocyanate solutions by double potential-step chronocoulometry F. C. ANSON, J. H. CHRISTIE AND R. A. OSTERYOUNG (Thousand Oaks, Calif., U.S.A.)	343
The chronopotentiometric determination of transport numbers J. BROADHEAD AND G. J. HILLS (Southampton, Great Britain) . . . . .	354
Adsorption et impédance faradique. II. Etude expérimentale A. M. BATICLE ET F. PERDU (Bellevue, France) . . . . .	364
Chronoamperometrische Untersuchung von Bleiniederschlägen auf Goldelektroden E. SCHMIDT UND H. R. GYGAX (Bern, Schweiz) . . . . .	378
Influence of the solvent system on the orientation of 3-butenitrile and 3-dimethylamino-propionitrile in the co-ordination sphere of copper(I) and silver ions F. FARHA JR. AND R. T. IWAMOTO (Lawrence, Kan., U.S.A.) . . . . .	390
Electroreductions of bis- and tris-2,2'-bipyridine complexes of chromium(III) B. V. TUCKER, J. M. FITZGERALD, L. G. HARGIS AND L. B. ROGERS (Lafayette, Ind., U.S.A.) . . . . .	400
Chloro complexes of copper(II) and copper(I) in methanol, ethanol, 2-propanol, 2-butanol and acetone S. E. MANAHAN AND R. T. IWAMOTO (Lawrence, Kan., U.S.A.) . . . . .	411
On the increase of sensitivity and specificity in the oscillopolarography of uranium A. MORALES AND F. GONZÁLEZ V. (Santiago, Chile) . . . . .	418
Amperometric determination of thorium and lanthanum in presence of nitrate A. K. MUKHERJI (Philadelphia, Pa., U.S.A.) . . . . .	425
Evaluation of the characteristics of exchange reactions. I. Exchange reaction at a solid zinc electrode in alkali J. P. G. FARR AND N. A. HAMPSON (Birmingham and Loughborough, Great Britain)	433
<i>Review</i> Elektrische Methoden zum Studium der Elektrodenkinetik P. MAZUREK (Dresden, Deutschland) . . . . .	442
<i>Short communication</i> Evaluation of the characteristics of exchange reactions. II. Evaluation of data from double impulse experiments J. P. G. FARR, N. A. HAMPSON AND M. E. WILLIAMSON (Birmingham and Loughborough, Great Britain) . . . . .	462
<i>Book reviews</i> . . . . .	465
<i>Author index</i> . . . . .	473
<i>Subject index</i> . . . . .	474

## TREATISE ON ELECTROCHEMISTRY

Second, completely revised edition

by G. KORTÜM

*Professor of Physical Chemistry, University of Tübingen, Germany*

7 x 10", xxii + 637 pages, 71 tables, 151 illus., 882 lit.refs., 1965, Dfl. 85.00, £ 8.10.0, \$ 30.00

**Contents:** 1. Definitions and fundamental laws. 2. Fundamental principles of thermodynamics. 3. The solvation of ions. 4. Weak and strong electrolytes. 5. Theory of ionic interaction. 6. Association and incomplete dissociation of strong electrolytes. 7. The results and applications of conductance measurements. 8. Electromotive forces. 9. Practical applications of potentiometric measurements. 10. Acids and bases. 11. Potential differences at phase boundaries. 12. Electrical polarization and the kinetics of electrode processes. 13. Applications of electrochemical processes. Appendix. Subject index.

## OXIDATION AND COMBUSTION REVIEWS

edited by C. F. H. TIPPER,

*Department of Inorganic, Physical and Industrial Chemistry, University of Liverpool, Great Britain*

Volume 1

6 x 9", viii + 344 pages, 29 tables, 45 illus., 815 lit.refs., 1965, Dfl. 47.50, 95s., \$ 17.00

**Contents:** 1. Application of the theory of branched chain reactions in low temperature combustion. 2. Oxidation reactions induced by ionising radiation. 3. Gas phase photo-oxidation. 4. Oxidation reactions involving nitrogen dioxide. 5. Oxidative degradation high polymers. 6. The heterogeneous selective oxidation of hydrocarbons. Author and subject indexes.

Volume 2 in preparation

## ATMOSPHERIC OXIDATION AND ANTIOXIDANTS

by G. SCOTT,

*Head of Works Research and Development Department, Dyestuffs Division, Imperial Chemical Industries Ltd., Grangemouth, Stirlingshire, Great Britain*

7 x 10", xii + 528 pages, 172 tables, 174 illus., 1206 lit.refs., 1965, Dfl. 72.50, £ 7.5.0, \$ 26.00

**Contents:** 1. The historical development of antioxidants. 2. Peroxides. 3. Autoxidation. 4. Antioxidants: radical chain-breaking mechanisms. 5. Antioxidants: Preventive mechanisms. 6. Measurement of oxidative deterioration. 7. Oxidative deterioration of saturated oils and polymers. 8. Oxidation of olefinic oils, fats and polymers. 9. Degradation of vulcanised rubber. 10. Mechano-oxidation of polymers. Index.



ELSEVIER PUBLISHING COMPANY

AMSTERDAM

LONDON

NEW YORK

